SOME ASPECTS OF THE GEOCHEMISTRY OF GALLIUM IN SILICATE ROCKS AND STONY METEORITES

by

J.P. WILLIS

Department of Geochemistry,
University of Cape Town.

VOLUME 3

Figures

November, 1978

Thesis submitted in fulfilment of the requirements for the degree of Ph.D. at the University of Cape Town

CONTENTS

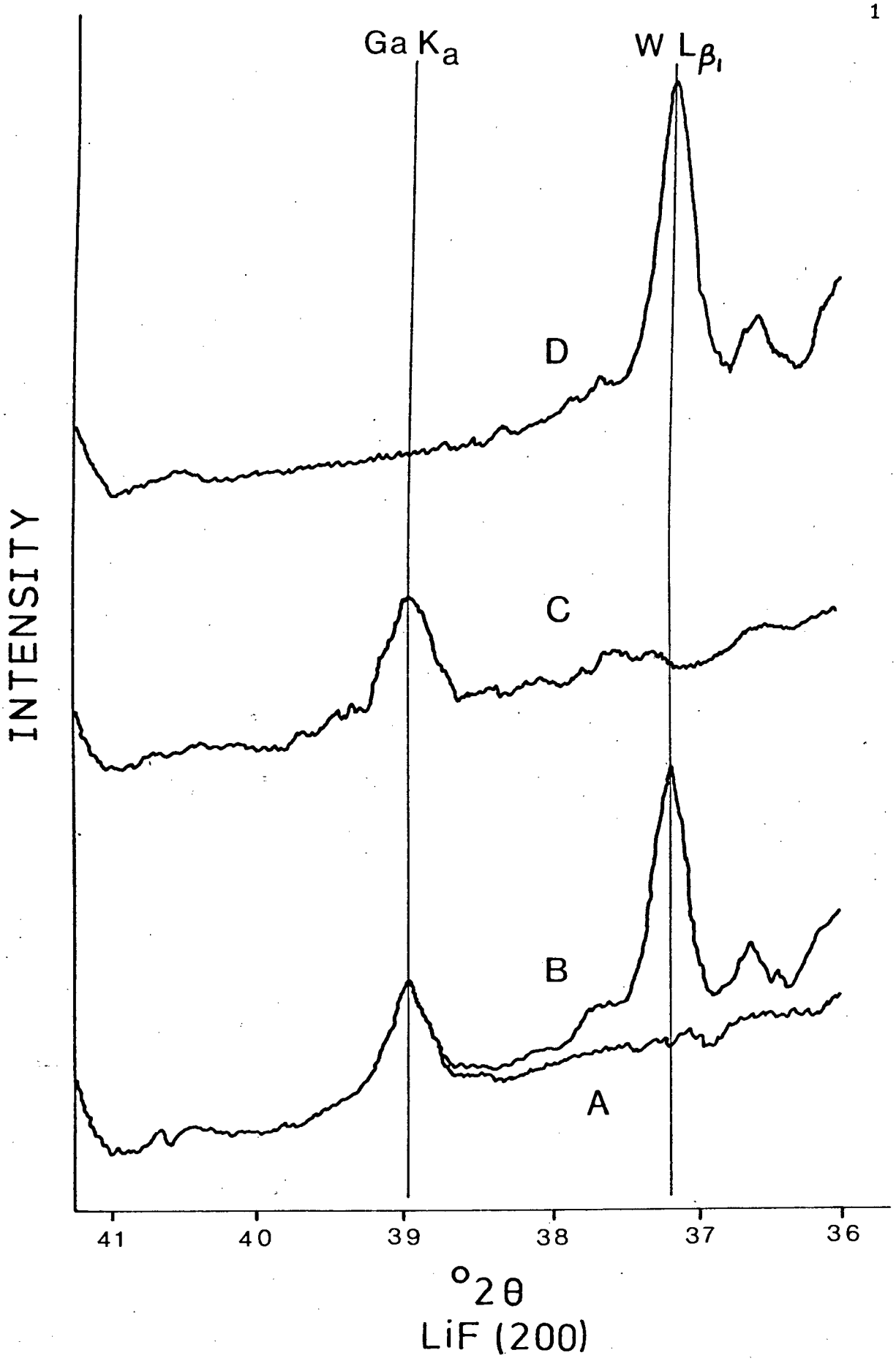

Fig. 1. Sample contamination introduced during the grinding process by steel and tungsten carbide vessels. The test sample is a spotted anorthosite from the B.I.C. containing 17.5 ppm Ga. A. Carbon steel vessel. B. Tungsten carbide vessel. C. Stainless steel vessel. D. 335 ppm W in quartz.

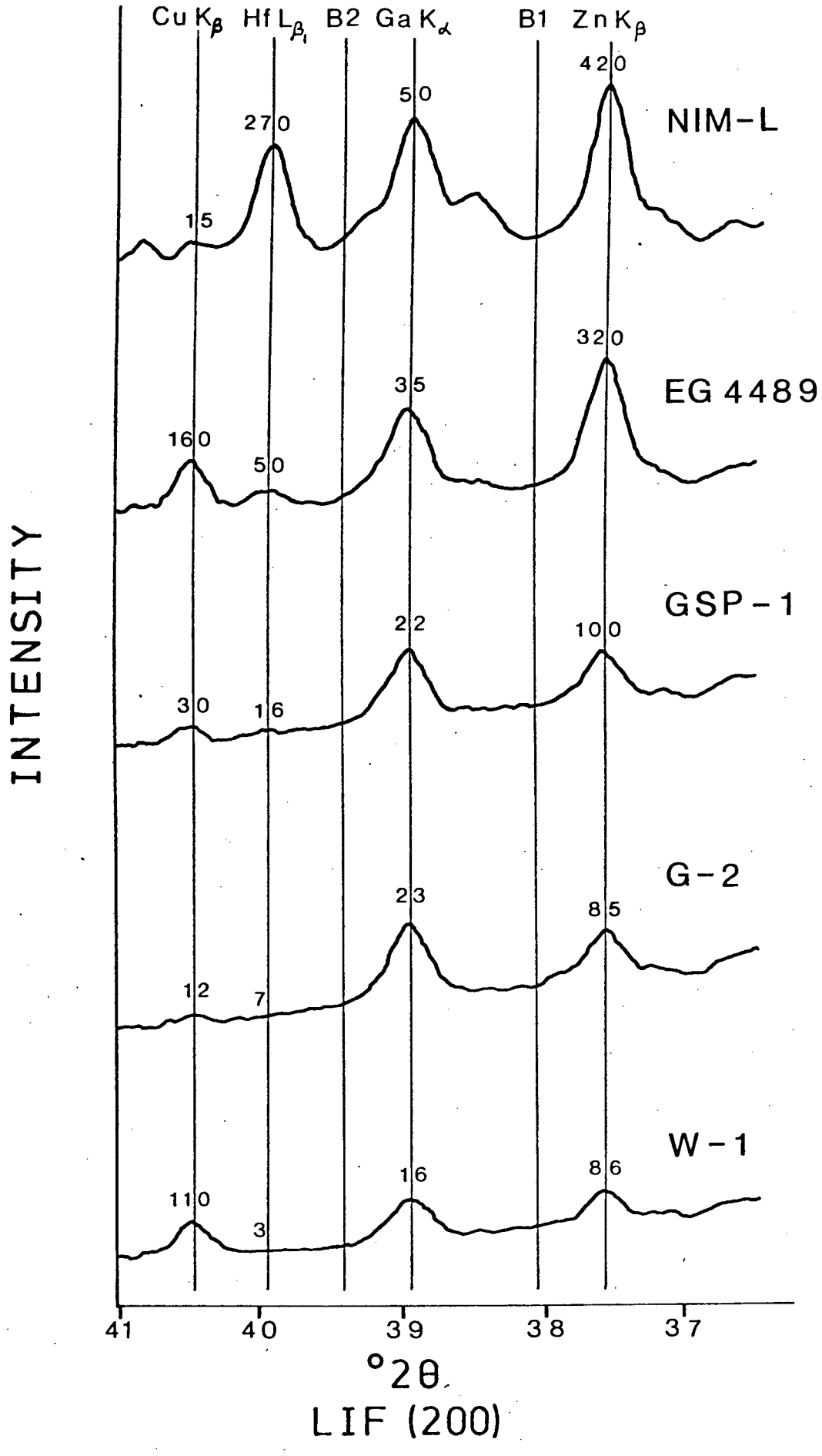

Fig. 2. Wavelength scans showing Zn, Ga, Hf and Cu lines for some rocks with Hf contents from 3-270 ppm. 3 ppm Hf is not detectable by this method. Concentrations of Zn, Ga, Hf and Cu given in ppm.

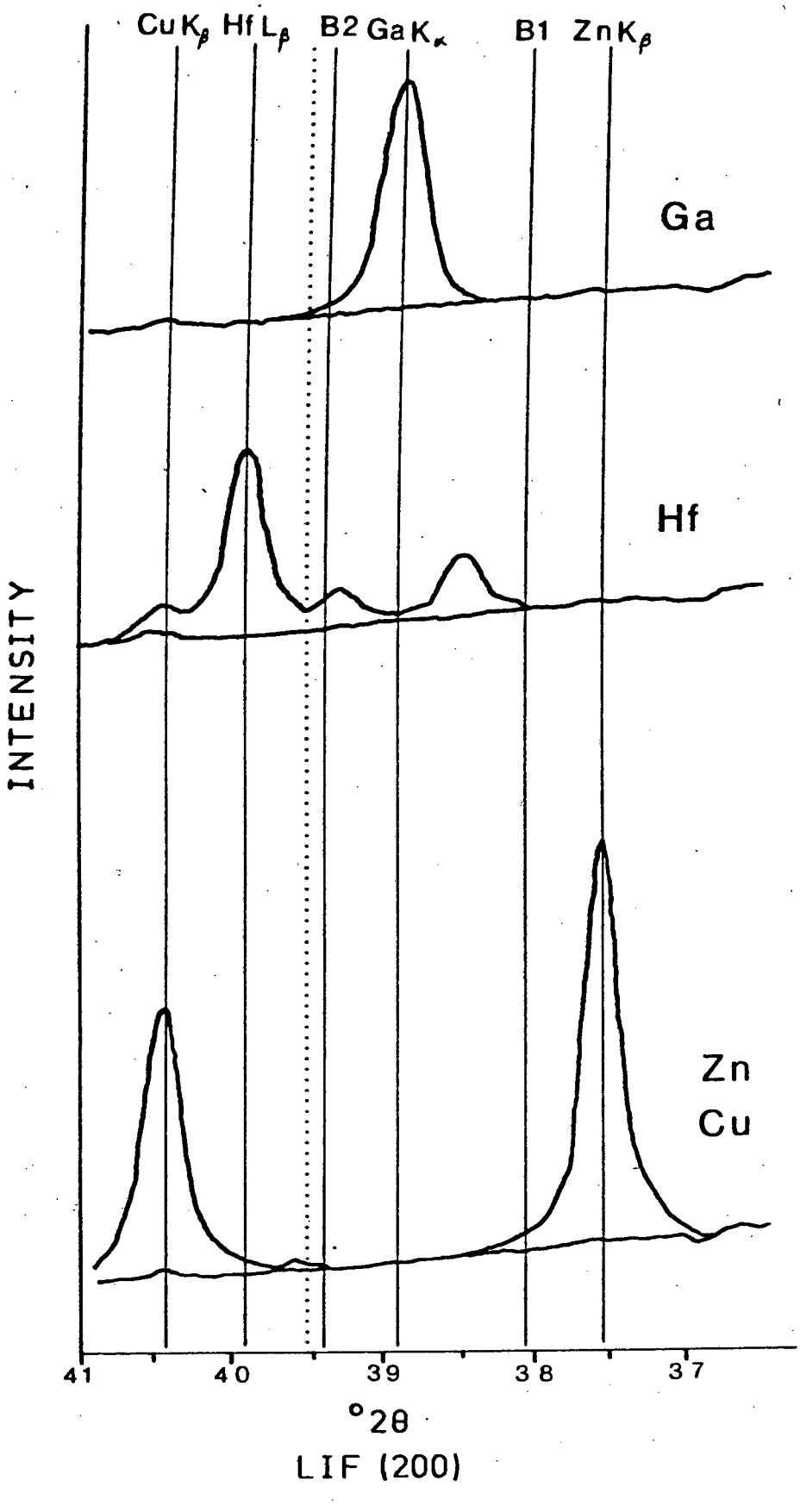

Fig. 3. Wavelength scans of blank samples doped with Ga, Hf, Zn and Cu illustrating potential line interferences.

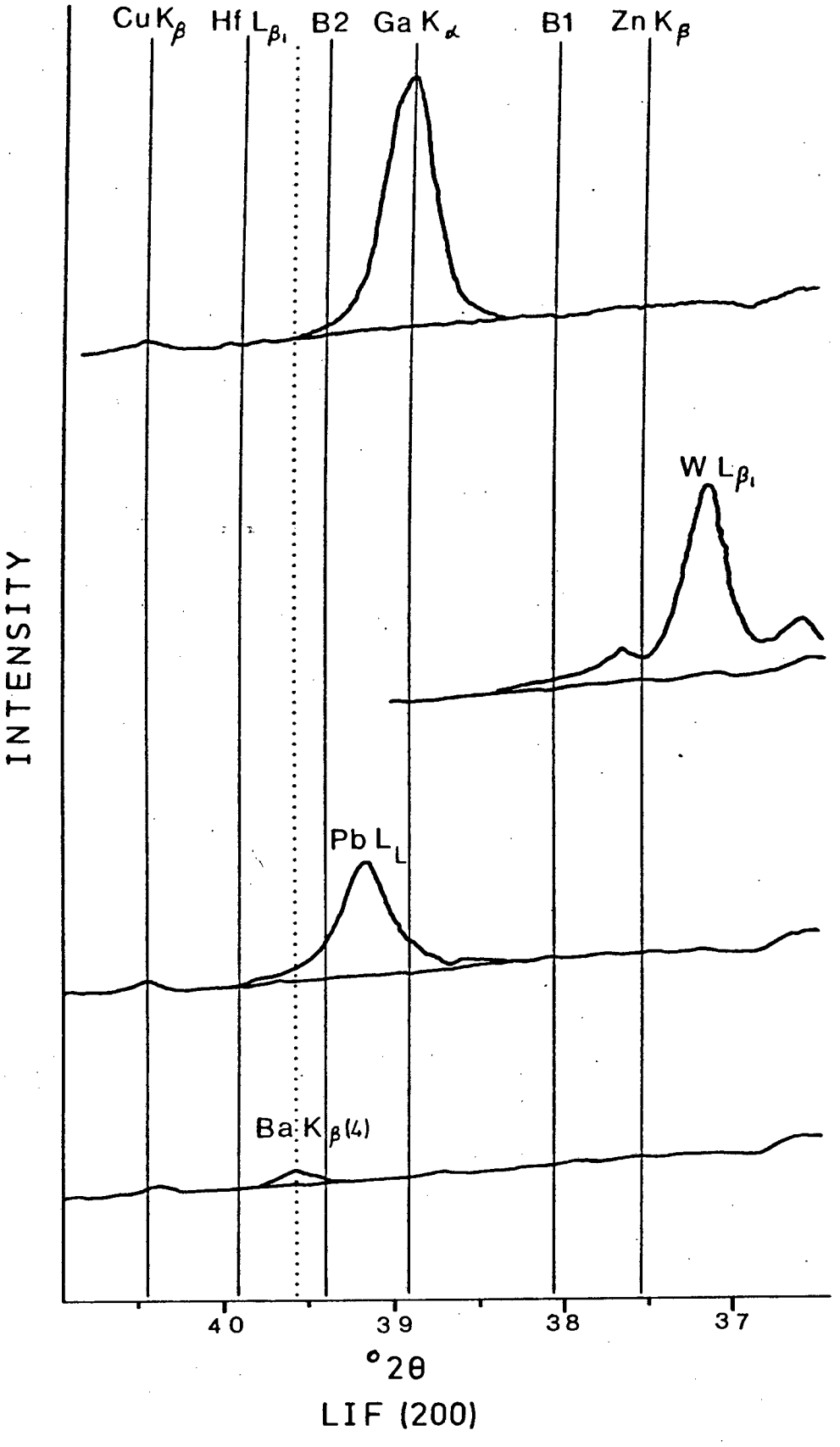

Fig. 4. Wavelength scans of blank samples doped with Ga, W, Pb and Ba illustrating potential line interferences.

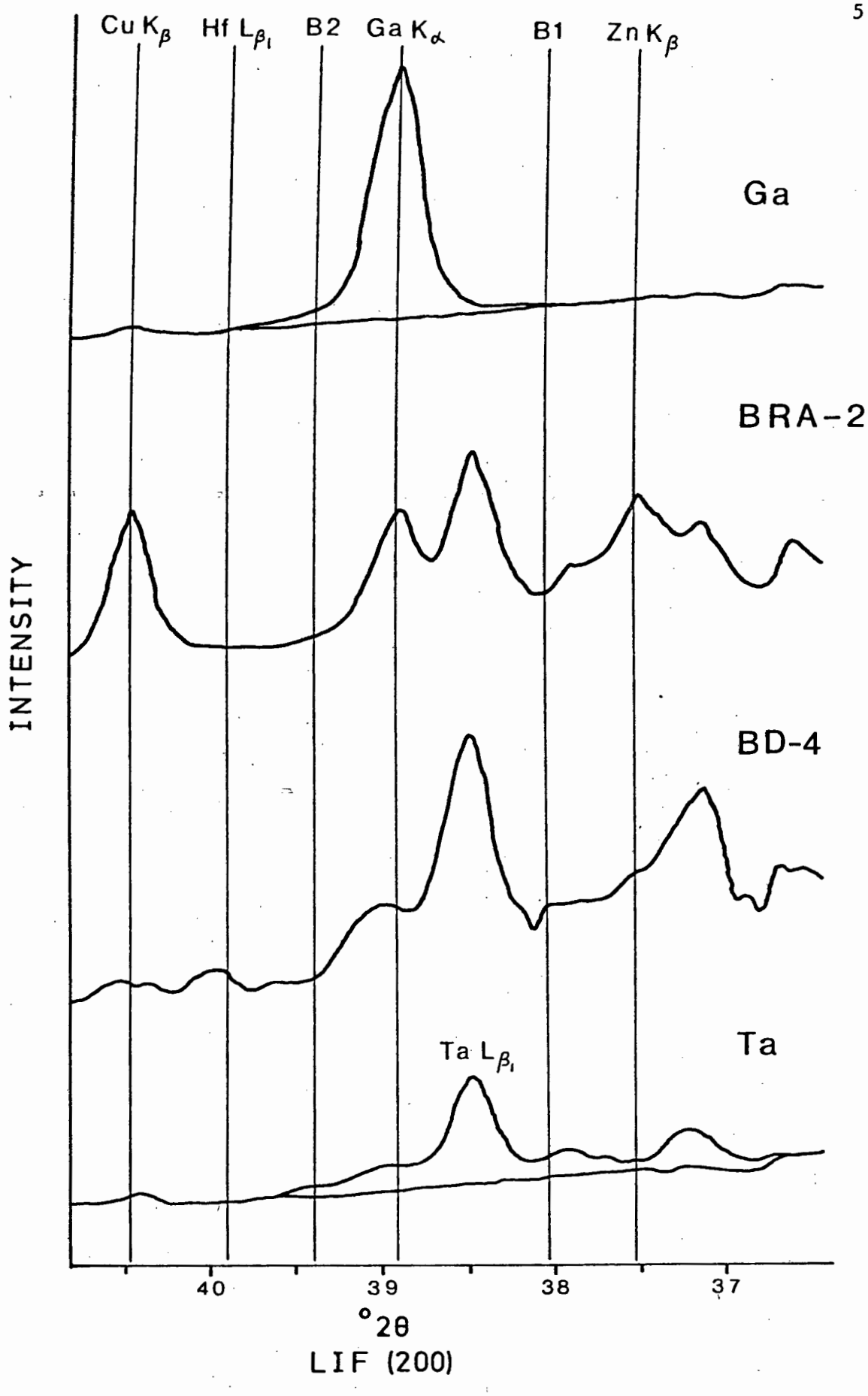

Fig. 5. Wavelength scans of samples containing Ta illustrating potential line interference on Ga. Sample Ta is quartz doped with 230 ppm Ta.

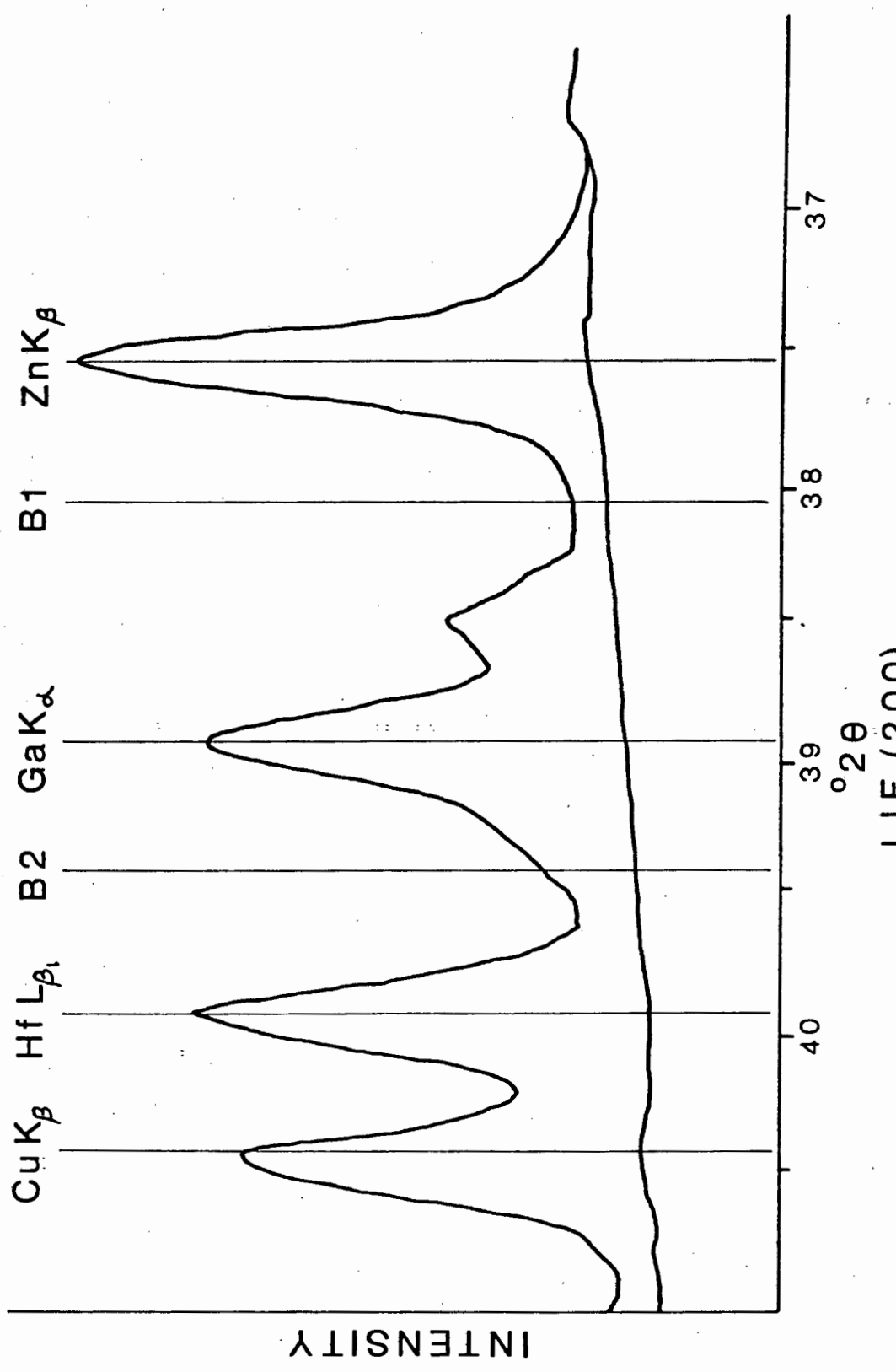

Fig. 6. Wavelength scan of a blank sample doped with Ga, Zn, Hf and Cu illustrating problems in the determination of background.

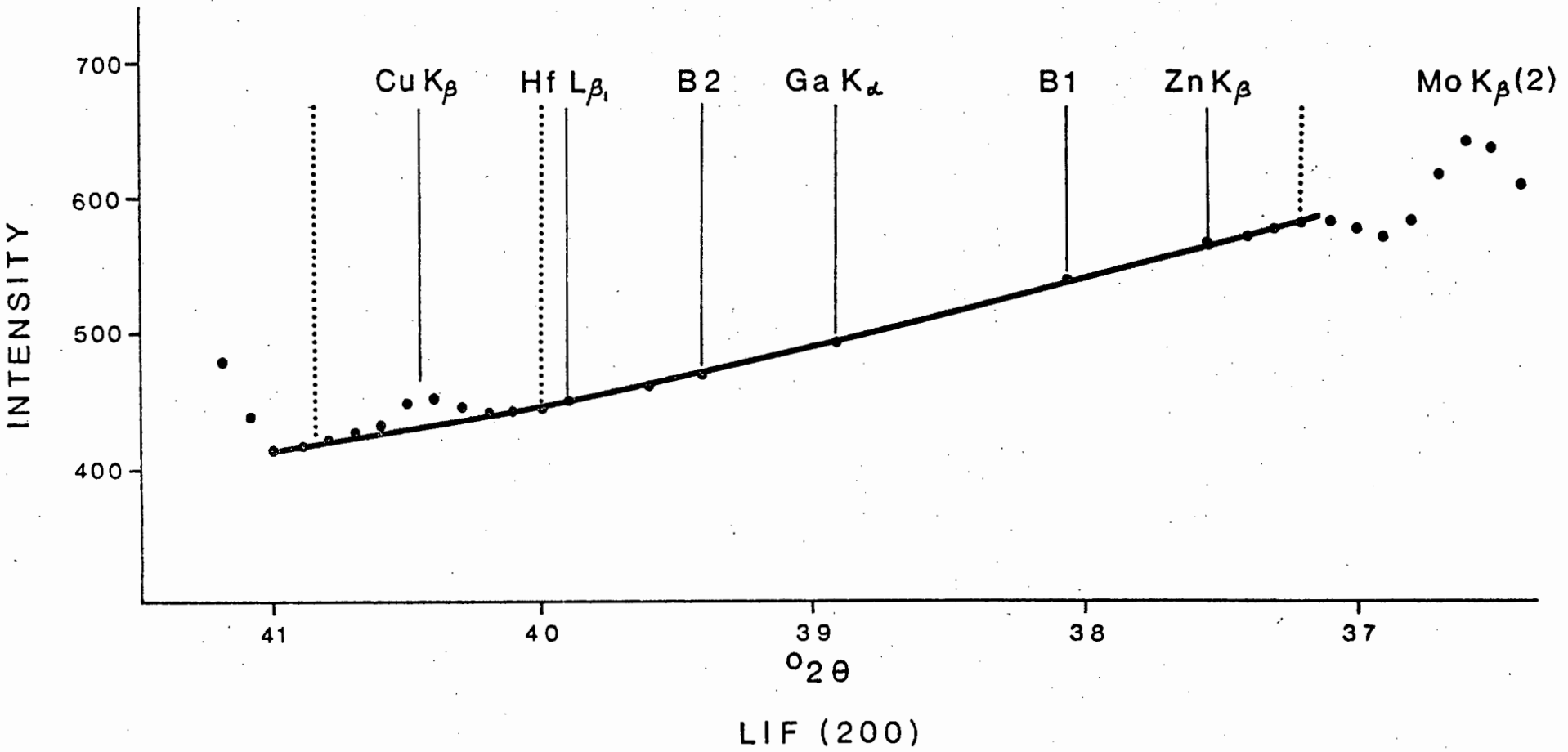

Fig. 7. Point count plot of a blank sample across the Ga wavelength region. Angles at which measurements were made for samples and standards are shown with a solid line. Blanks and interference standards were counted at extra positions shown with dotted lines.

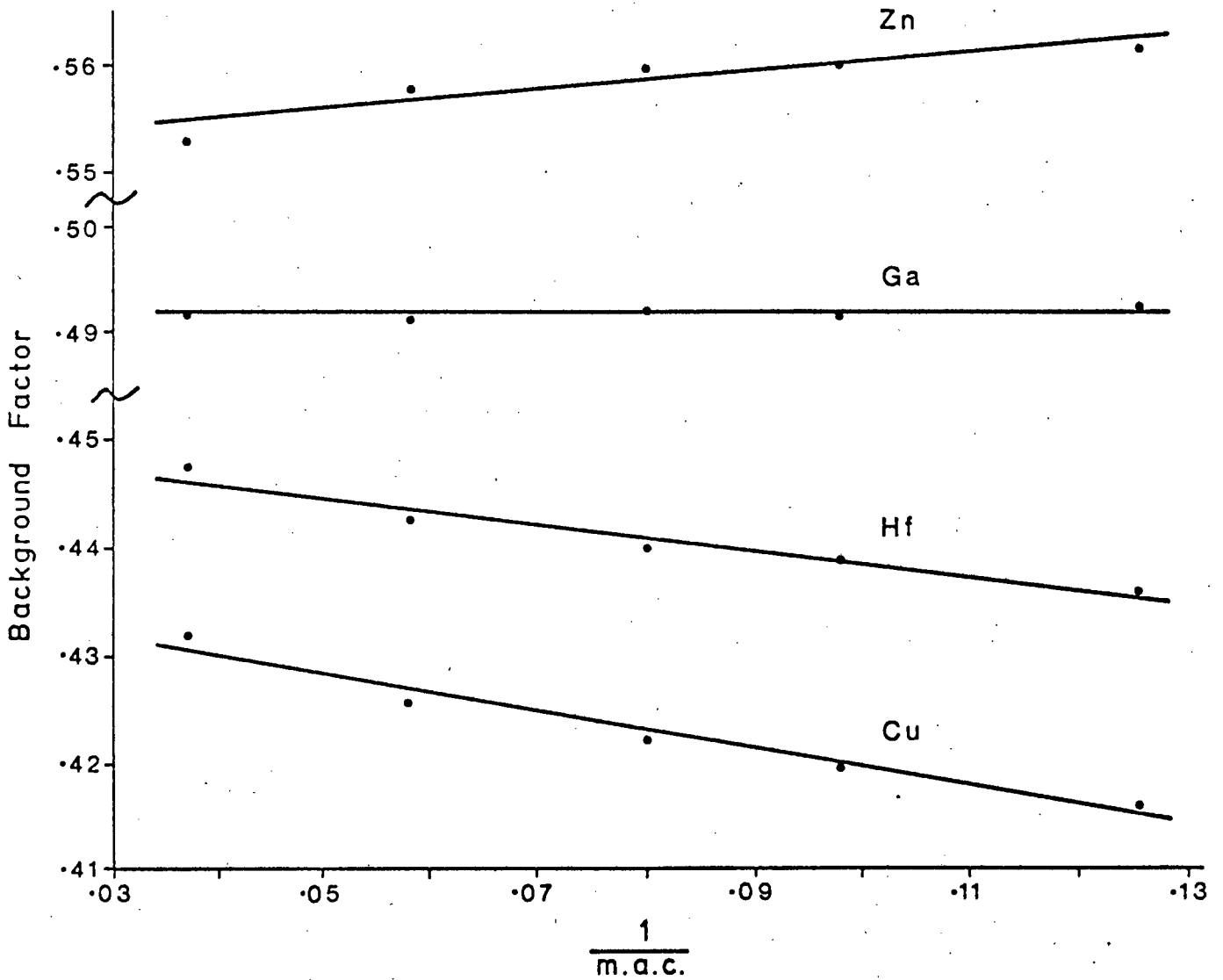

Fig. 8. Background factors of blank samples for Zn, Ga, Hf and Cu plotted against reciprocal mass absorption coefficient.

X-RAY FLUORESCENCE ANALYSIS FOR GALLIUM

GALLIUM RUN, OCTOBER, 1974.

DEAD TIME IS .00000145 SECONDS
NUMBER OF COUNTS ON MO COMPTON PEAK IS 400000.

SAMPLE NO.	GA/AL X10000	GALLIUM PPM	COUNTING ERROR PPM	COUNTING ERROR %	DETECTION LIMIT PPM	COUNTING TIME SEC	ZINC PPM	ZINC DL	HAFNIUM PPM	HAFNIUM DL	COPPER PPM	COPPER DL	N	M.A.C. RB KA	CMPTN SEC
HSS-51	.00	9.99	.17	1.7	.36	1080.	82.2	7.5	.5	4.1	95.0	8.8	4	15.790	39.09
HSS-51	.00	9.87	.17	1.7	.36	1080.	78.9	7.5	.2	4.1	98.7	8.8	4	15.744	38.96
HSS-52B	.00	15.05	.22	1.5	.44	400.	67.9	6.5	3.4	4.9	54.6	7.4	4	10.886	26.12
HSS-52B	.00	15.40	.22	1.5	.44	400.	71.6	6.5	3.4	4.9	60.8	7.5	4	10.999	26.42
ZNGAHFCU B	.00	93.61	.40	.4	.63	400.	845.2	8.9	588.9	6.9	684.7	12.0	5	17.083	42.51
EG 4489	.00	33.65	.20	.6	.37	800.	315.7	7.7	50.1	4.2	160.5	9.1	4	13.998	34.35
G-2 SP	.00	21.09	.16	.8	.31	800.	82.1	6.5	7.9	3.5	12.8	7.5	4	10.607	25.38
BO 33	.00	31.28	.39	1.2	.72	240.	215.8	10.6	16.4	8.0	48.4	12.3	4	15.219	37.56
BO 33	.00	31.82	.39	1.2	.72	240.	219.3	10.5	18.2	8.0	48.9	12.3	4	15.213	37.56
BO 41	.00	24.27	.35	1.4	.66	240.	170.6	9.7	5.7	7.3	10.2	11.3	4	13.353	32.64
BO 41	.00	24.52	.35	1.4	.66	240.	173.4	9.7	4.4	7.3	7.8	11.3	4	13.352	32.64
B-1 SP	.00	16.39	.20	1.2	.39	800.	87.3	8.2	.3	4.4	108.6	9.5	4	15.464	38.22
G-1 SP	.00	18.72	.16	.8	.30	800.	93.2	6.3	5.0	3.3	15.9	7.2	4	10.185	24.26
NIM-G	.00	27.00	.16	.6	.30	800.	44.9	6.2	10.9	3.3	15.8	7.1	4	9.865	23.42
MT PADBURY	.00	2.65	.18	6.8	.41	1400.	.3	7.3	.5	4.5	58.3	8.5	3	21.209	53.42
MT PADBURY	.00	2.41	.18	7.5	.40	1400.	2.8	7.3	-1.4	4.5	52.4	8.5	2	21.032	52.95
PATBAR	.00	1.97	.20	10.2	.45	1400.	3.0	8.1	-1.3	5.0	41.6	9.5	2	24.121	61.12
PATBAR	.00	1.94	.20	10.4	.45	1400.	3.3	8.1	1.8	5.1	35.8	9.5	3	24.169	61.25
ZNGAHFCU B	.00	92.99	.39	.4	.63	400.	835.2	8.9	585.7	6.9	670.6	12.1	5	17.041	42.40
HSS-131	.00	4.06	.13	3.2	.29	1400.	82.9	5.2	.0	3.2	29.9	6.0	3	13.188	32.20

Fig. 9. Example of output from the computer program calculating element concentrations and mass absorption coefficients.

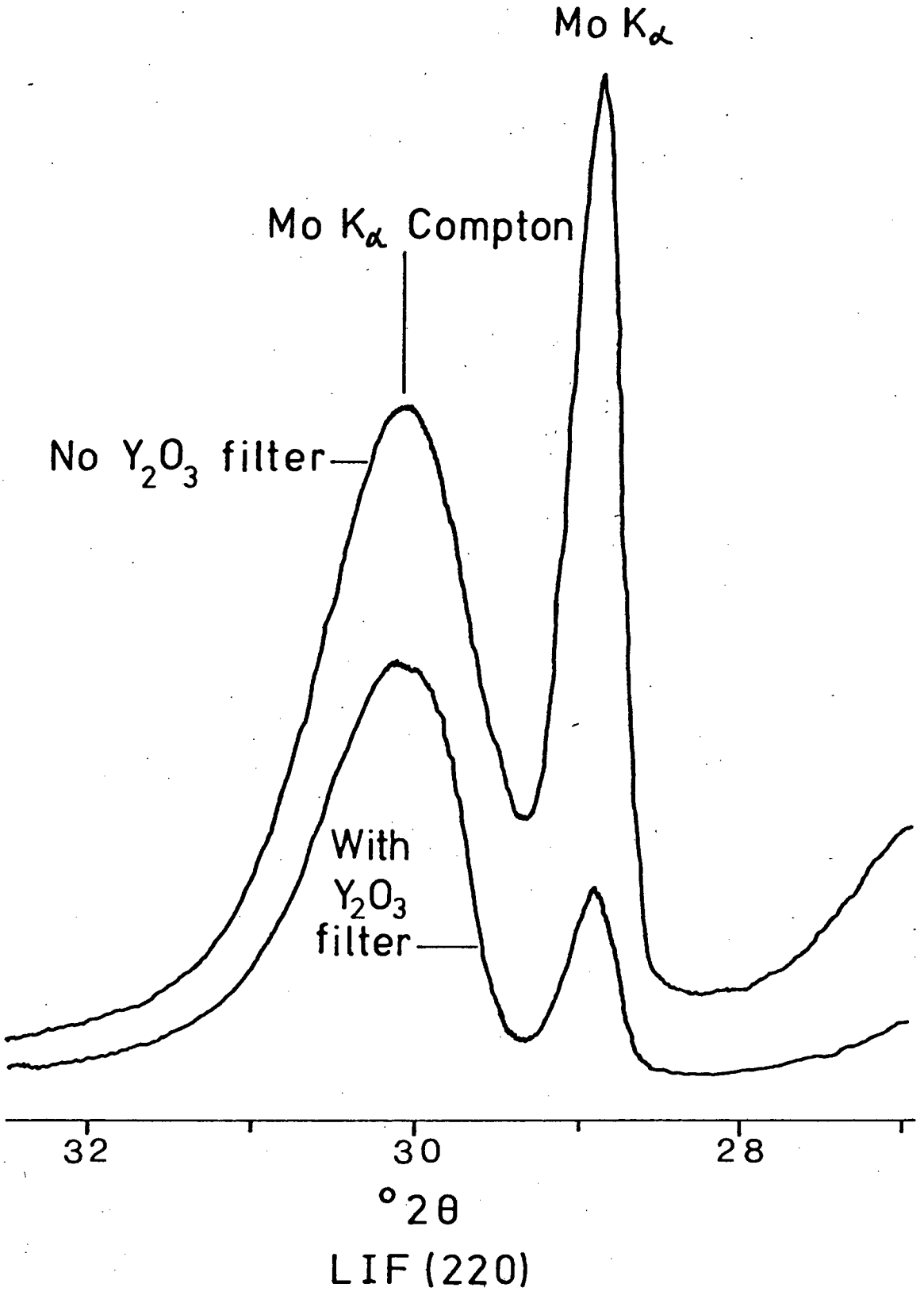

Fig. 10. Wavelength scan showing Mo Kα tube line and associated Compton peak. The sample is quartz and the analysing crystal LiF(220). Note the effect of the Y_2O_3 filter in reducing the Mo Kα intensity relative to that of the Compton peak.

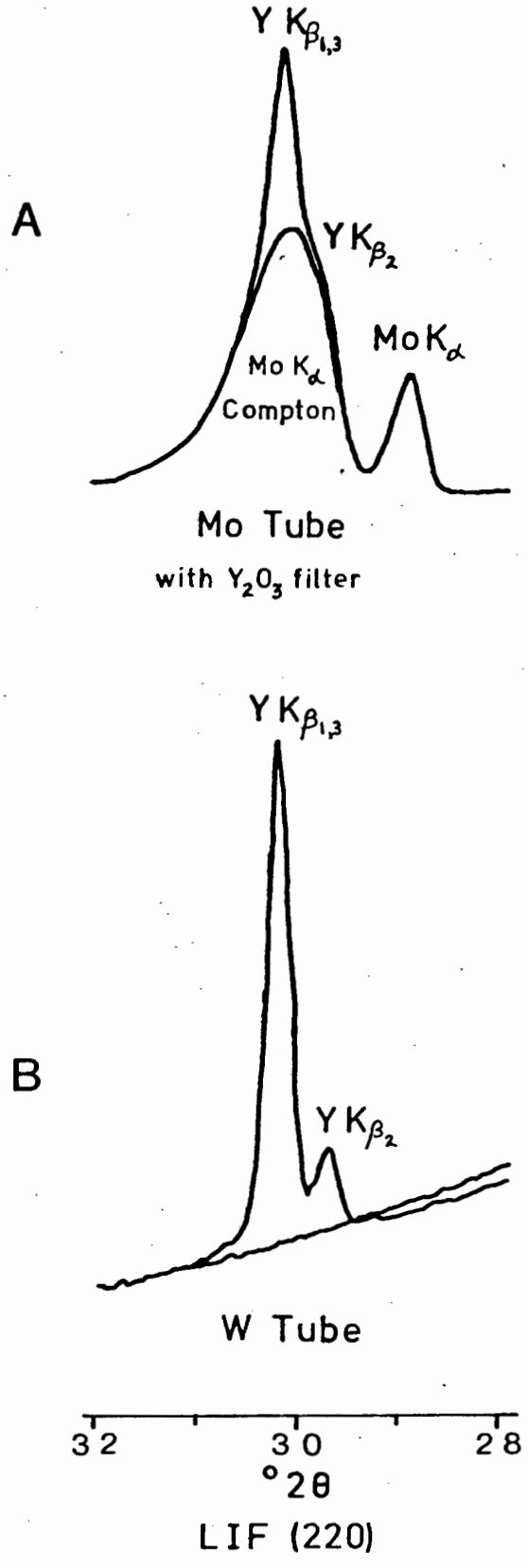

Fig. 11. Wavelength scans illustrating interference of the Y Kβ lines on the Mo Kα Compton peak. Samples are quartz, and quartz doped with 2000 ppm Y.

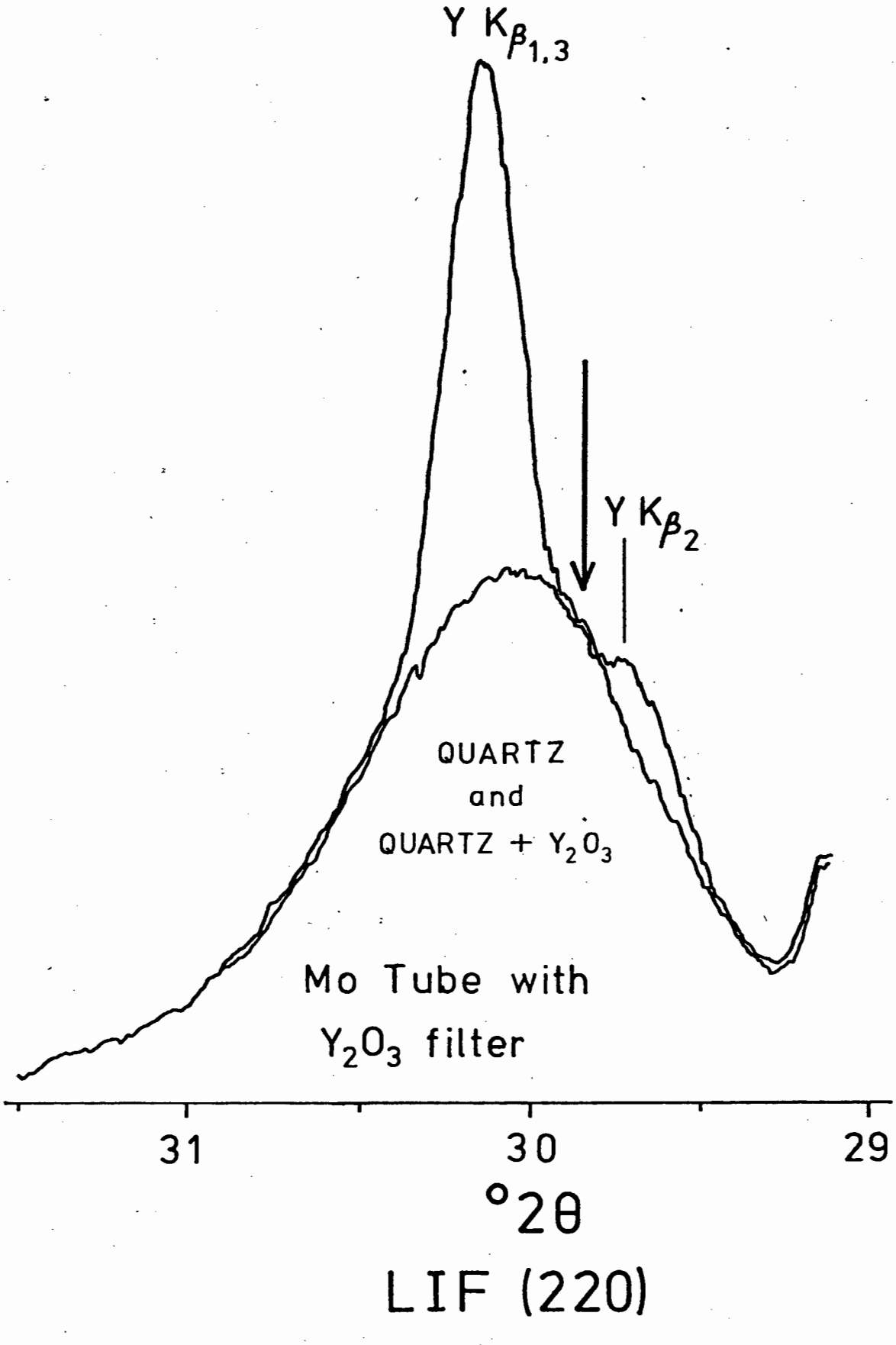

Fig. 12. An expanded wavelength scan of Fig. 11(A). The arrow indicates the angle at which the Compton peak intensity is measured for the determination of mass absorption coefficients.

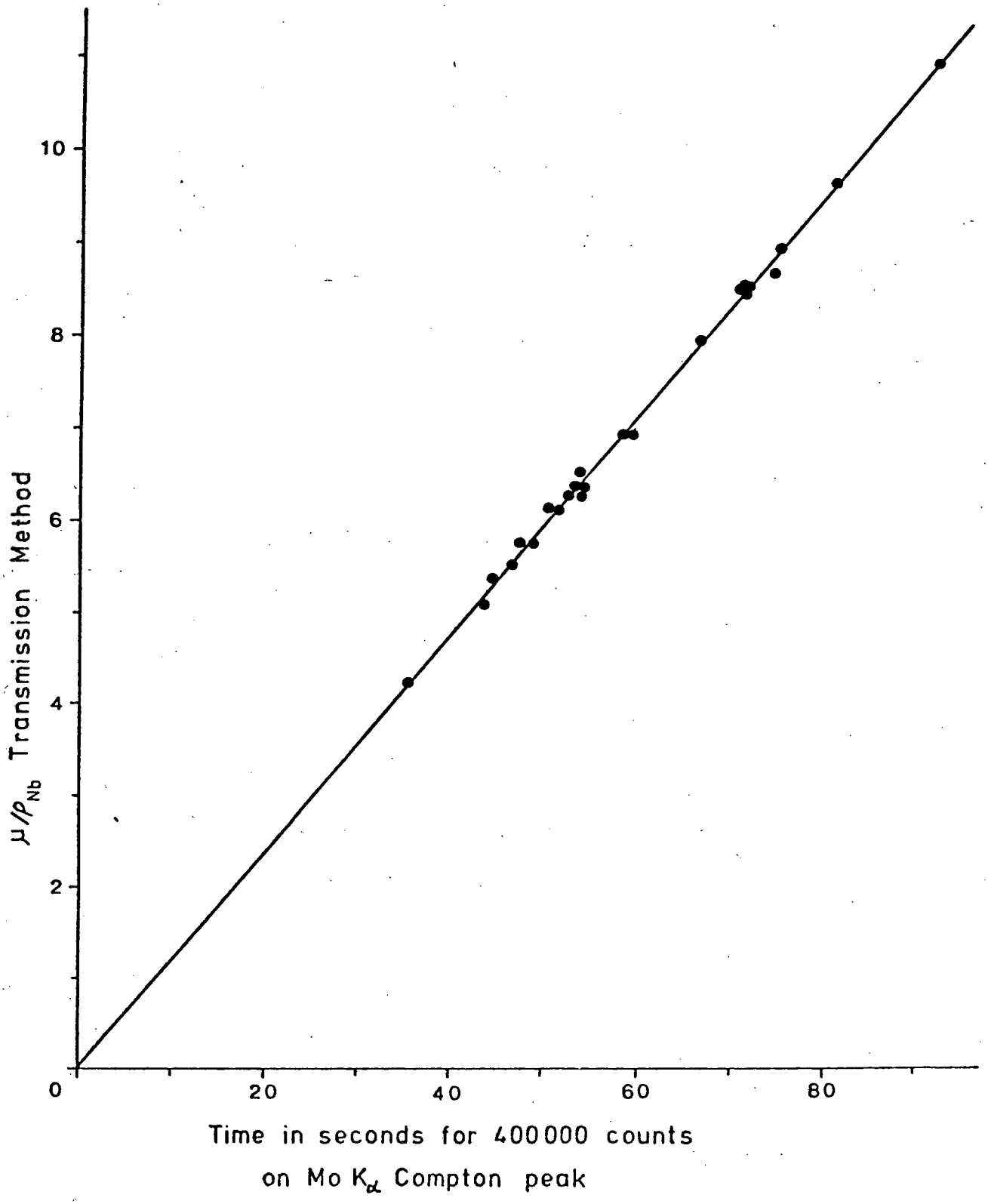

Fig. 13. Plot of the m.a.c. at Nb Kα measured by the transmission method against time required to measure a fixed number of counts on the Mo Kα Compton peak using a Y_2O_3 filter. Intensity was measured at an angle of $-0.15^{\circ}2\theta$ from the Compton peak maximum with a LiF(220) crystal.

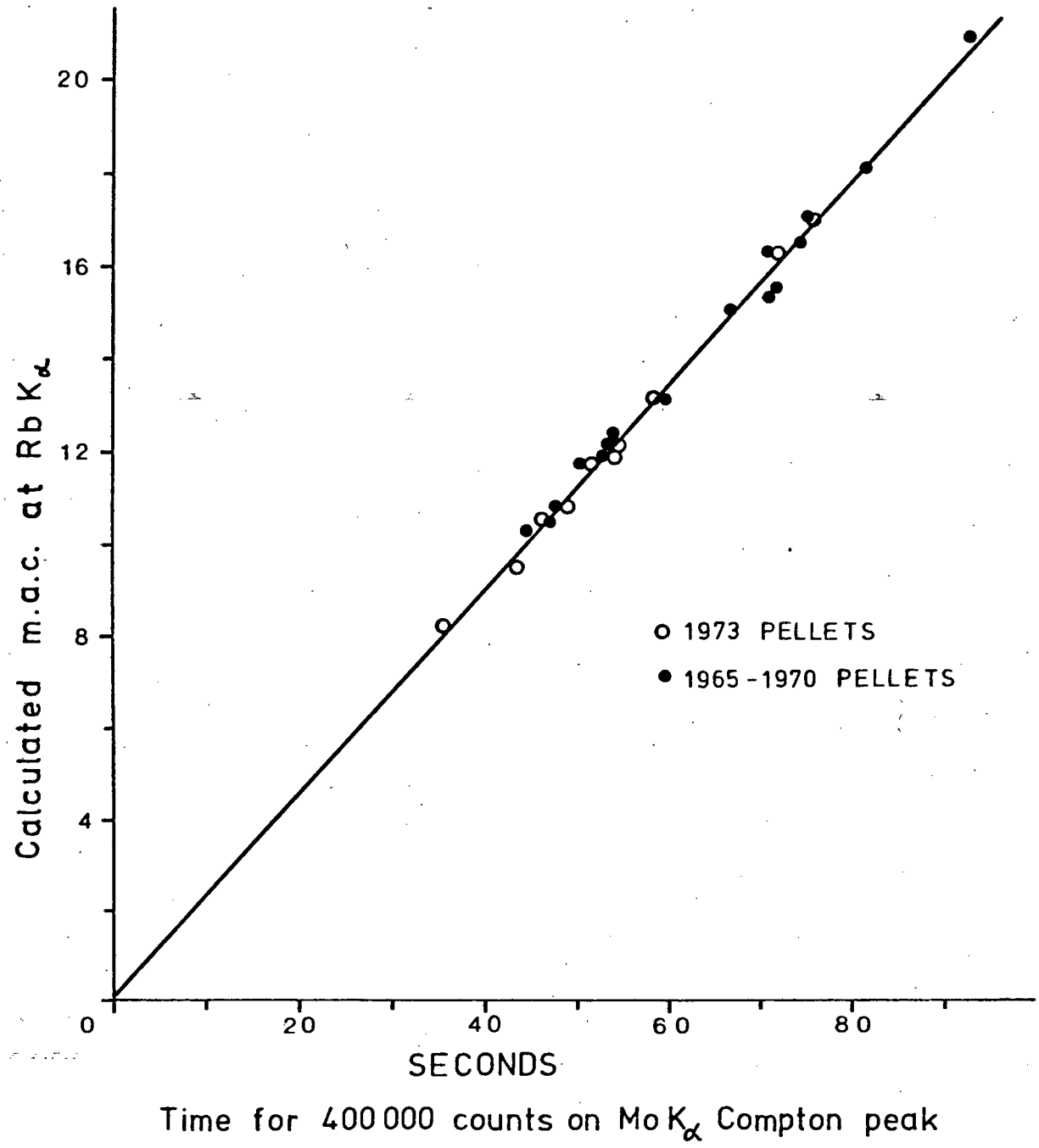

Fig. 14. Plot of m.a.c's for Rb Kα calculated from Philips tables versus Mo Kα Compton time.

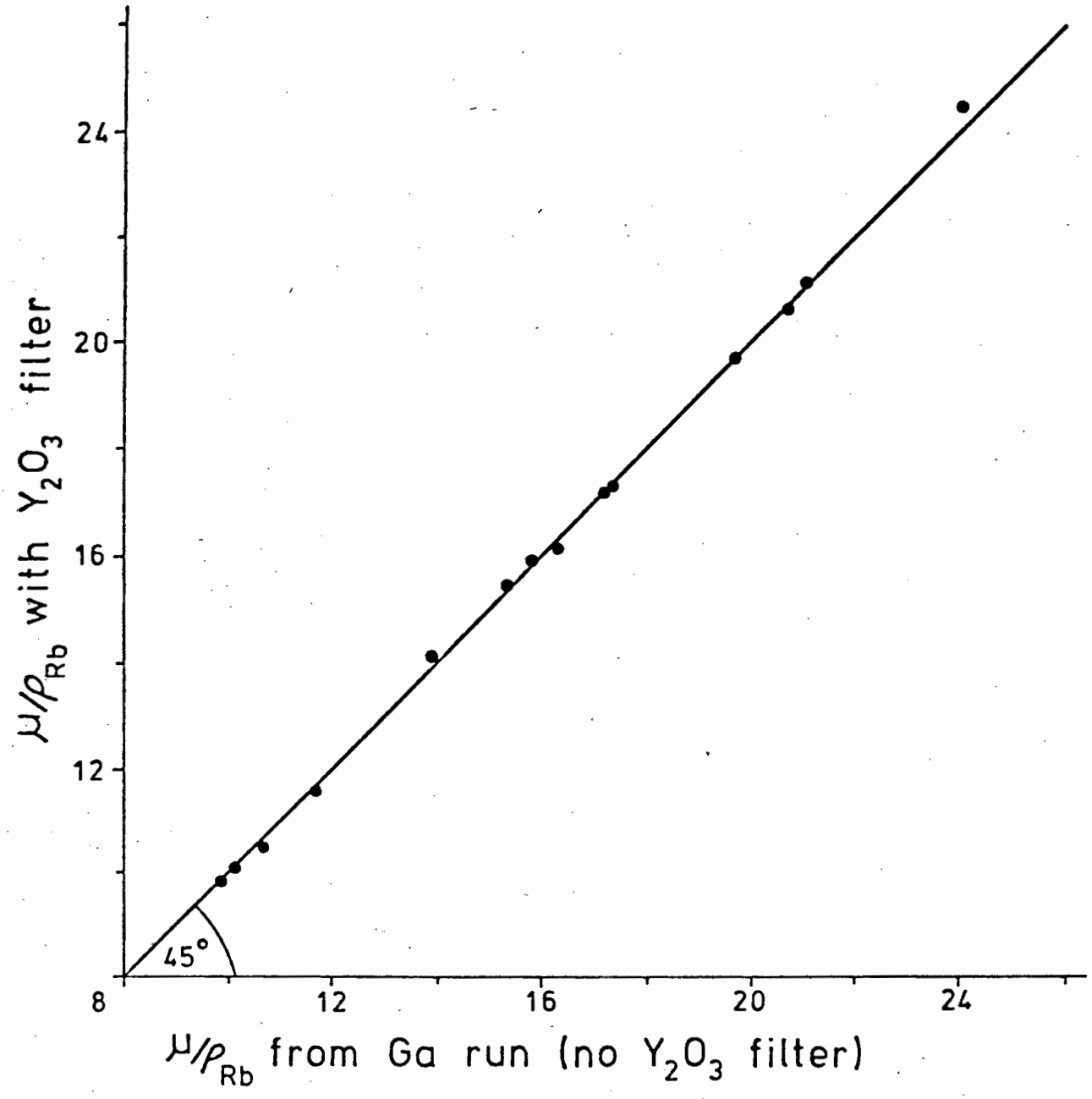

Fig. 15. Plot comparing m.a.c's measured by the Mo Kα Compton peak method with and without an Y_2O_3 filter.

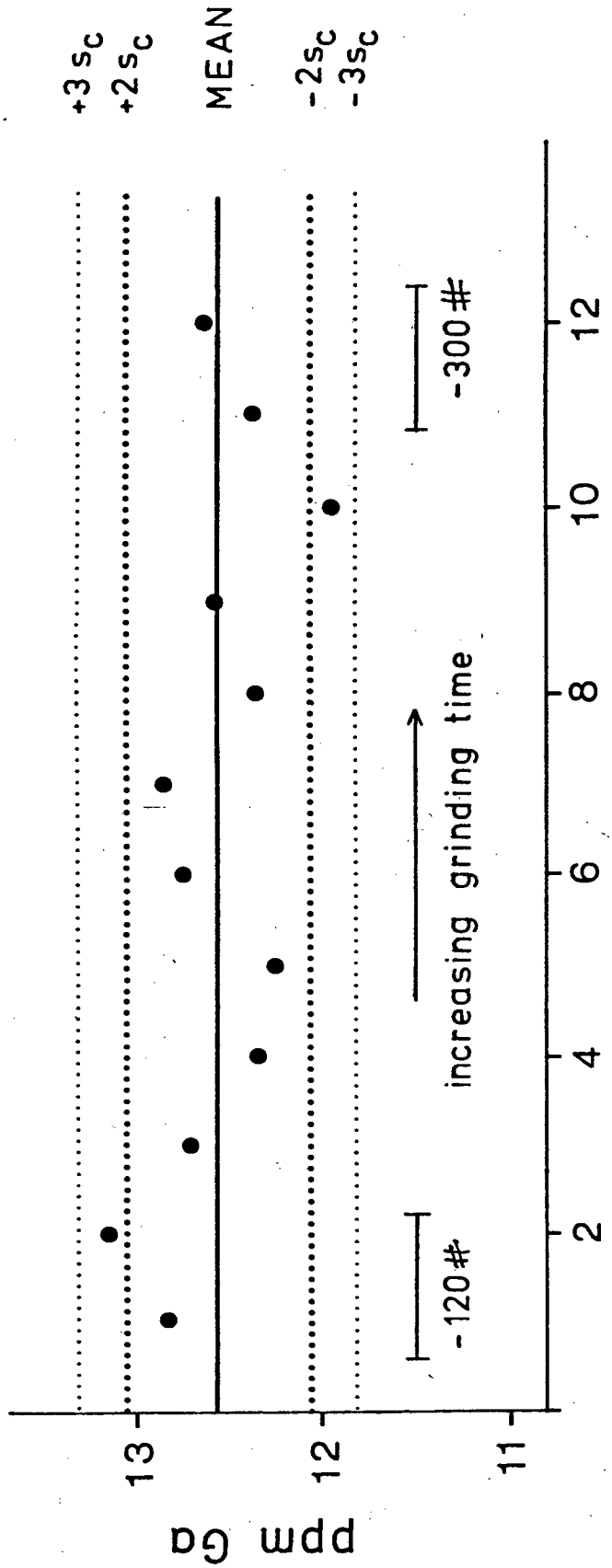

Fig. 16. Plot indicating the effect of particle size on measured Ga concentration. Twelve 4g aliquots of -120 # powder of OK 227, a gabbro-picrite (olivine cumulate), were ground in an automatic agate mortar for times varying from 15 to 60 minutes, after which the finest sample was -300 #. The mean value of the measured Ga contents is indicated together with $2s_c$ and $3s_c$ limits due to counting statistics alone.

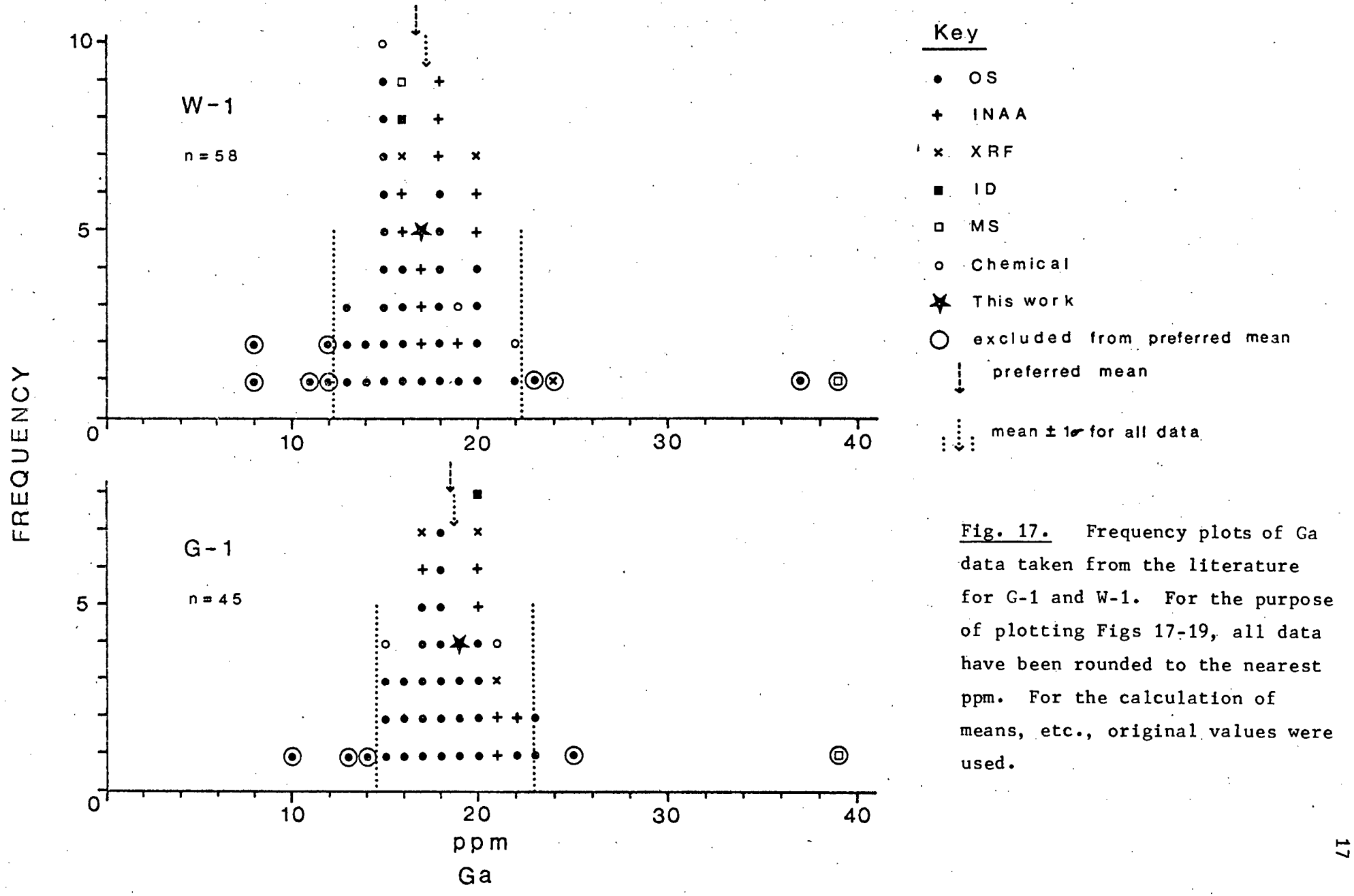

Fig. 17. Frequency plots of Ga data taken from the literature for G-1 and W-1. For the purpose of plotting Figs 17-19, all data have been rounded to the nearest ppm. For the calculation of means, etc., original values were used.

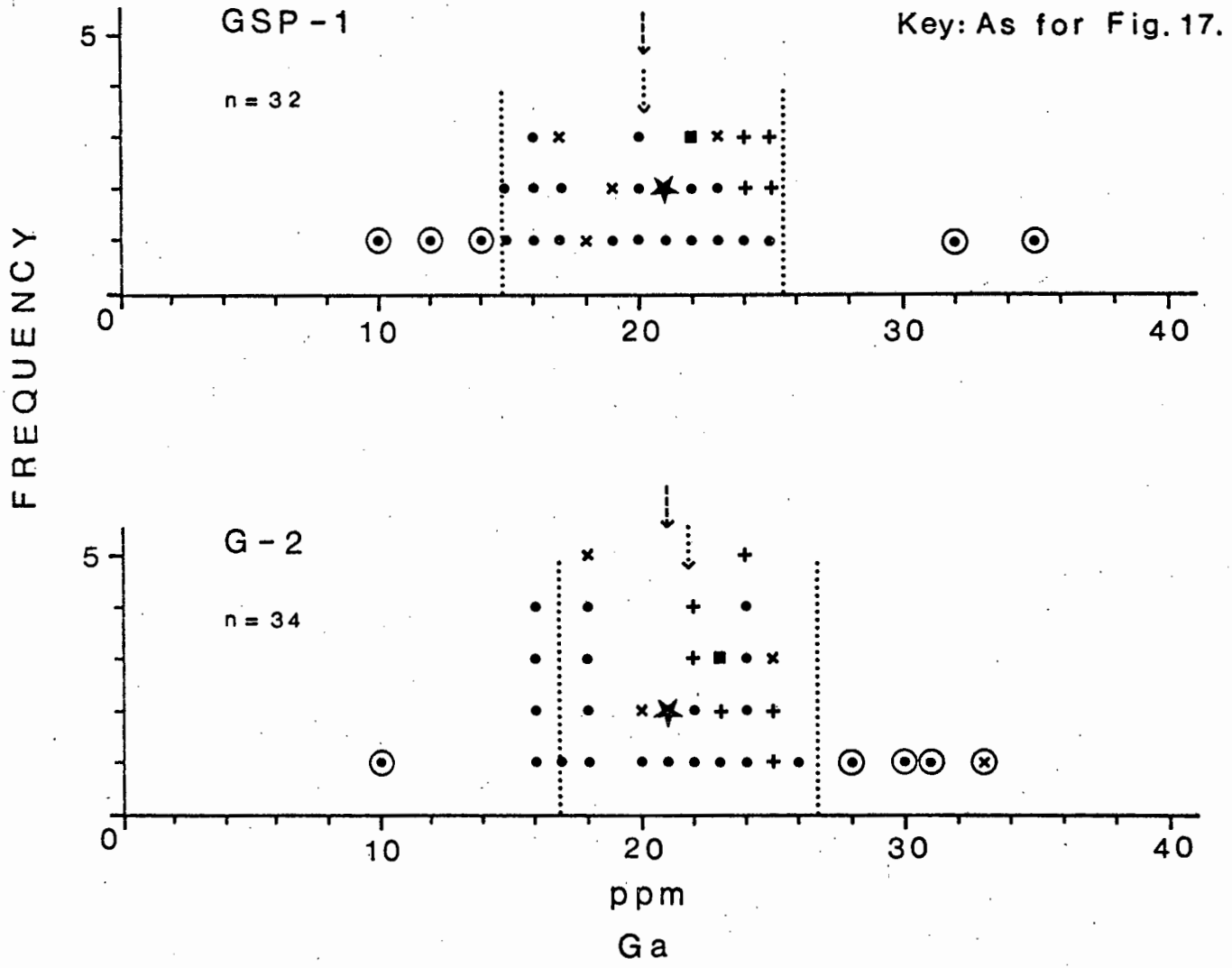

Fig. 18. Frequency plots of Ga data taken from the literature for G-2 and GSP-1.

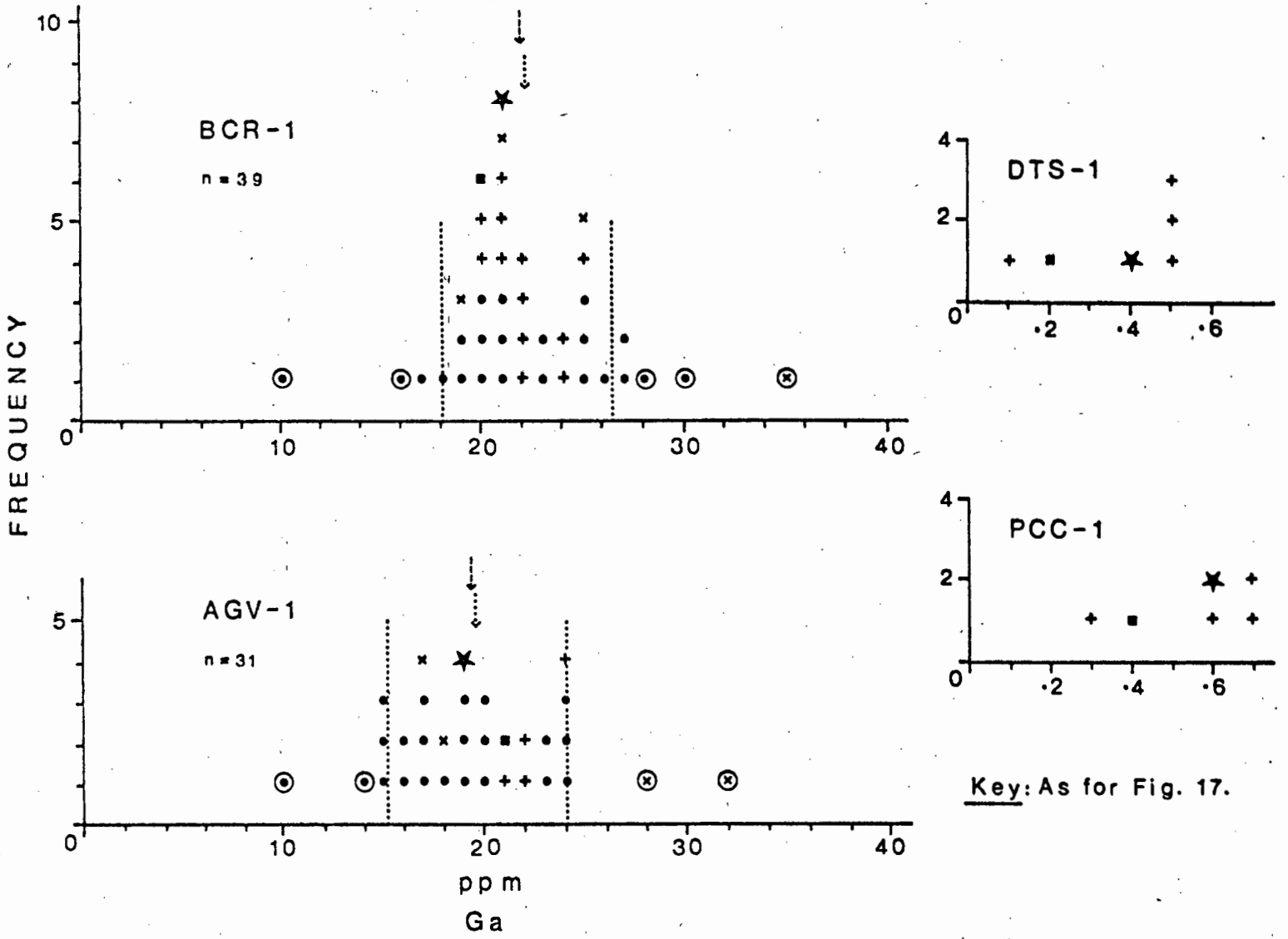

Fig. 19. Frequency plots of Ga data taken from the literature for AGV-1, BCR-1, PCC-1 and DTS-1. As discussed in the text, only data ⩽ 1 ppm Ga have been accepted for PCC-1 and DTS-1.

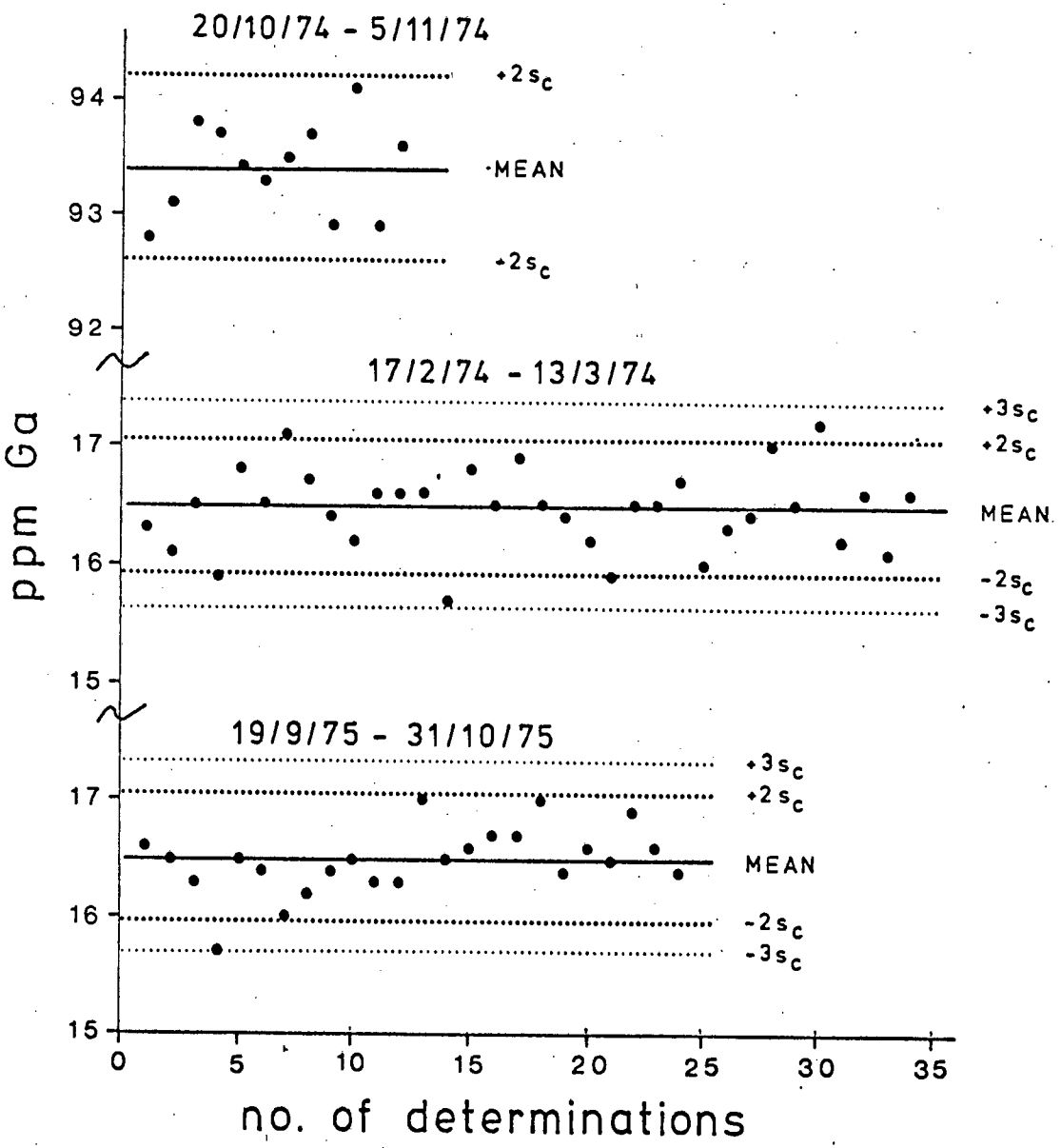

Fig. 20. Plots showing the precision of various analytical runs for the determination of Ga. A monitor sample was analysed repeatedly during each run, and the results are plotted for three separate runs. Error limits are those expected from counting statistics alone.

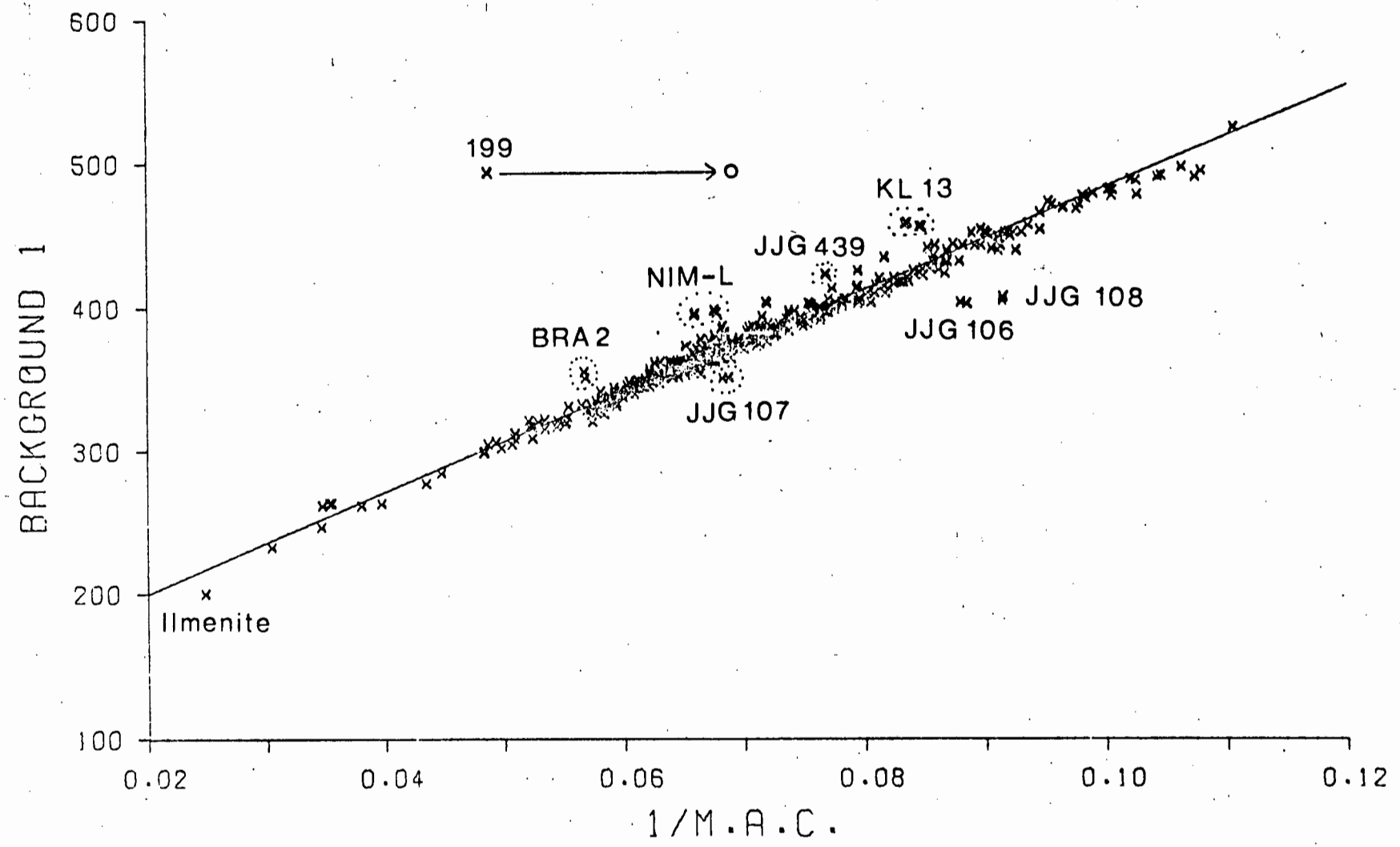

FIG. 21. Corrected background intensity at B1 plotted against reciprocal m.a.c. for a typical analytical run. M.a.c. for NIM-L determined by the transmission method at Rb Kα.

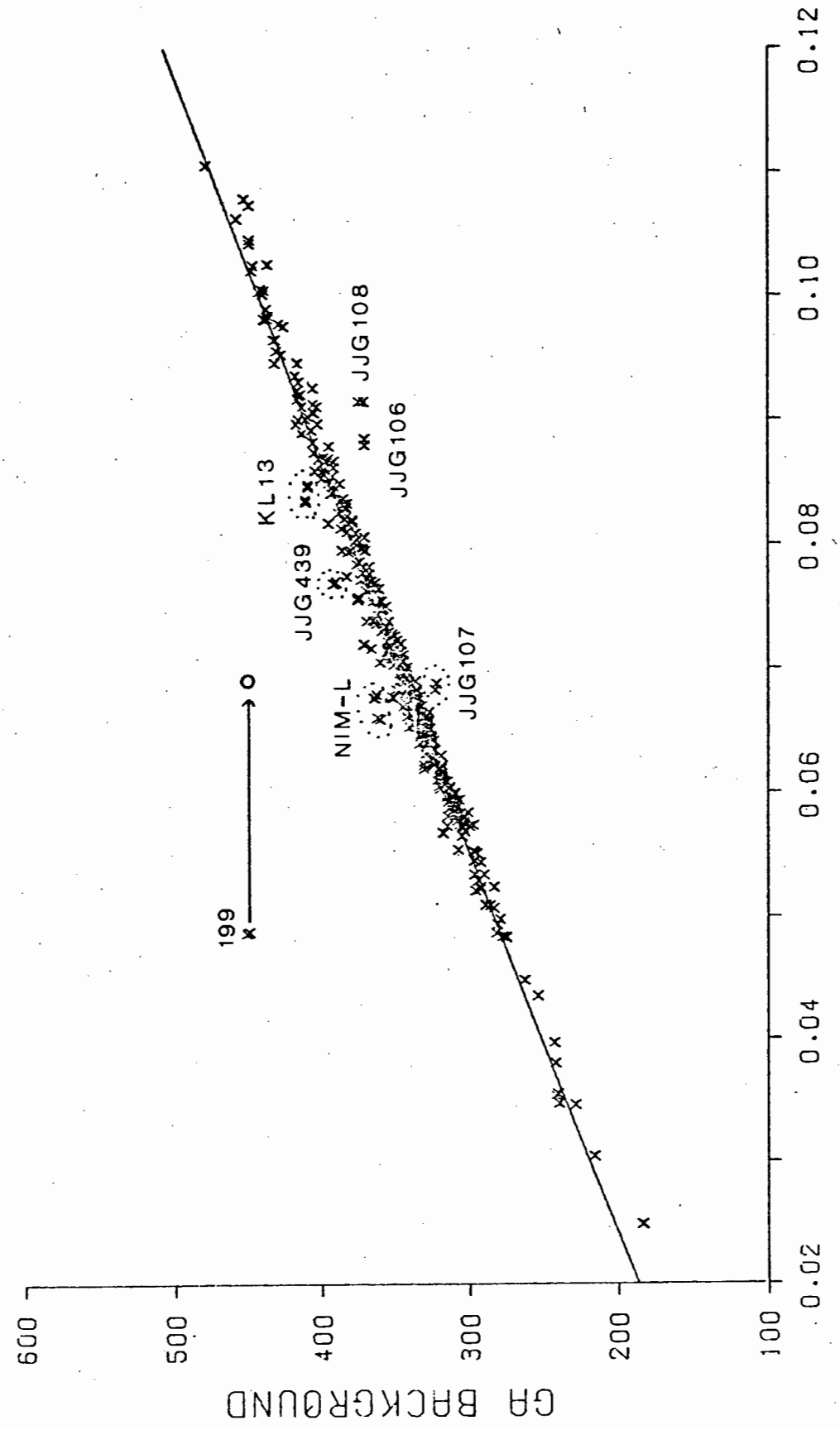

FIG. 22. Calculated background intensity at Ga Kα plotted against reciprocal m.a.c. Same run as Fig. 21.

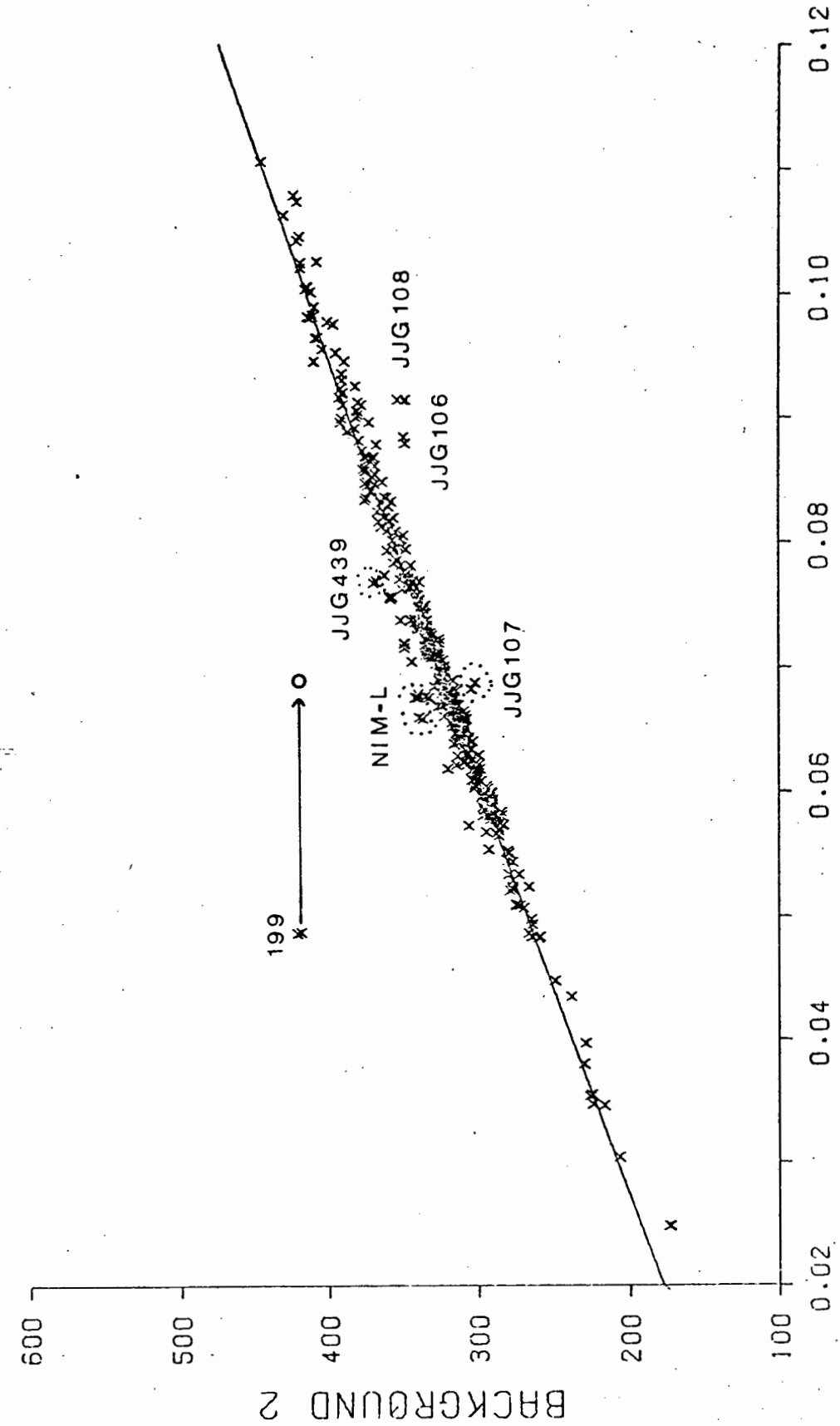

FIG. 23. Corrected background intensity at B2 plotted against reciprocal m.a.c. Same run as Fig. 21.

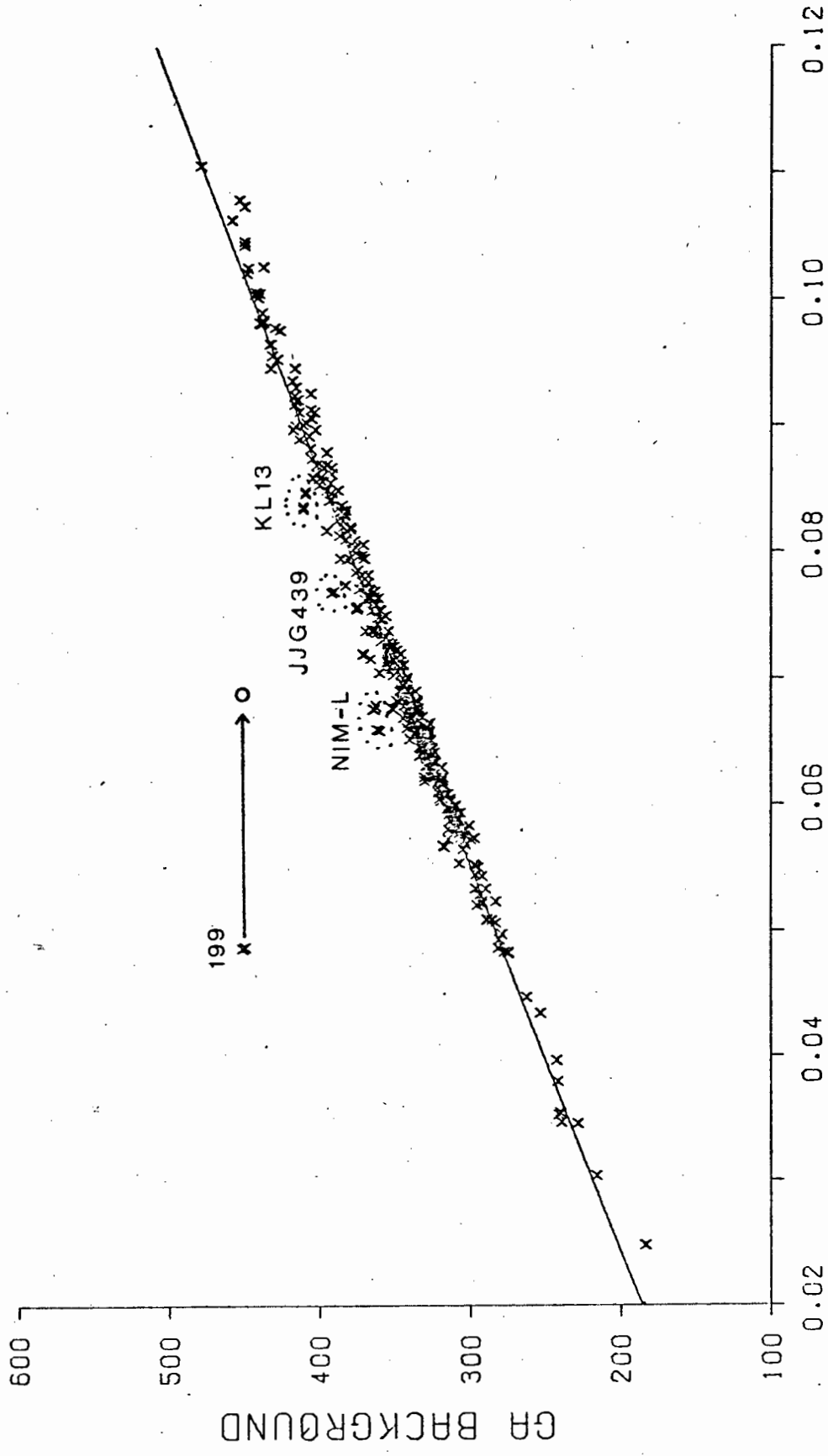

FIG. 24. Calculated background intensity at Ga Kα plotted against reciprocal m.a.c. after correction of m.a.c. for JJG 106, 107 and 108. Same run as Fig. 21.

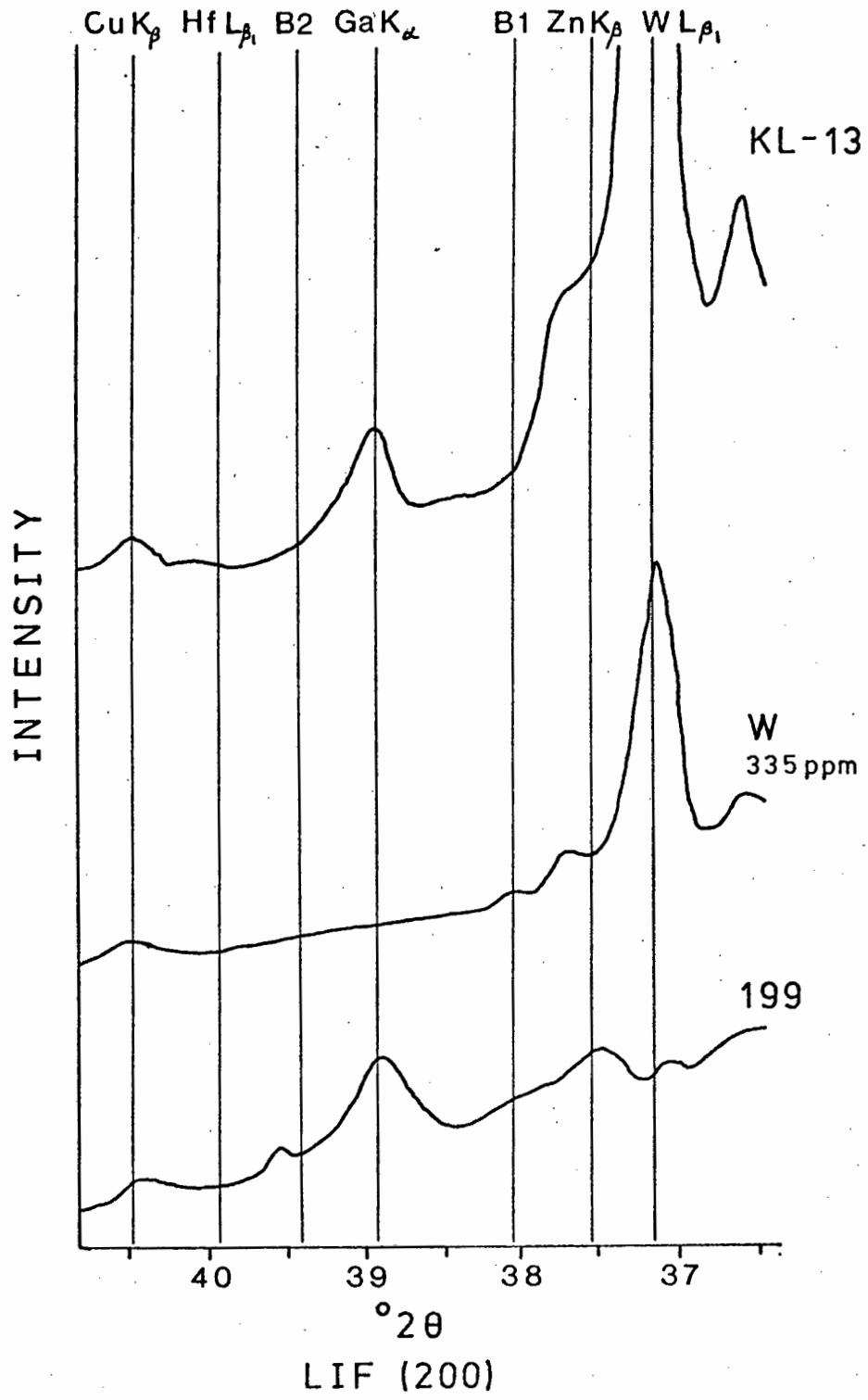

Fig. 25. Wavelength scans for KL-13, phlogopite 199 and a W-doped blank.

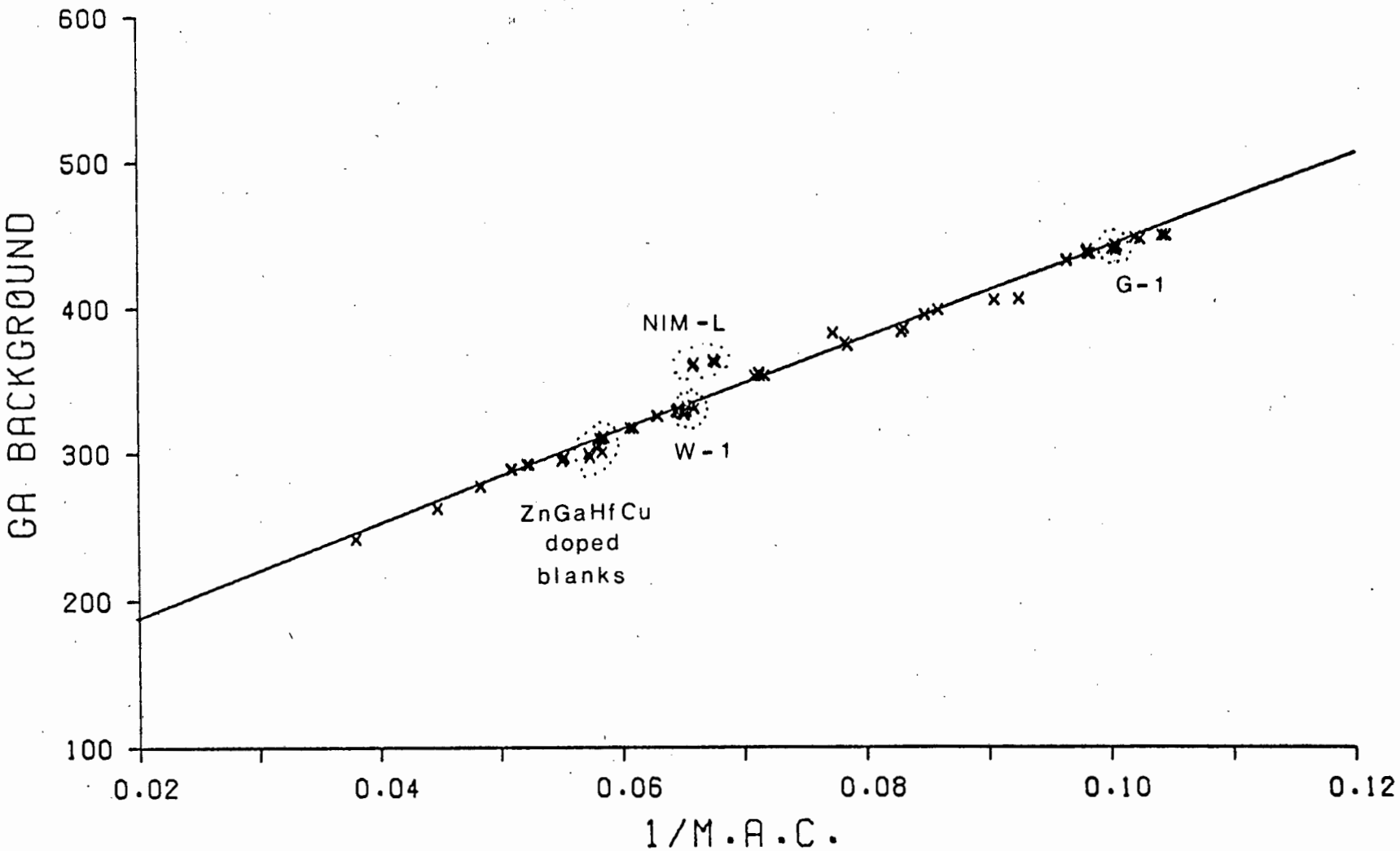

FIG. 26. Background intensities at Ga Kα of some standard rocks, meteorites and doped blanks plotted against reciprocal m.a.c.

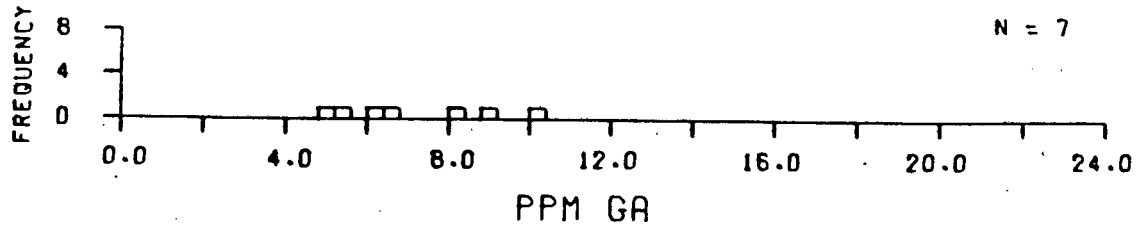

MESOSIDERITES.

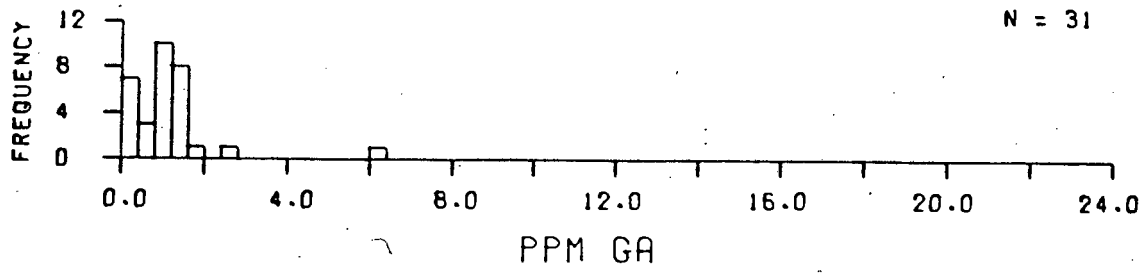

ACHONDRITES.

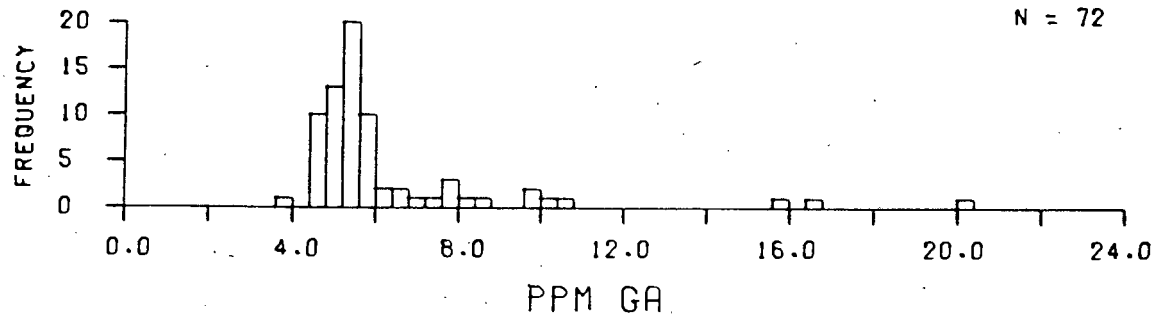

CHONDRITES.

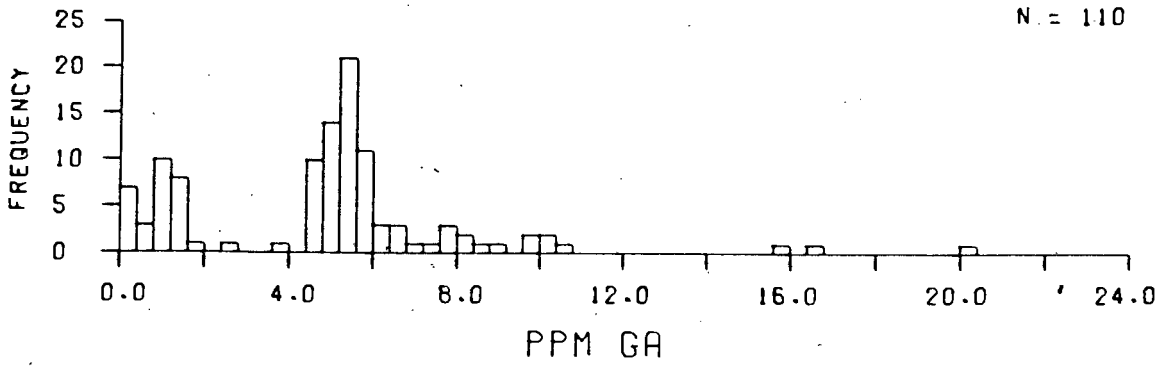

ALL METEORITES.

FIG. 27. METEORITES.

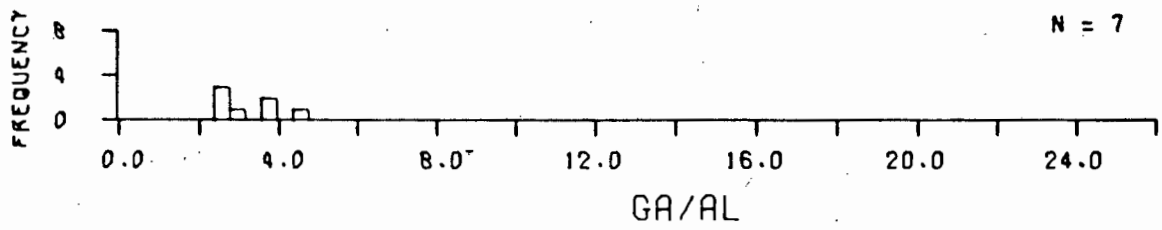

MESØSIDERITES.

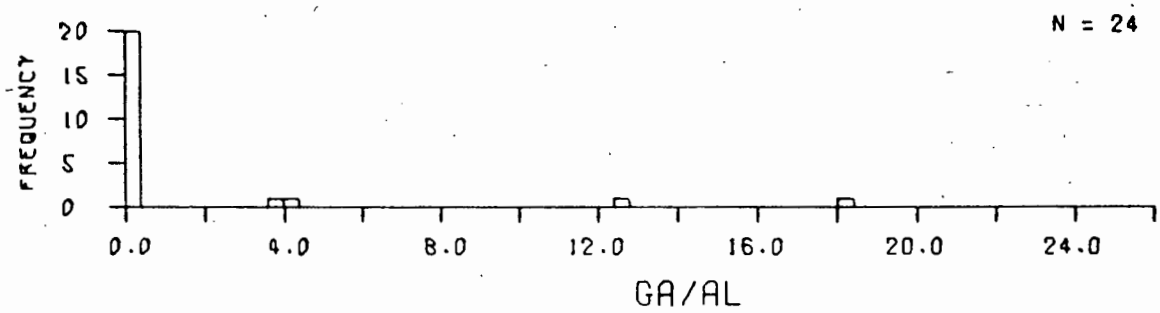

ACHØNDRITES.

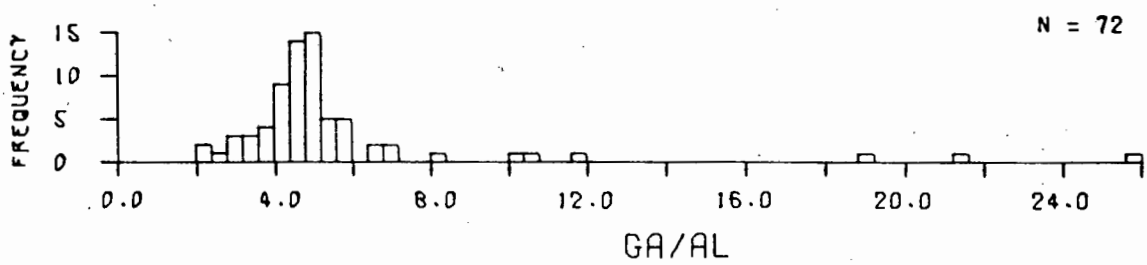

CHØNDRITES.

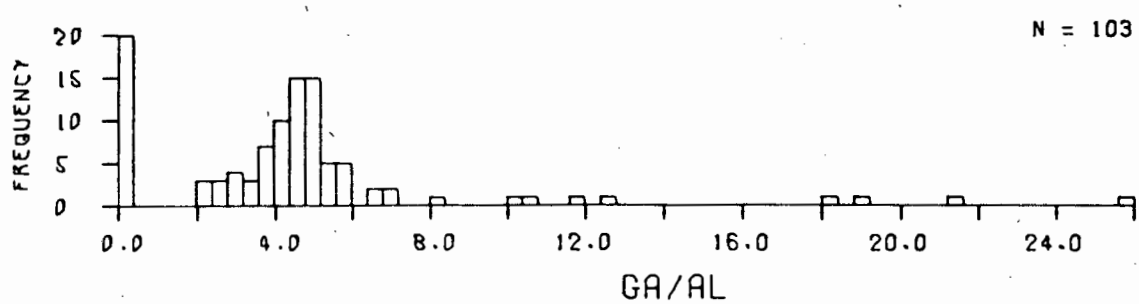

ALL METEØRITES.

FIG. 28. METEØRITES.

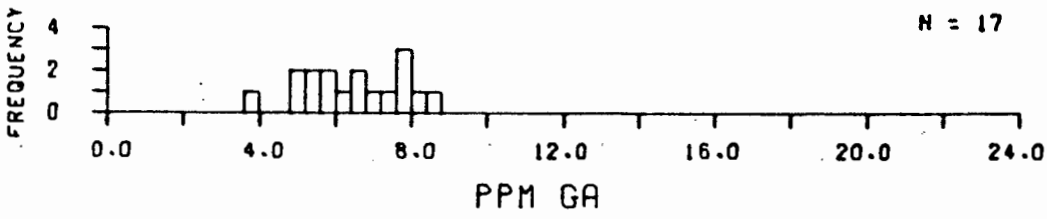

CARBONACEOUS CHONDRITES.

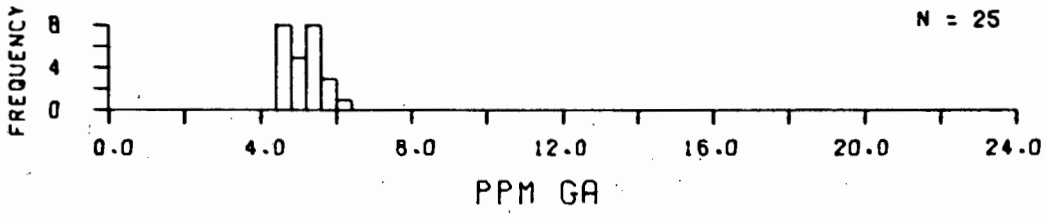

HYPERSTHENE CHONDRITES.

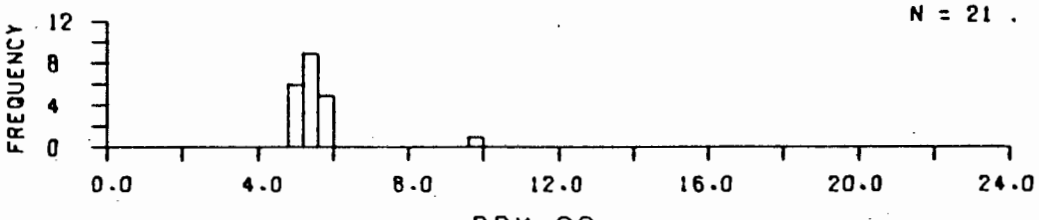

BRONZITE CHONDRITES.

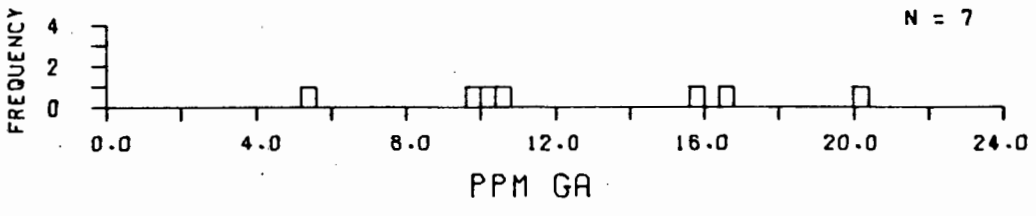

ENSTATITE CHONDRITES.

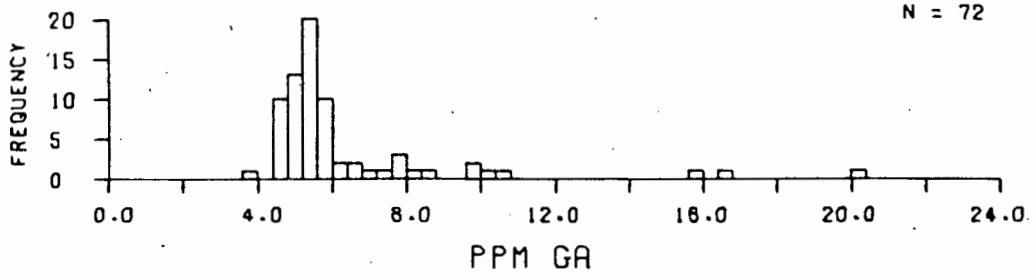

ALL CHONDRITES.

FIG. 29. CHONDRITIC METEORITES.

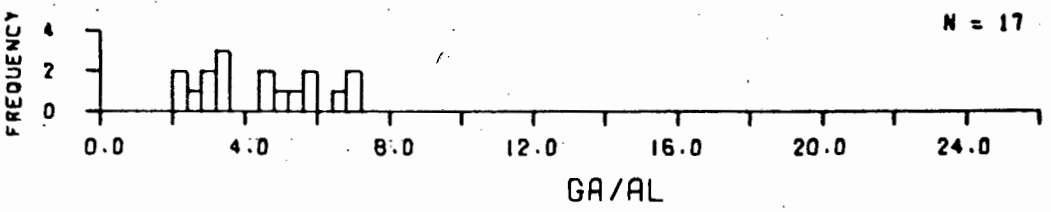

CARBONACEOUS CHONDRITES.

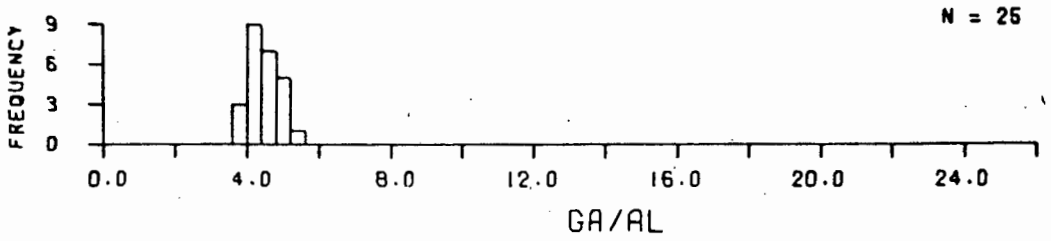

HYPERSTHENE CHONDRITES.

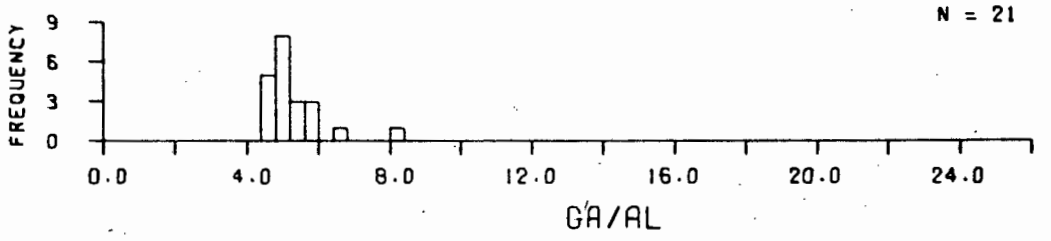

BRONZITE CHONDRITES.

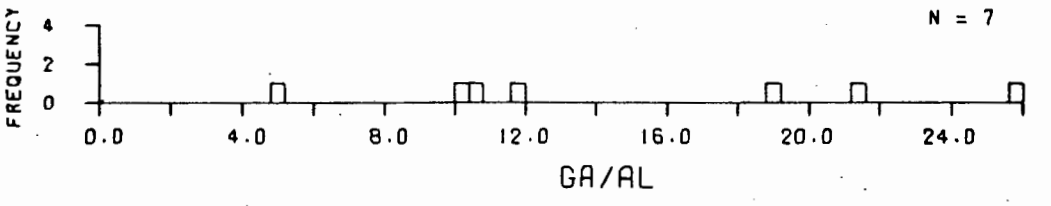

ENSTATITE CHONDRITES.

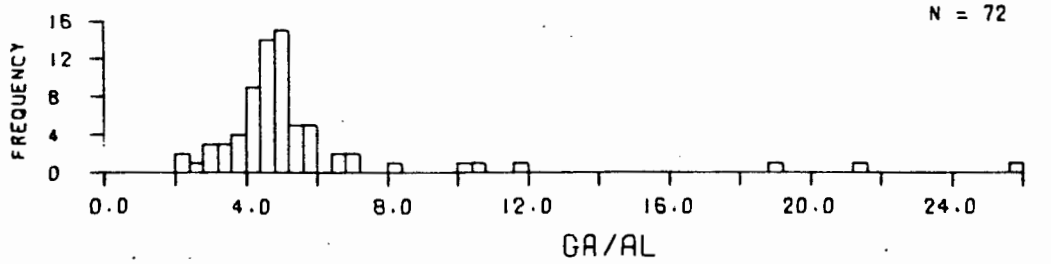

ALL CHONDRITES.

FIG. 30. CHONDRITIC METEORITES.

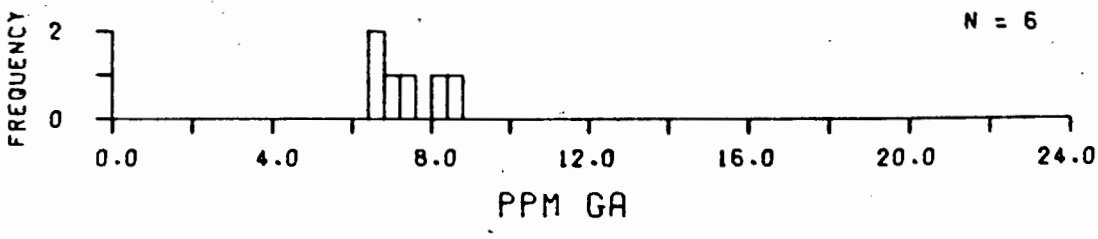

CARBONACEOUS CHONDRITES C3-0.

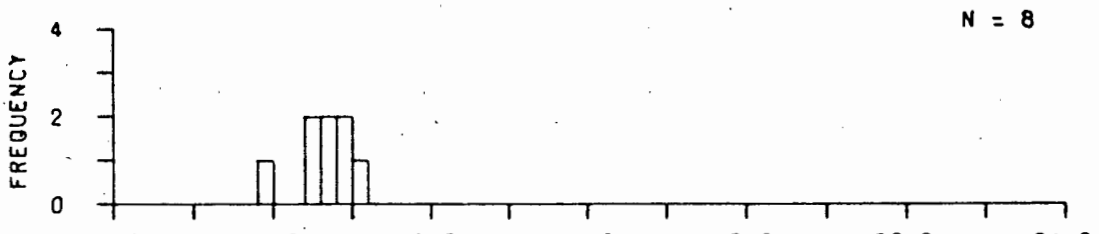

CARBONACEOUS CHONDRITES C3-V.

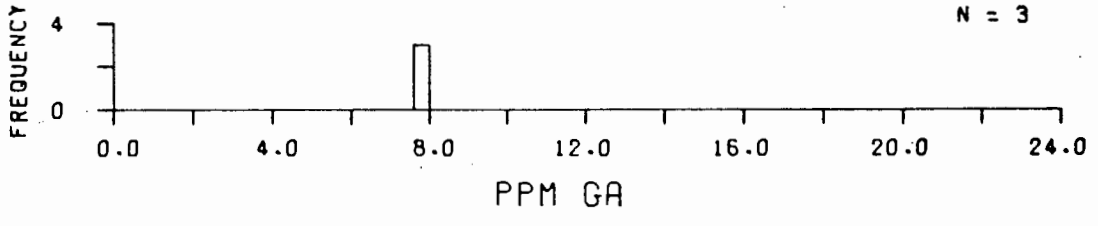

CARBONACEOUS CHONDRITES C2.

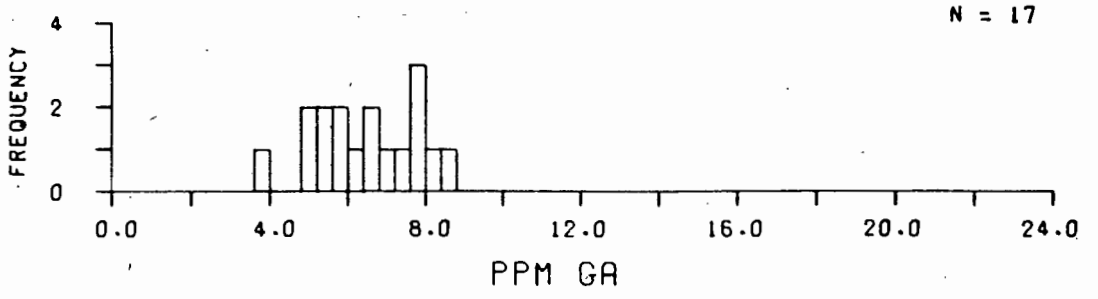

CARBONACEOUS CHONDRITES.

FIG. 31. CHONDRITIC METEORITES.

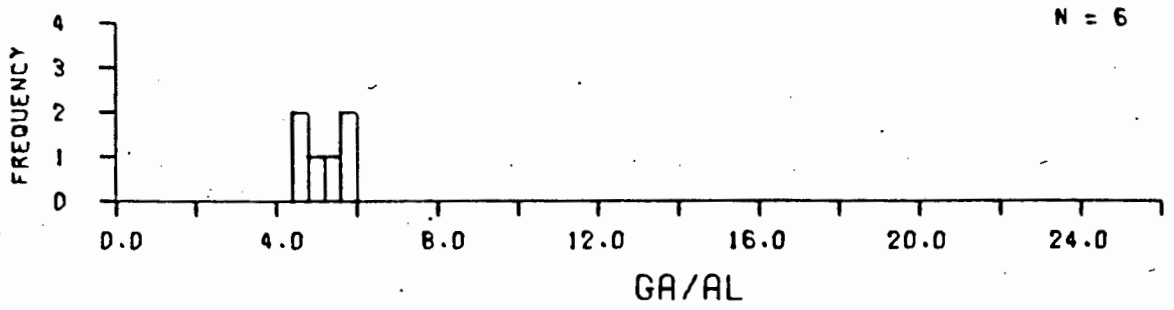

CARBONACEOUS CHONDRITES C3-O.

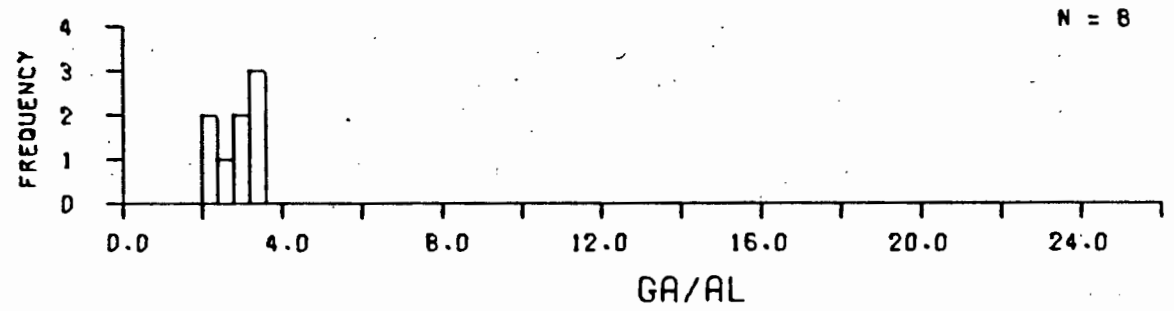

CARBONACEOUS CHONDRITES C3-V.

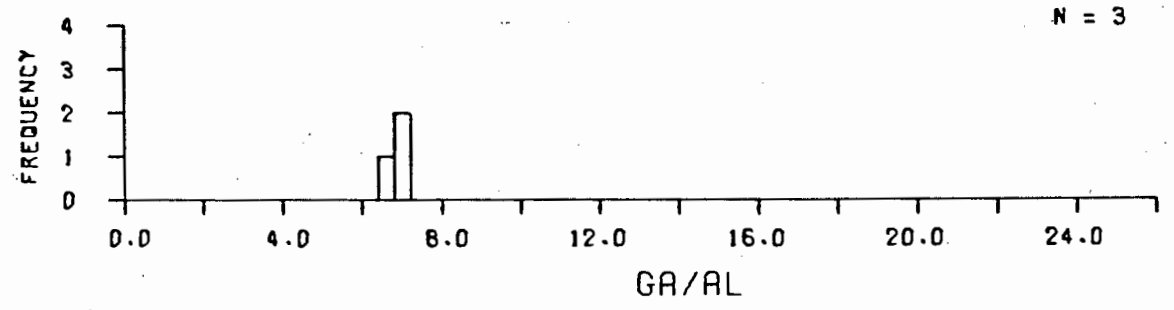

CARBONACEOUS CHONDRITES C2.

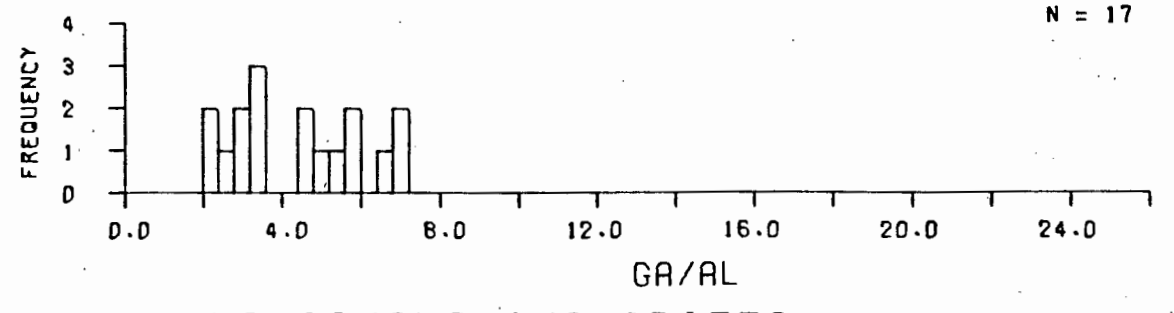

CARBONACEOUS CHONDRITES.

FIG. 32. CHONDRITIC METEORITES.

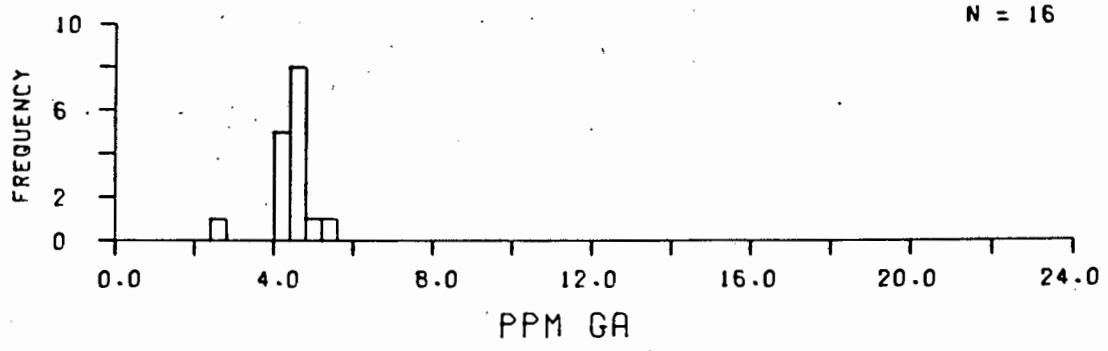

HYPERSTHENE CHONDRITES (NM FRACTION).

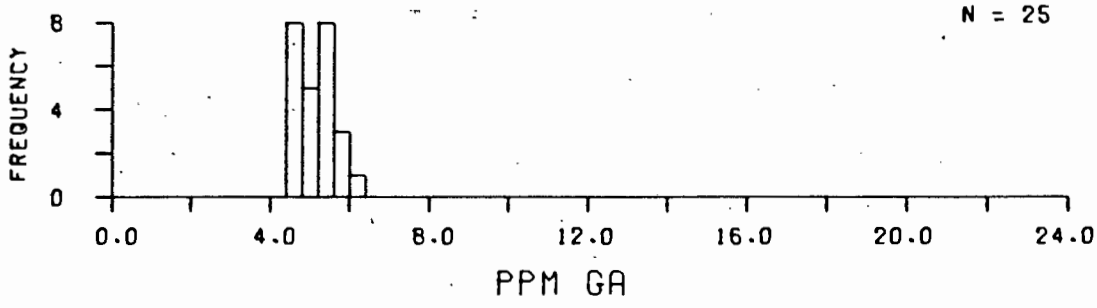

HYPERSTHENE CHONDRITES.

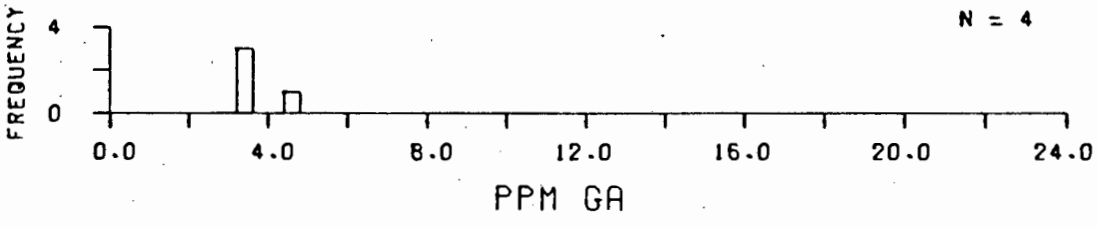

BRONZITE CHONDRITES (NM FRACTION).

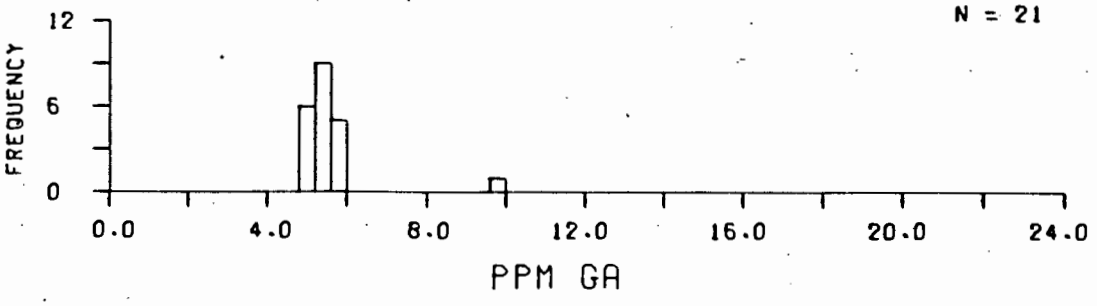

BRONZITE CHONDRITES.

FIG. 33. CHONDRITIC METEORITES.

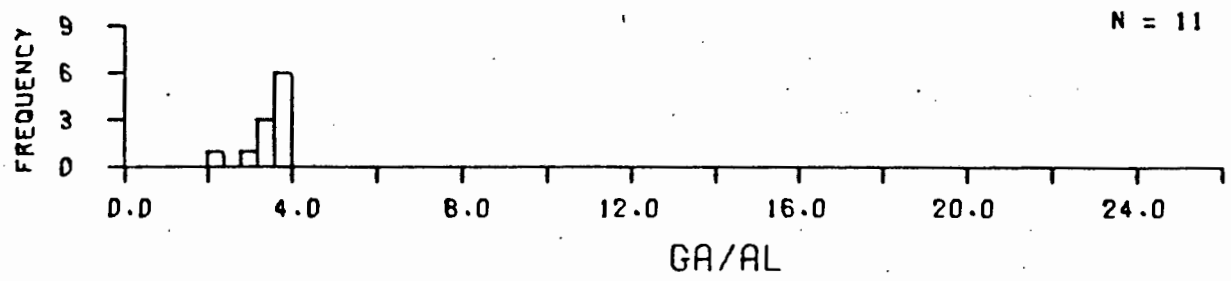

HYPERSTHENE CHONDRITES (NM FRACTION)

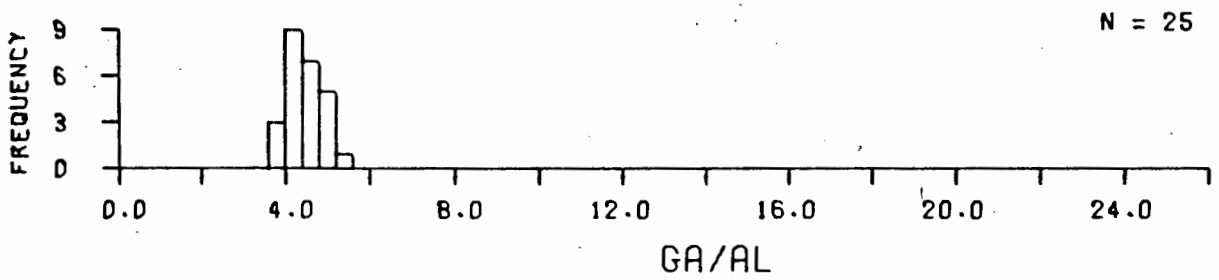

HYPERSTHENE CHONDRITES.

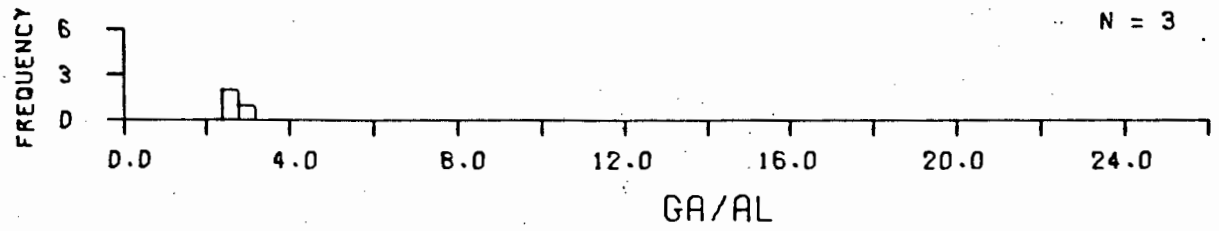

BRONZITE CHONDRITES (NM FRACTION).

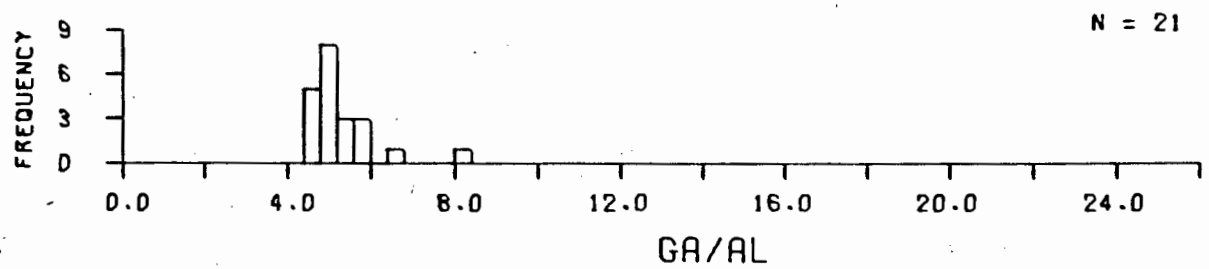

BRONZITE CHONDRITES.

FIG. 34. CHONDRITIC METEORITES.

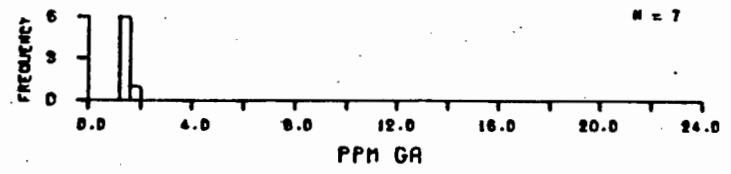

EUCRITES.

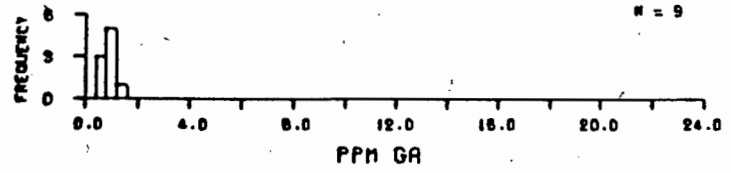

HOWARDITES.

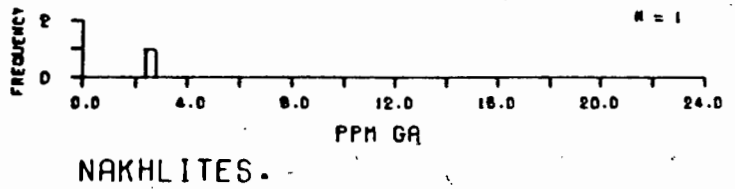

NAKHLITES.

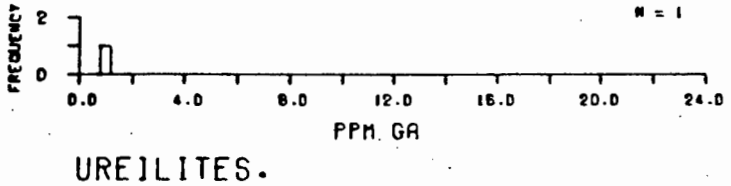

UREILITES.

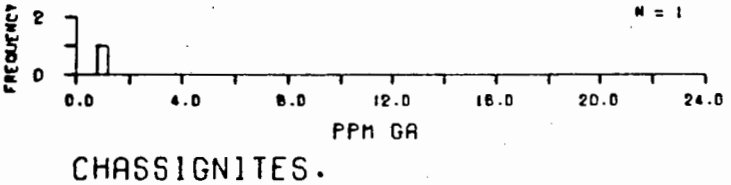

CHASSIGNITES.

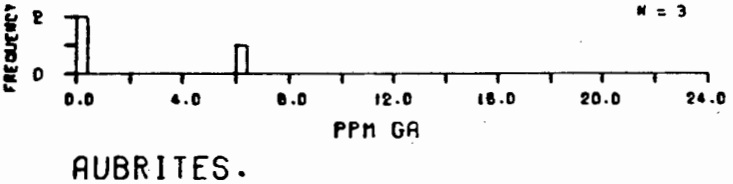

AUBRITES.

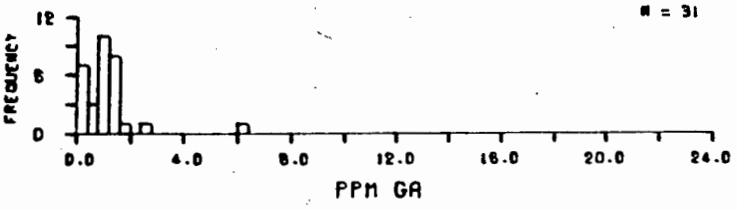

ALL ACHONDRITIC METEORITES.

FIG. 35. ACHONDRITIC METEORITES.

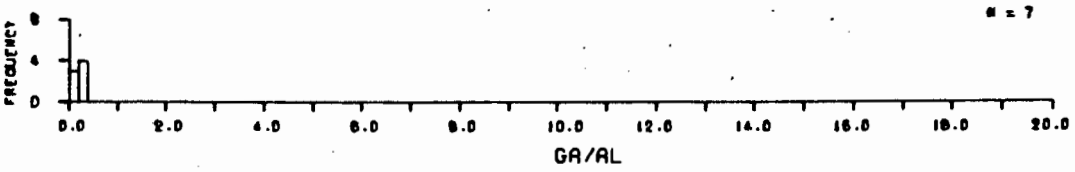

EUCRITES.

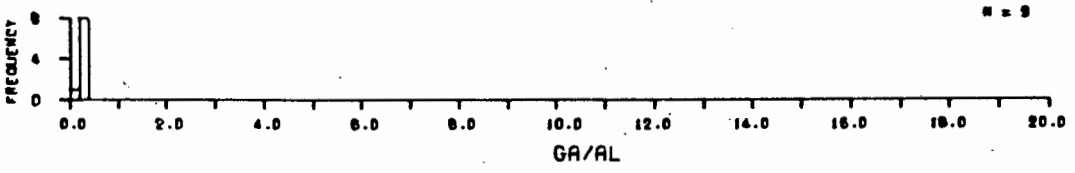

HOWARDITES.

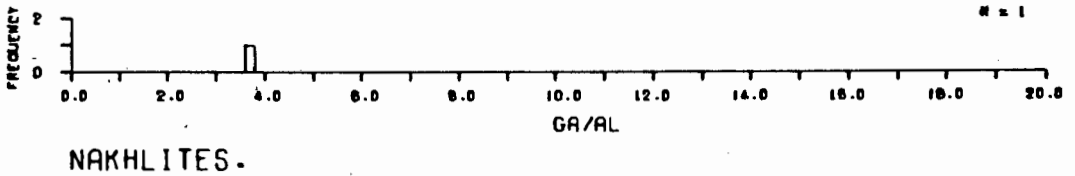

NAKHLITES.

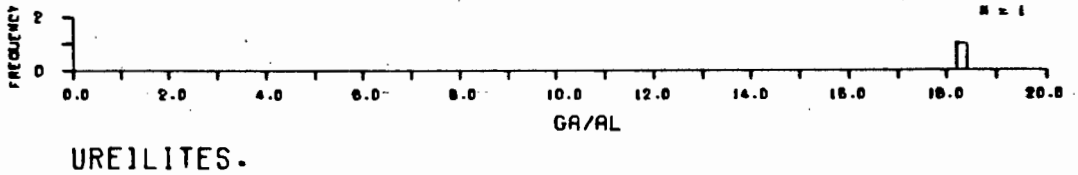

UREILITES.

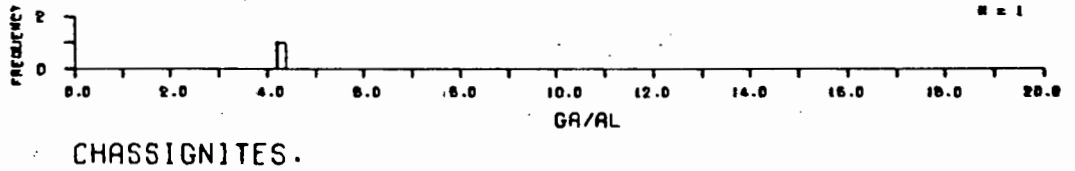

CHASSIGNITES.

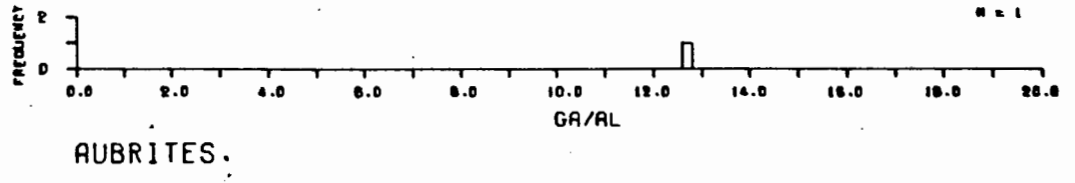

AUBRITES.

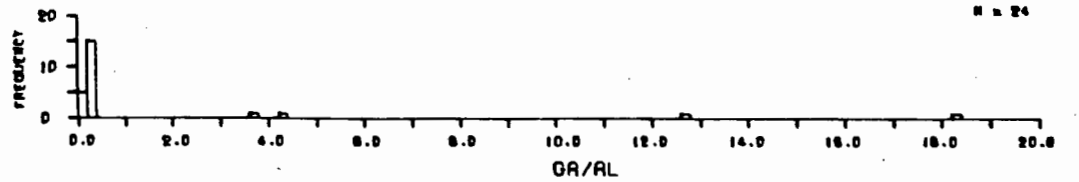

ALL ACHONDRITIC METEORITES.

FIG. 36. ACHONDRITIC METEORITES.

KEY TO FIG. 37

⊡	CARBONACEOUS CHONDRITES.
△	BRONZITE CHONDRITES (H GROUP).
B	H GROUP, NON-MAGNETIC FRACTIONS.
◇	HYPERSTHENE CHONDRITES (L GROUP).
U	LL3 UNEQUILIBRATED CHONDRITE.
#	LL6 AMPHOTERITES.
H	L GROUP, NON-MAGNETIC FRACTIONS.
⌘	ENSTATITE CHONDRITES.
E	ENSTATITES, NON-MAGNETIC FRACTIONS.
✳	EUCRITE ACHONDRITES.
X	HOWARDITE ACHONDRITES.
Y	NAKHLITE.
⧖	UREILITE.
D	DIOGENITES.
A	AUBRITES.
+	CHASSIGNITE.
M	MESOSIDERITES, NON-MAGNETIC FRACTIONS.
✿	MESOSIDERITES.
S	MESOSIDERITES, SILICATE FRACTIONS.
⏀	SHERGOTTITE.
@	ANGRITE.

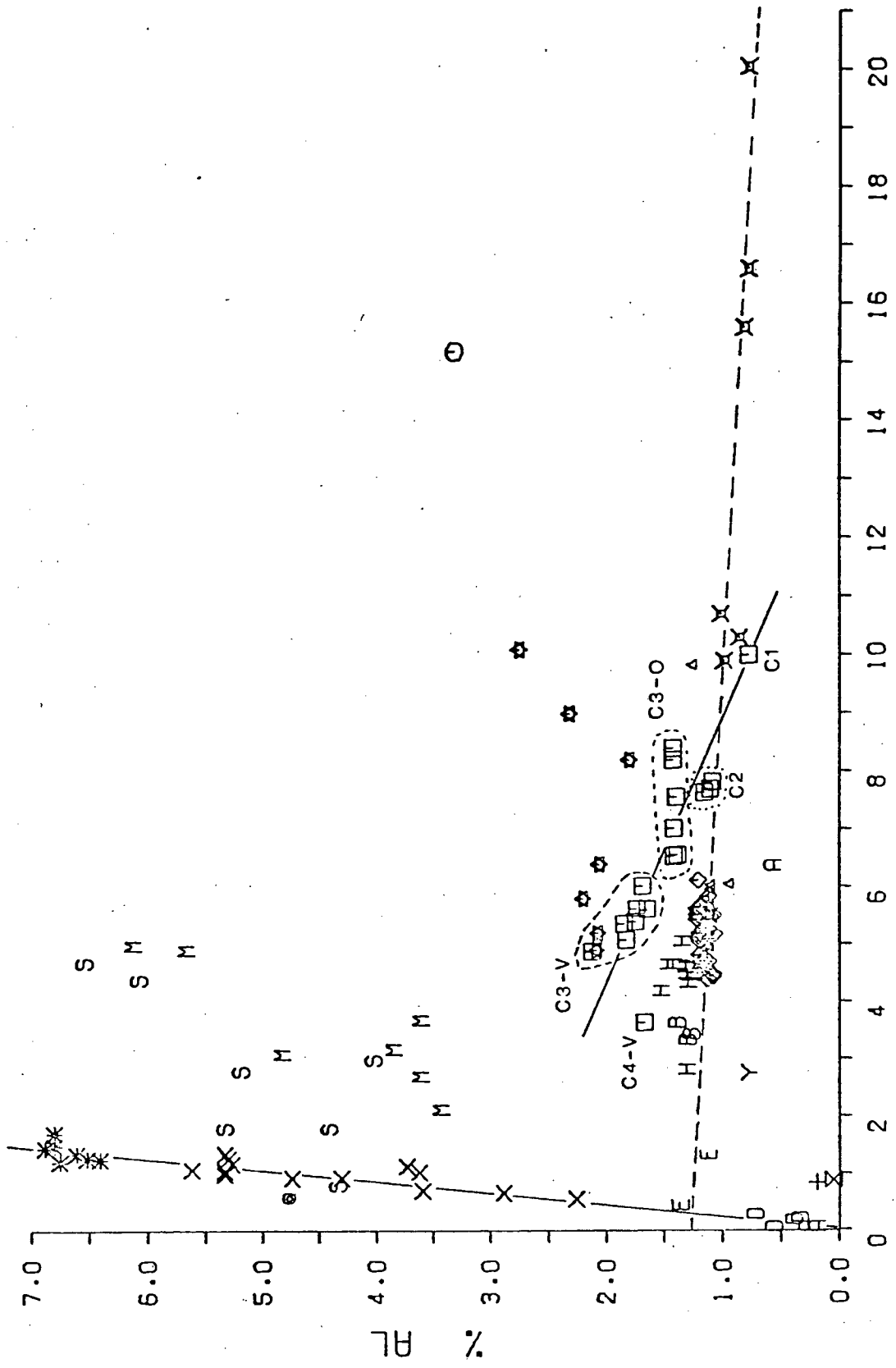

FIG. 37. A GA - AL PLOT FOR ALL METEORITES.

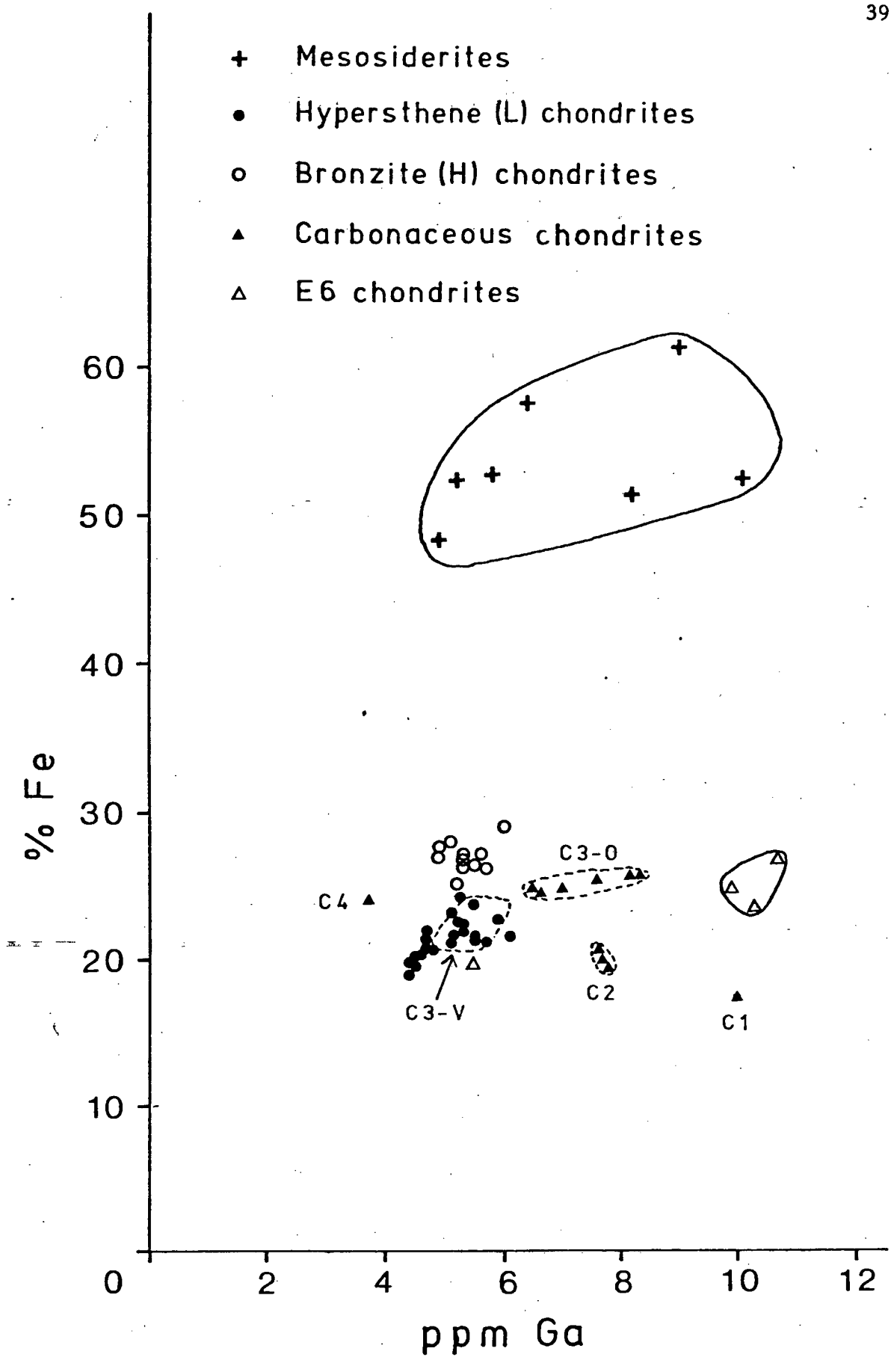

Fig. 38. A Ga-Fe plot for selected classes of meteorites. The area in which C3-V meteorites plot is shown, but the individual points are omitted.

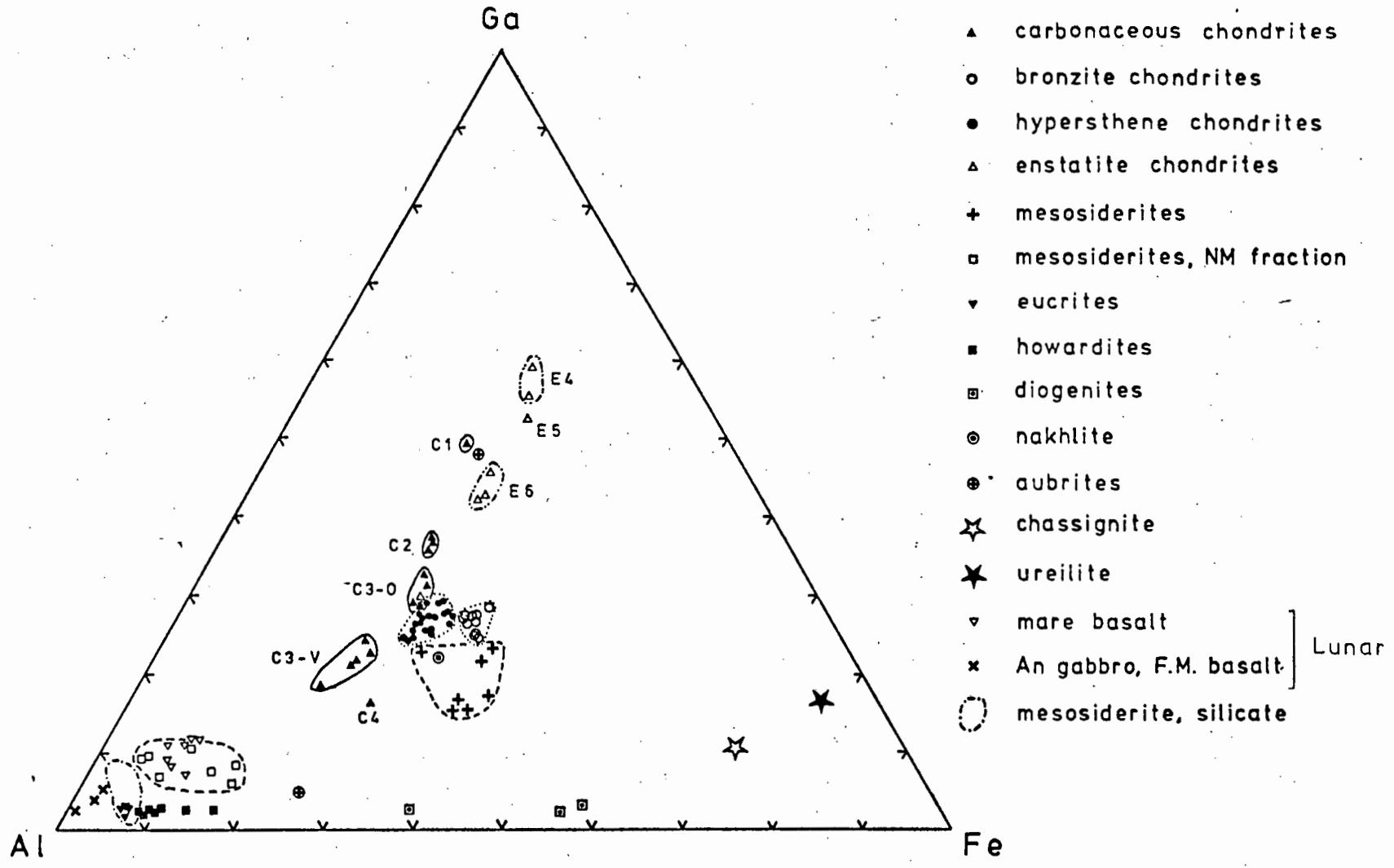

Fig. 39. A Ga-Al-Fe ternary plot for all meteorites, ppm Ga (x4), % Al (x30) and % Fe (x1).

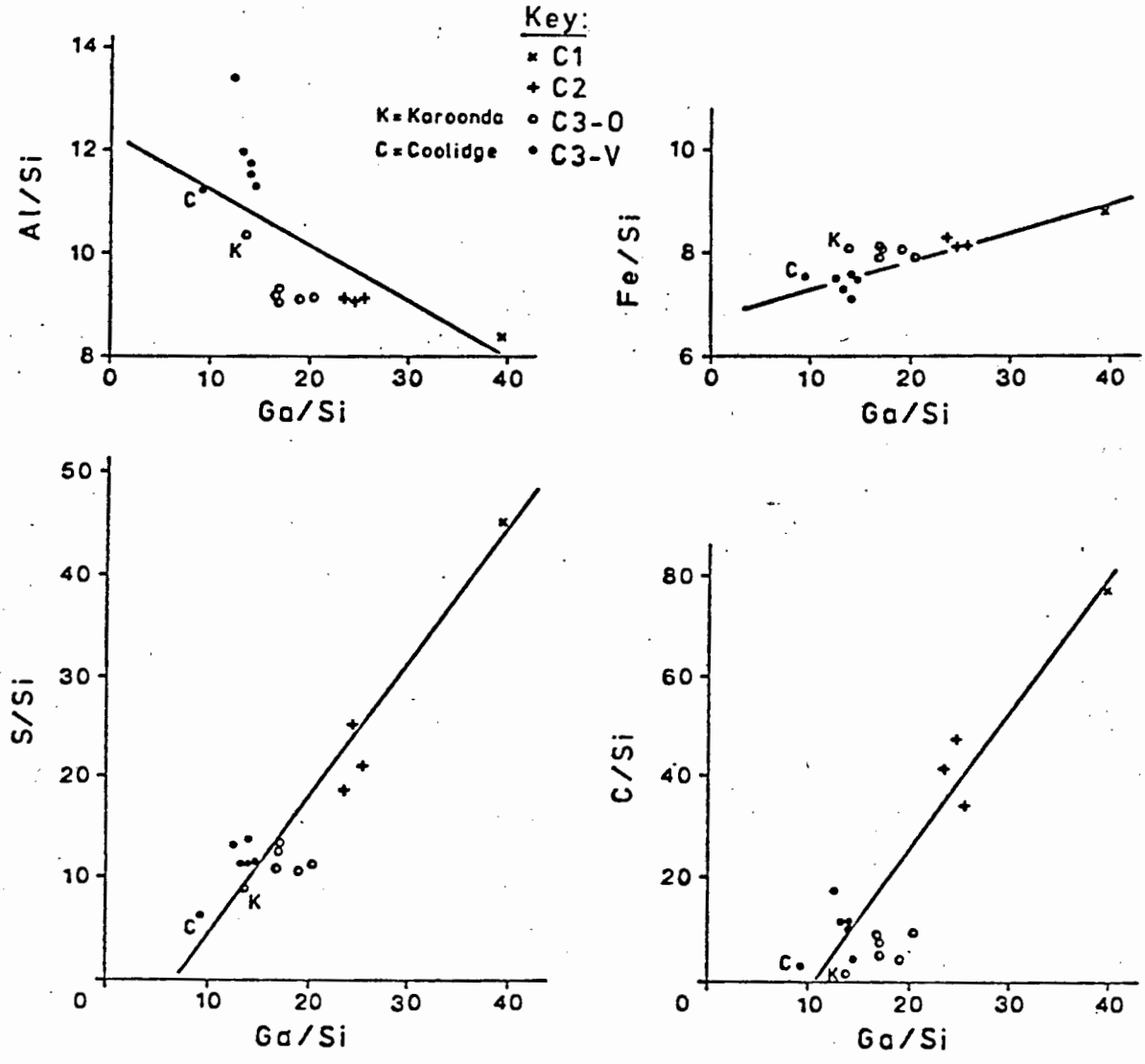

Fig. 40. Plots of Ga/Si - Al/Si, Ga/Si - Fe/Si, Ga/Si - C/Si and Ga/Si - S/Si for carbonaceous chondrites. Note: All ratios are atomic ratios.

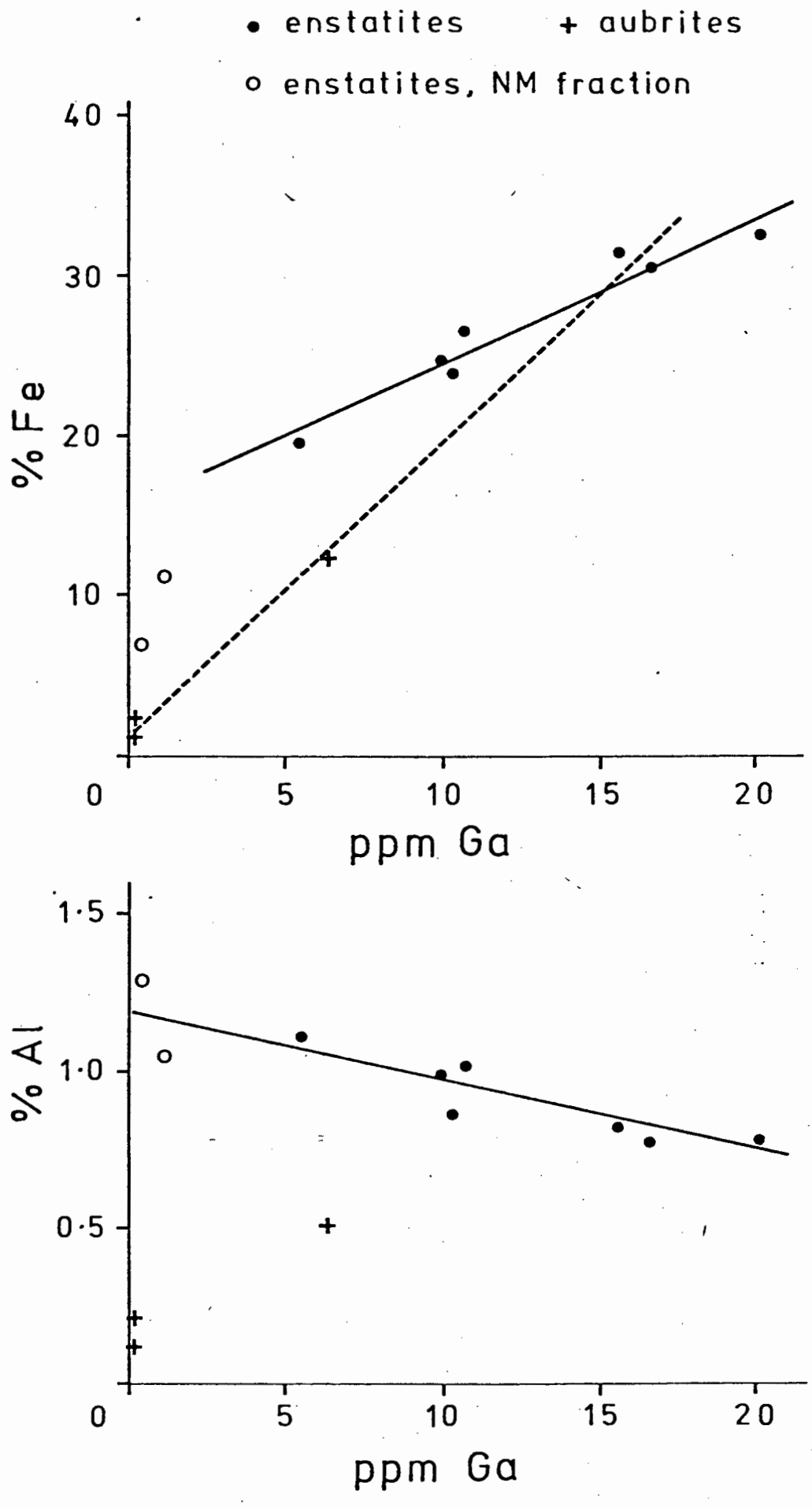

Fig. 41. Ga - Fe and Ga - Al plots for enstatite chondrites and enstatite achondrites (aubrites).

Figs 42 - 72. Frequency distribution diagrams (histograms) of the Ga distributions (A) and Ga/Al distributions (B) for all rocks analysed in this work. In Figs 42 - 67, Q = quartz, A = alkali feldspar, P = plagioclase, F = felspathoids, M = mafic and related minerals. Tables 34 and 38 should be read in conjunction with these diagrams.

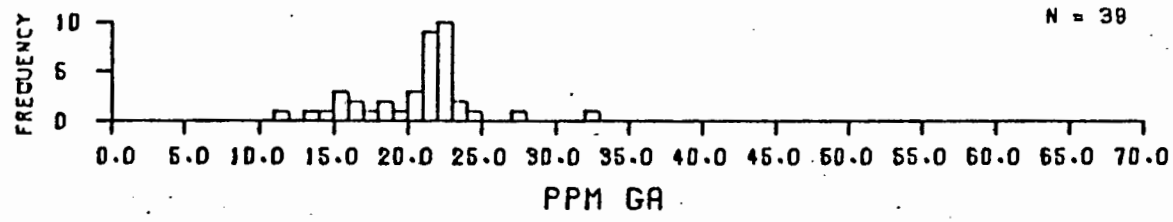

900000 METAMORPHIC ROCKS.

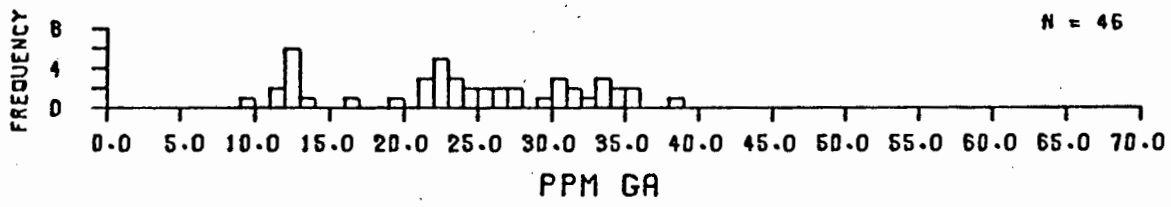

400000 SEDIMENTARY ROCKS.

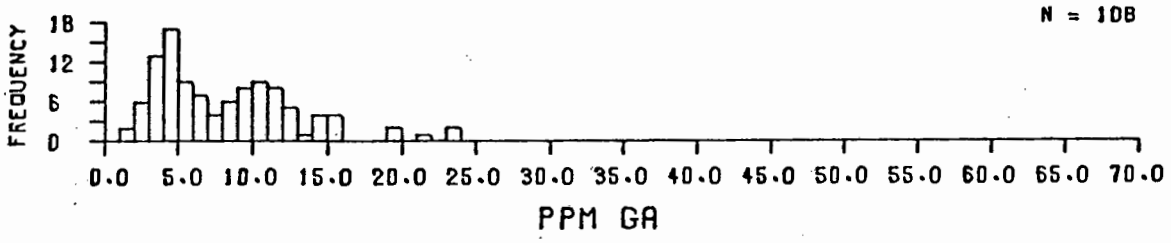

300000 VOLCANIC ROCKS (CHEMICAL).

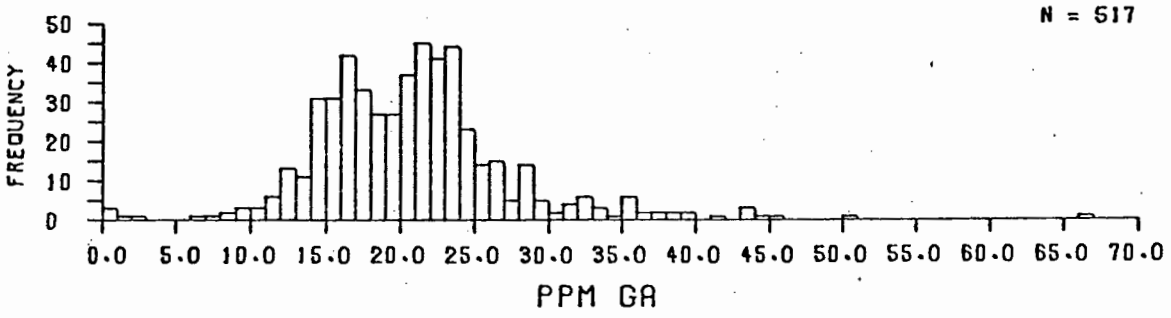

200000 VOLCANIC ROCKS (MINERALOGICAL).

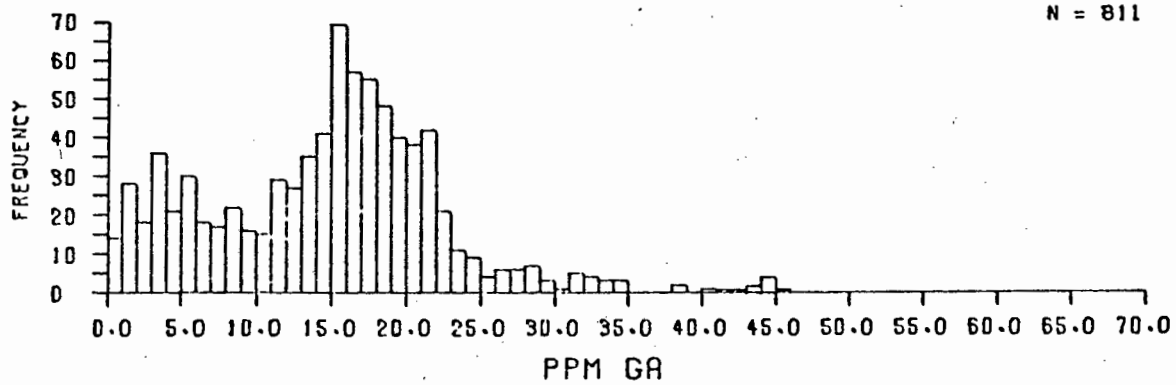

100000 PLUTONIC & HYPABYSSAL ROCKS.

FIG. 42A. ALL ROCKS.

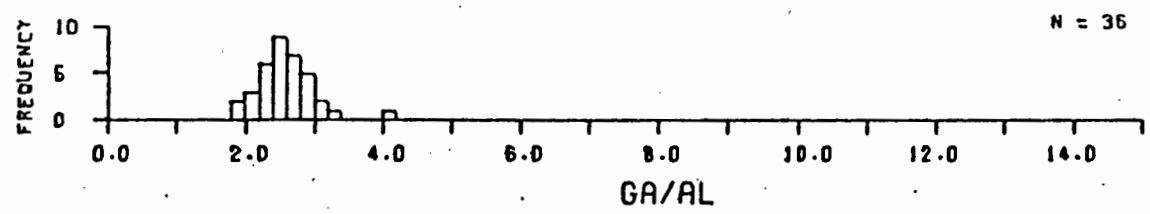

900000 METAMORPHIC ROCKS.

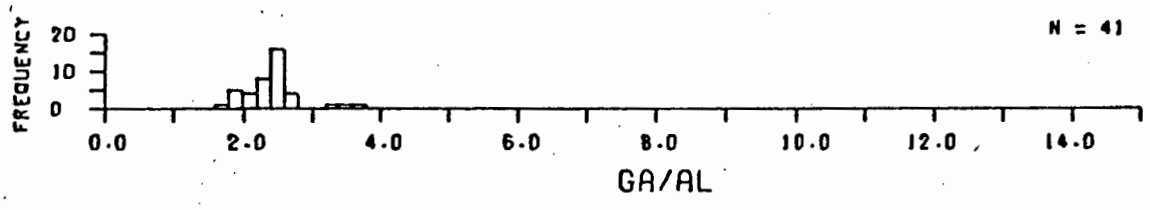

400000 SEDIMENTARY ROCKS.

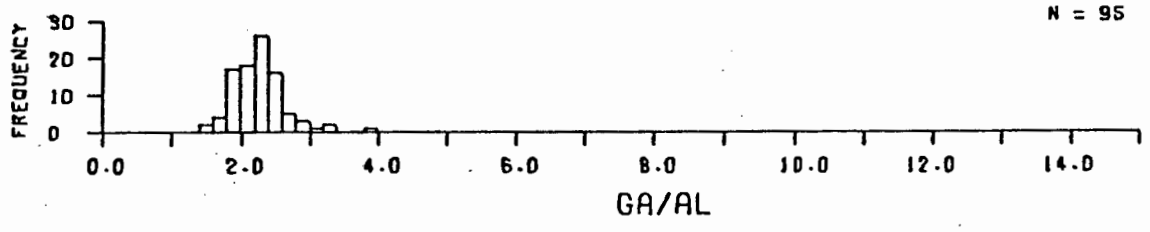

300000 VOLCANIC ROCKS (CHEMICAL).

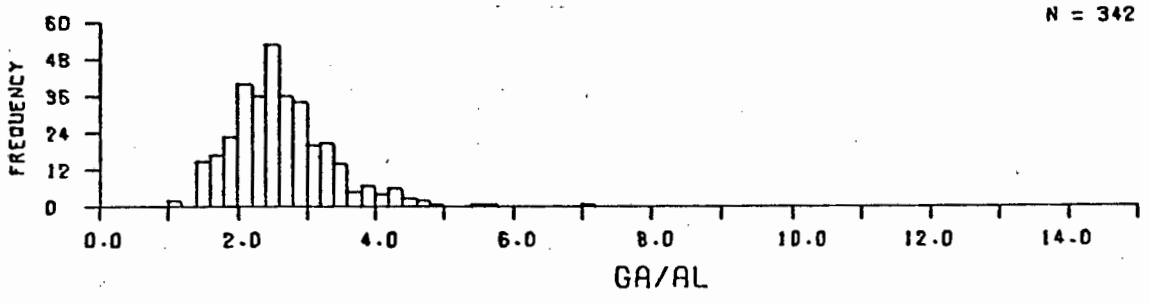

200000 VOLCANIC ROCKS (MINERALOGICAL).

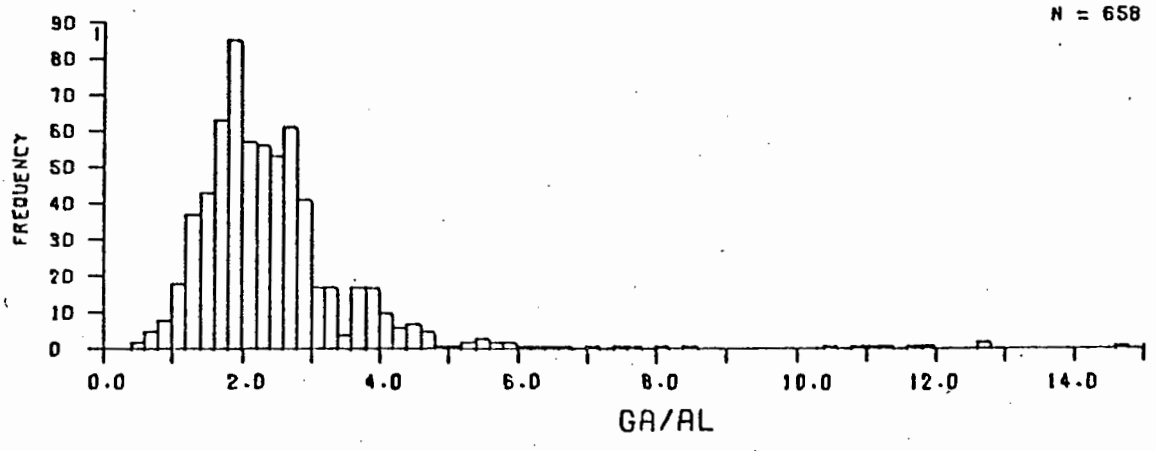

100000 PLUTONIC & HYPABYSSAL ROCKS.

FIG. 42B. ALL ROCKS.

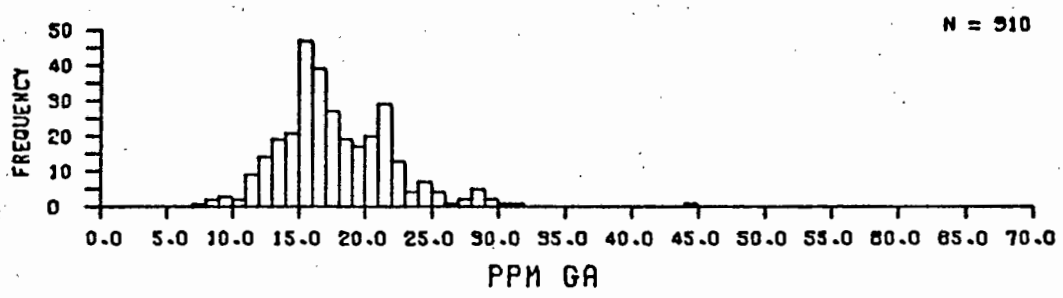

140000 A + P +- Q ROCKS.

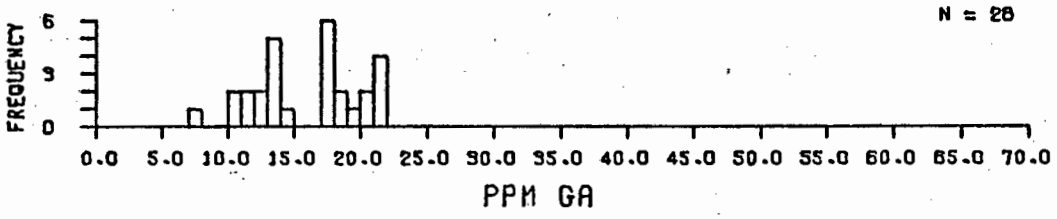

130000 A + P + Q ROCKS.

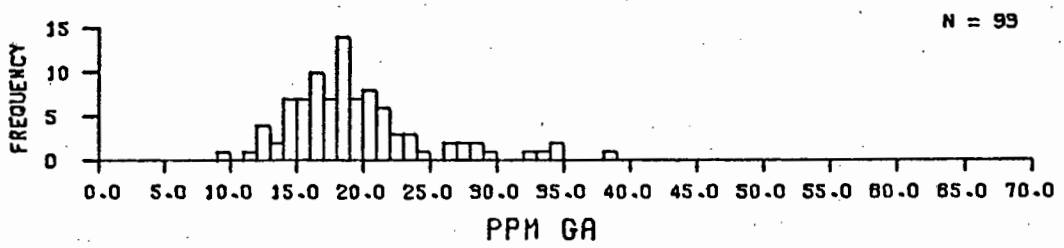

120000 Q + A + P ROCKS.

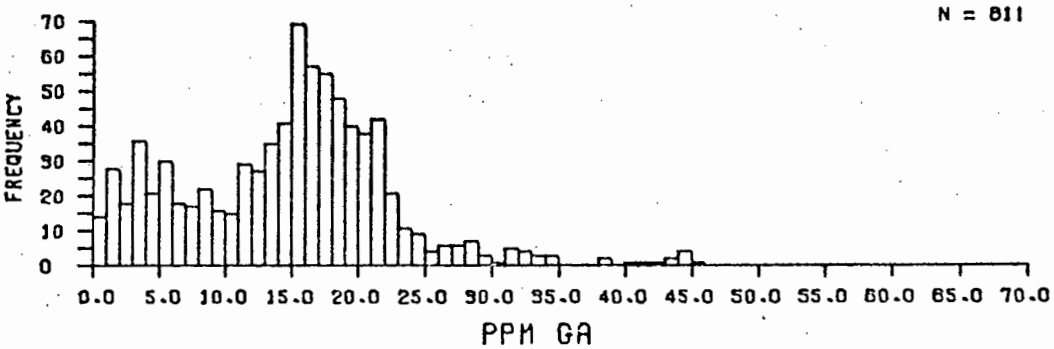

100000 ALL ROCKS.

FIG. 43A. PLUTONIC & HYPABYSSAL ROCKS.

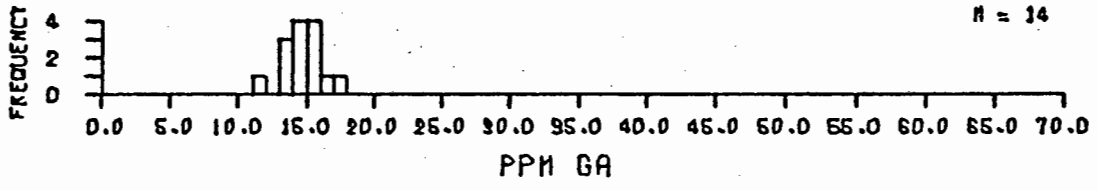

190000 LAMPROPHYRES.

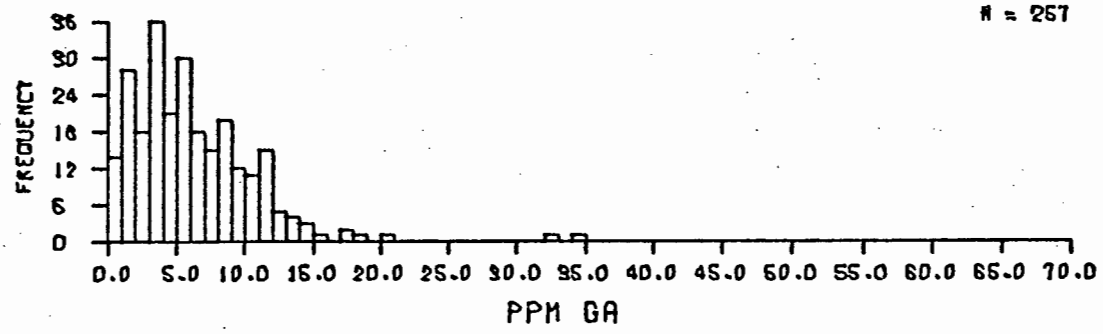

180000 ULTRAMAFIC ROCKS.

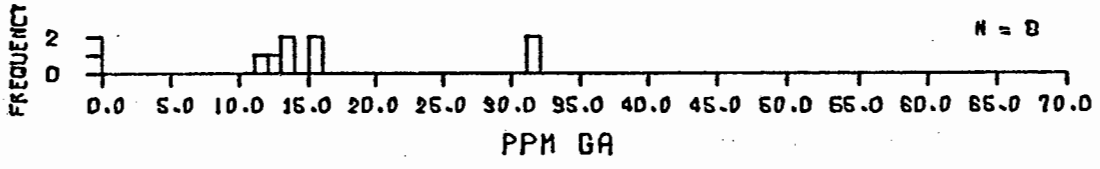

170000 F +- A +- P ROCKS.

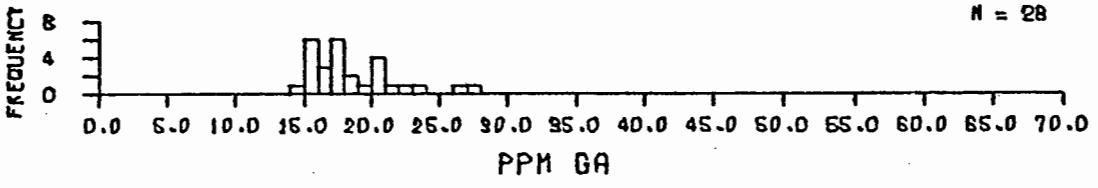

160000 A + P + F ROCKS.

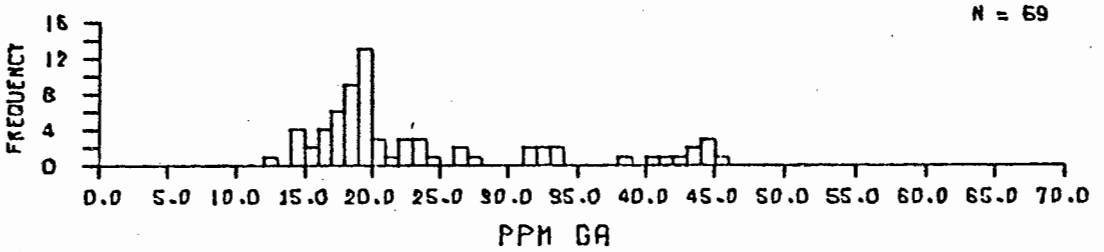

150000 A + P +- F ROCKS.

FIG. 44A. PLUTONIC & HYPABYSSAL ROCKS.

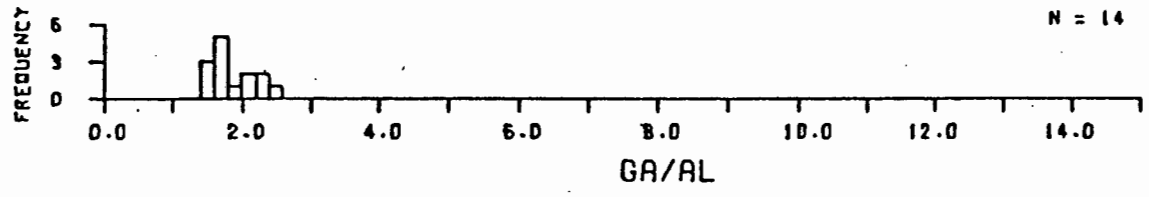

190000 LAMPROPHYRES.

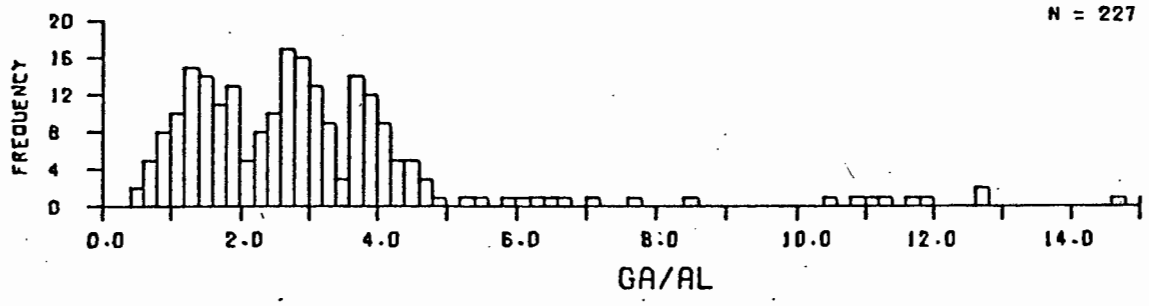

180000 ULTRAMAFIC ROCKS.

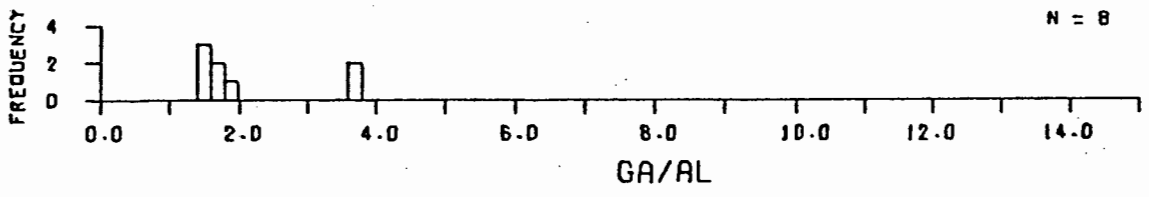

170000 F +- A +- P ROCKS.

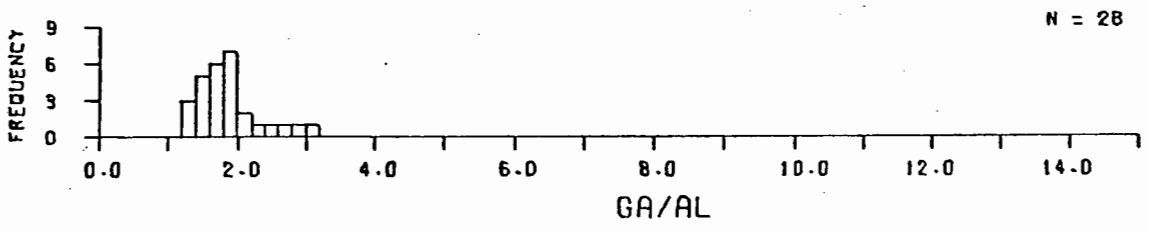

160000 A + P + F ROCKS.

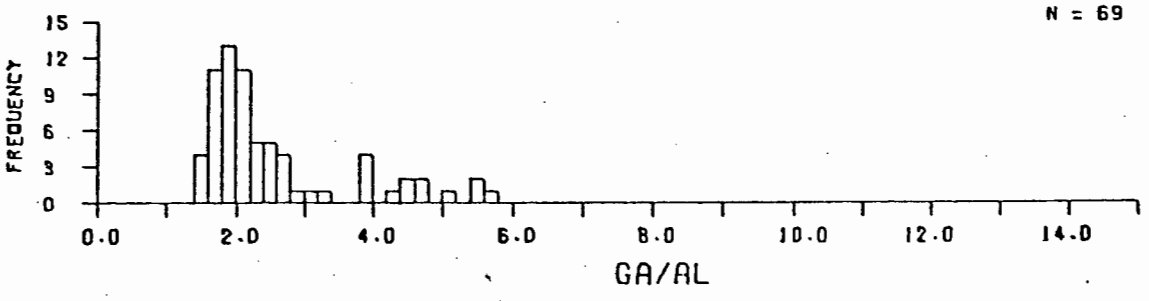

150000 A + P +- F ROCKS.

FIG. 44B. PLUTONIC & HYPABYSSAL ROCKS.

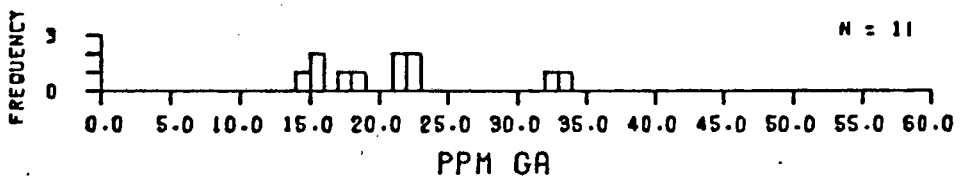

122900 FINE-GRAINED GRANITES.

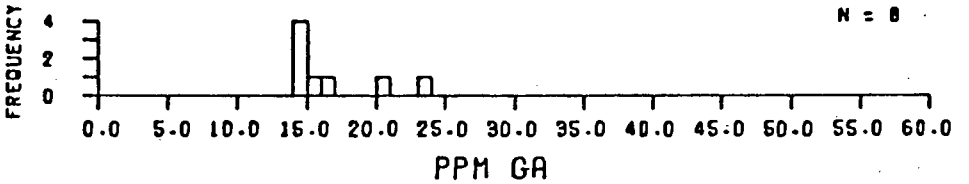

122600 MONZOGRANITES.

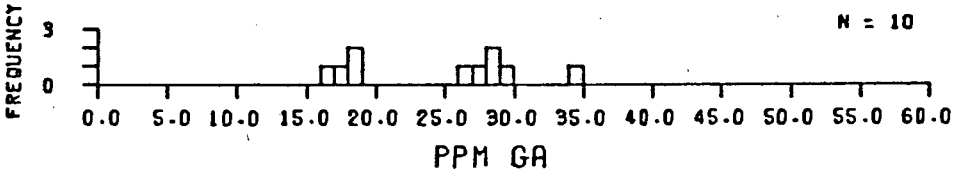

122200 GRANOPHYRES.

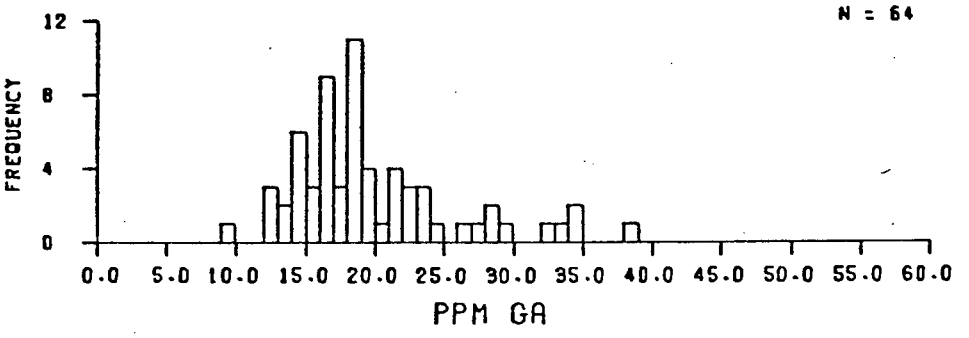

122000 GRANITES.

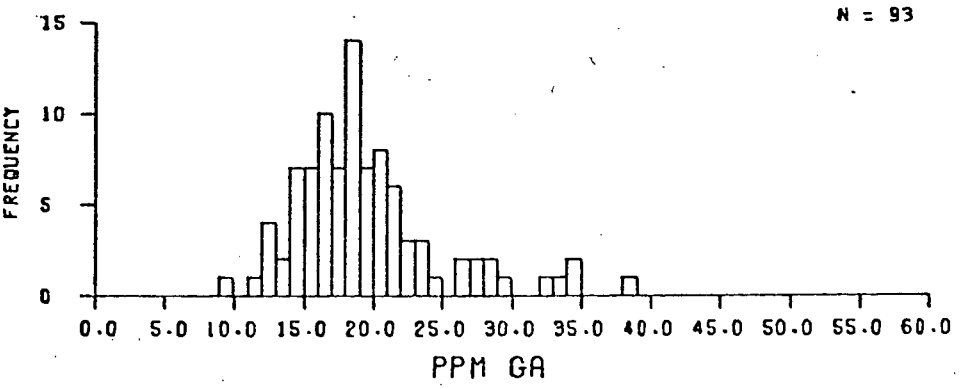

120000 Q + A + P ROCKS.

FIG. 45A. GRANITIC ROCKS.

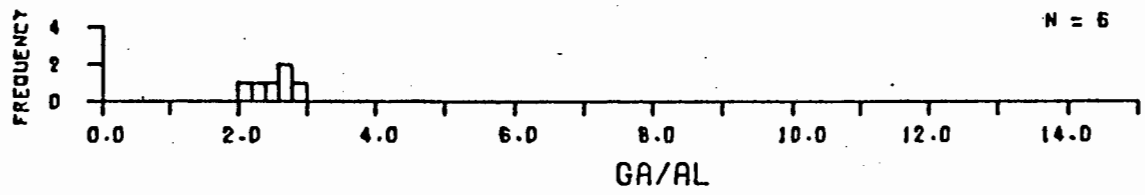

122900 FINE-GRAINED GRANITES.

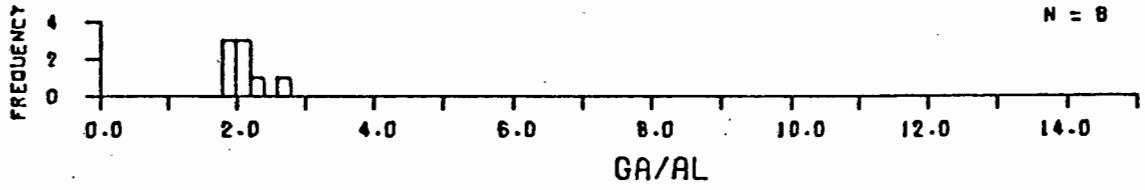

122600 MONZOGRANITES.

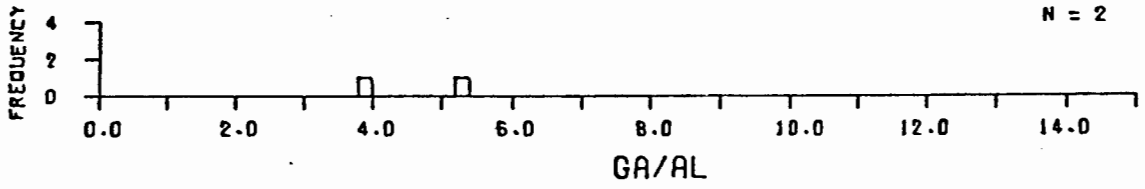

122200 GRANOPHYRES.

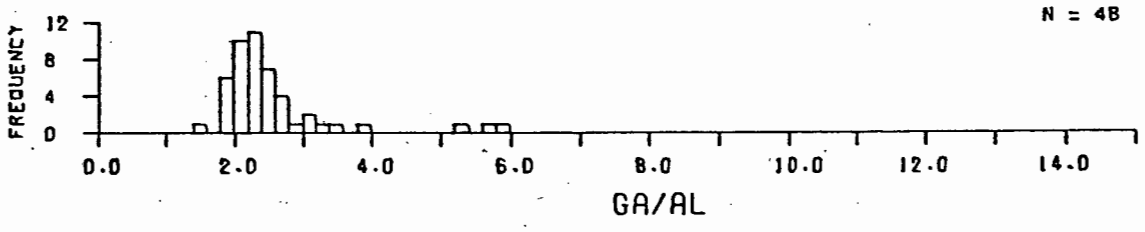

122000 GRANITES.

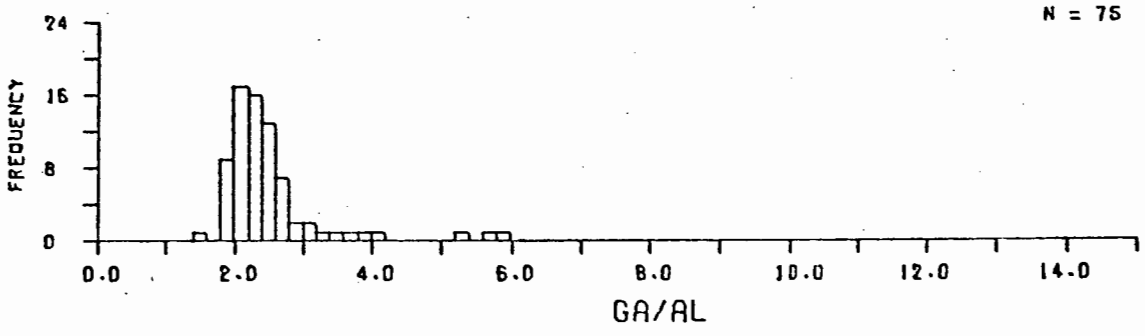

120000 Q + A + P ROCKS.

FIG. 45B. GRANITIC ROCKS.

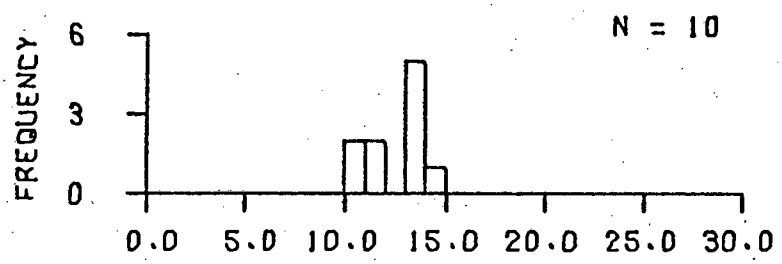

137000 QUARTZ GABBROS.

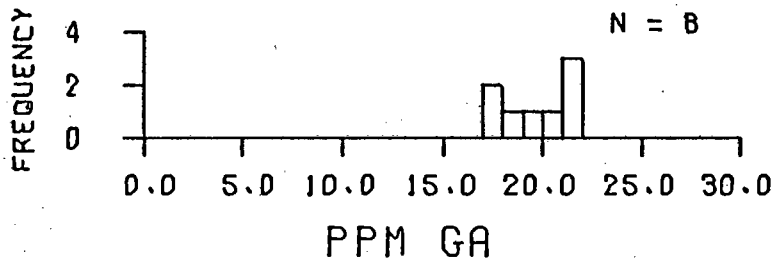

133000 QUARTZ MONZONITES.

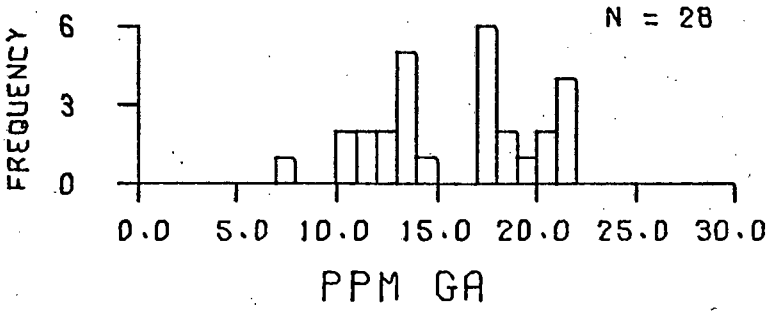

130000 A + P + Q ROCKS.

FIG. 46A. A + P + Q ROCKS.

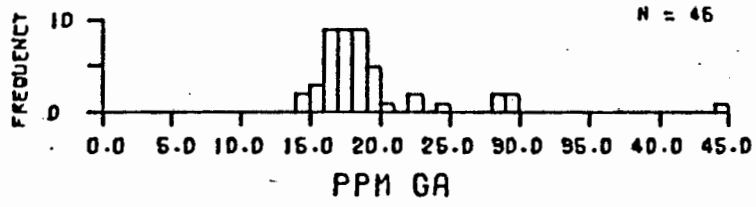

148000 ANORTHOSITES.

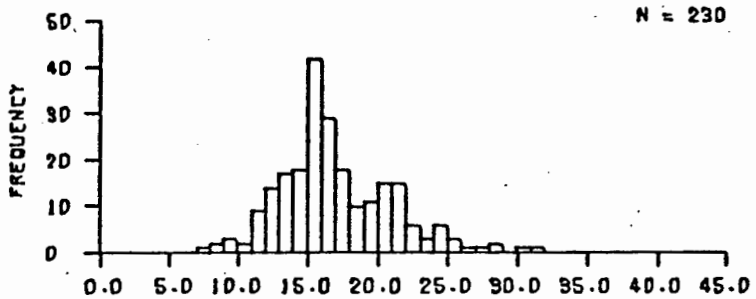

147000 GABBROID ROCKS.

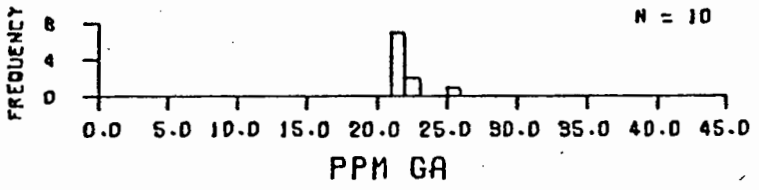

146000 DIORITES.

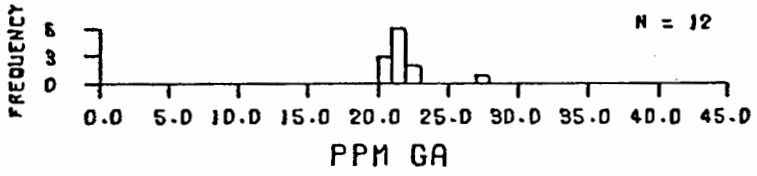

143000 MONZONITES.

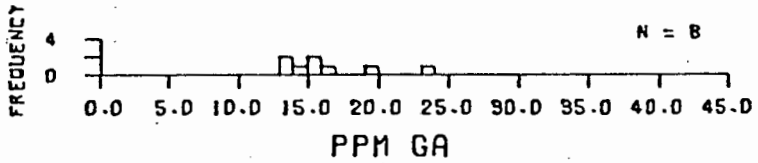

141000 ALKALI-FELDSPAR SYENITES.

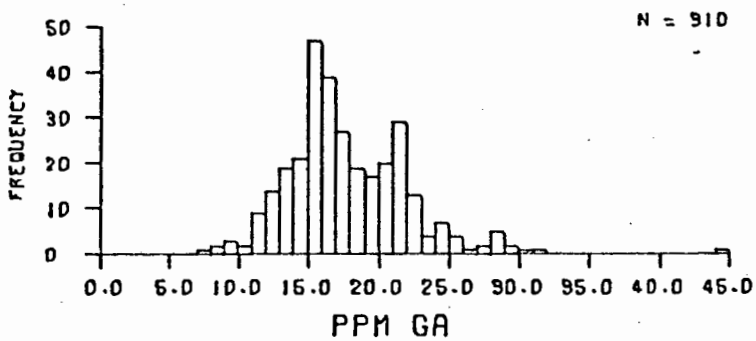

140000 A + P +- Q ROCKS.

FIG. 47A. A + P +- Q ROCKS.

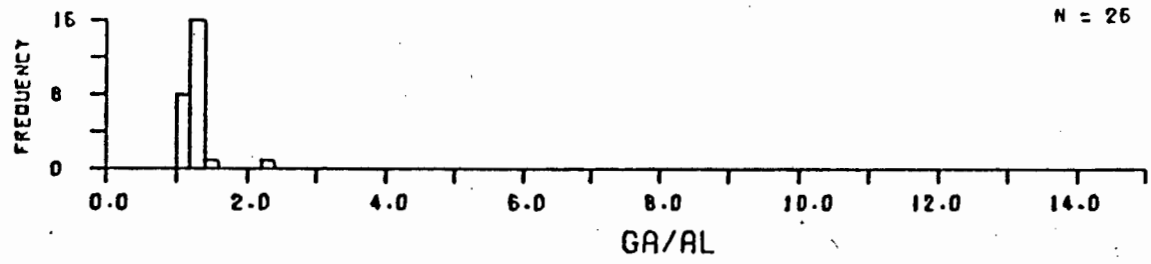

148000 ANORTHOSITES.

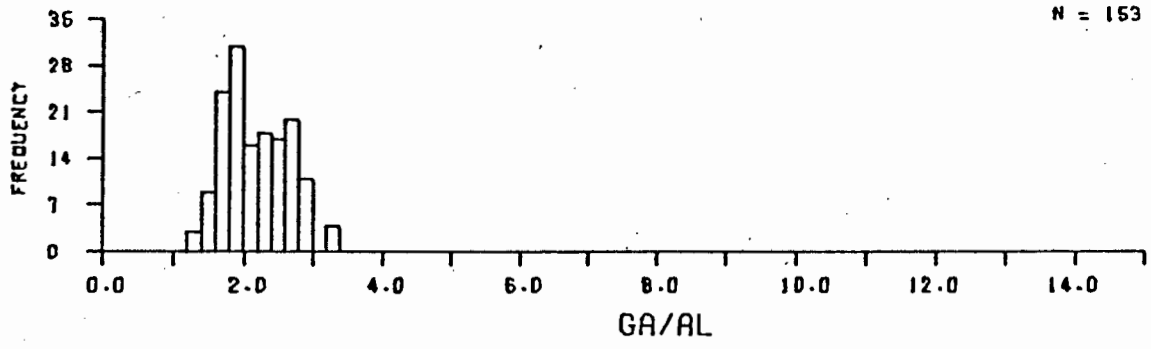

147000 GABBROID ROCKS.

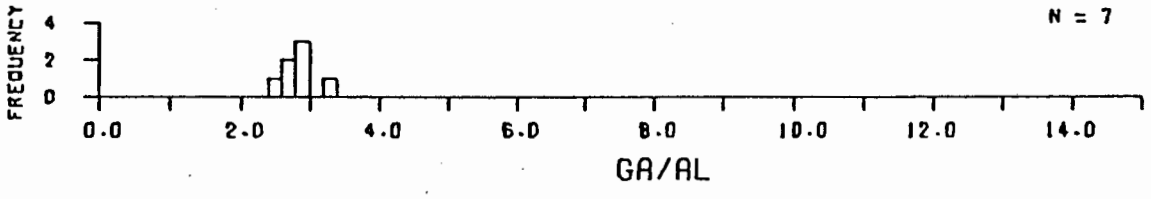

146000 DIORITES.

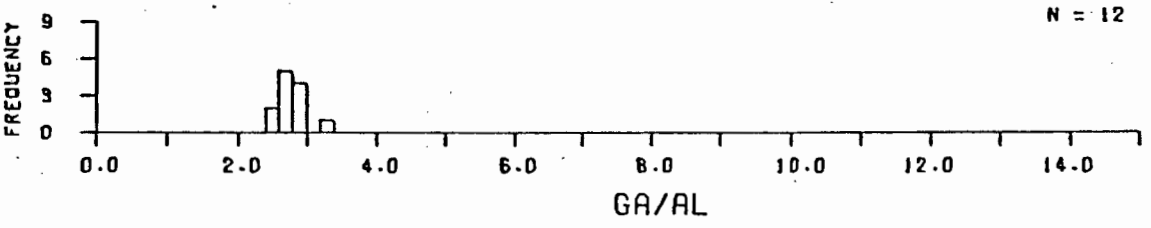

143000 MONZONITES.

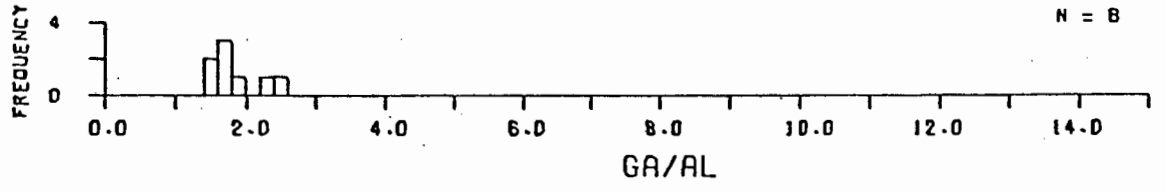

141000 ALKALI-FELDSPAR SYENITES.

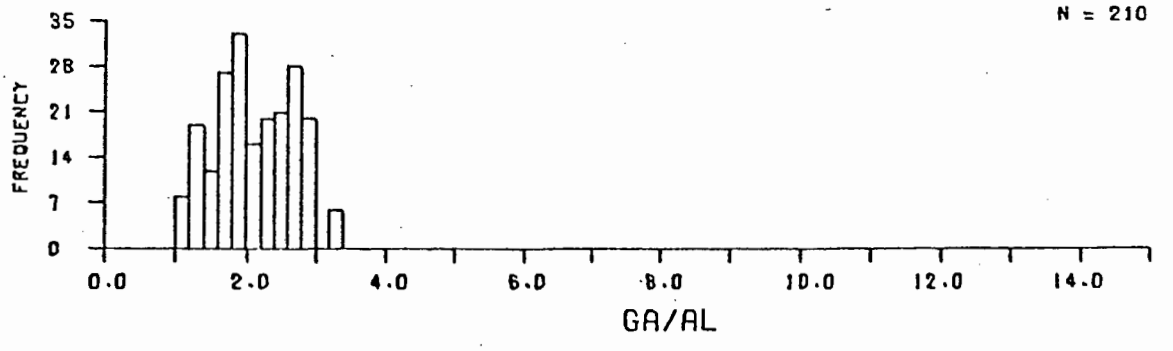

140000 A + P +- Q ROCKS.

FIG. 47B. A + P +- Q ROCKS.

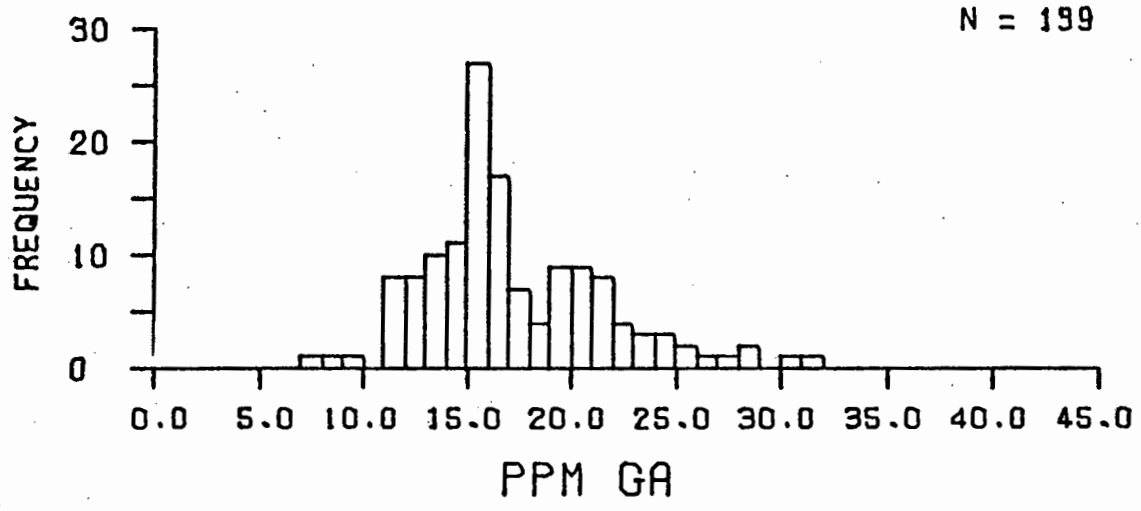

147200 PLAG + PYX ROCKS.

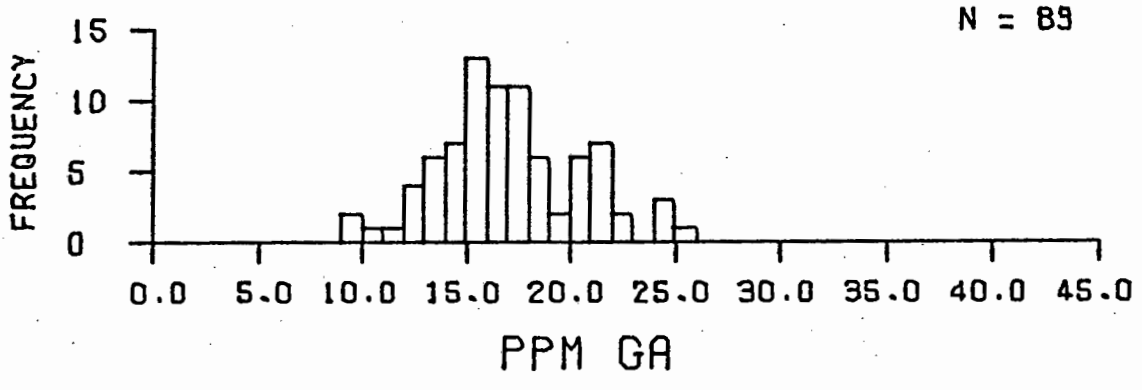

147100 PLAG + PYX + OL ROCKS.

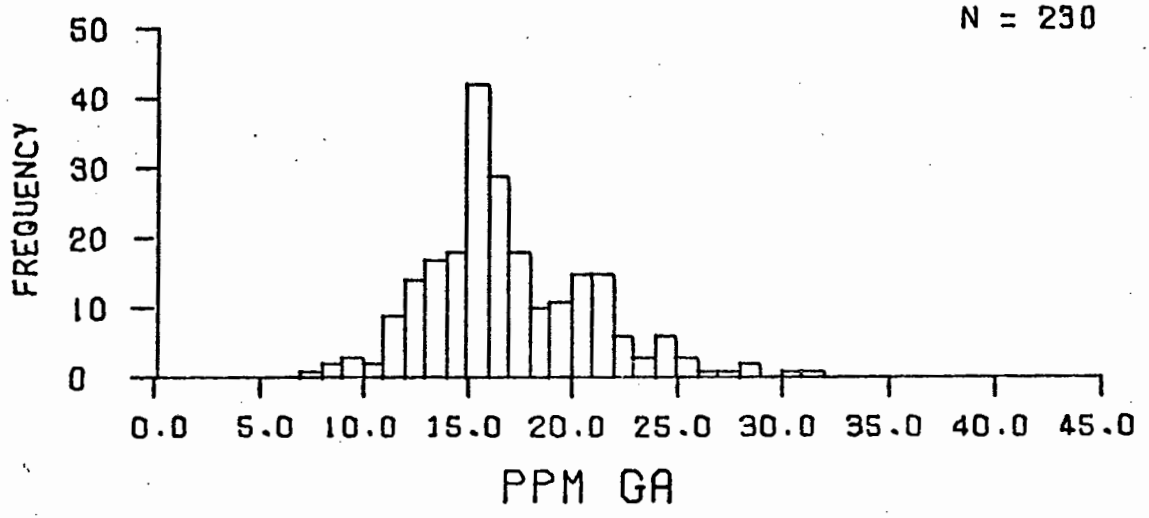

147000 GABBROID ROCKS.

FIG. 48A. GABBROID ROCKS.

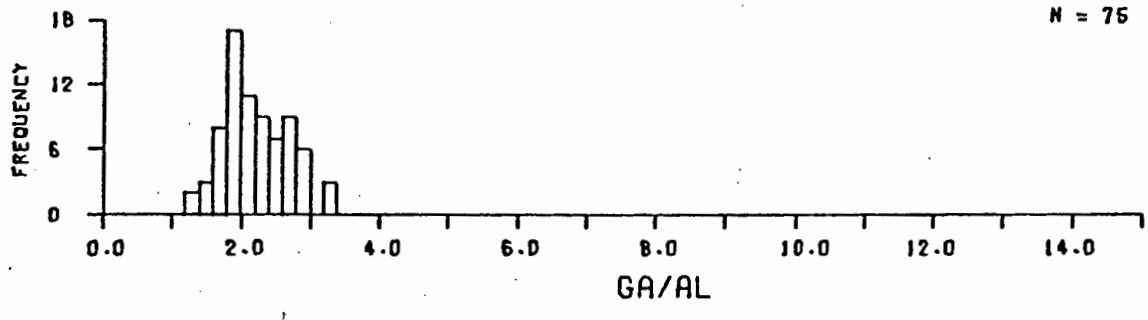

147200 PLAG + PYX ROCKS.

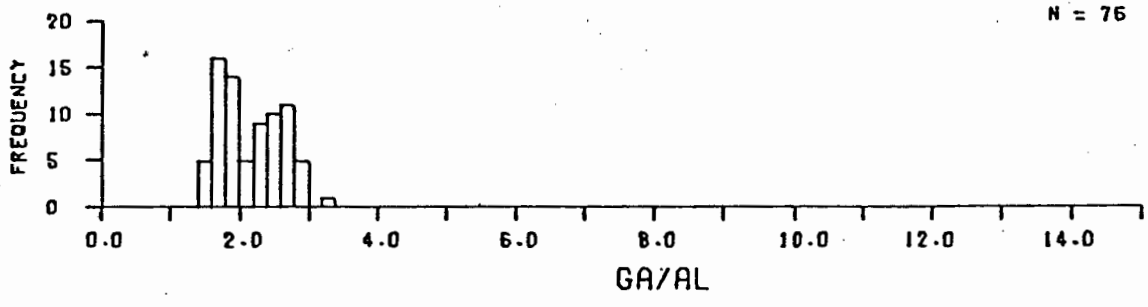

147100 PLAG + PYX + OL ROCKS.

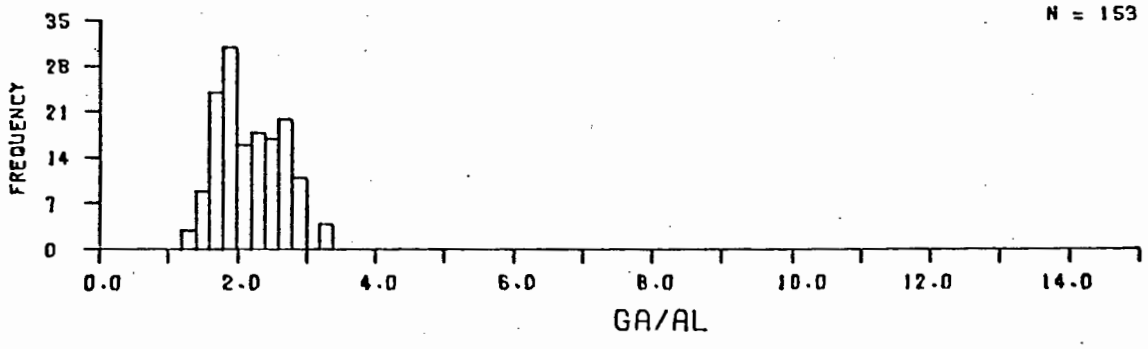

147000 GABBROID ROCKS.

FIG. 48B. GABBROID ROCKS.

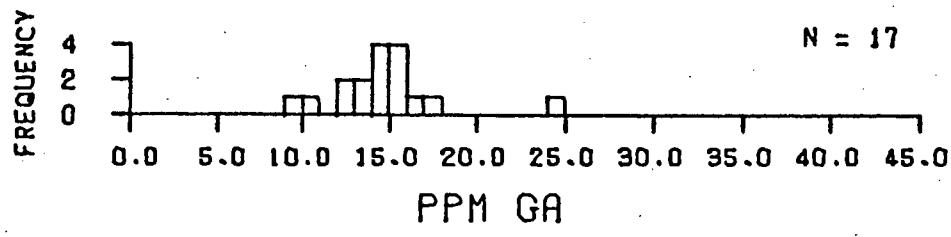

1471E2 GABBR0-P1CRITES.

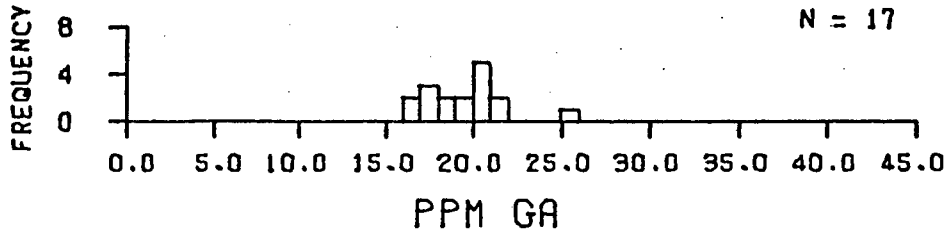

1471E1 0LIVINE FERR0GABBR0S.

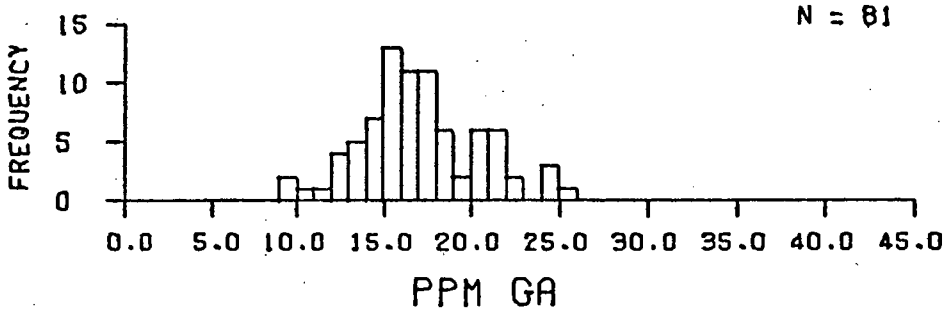

1471E0 0LIVINE GABBR0S.

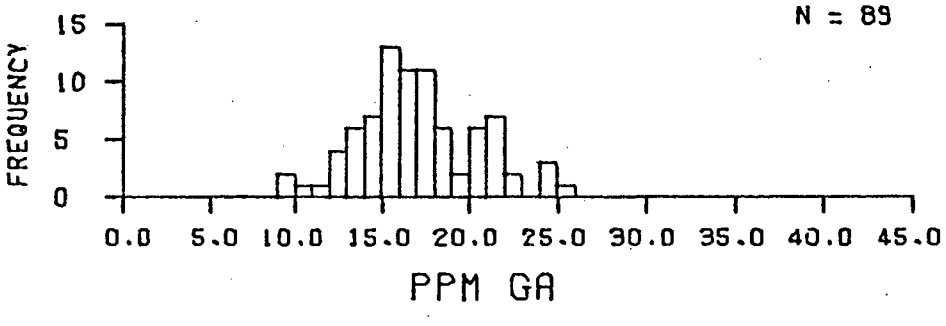

147100 PLAG + PYX + 0L R0CKS.

FIG. 49A. GABBR0ID R0CKS.

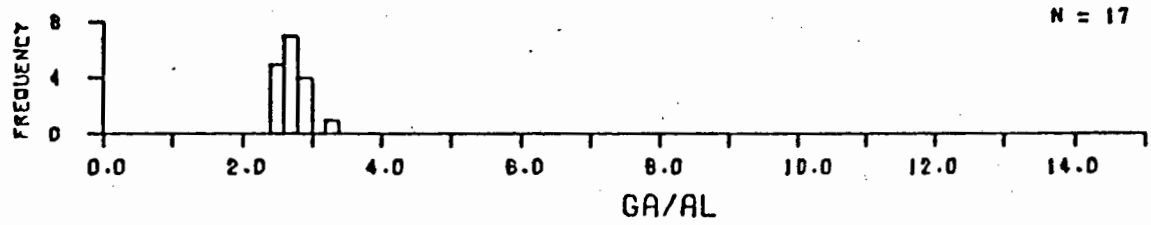

1471E2 GABBRO-PICRITES.

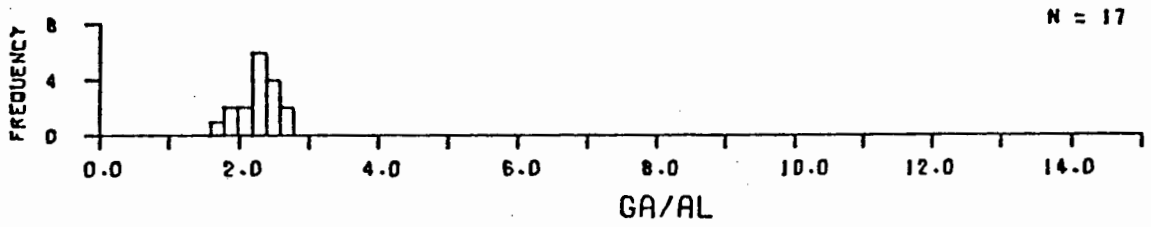

1471E1 OLIVINE FERROGABBROS.

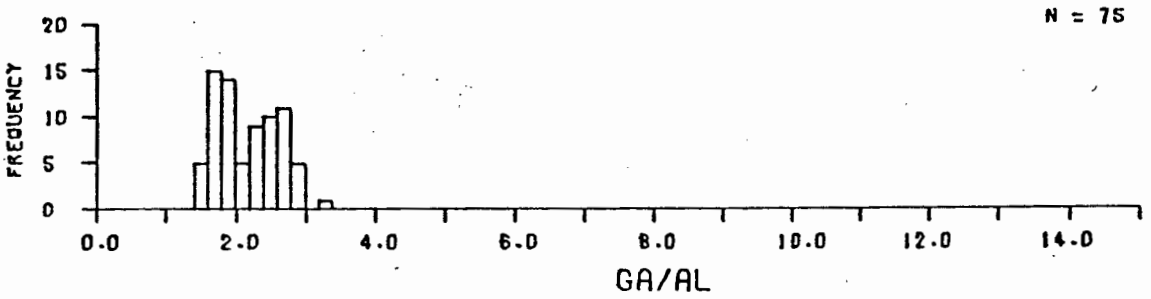

1471E0 OLIVINE GABBROS.

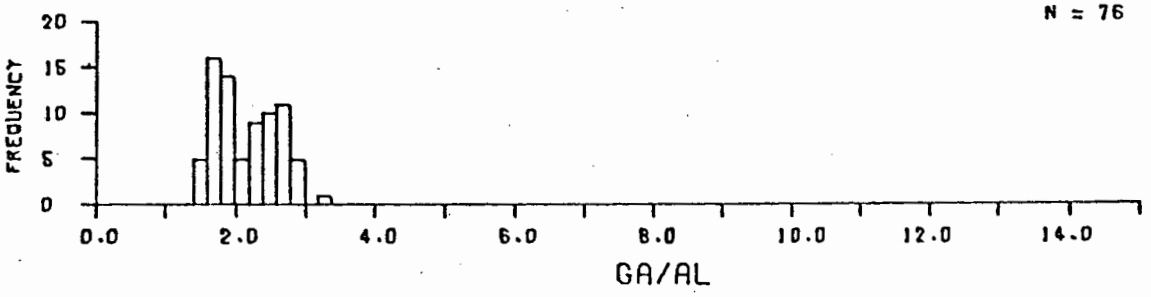

147100 PLAG + PYX + OL ROCKS.

FIG. 49B. GABBROID ROCKS.

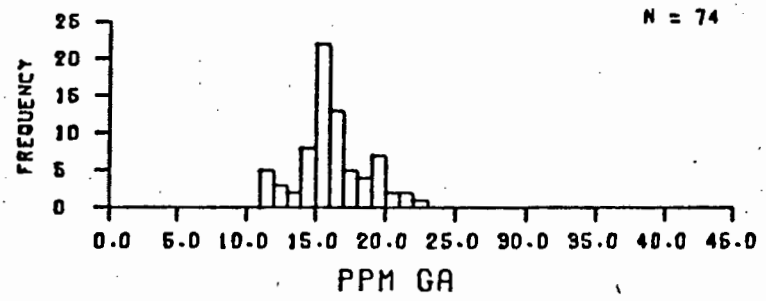

1472AD DOLERITES.

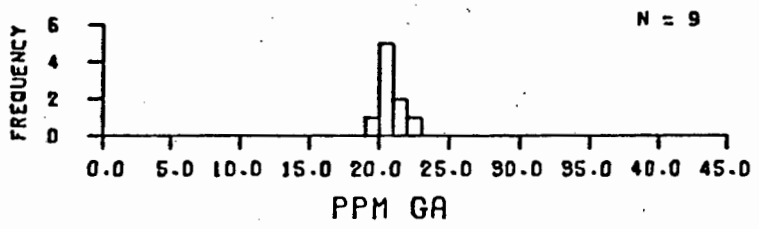

147282 OPX FERROGABBROS.

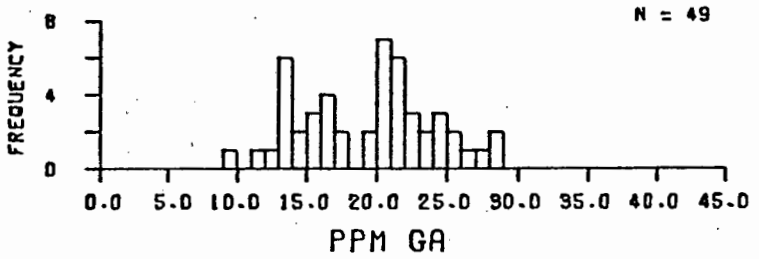

147280 GABBROS.

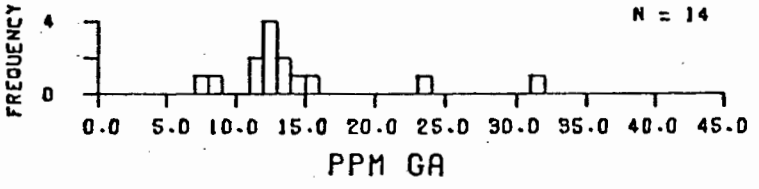

147220 NORITES.

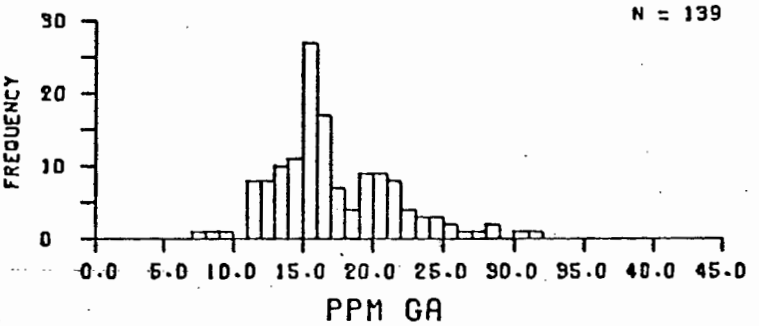

147200 PLAG + PYX ROCKS.

FIG. 50A. GABBROID ROCKS.

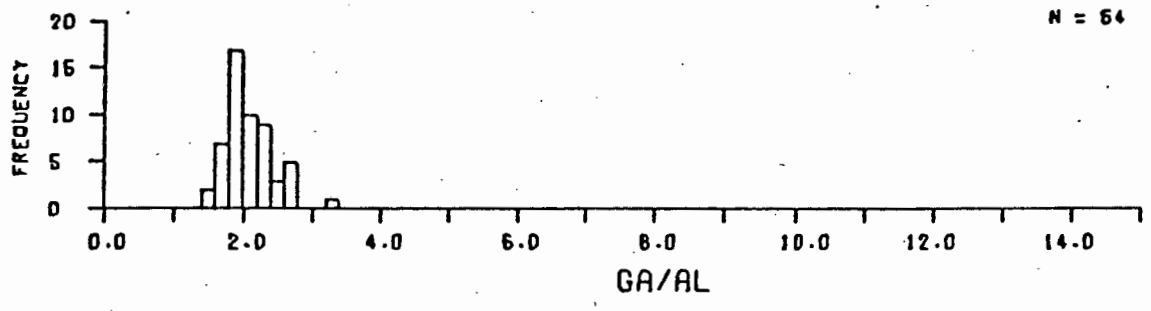

1472A0 D0LERITES.

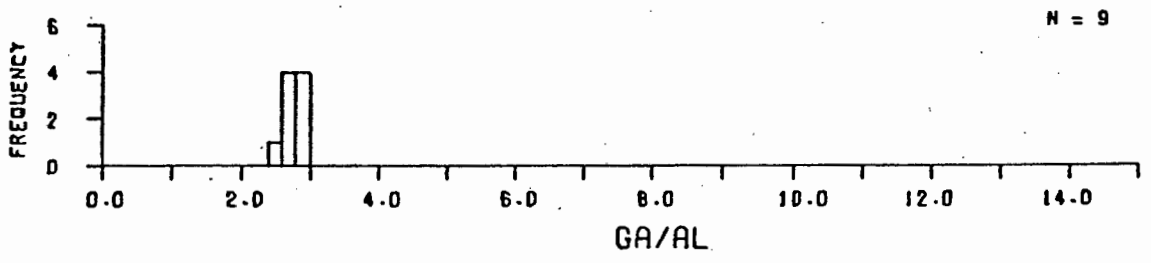

147282 FERR0GABBR0S.

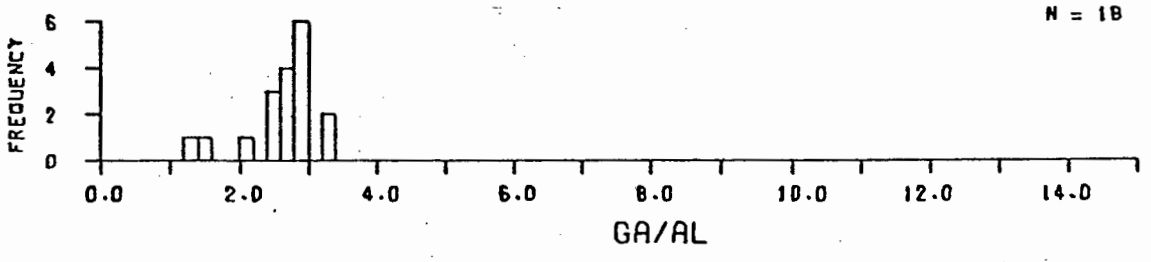

147280 GABBR0S.

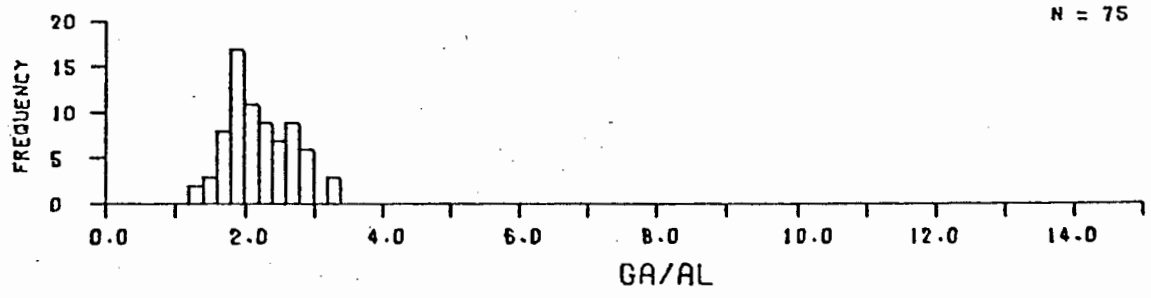

147200 PLAG + PYX R0CKS.

FIG. 50B. GABBR0ID R0CKS.

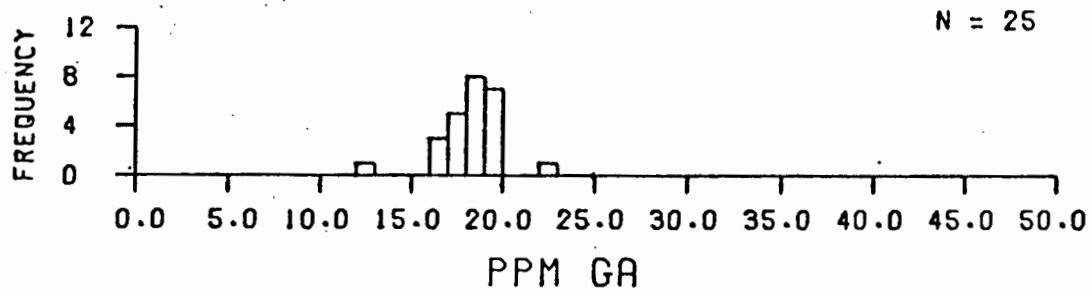

157300 NEPH-BEARING OL GABBROS.

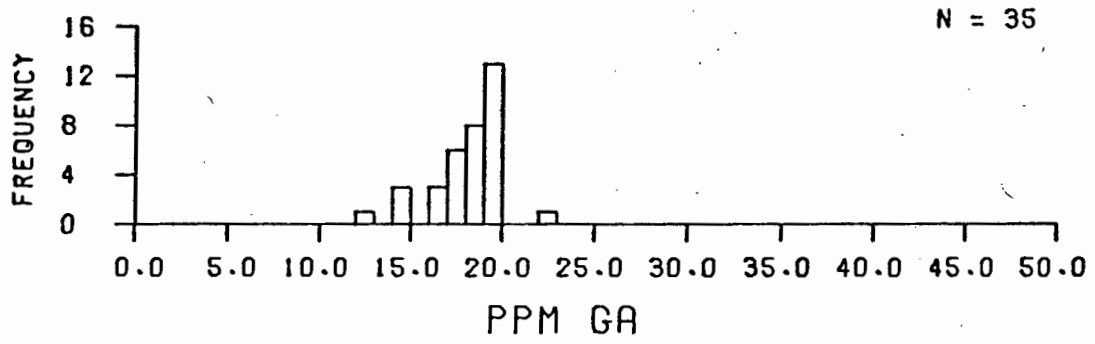

157000 FOID-BEARING GABBROS.

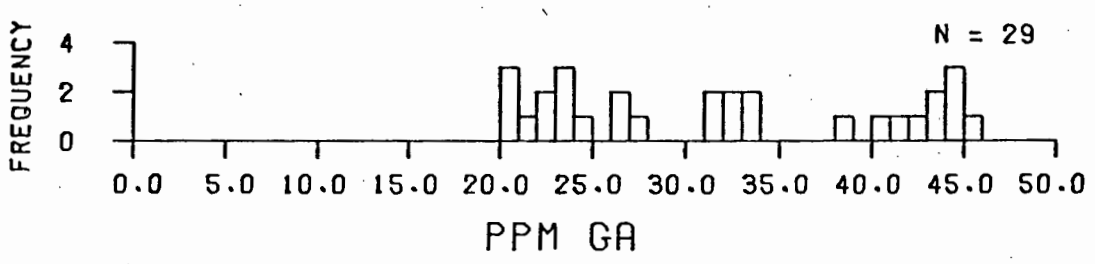

152000 FOID-BEARING SYENITES.

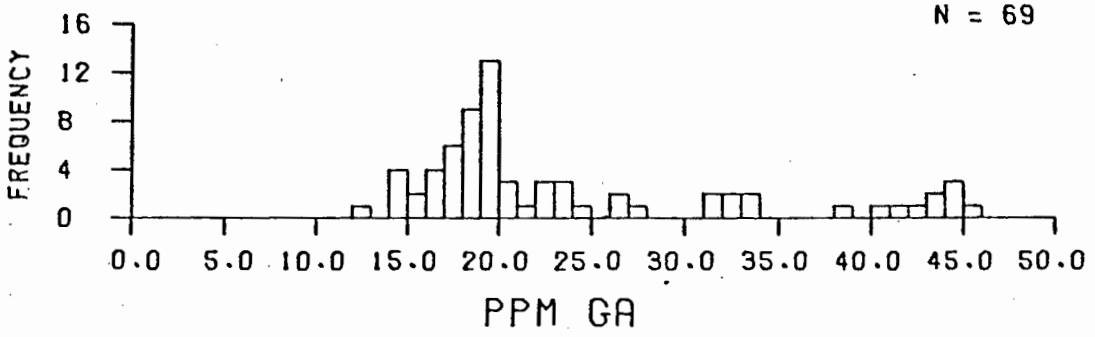

150000 A + P +- F ROCKS.

FIG. 51A. A + P +- F ROCKS.

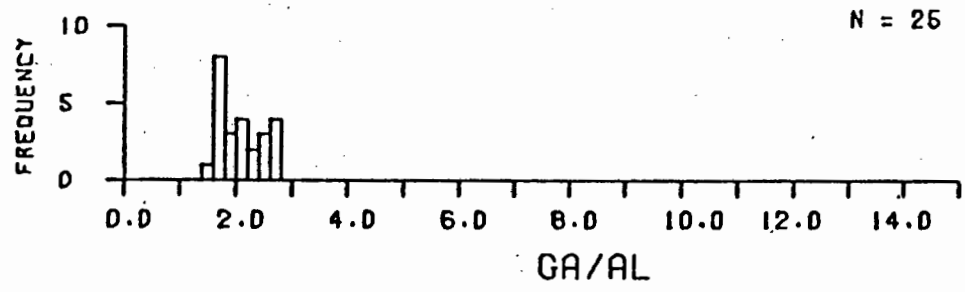

157300 NEPH-BEARING OL GABBROS.

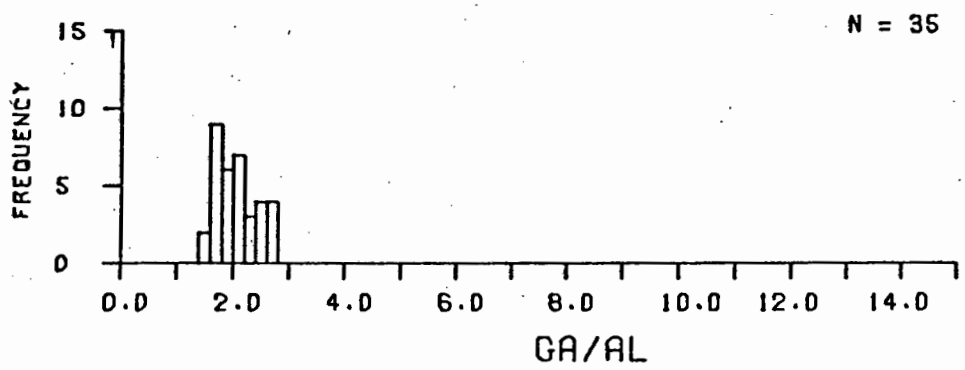

157000 FOID-BEARING GABBROS.

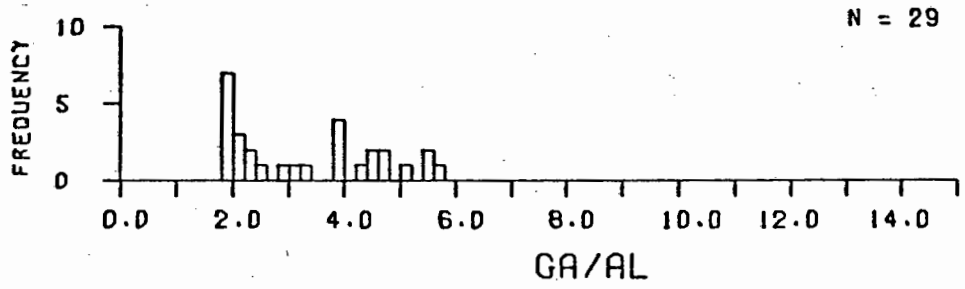

152000 FOID-BEARING SYENITES.

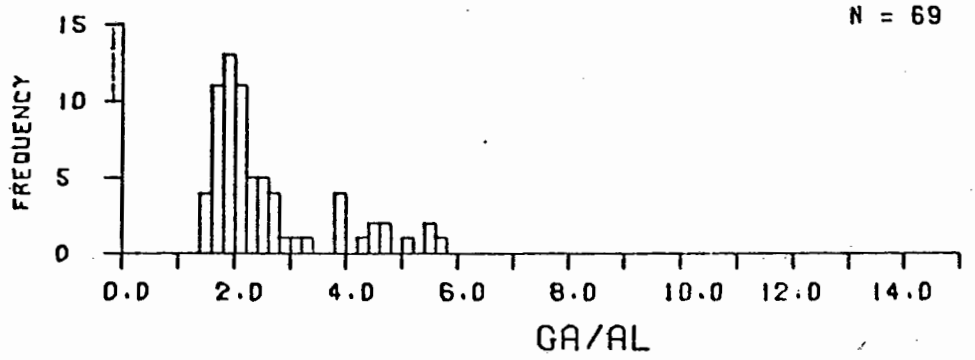

150000 A + P +- F ROCKS.

FIG. 51B. A + P +- F ROCKS.

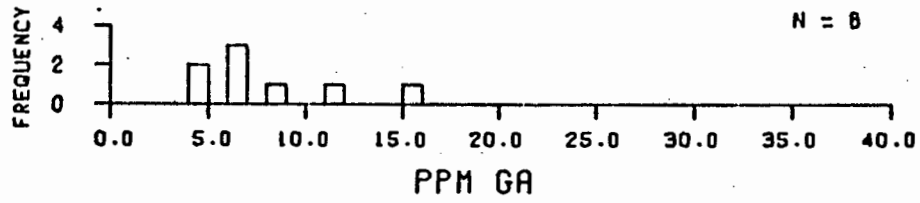

183000 0L + PYX + PLAG R0CKS.

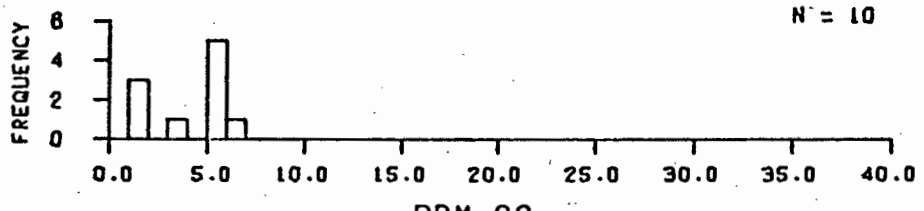

181600 HARZBURGITES.

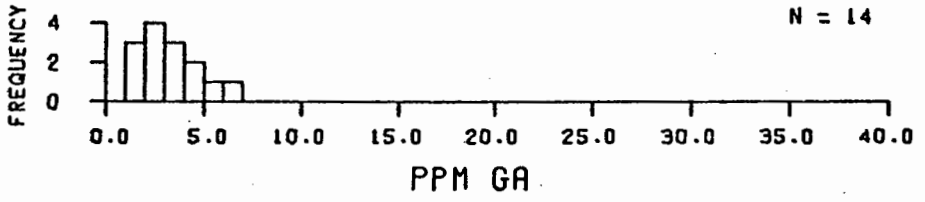

181200 PYR0XENITES.

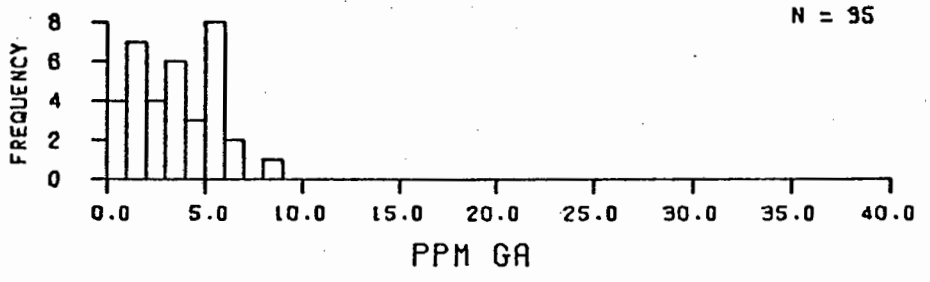

181000 0L + PYX R0CKS.

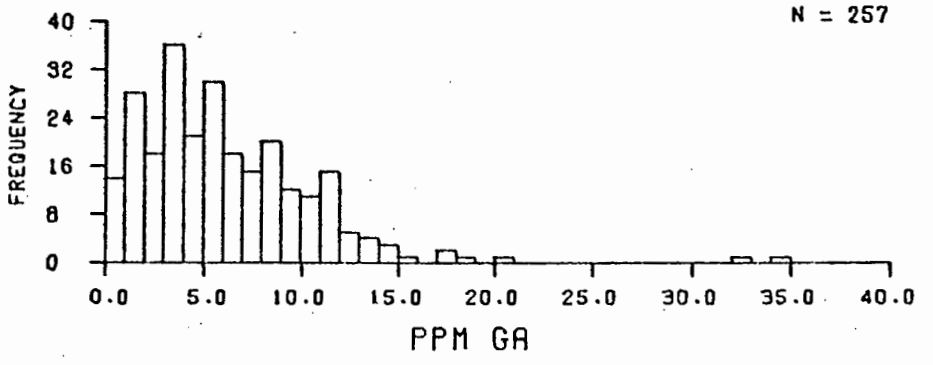

180000 ULTRAMAFIC R0CKS.

FIG. 53A. ULTRAMAFIC R0CKS.

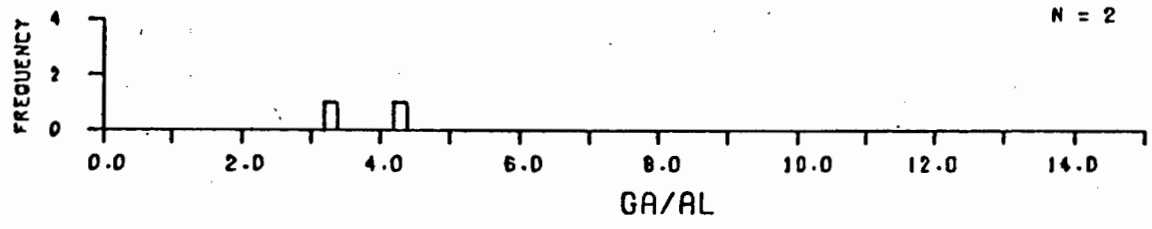

183000 OL + PYX + PLAG ROCKS.

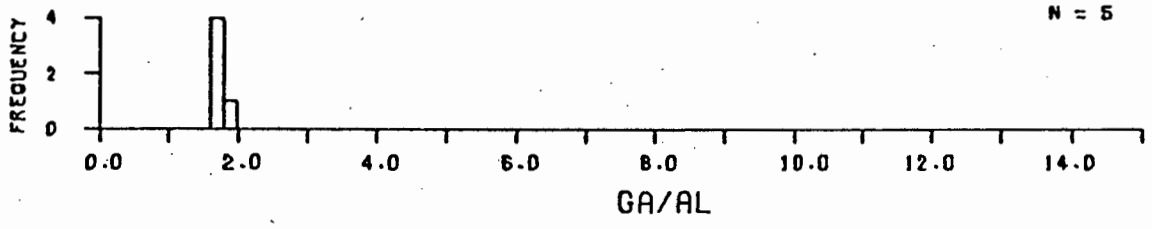

181600 HARZBURGITES.

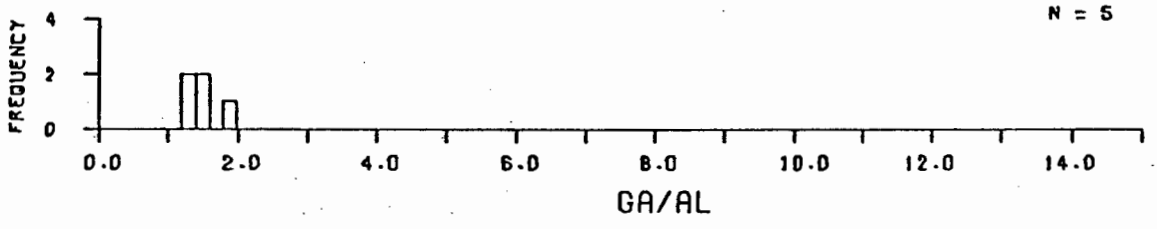

181200 PYROXENITES.

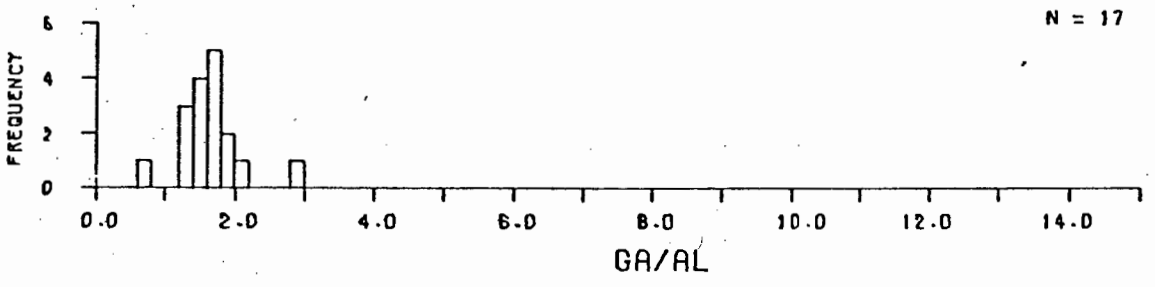

181000 OL + PYX ROCKS.

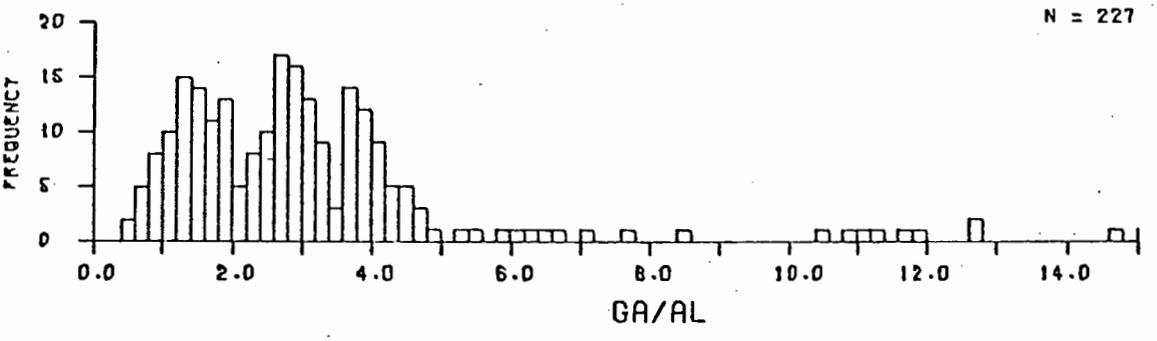

180000 ULTRAMAFIC ROCKS.

FIG. 53B. ULTRAMAFIC ROCKS.

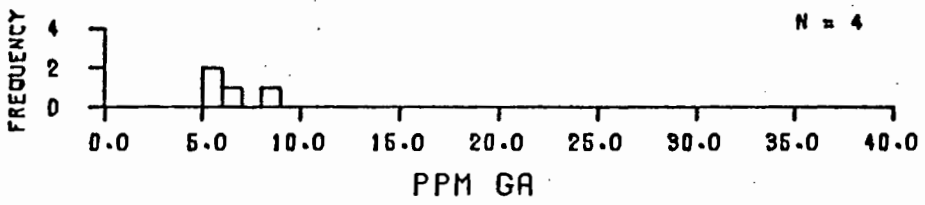

187400 NON-MICA CARB.-RICH KIMBERLITE.

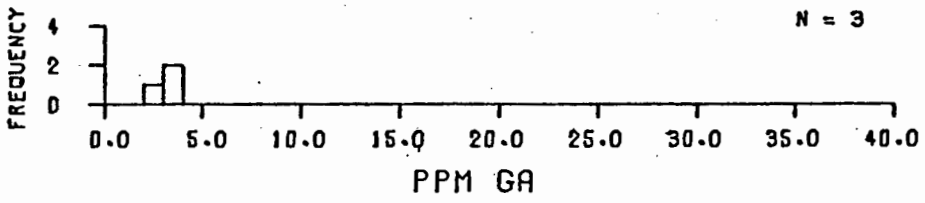

187300 CARBONATITIC KIMBERLITE.

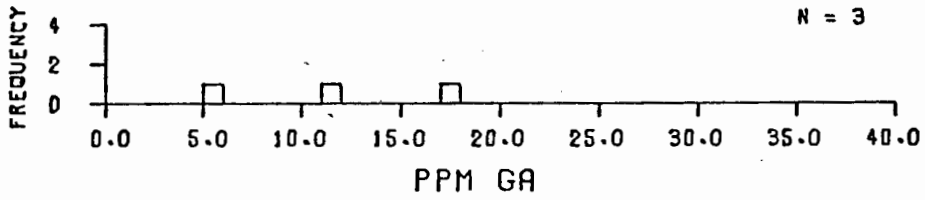

187200 NON-MICACEOUS KIMBERLITES.

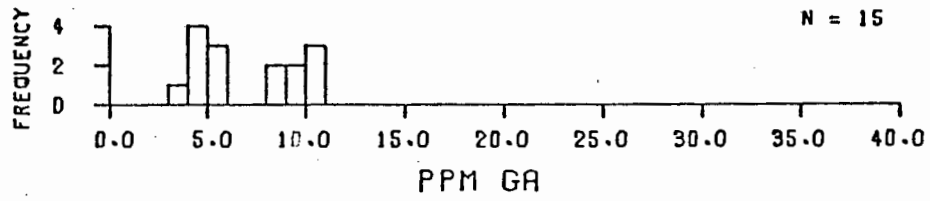

187100 MICA-RICH KIMBERLITES.

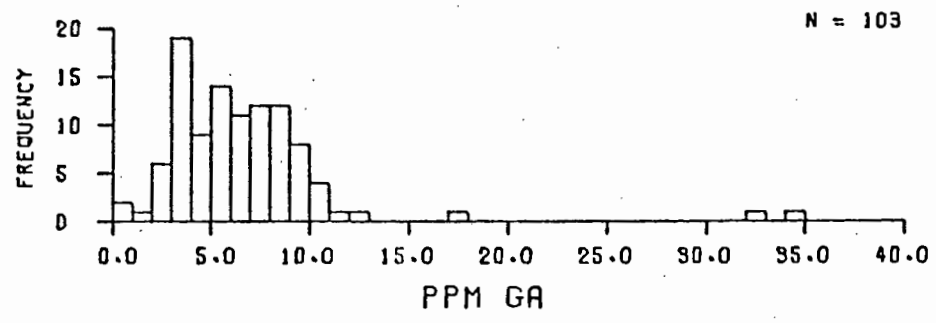

187000 KIMBERLITES.

FIG. 54A. KIMBERLITES.

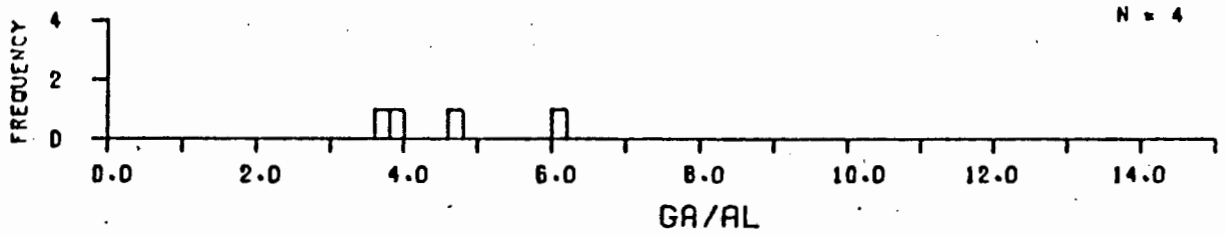

187400 NON-MICA CARBONATE-RICH KIMBERLITES.

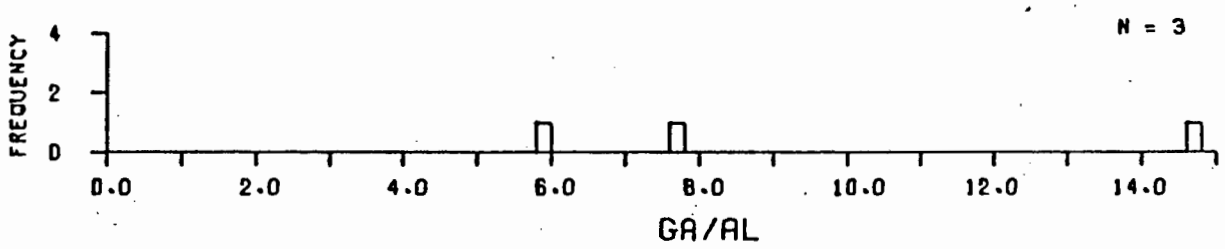

187300 CARBONATITIC KIMBERLITES.

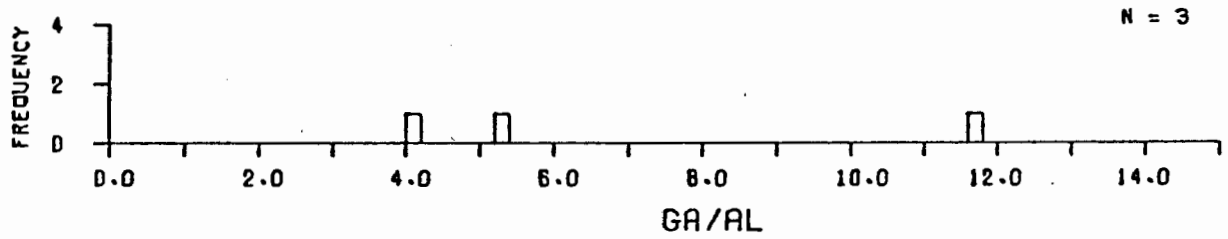

187200 NON-MICACEOUS KIMBERLITES.

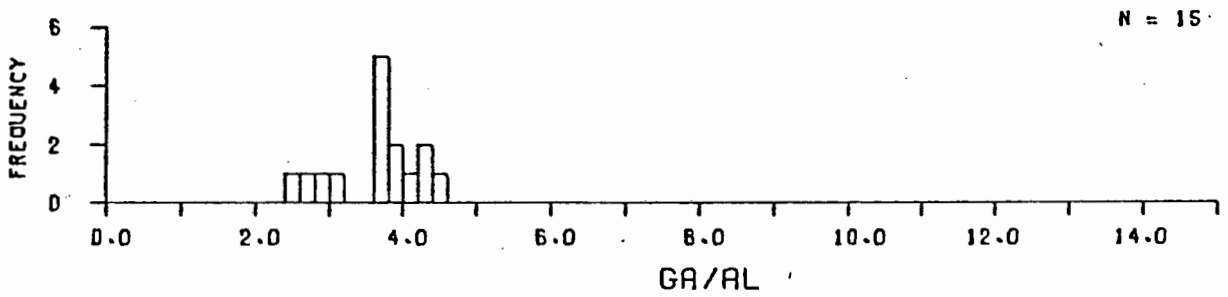

187100 MICA-RICH KIMBERLITES.

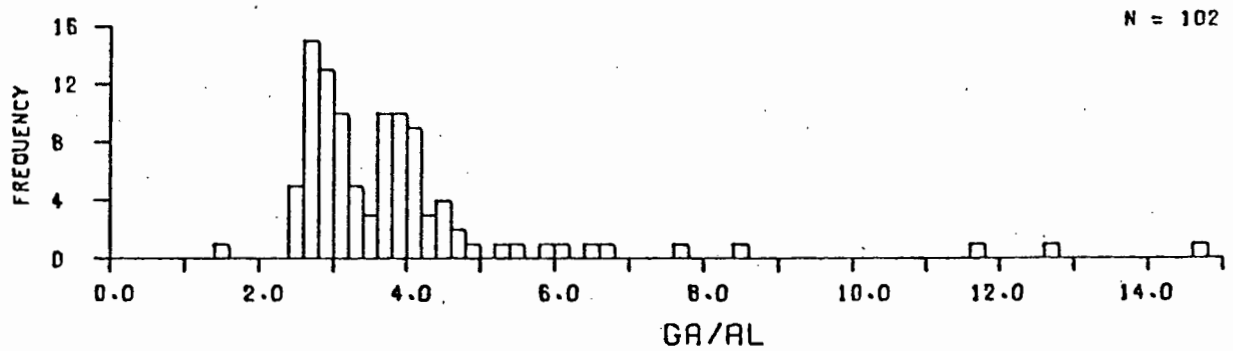

187000 KIMBERLITES.

FIG. 54B. KIMBERLITES.

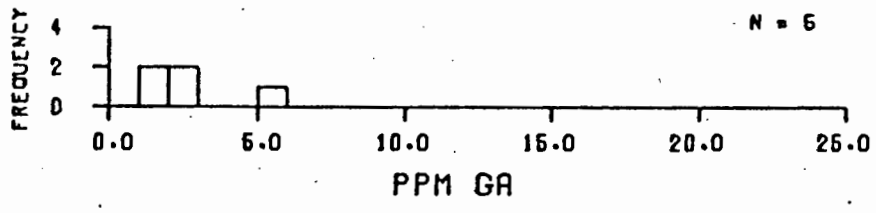

188A00 PERIDOTITE XENOLITHS.

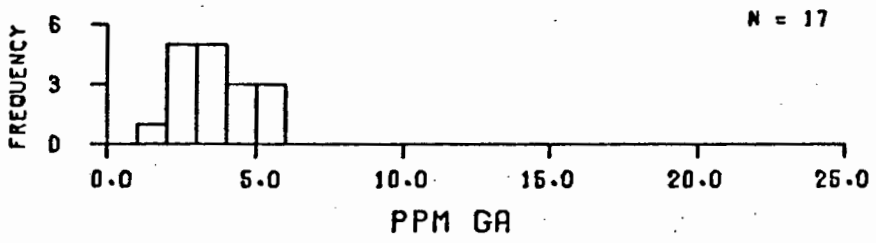

188900 PYROXENITE XENOLITHS.

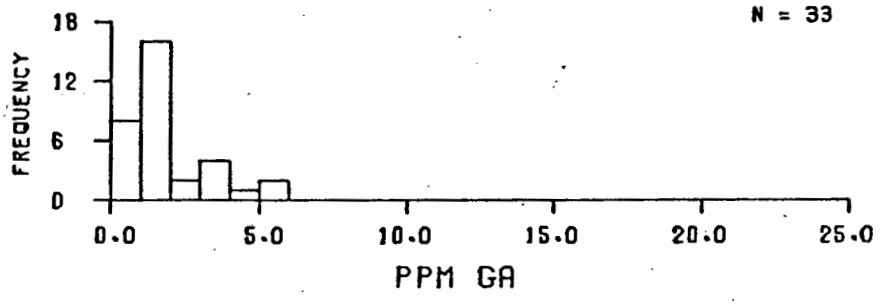

188810 CP XENOLITHS.

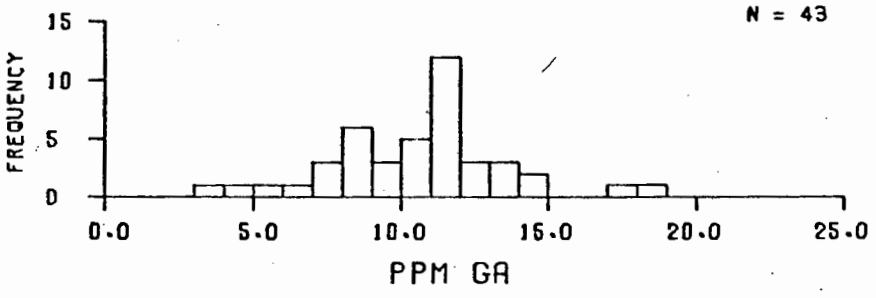

188100 ECLOGITE XENOLITHS.

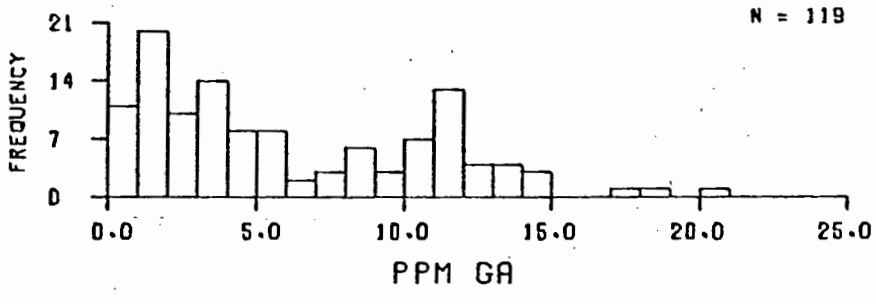

188000 XENOLITHS.

FIG. 55A. KIMBERLITIC XENOLITHS.

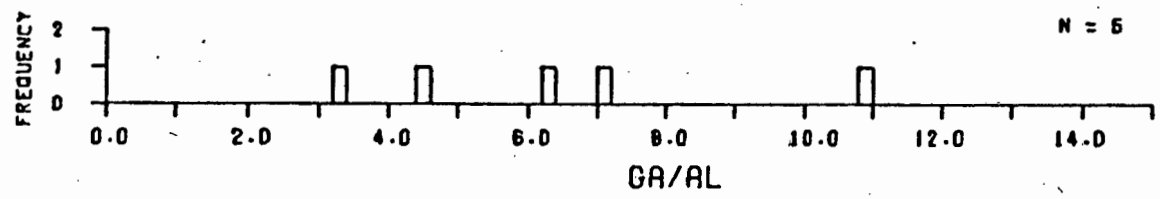

188A00 PERIDOTITE XENOLITHS.

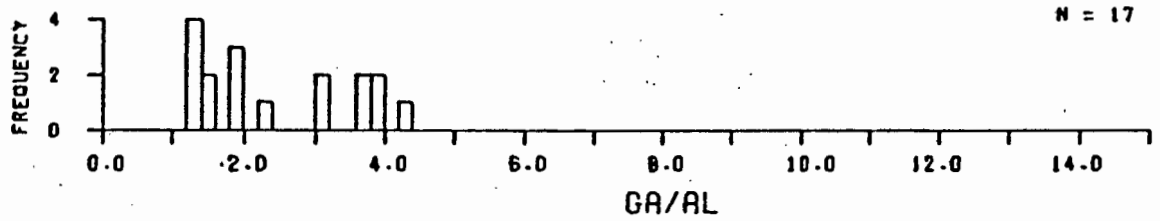

188900 PYROXENITE XENOLITHS.

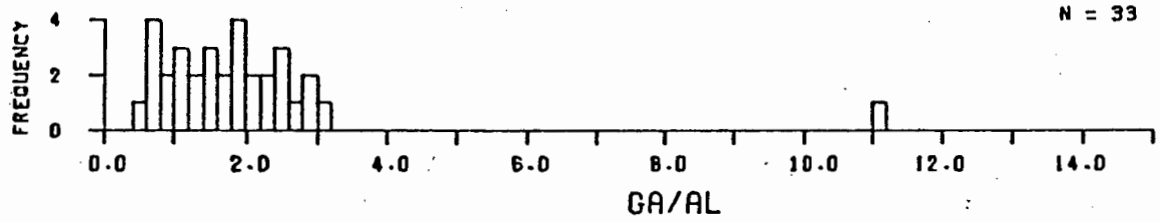

188810 CP XENOLITHS.

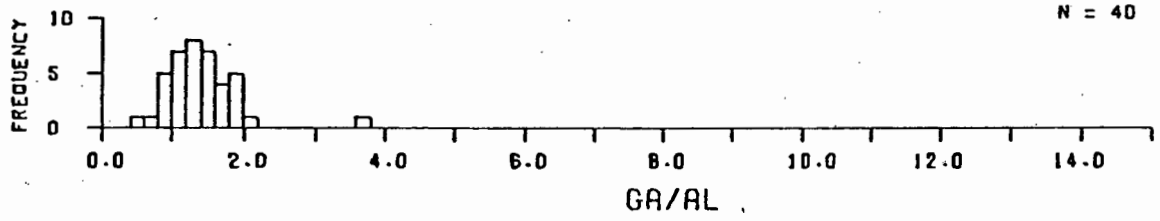

188100 ECLOGITE XENOLITHS.

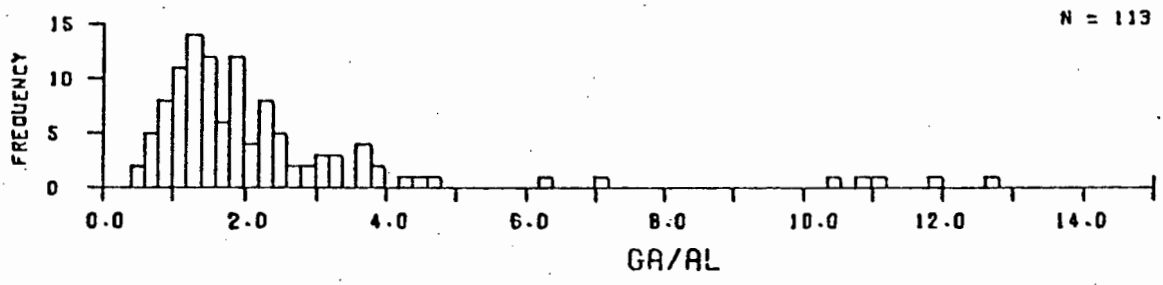

188000 ALL XENOLITHS.

FIG. 55B. KIMBERLITIC XENOLITHS.

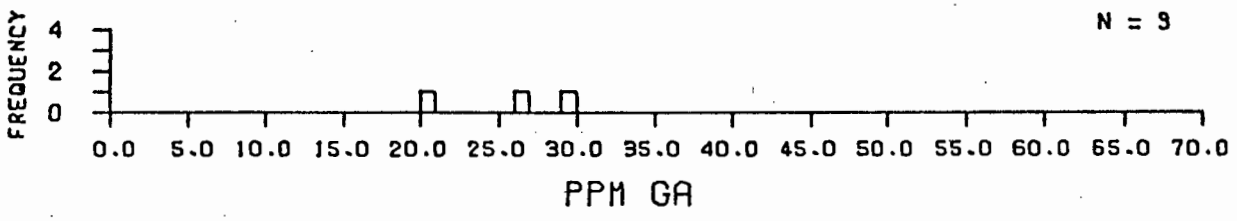

230000 A + P + Q ROCKS.

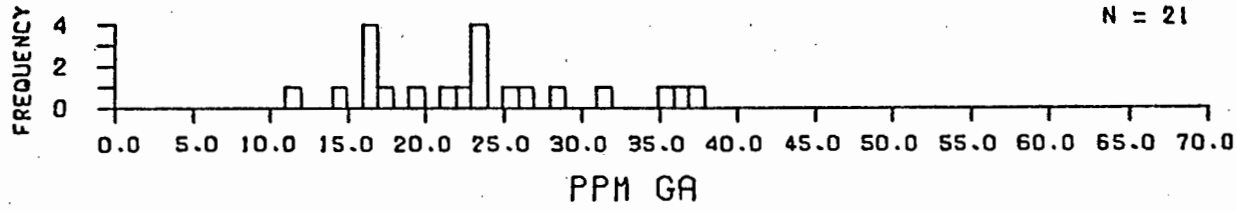

220000 Q + A + P ROCKS.

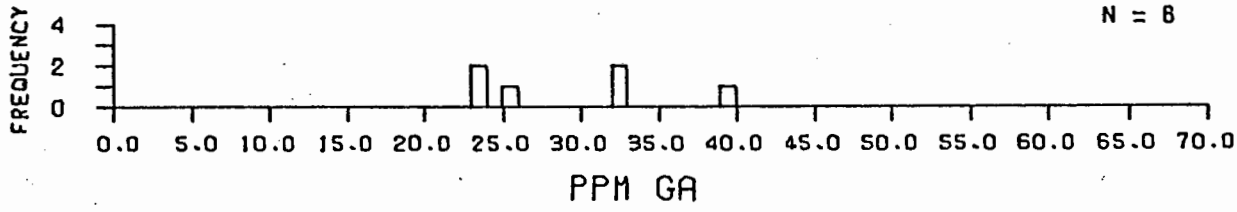

210000 GLASSY ROCKS.

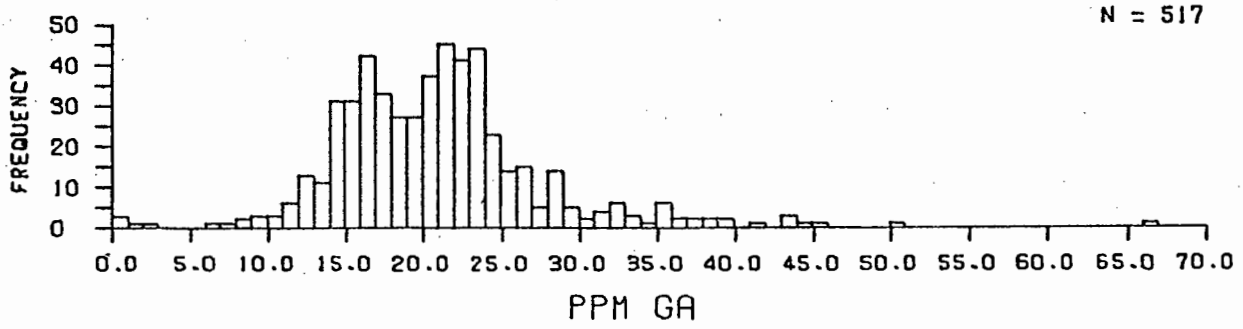

200000 VOLCANIC ROCKS.

FIG. 56A. VOLCANIC ROCKS.

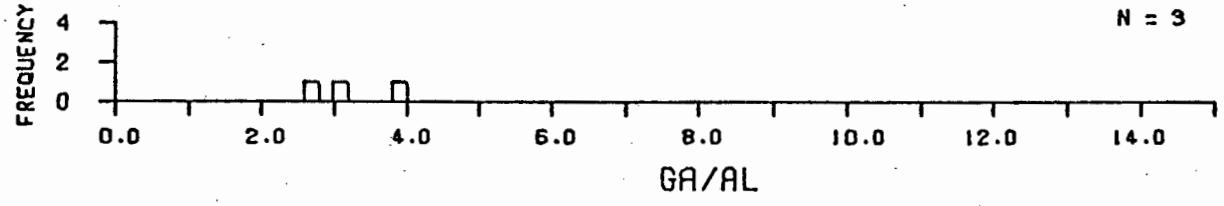

230000 A + P + Q ROCKS.

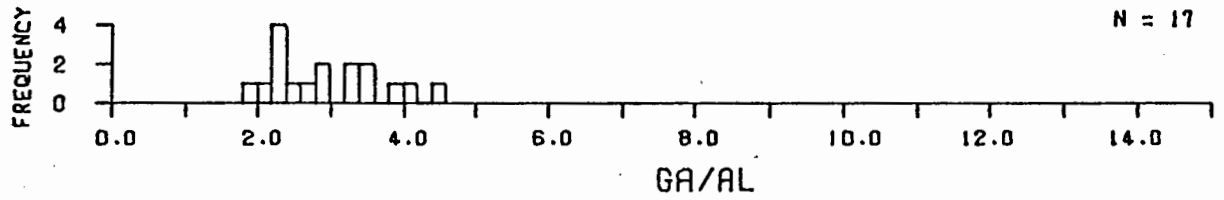

220000 Q + A + P ROCKS.

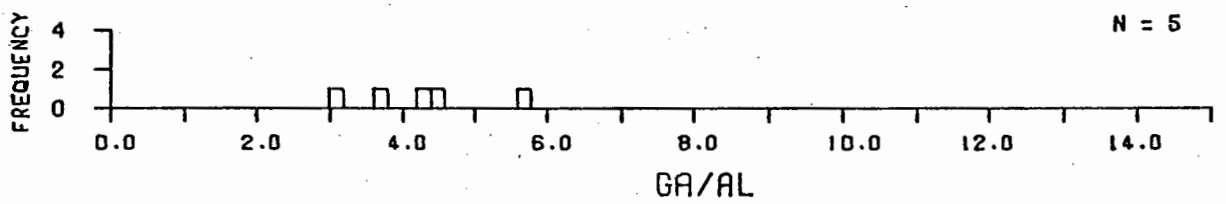

210000 GLASSY ROCKS.

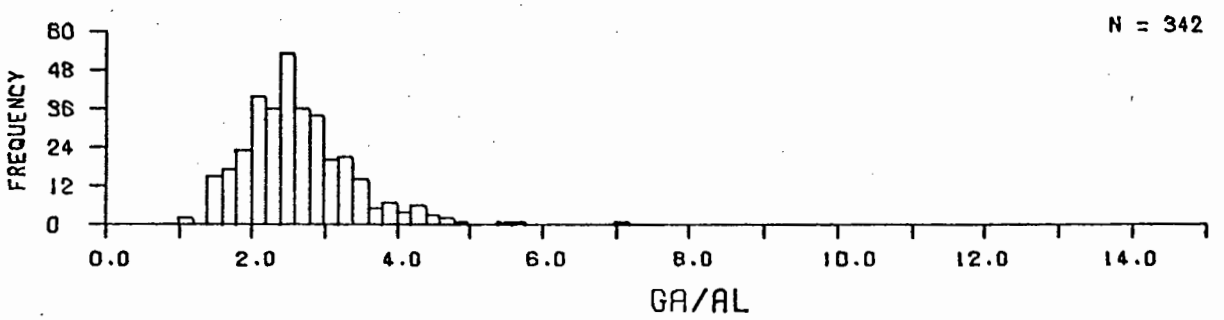

200000 VOLCANIC ROCKS.

FIG. 56B. VOLCANIC ROCKS.

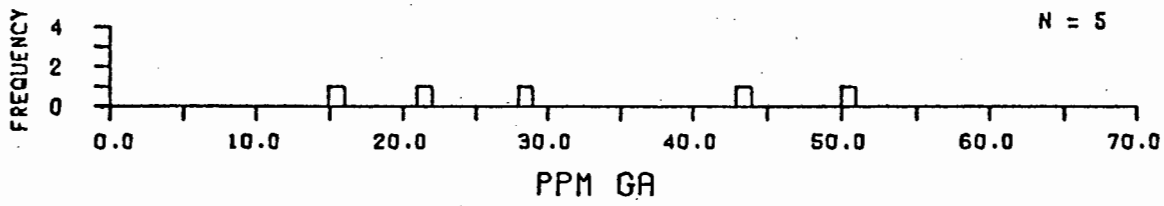

290000 FRAGMENTAL ROCKS.

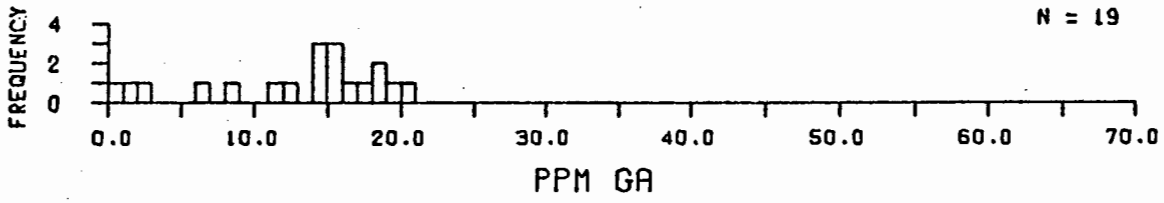

280000 ULTRAMAFIC ROCKS.

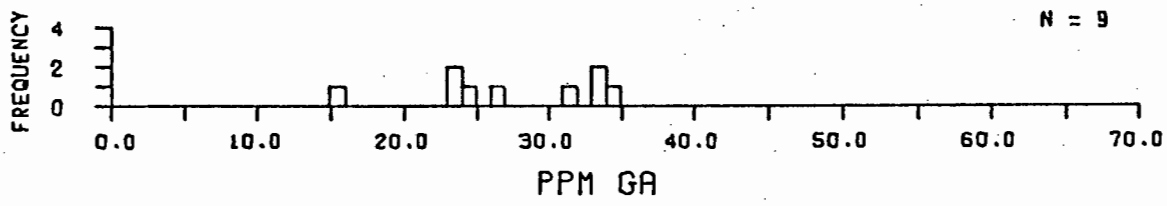

270000 F +- A +- P ROCKS.

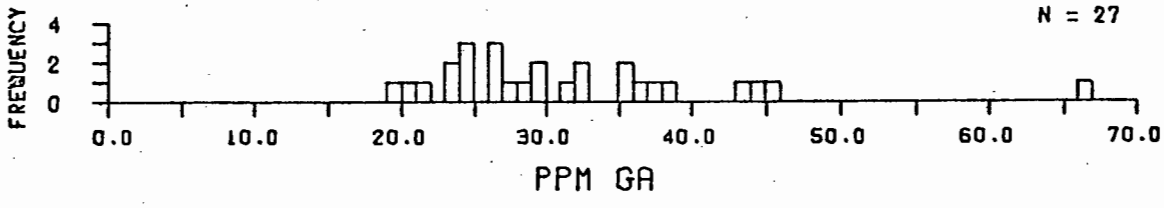

260000 A + P + F ROCKS.

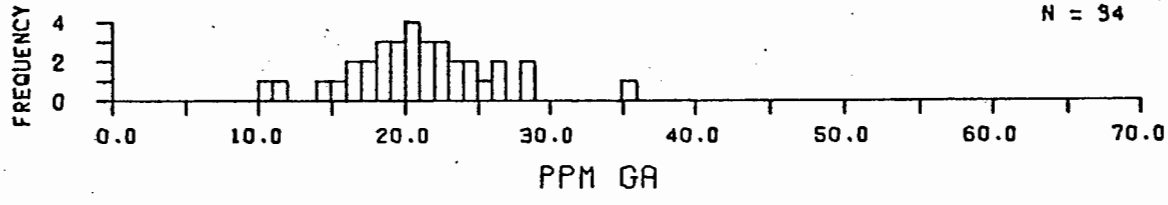

250000 A + P +- F ROCKS.

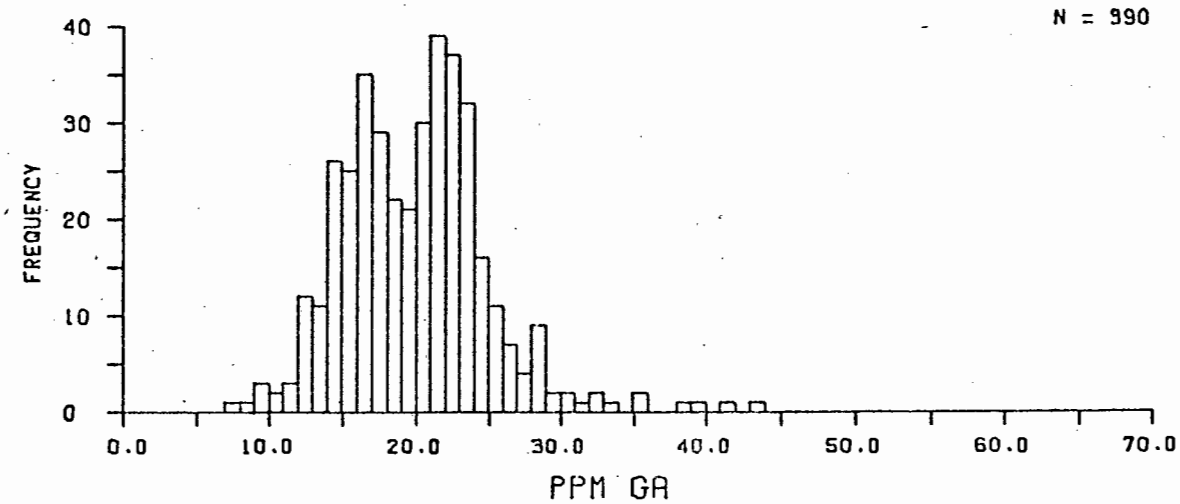

240000 A + P +- Q ROCKS.

FIG. 57A. VOLCANIC ROCKS.

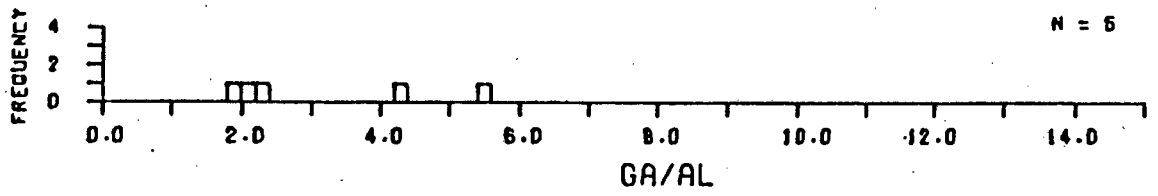

290000 FRAGMENTAL ROCKS.

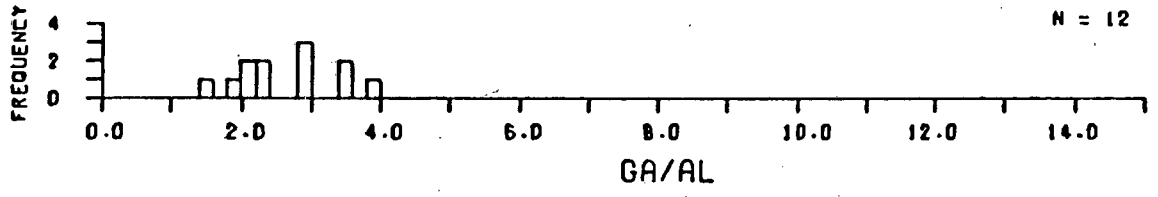

280000 ULTRAMAFIC ROCKS.

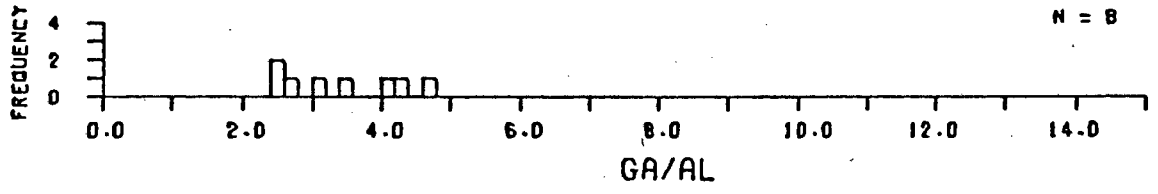

270000 F +- A +- P ROCKS.

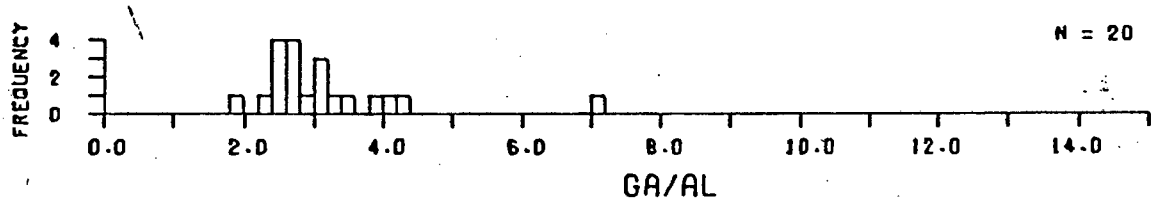

260000 A + P + F ROCKS.

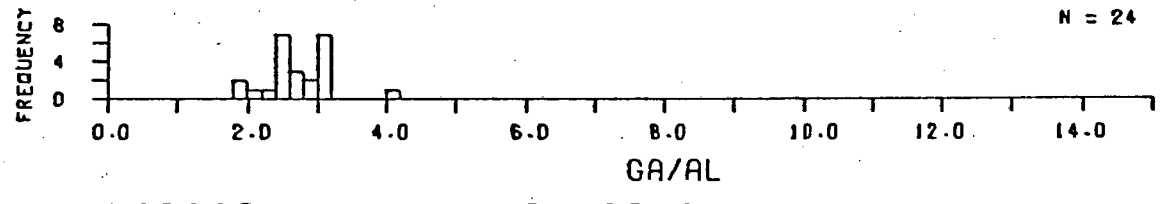

250000 A + P +- F ROCKS.

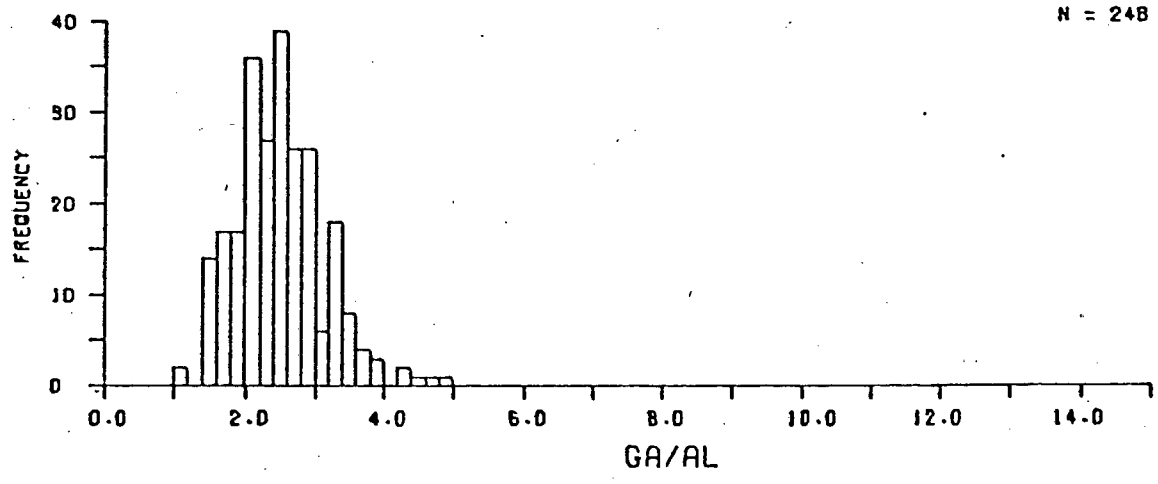

240000 A + P +- Q ROCKS.

FIG. 57B. VOLCANIC ROCKS.

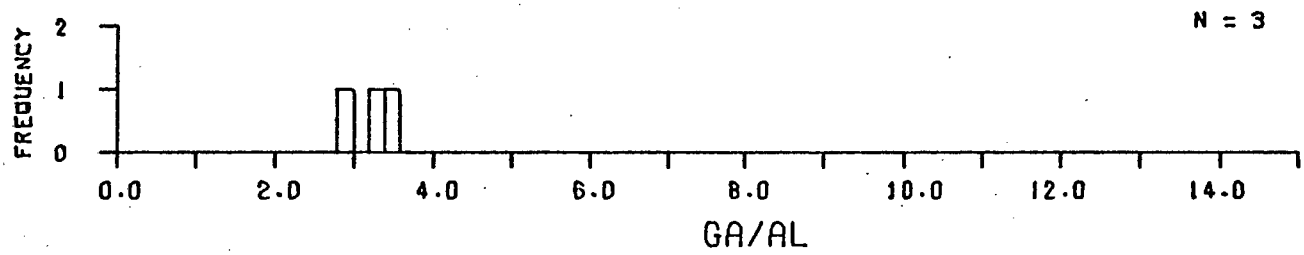

224000 DACITES.

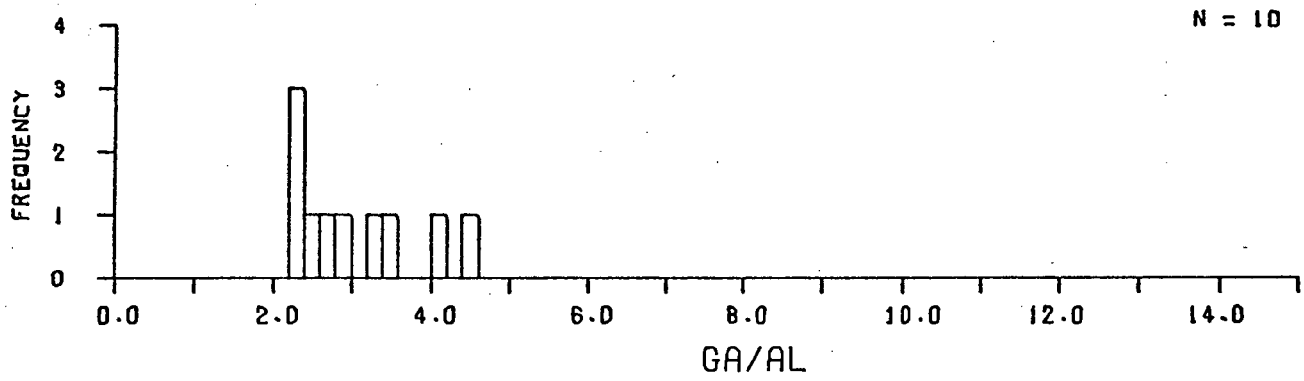

222000 RHYOLITES.

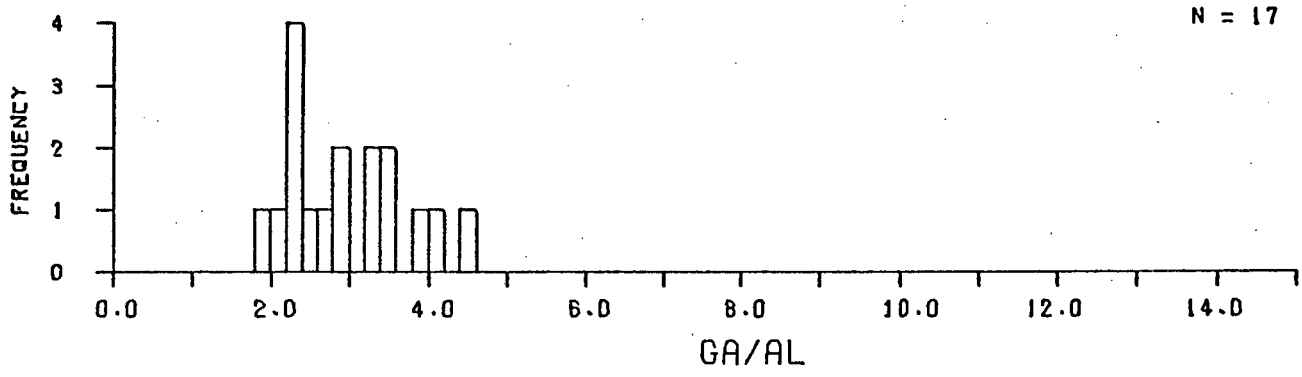

220000 Q + A + P ROCKS.

FIG. 58B. Q + A + P ROCKS.

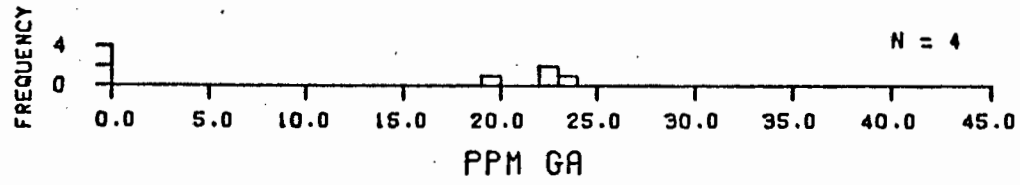

246000 ANDESITES.

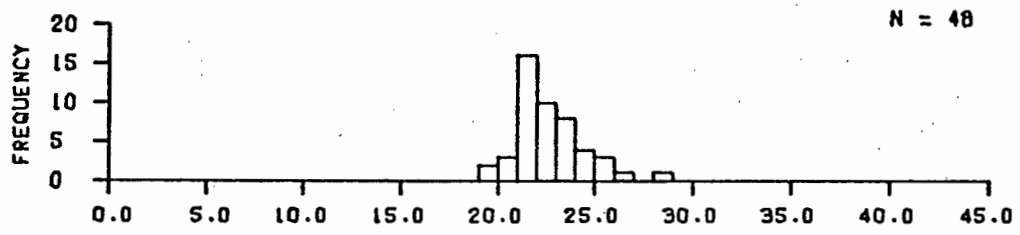

245000 LATITE BASALTS.

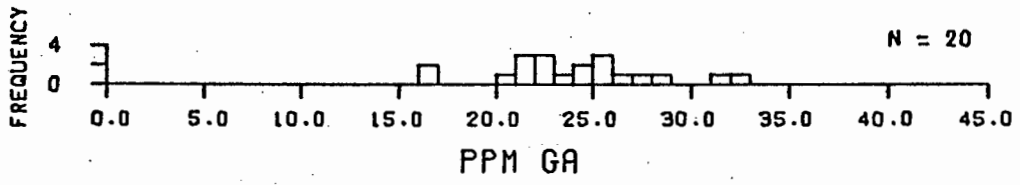

244000 LATITE ANDESITES.

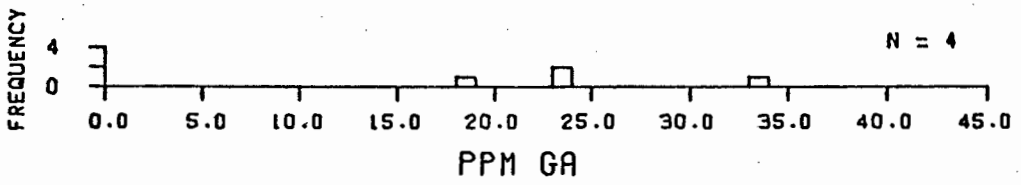

243000 LATITES.

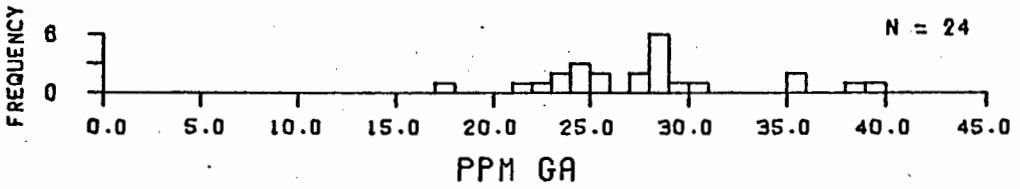

242000 TRACHYTES.

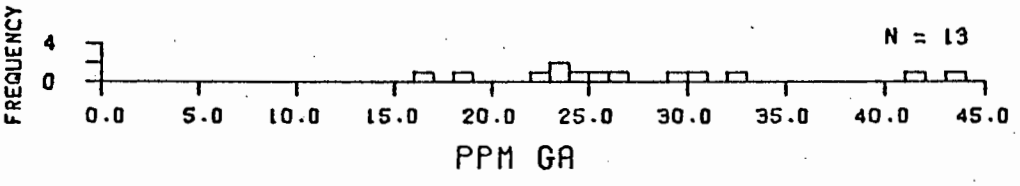

241000 ALKALI TRACHYTES.

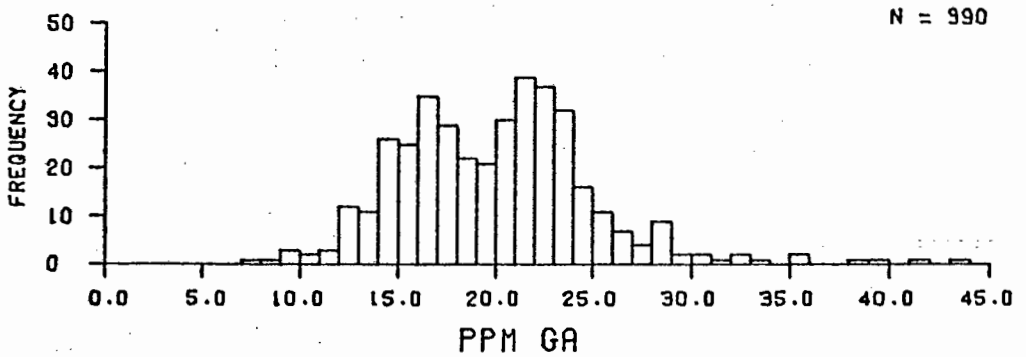

240000 A + P +- Q ROCKS.

FIG. 59A. A + P +- Q ROCKS.

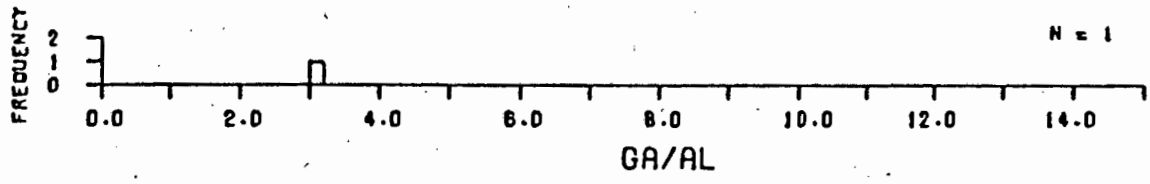

246000 ANDESITES.

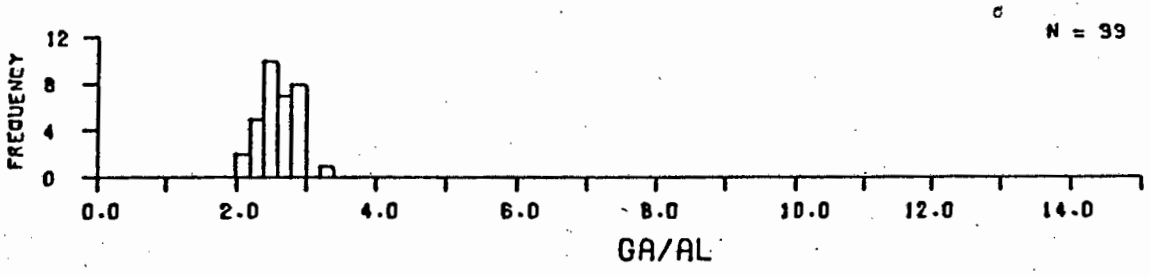

245000 LATITE BASALTS.

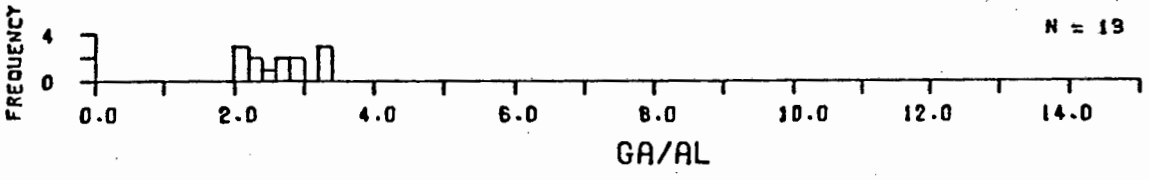

244000 LATITE ANDESITES.

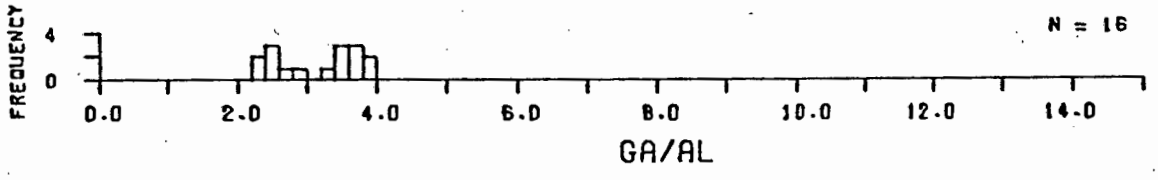

242000 TRACHYTES.

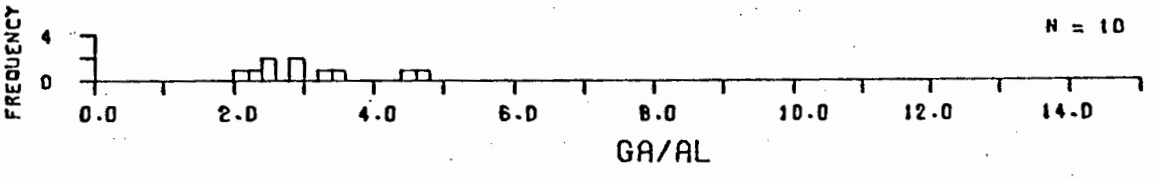

241000 ALKALI TRACHYTES.

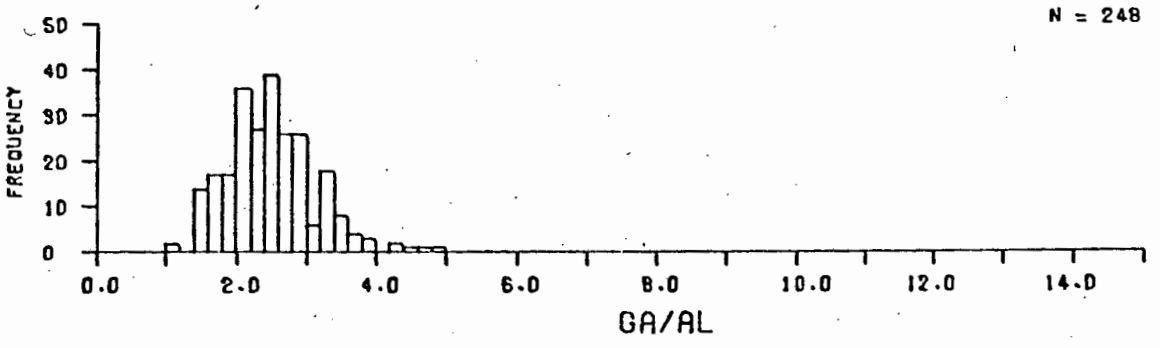

240000 A + P +- Q ROCKS.

FIG. 59B. A + P +- Q ROCKS.

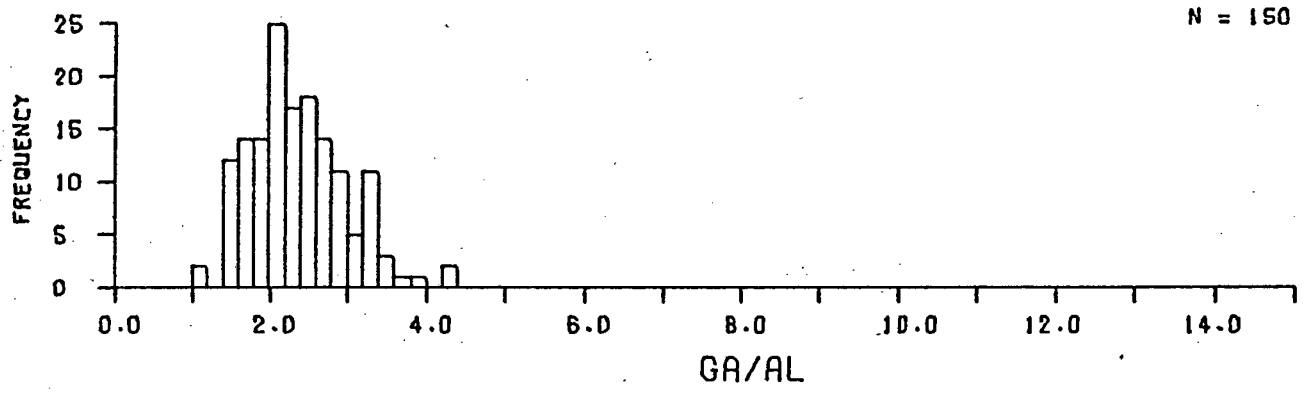

247200 PLAG + PYX ROCKS.

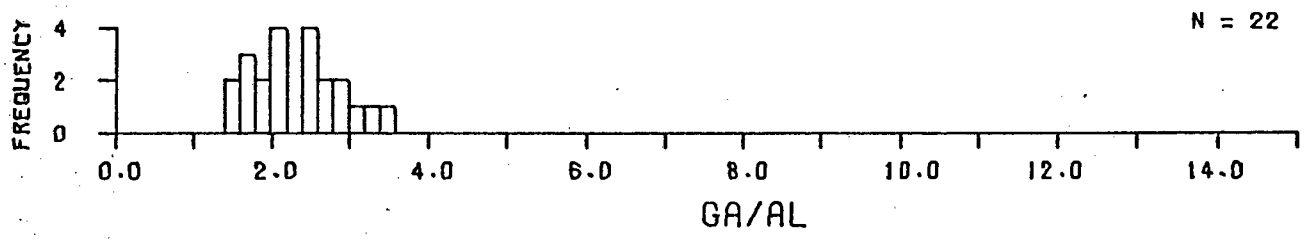

247100 PLAG + PYX + OL ROCKS.

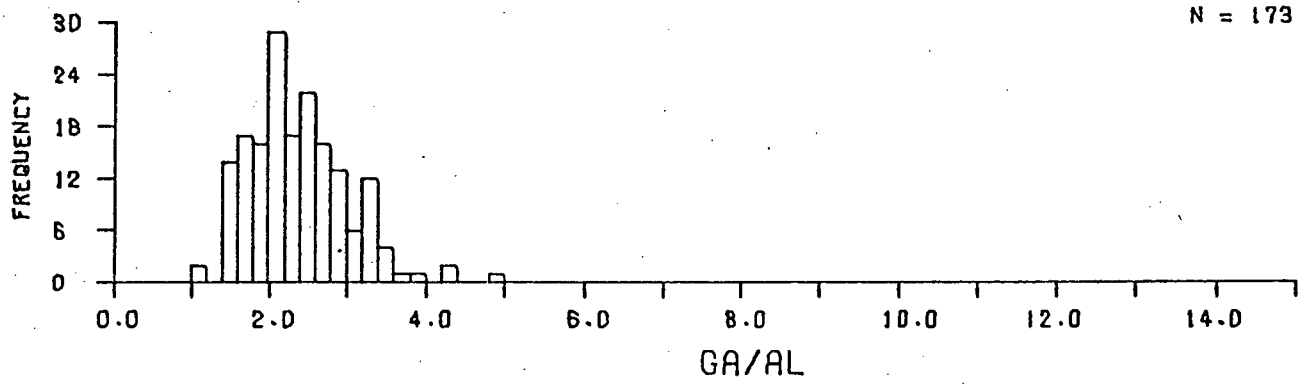

247000 BASALTIC ROCKS.

FIG. 60B. BASALTIC ROCKS.

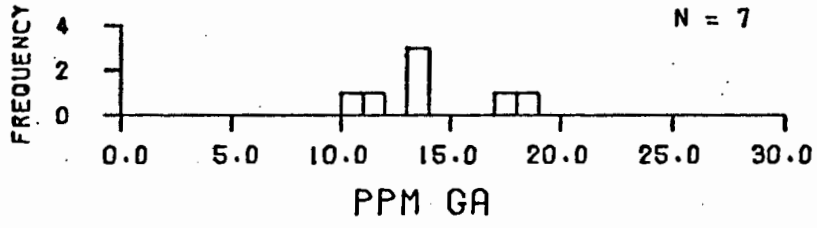

247111 PICRITIC BASALTS.

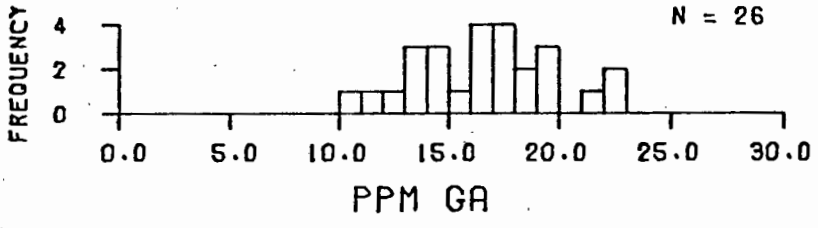

247110 OLIVINE BASALTS.

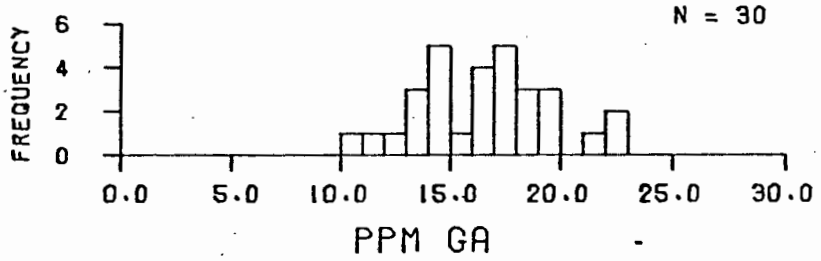

247100 PLAG + PYX + OL ROCKS.

FIG. 61A. PLAG + PYX + OL ROCKS.

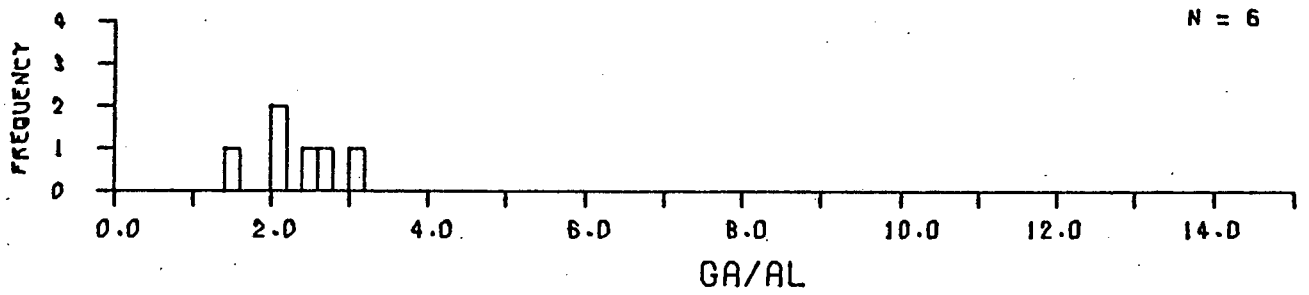

247111 PICRITIC BASALTS.

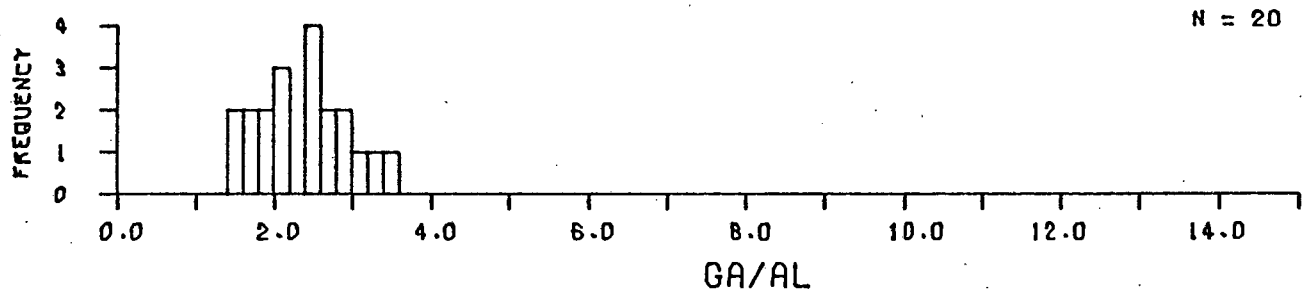

247110 OLIVINE BASALTS.

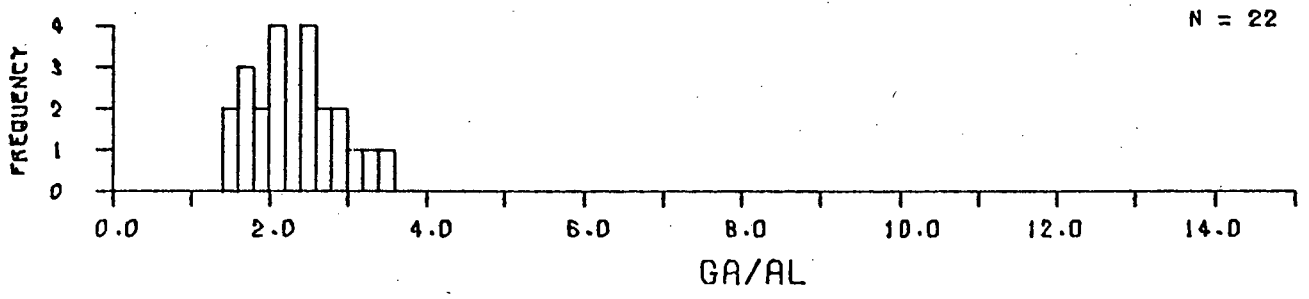

247100 PLAG + PYX + OL ROCKS.

FIG. 61B. PLAG + PYX + OL ROCKS.

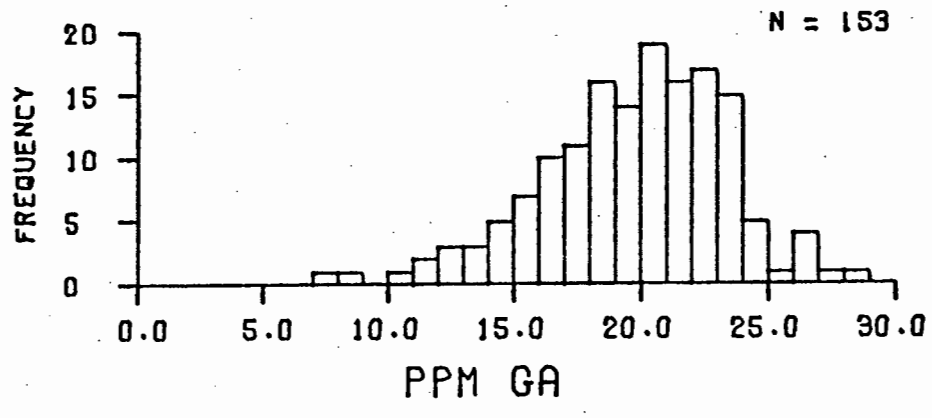

247220 BASALTS.

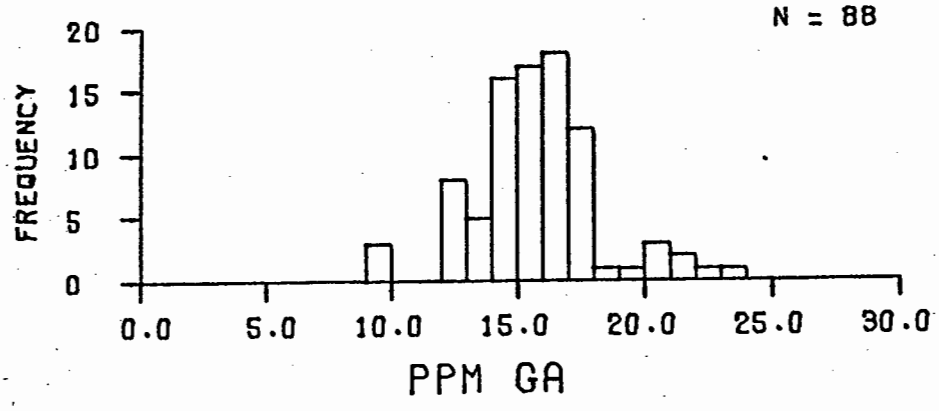

247210 THOLEIITE BASALTS.

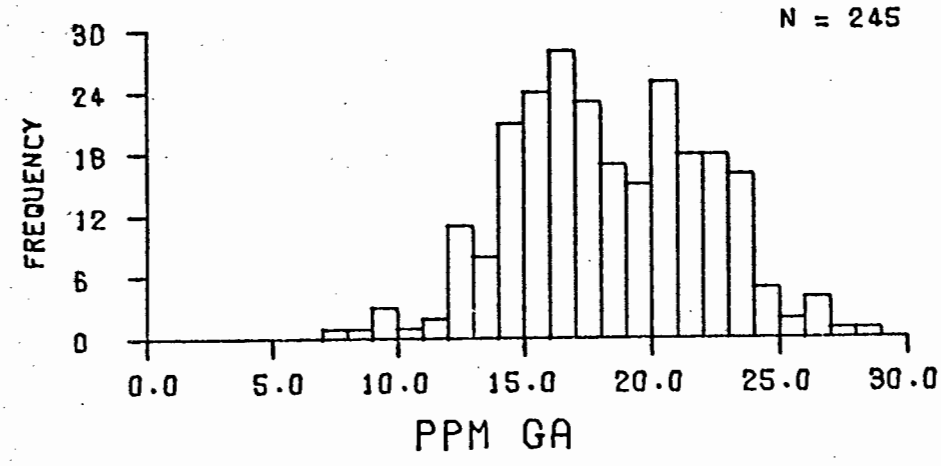

247200 PLAG + PYX ROCKS.

FIG. 62A. PLAG + PYX ROCKS.

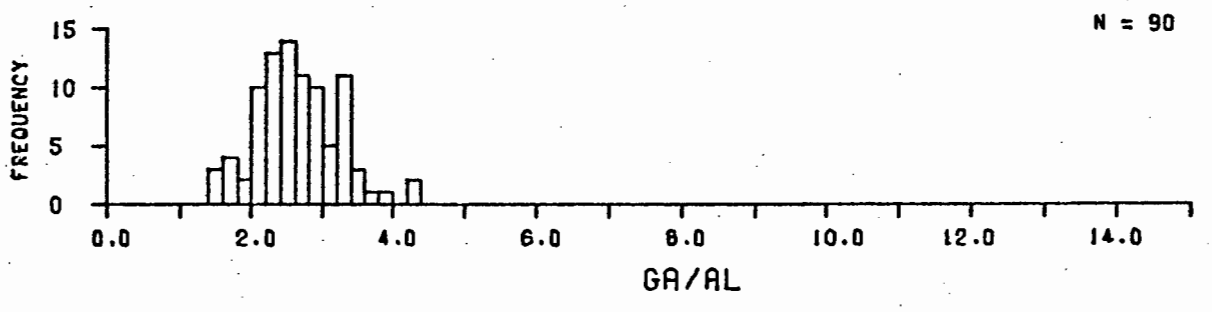

247220 BASALTS.

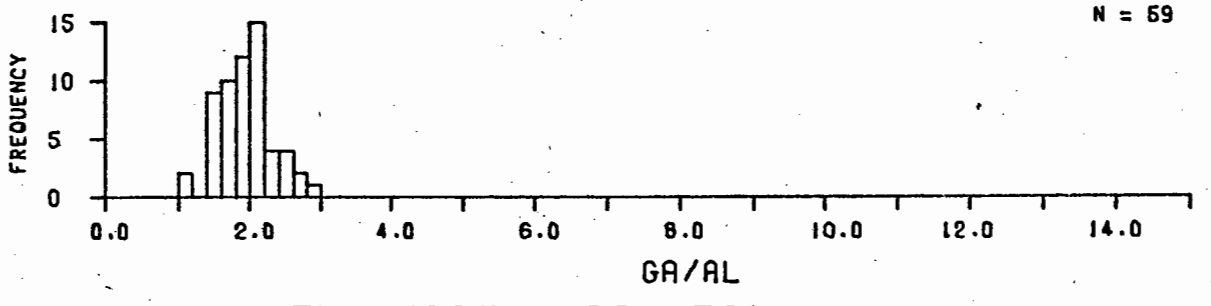

247210 THOLEIITE BASALTS.

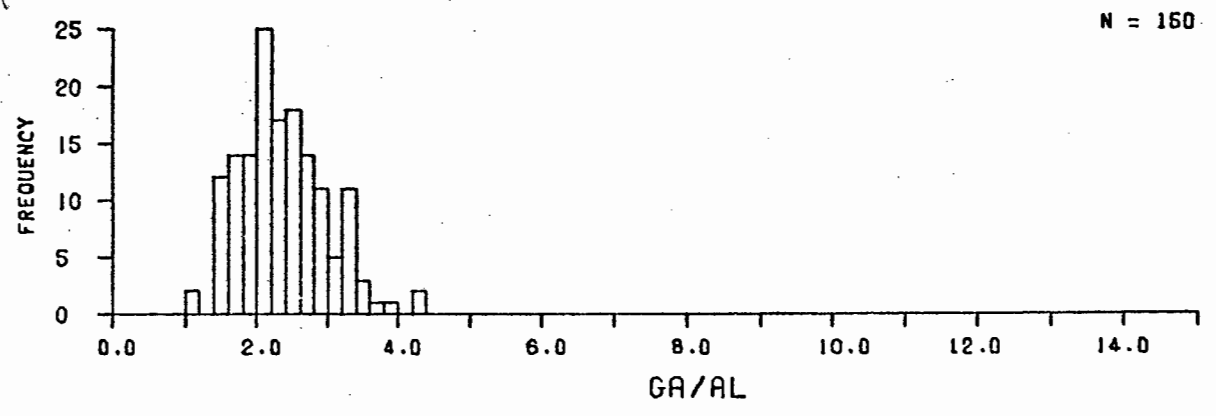

247200 PLAG + PYX ROCKS.

FIG. 62B. PLAG + PYX ROCKS.

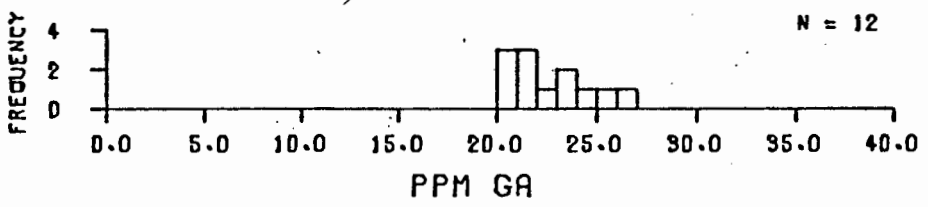

257100 HAWAIITES.

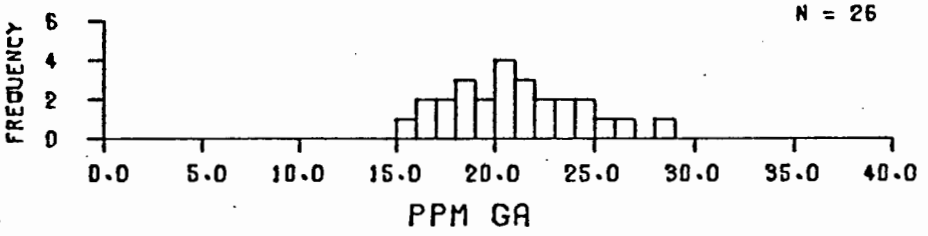

257100 ALKALI OLIVINE BASALTS.

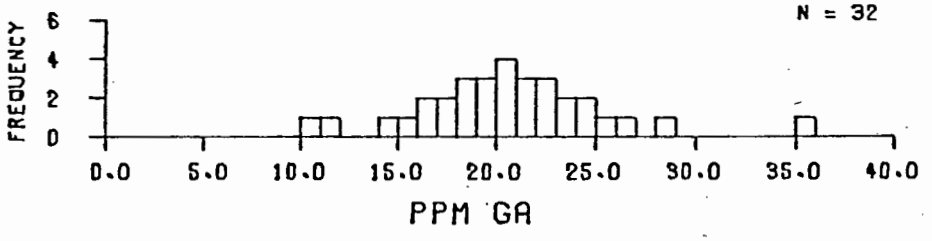

257000 FOID-BEARING BASALTIC ROCKS.

FIG. 63A. FOID-BEARING BASALTIC ROCKS.

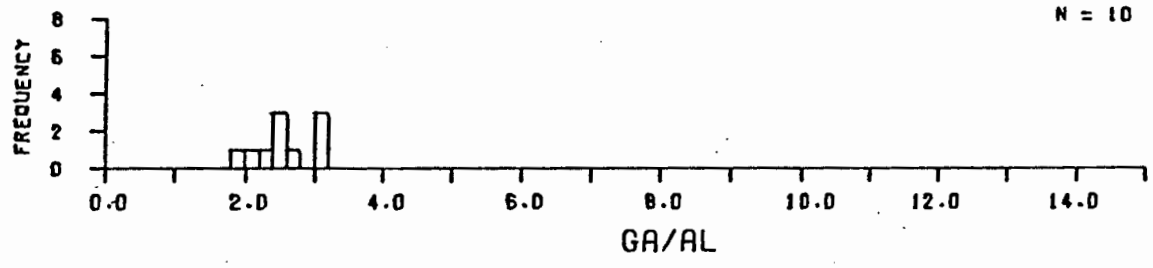

257110 HAWAIITES.

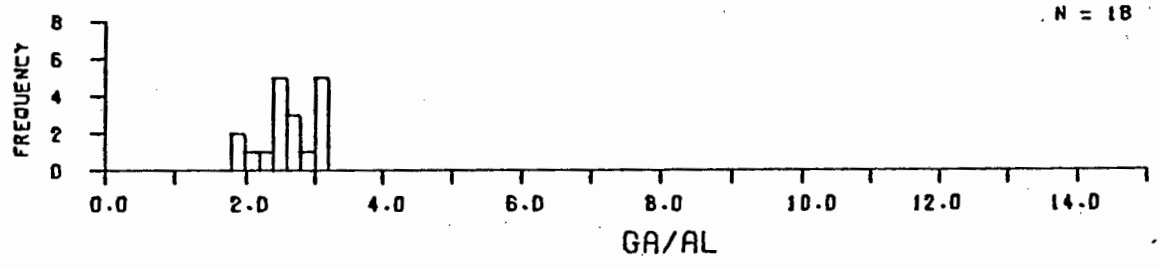

257100 ALKALI OLIVINE BASALTS.

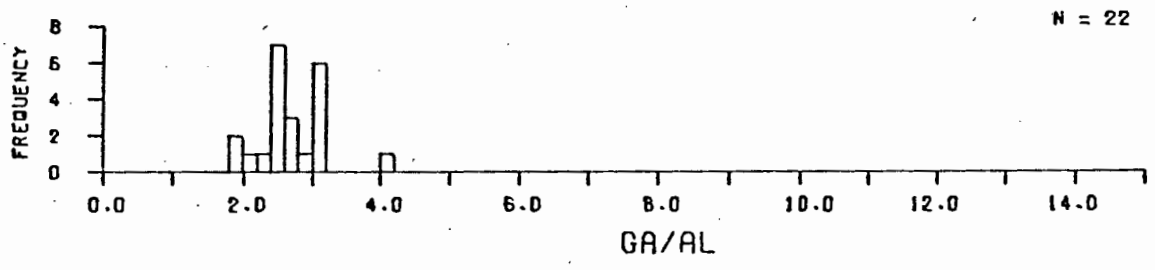

257000 FOID-BEARING BASALTIC ROCKS.

FIG. 63B. FOID-BEARING BASALTIC ROCKS.

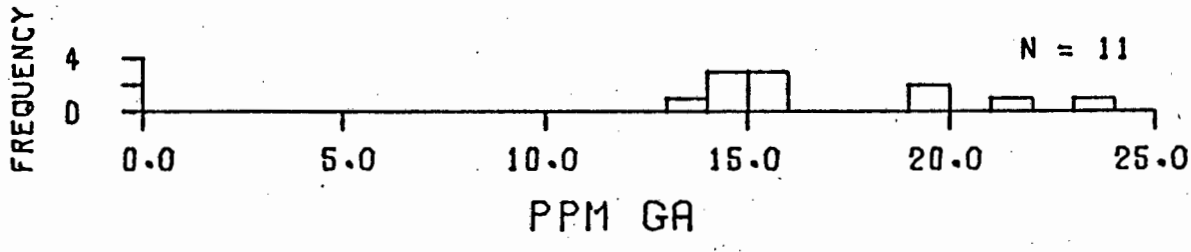

312000 CALC-ALKALINE TYPE.

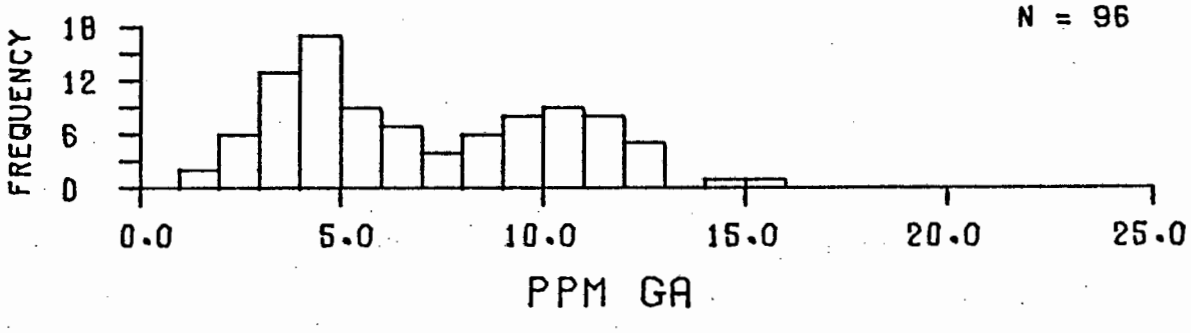

311000 THOLEIITIC TYPE.

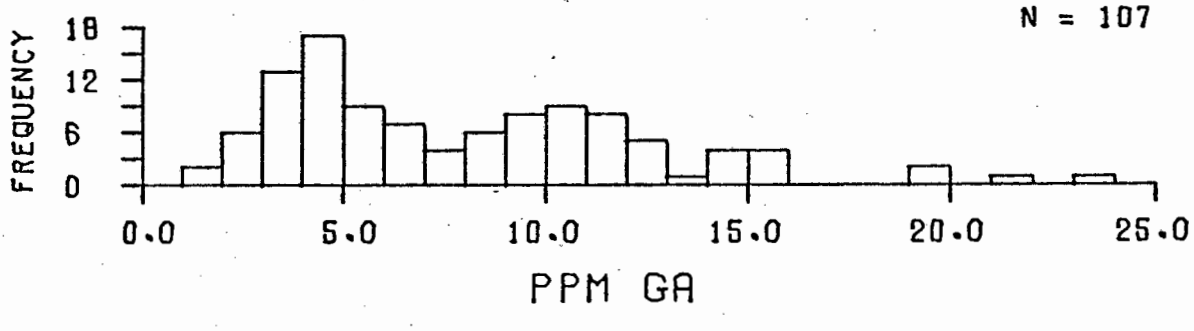

310000 SUBALKALINE ROCKS.

FIG. 64A. VOLCANIC ROCKS.

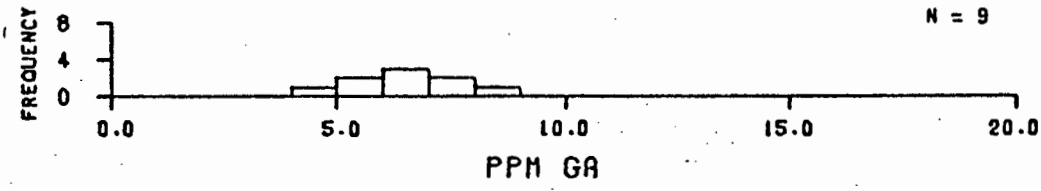

BASALTIC K0MATIITES (GELUK TYPE).

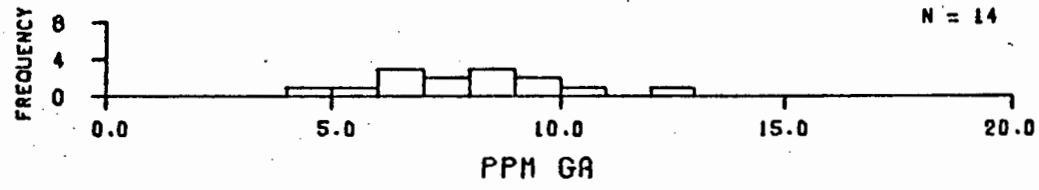

BASALTIC K0MATIITES (BADPLAAS TYPE).

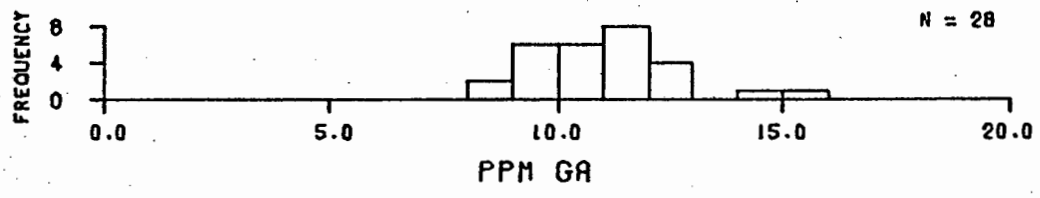

BASALTIC K0MATIITES (BARBERT0N TYPE).

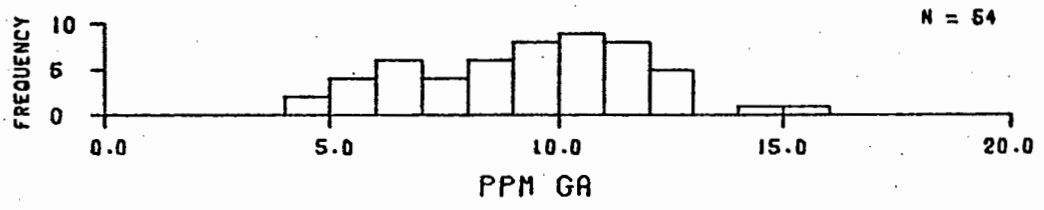

311700 ALL BASALTIC K0MATIITES.

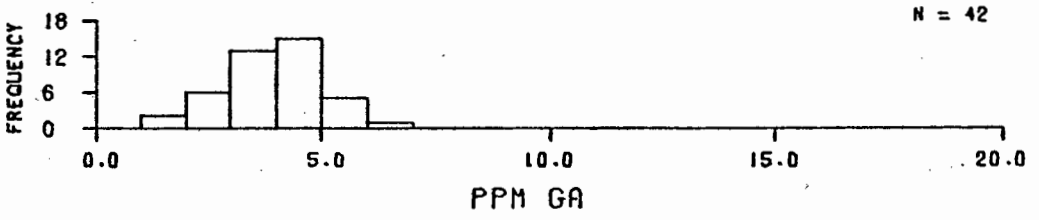

311600 PERID0TITIC K0MATIITES.

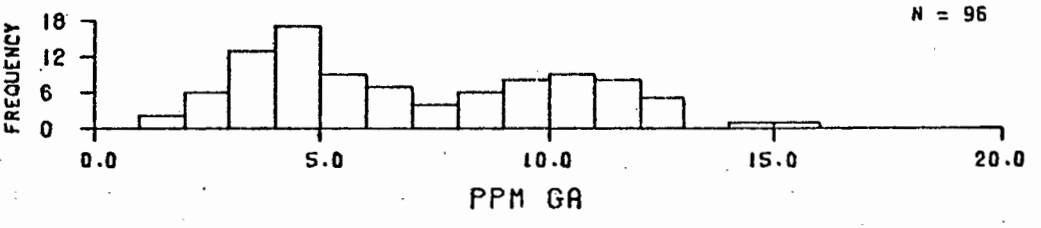

311000 SUBALK. TH0LEIITIC R0CKS.

FIG. 65A. SUBALKALINE TH0LEIITIC R0CKS.

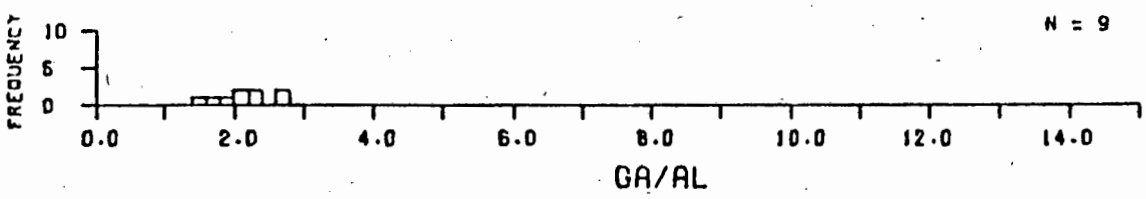

BASALTIC KØMATIITES (GELUK TYPE).

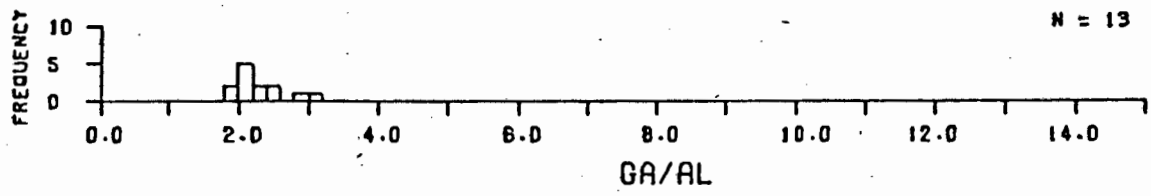

BASALTIC KØMATIITES (BADPLAAS TYPE).

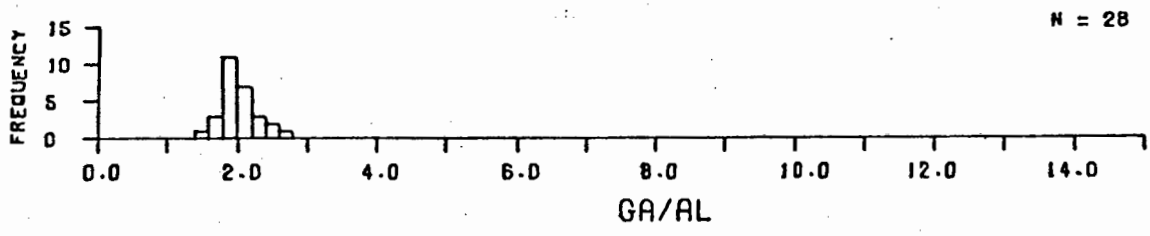

BASALTIC KØMATIITES (BARBERTØN TYPE).

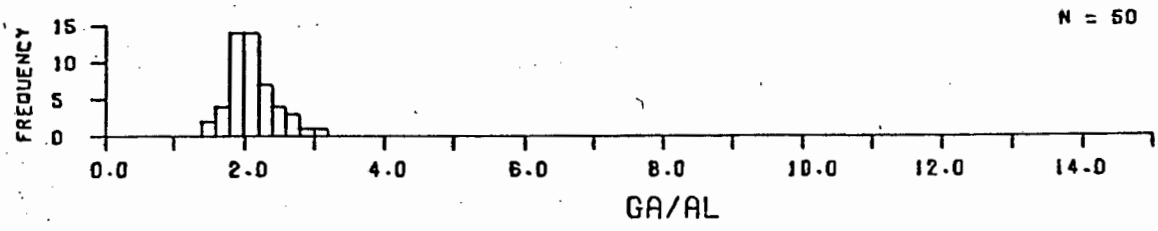

311700 ALL BASALTIC KØMATIITES.

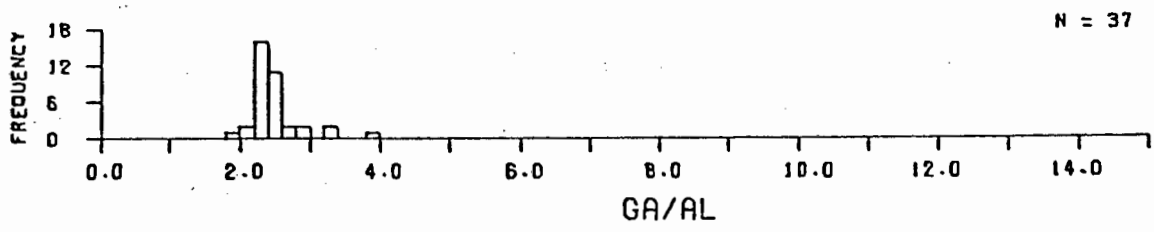

311600 PERIDØTITIC KØMATIITES.

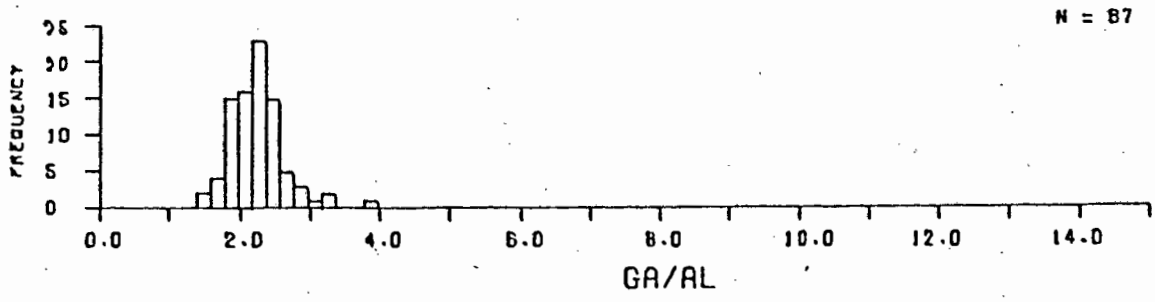

311000 SUBALKALINE THØLEIITIC RØCKS.

FIG. 65B. SUBALKALINE THØLEIITIC RØCKS.

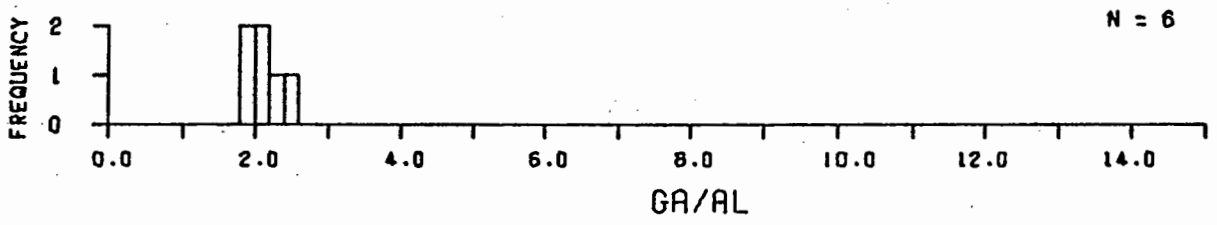

312400 DACITES.

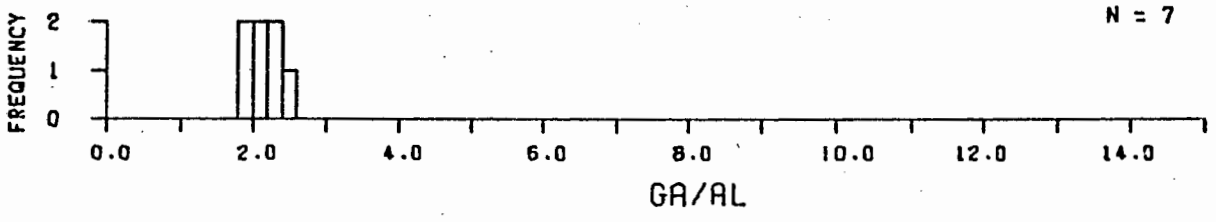

312000 CALC-ALKALINE ROCKS.

FIG. 66B. CALC-ALK SUBALKALINE ROCKS.

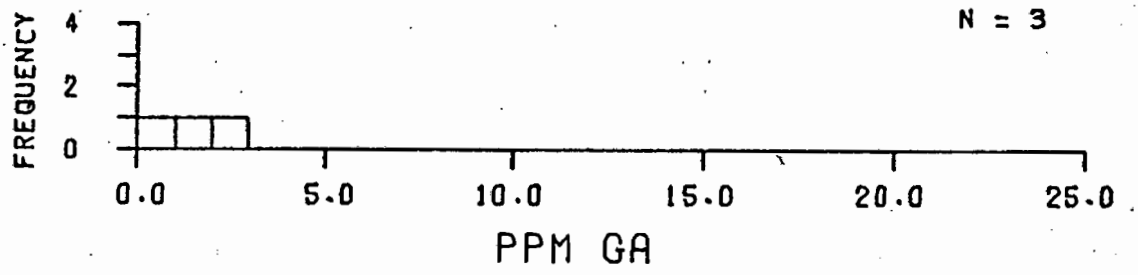

286000 SERPENTINITES.

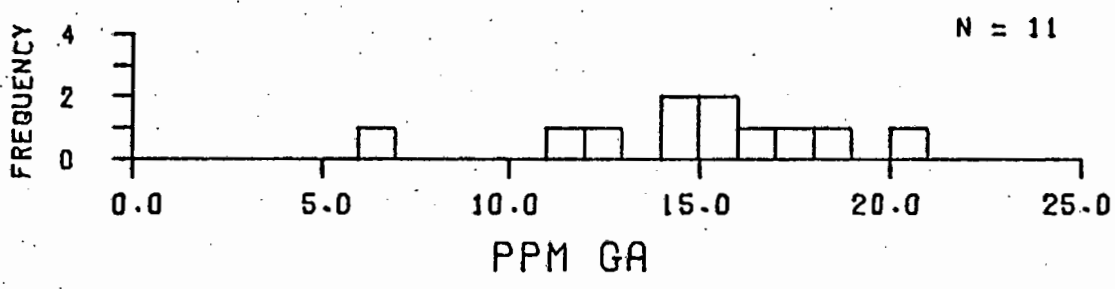

283000 OL + PYX + PLAG ROCKS.

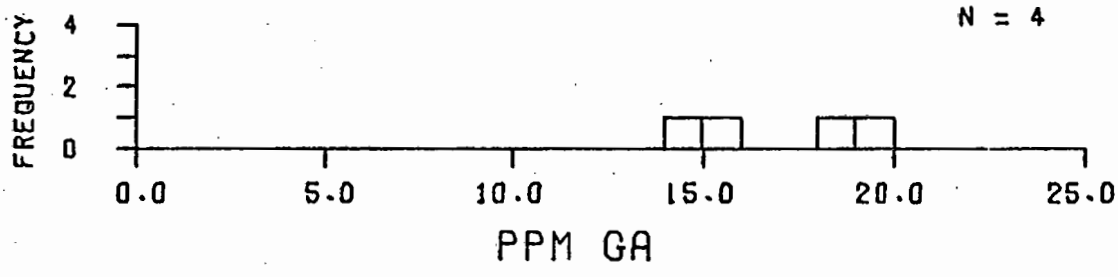

281100 LIMBURGITES.

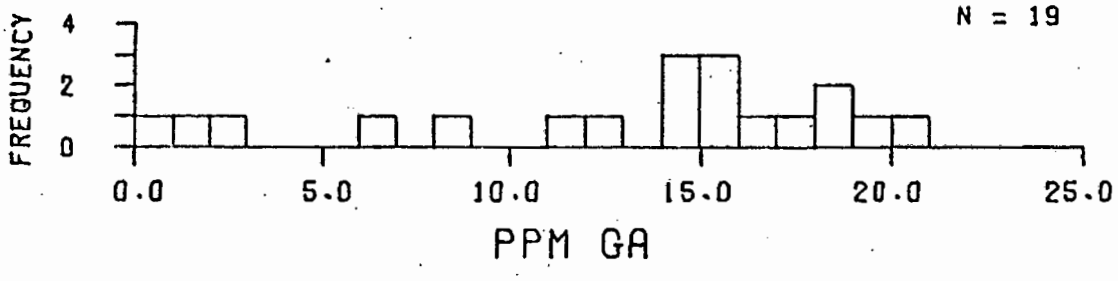

280000 ULTRAMAFIC ROCKS.

FIG. 67A. ULTRAMAFIC ROCKS.

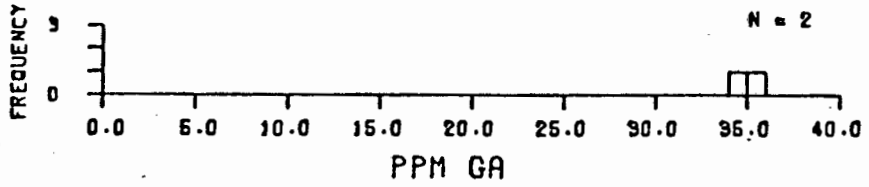

SILICEOUS SHALES (CLAY FRACTION).

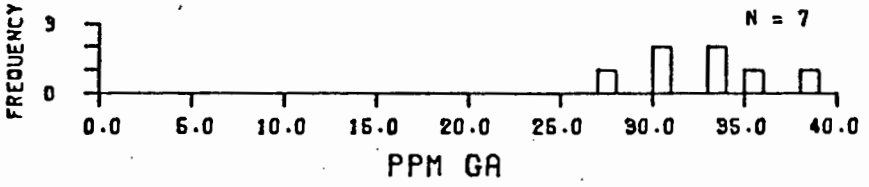

FELDSPATHIC SHALES (CLAY FRACTION).

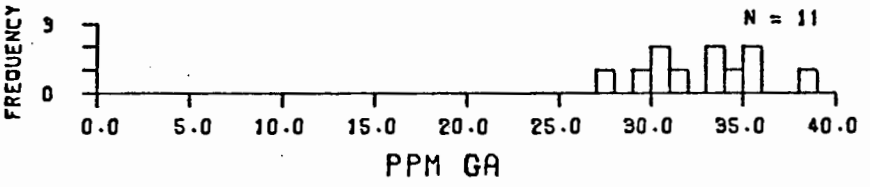

ALL SHALES (CLAY FRACTION).

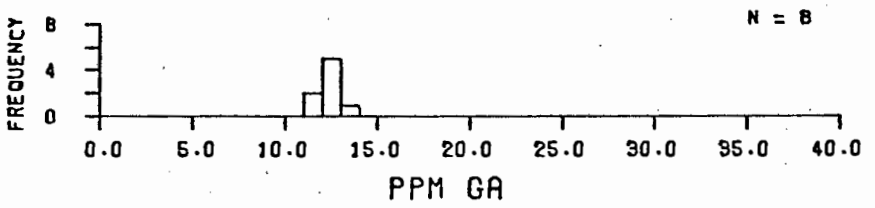

4T3000 SILICEOUS SHALES.

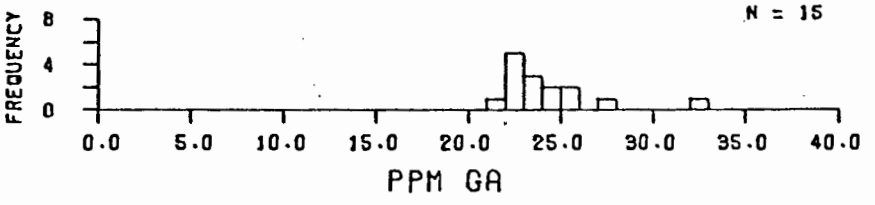

4T6000 FELDSPATHIC SHALES.

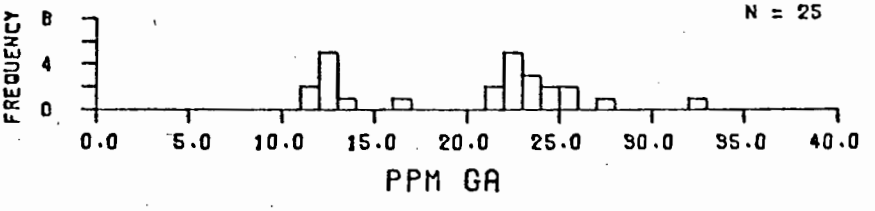

4T0000 ALL SHALES.

FIG. 68A. SHALES.

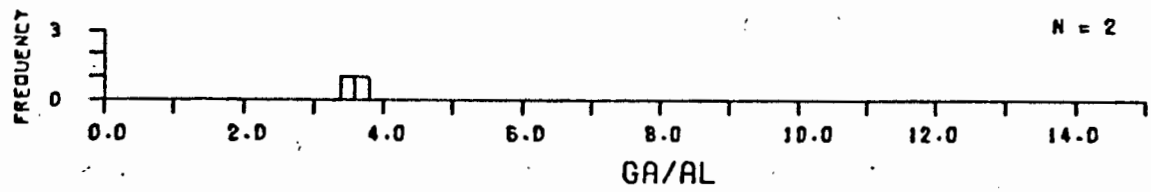

SILICEOUS SHALES (CLAY FRACTION).

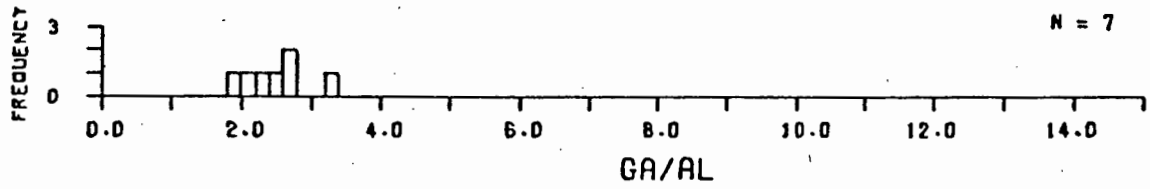

FELDSPATHIC SHALES (CLAY FRACTION).

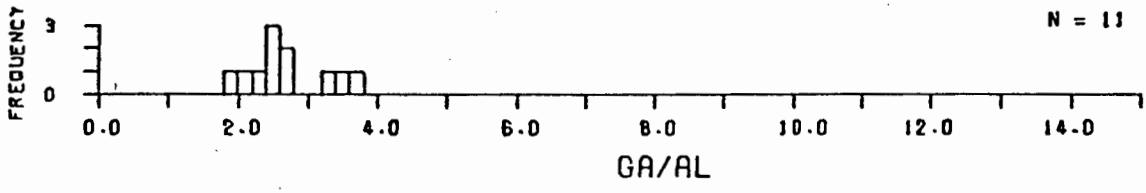

ALL SHALES (CLAY FRACTION).

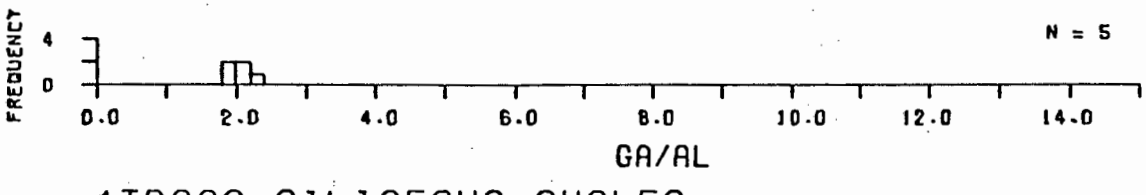

4T3000 SILICEOUS SHALES.

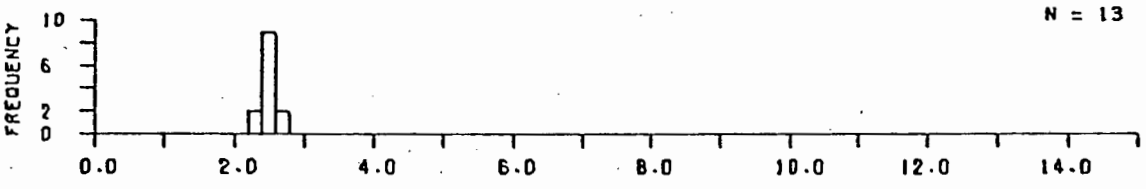

4T6000 FELDSPATHIC SHALES.

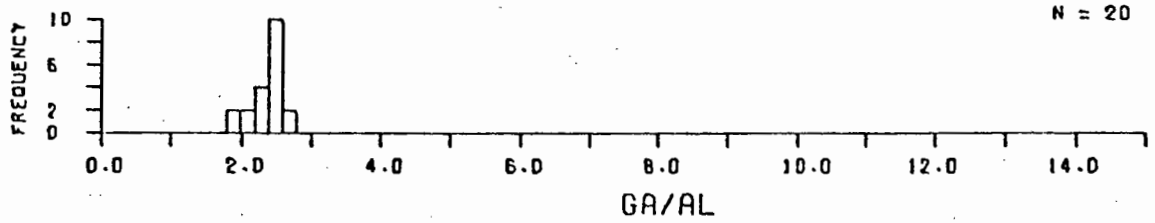

4T0000 ALL SHALES.

FIG. 68B. SHALES.

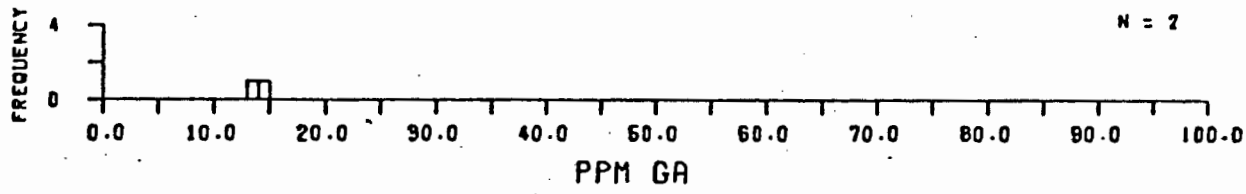

7N1300 HYPERSTHENES.

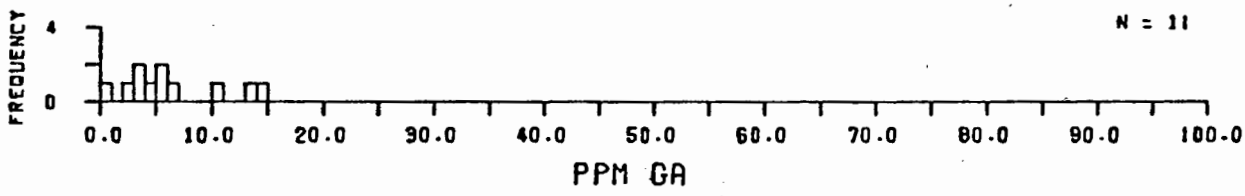

7N0000 ALL PYR0XENES.

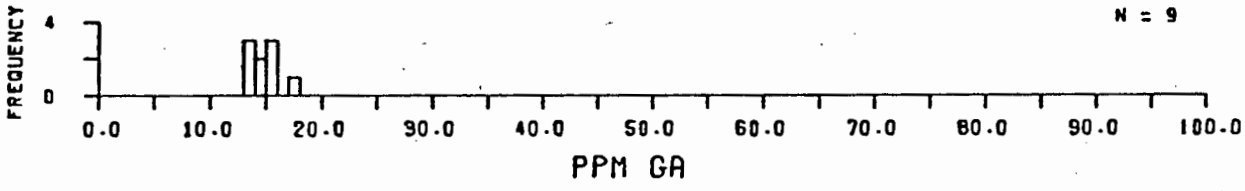

7MA100 PERTHITIC FELDSPARS.

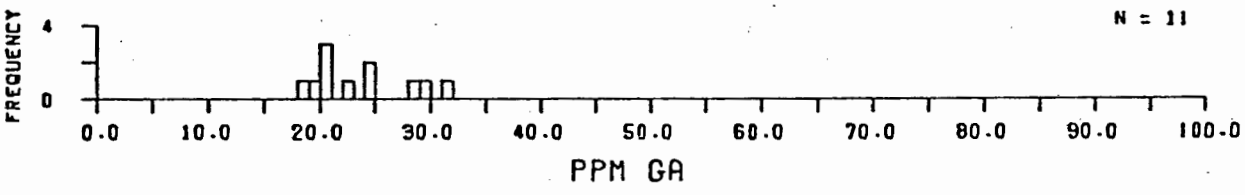

7M2000 PLAGI0CLASE FELDPSARS.

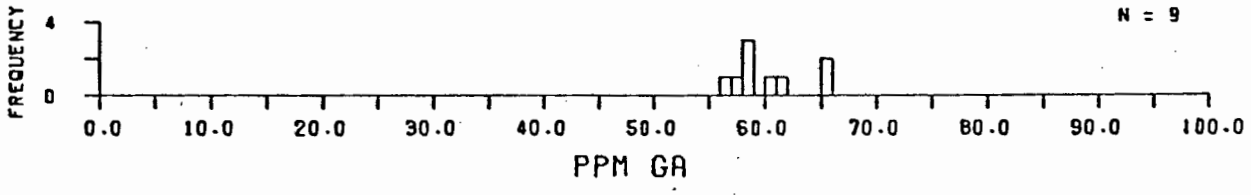

7P2100 BI0TITES.

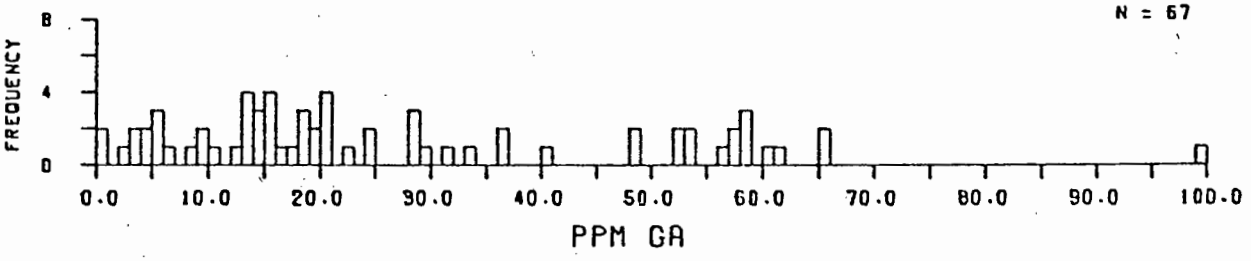

700000 ALL MINERALS.

FIG. 69A. MINERALS.

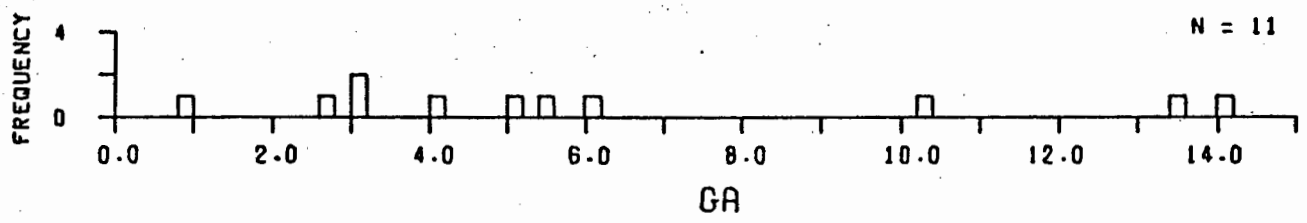

7N0000 PYR0XENES.

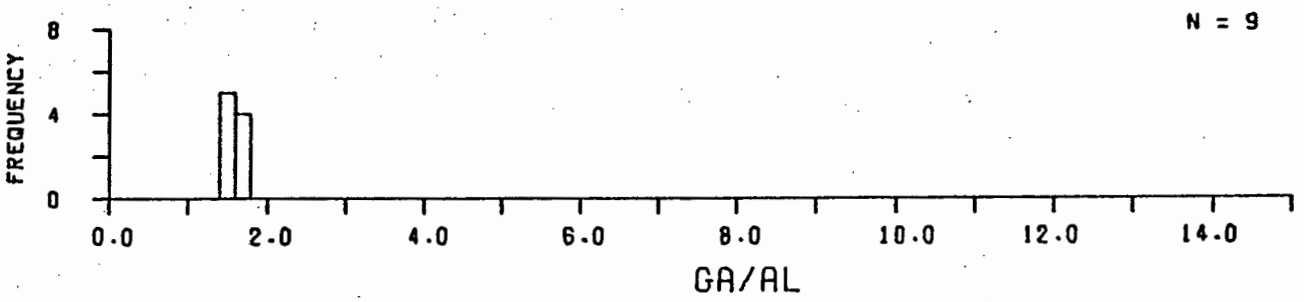

PERTHITIC FELDSPARS.

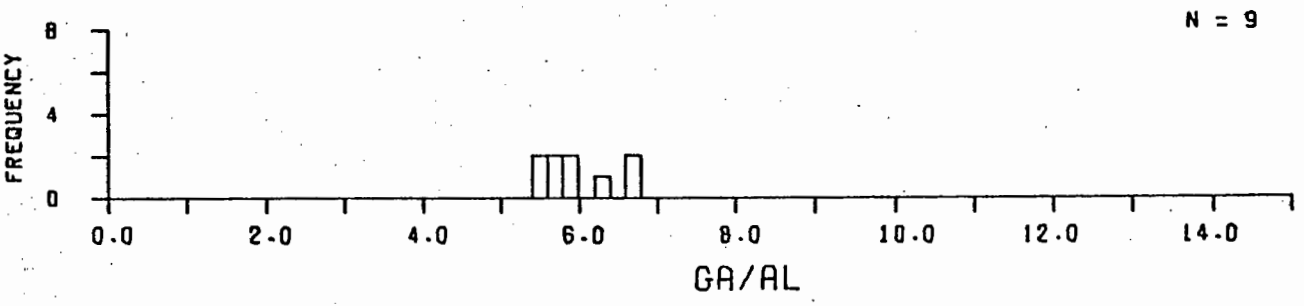

BI0TITES.

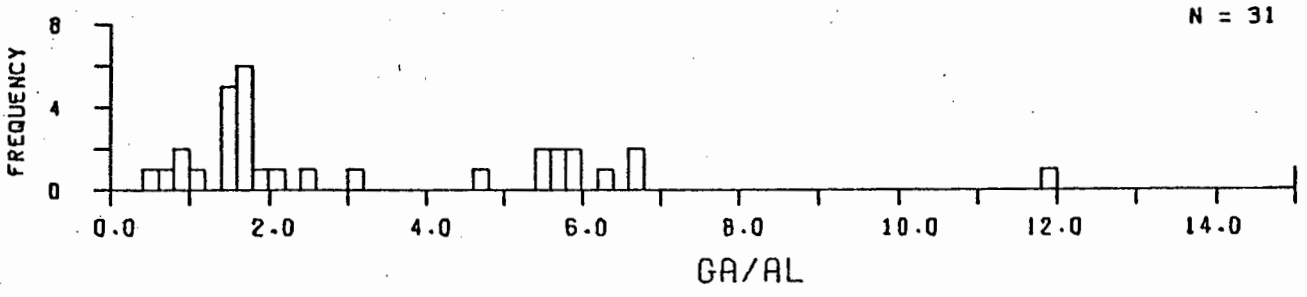

700000 ALL MINERALS.

FIG. 69B. MINERALS.

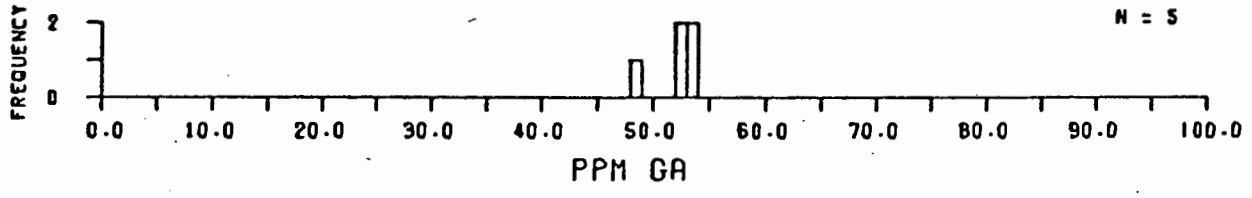

7DI200 MAGNETITES.

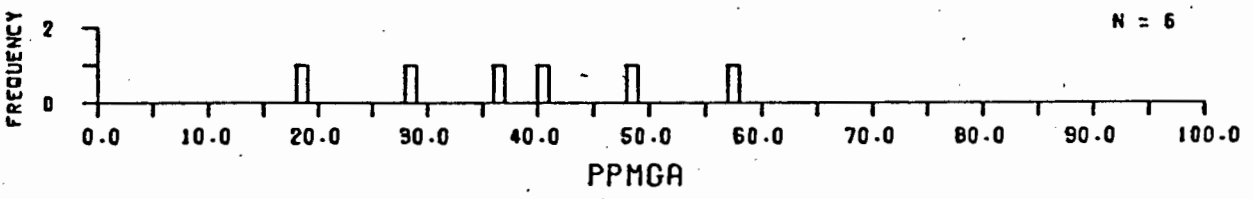

7DH000 CHR0MIUM SPINELS.

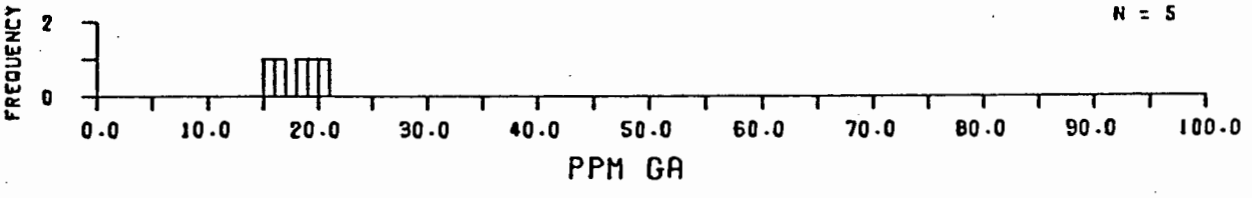

7E1100 ILMENITES.

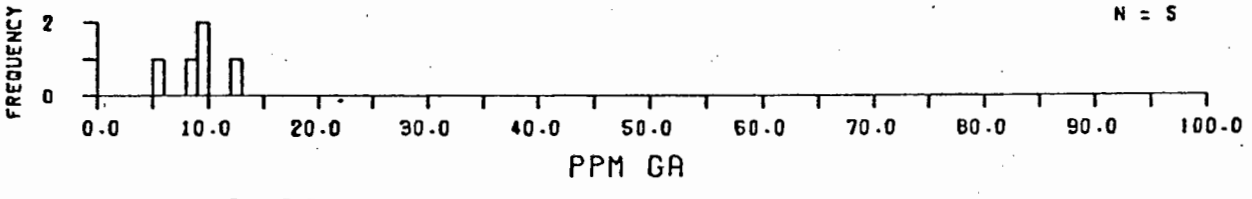

7Q4000 GARNETS.

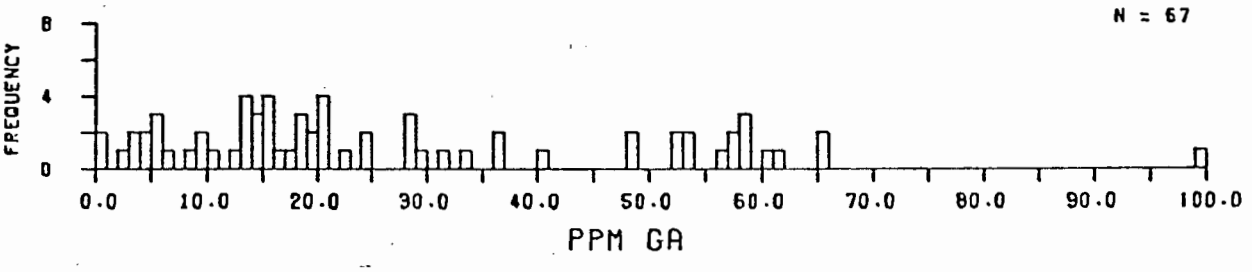

700000 ALL MINERALS.

FIG. 70A. MINERALS.

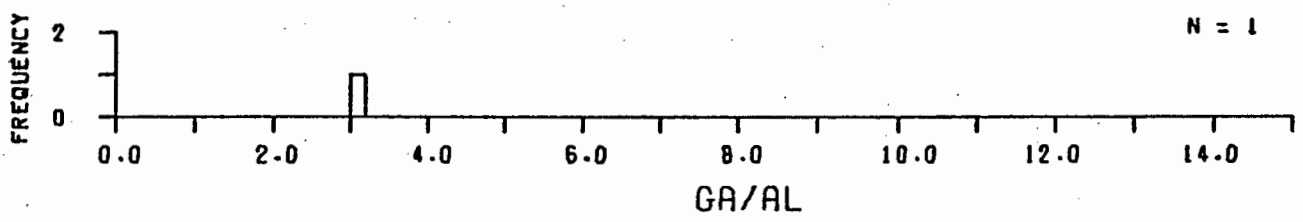

7DH000 CHR0MIUM SPINELS.

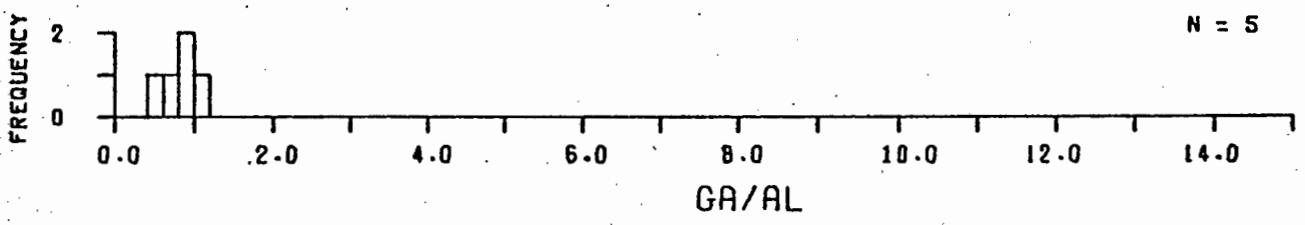

7Q4000 GARNETS.

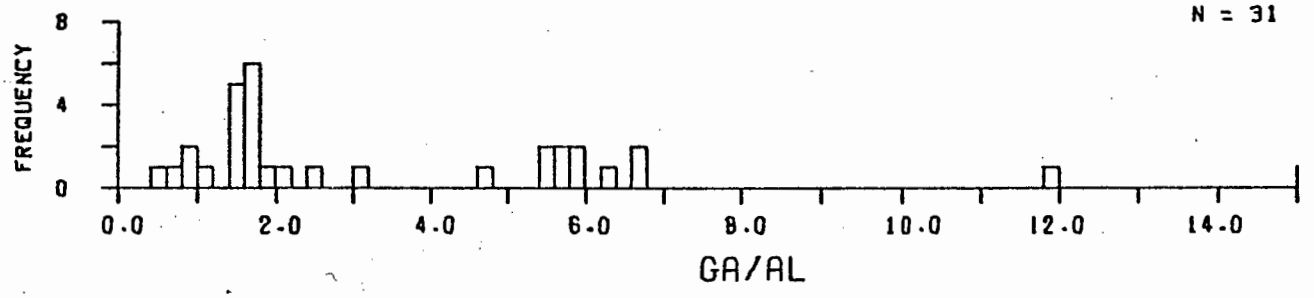

700000 ALL MINERALS.

FIG. 70B. MINERALS.

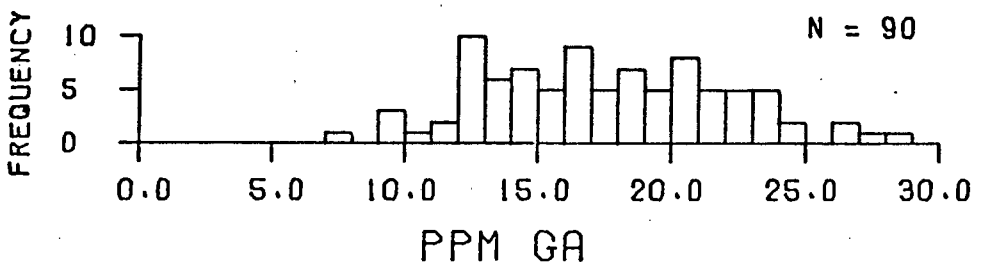

CONTINENTAL BASALTIC ROCKS.

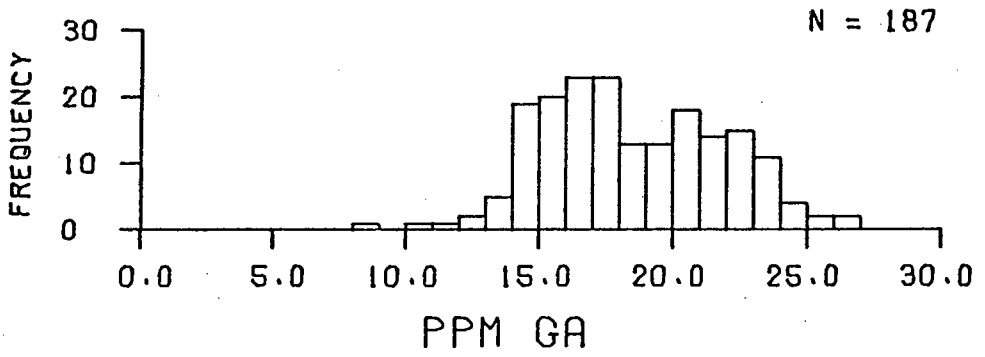

OCEANIC BASALTIC ROCKS.

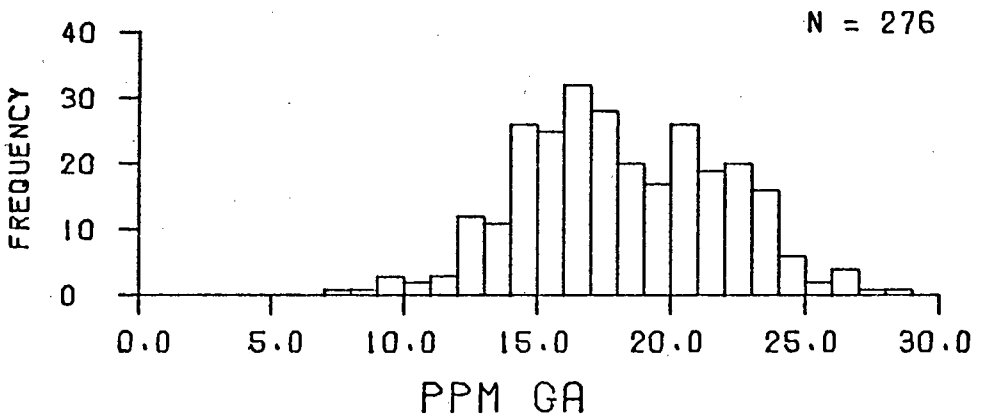

ALL BASALTIC ROCKS.

FIG. 71A. BASALTIC ROCKS.

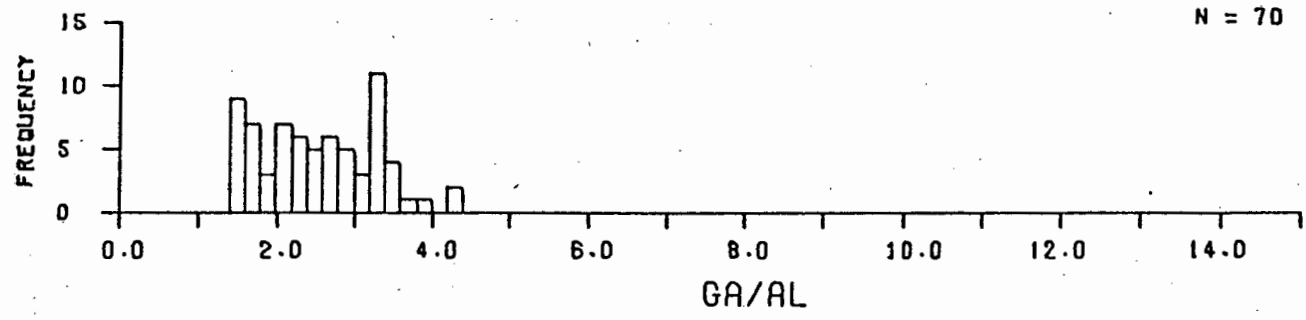

CONTINENTAL BASALTIC ROCKS.

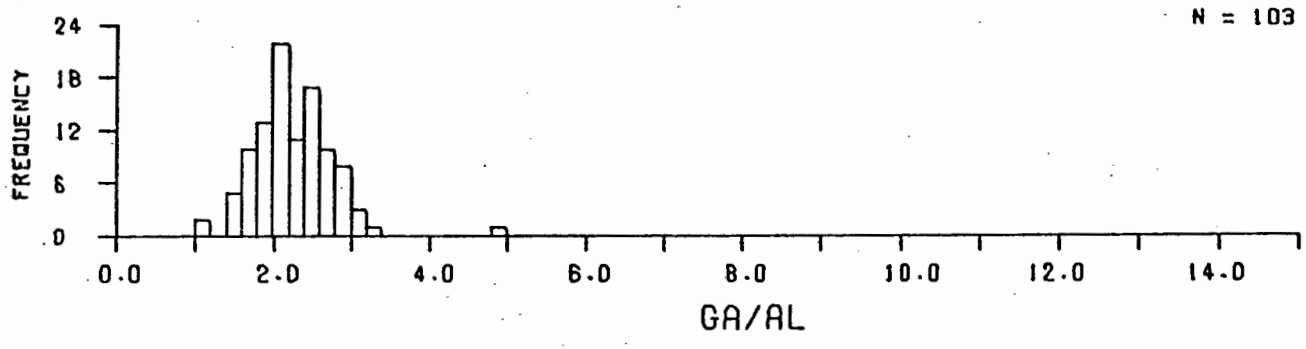

OCEANIC BASALTIC ROCKS.

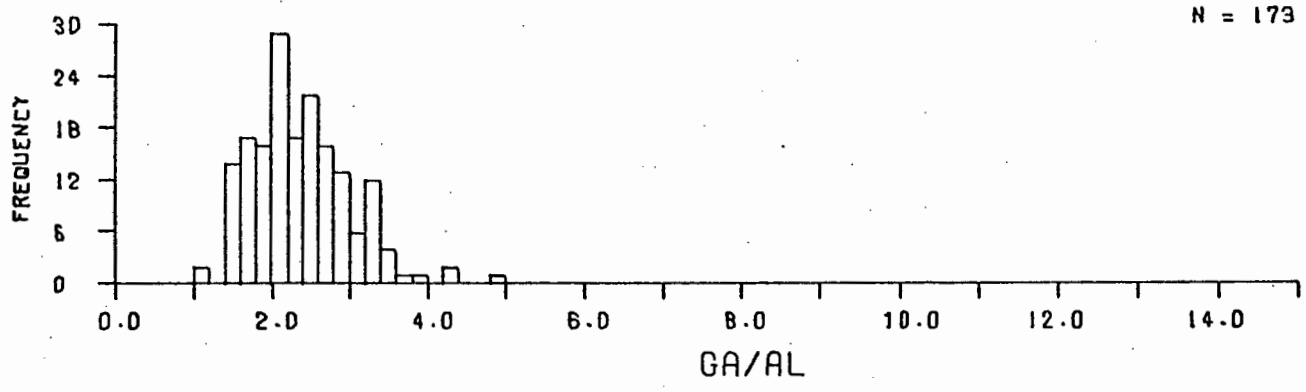

ALL BASALTIC ROCKS.

FIG. 71B. BASALTIC ROCKS.

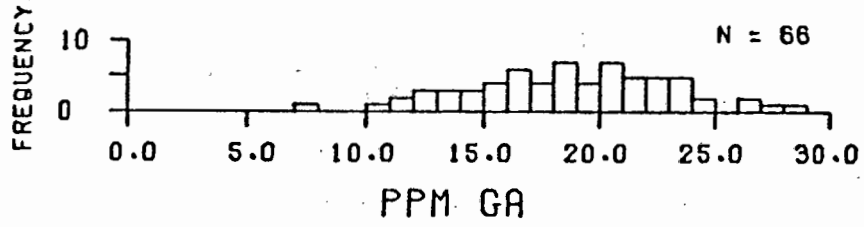

CONTINENTAL BASALTS.

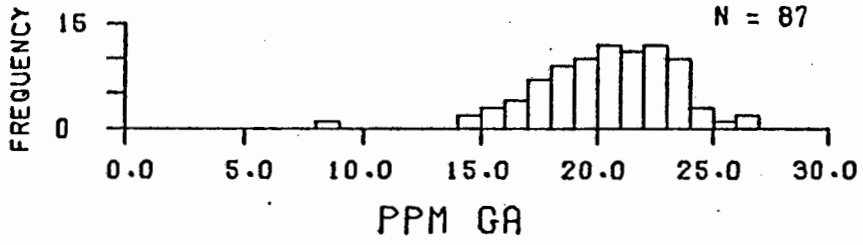

OCEANIC BASALTS.

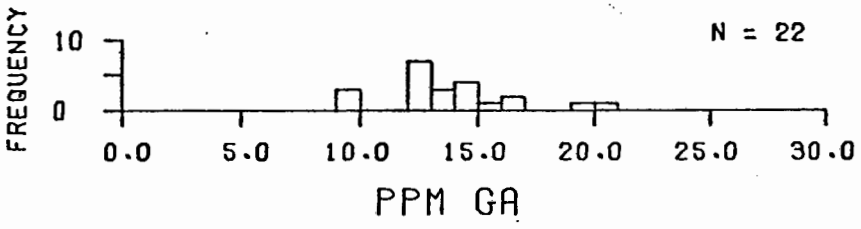

CONTINENTAL THOLEIITES.

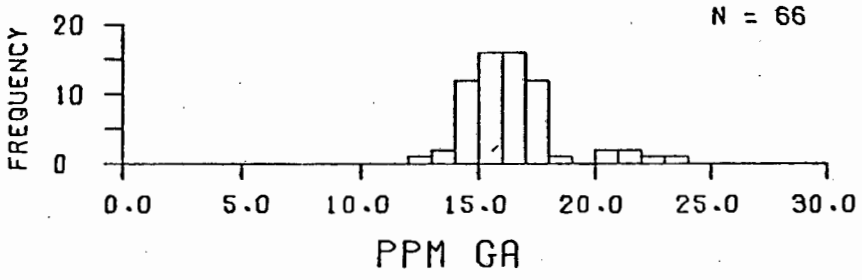

OCEANIC THOLEIITES.

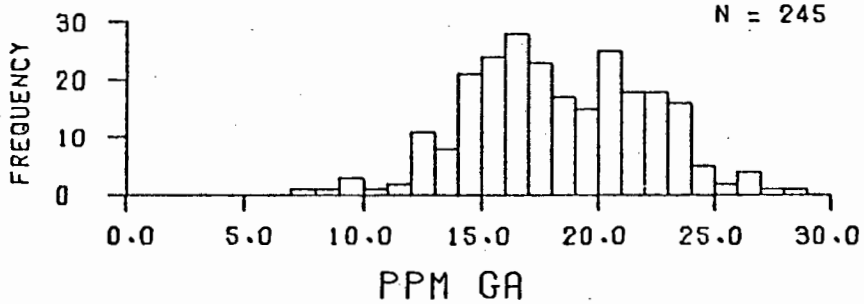

ALL PLAG + PYX ROCKS.

FIG. 72A. BASALTIC ROCKS.

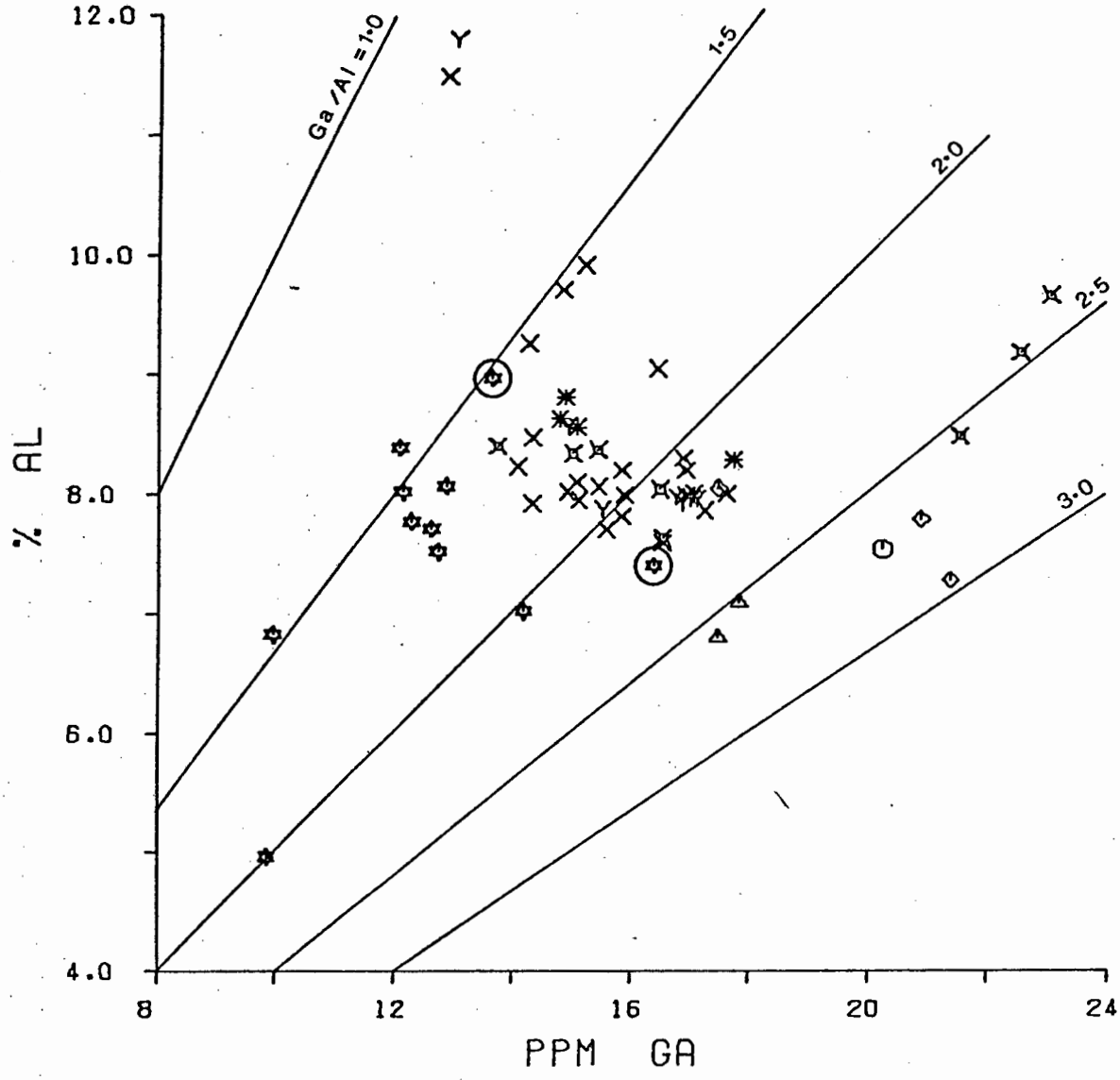

FIG. 73. GA-AL PLOT FOR THOLEIITE BASALTS.

- ✡ BARBERTON ROCKS.
- × MID-ATLANTIC RIDGE.
- Y PACIFIC OCEAN. ABYSSAL ROCKS.
- ✳ CARLSBERG RIDGE.
- ✡ JOIDES LEG 25 INDIAN OCEAN.
- ⊙ ICELAND.
- ◇ GALAPAGOS ISLANDS.
- △ HAWAIIAN ISLANDS.

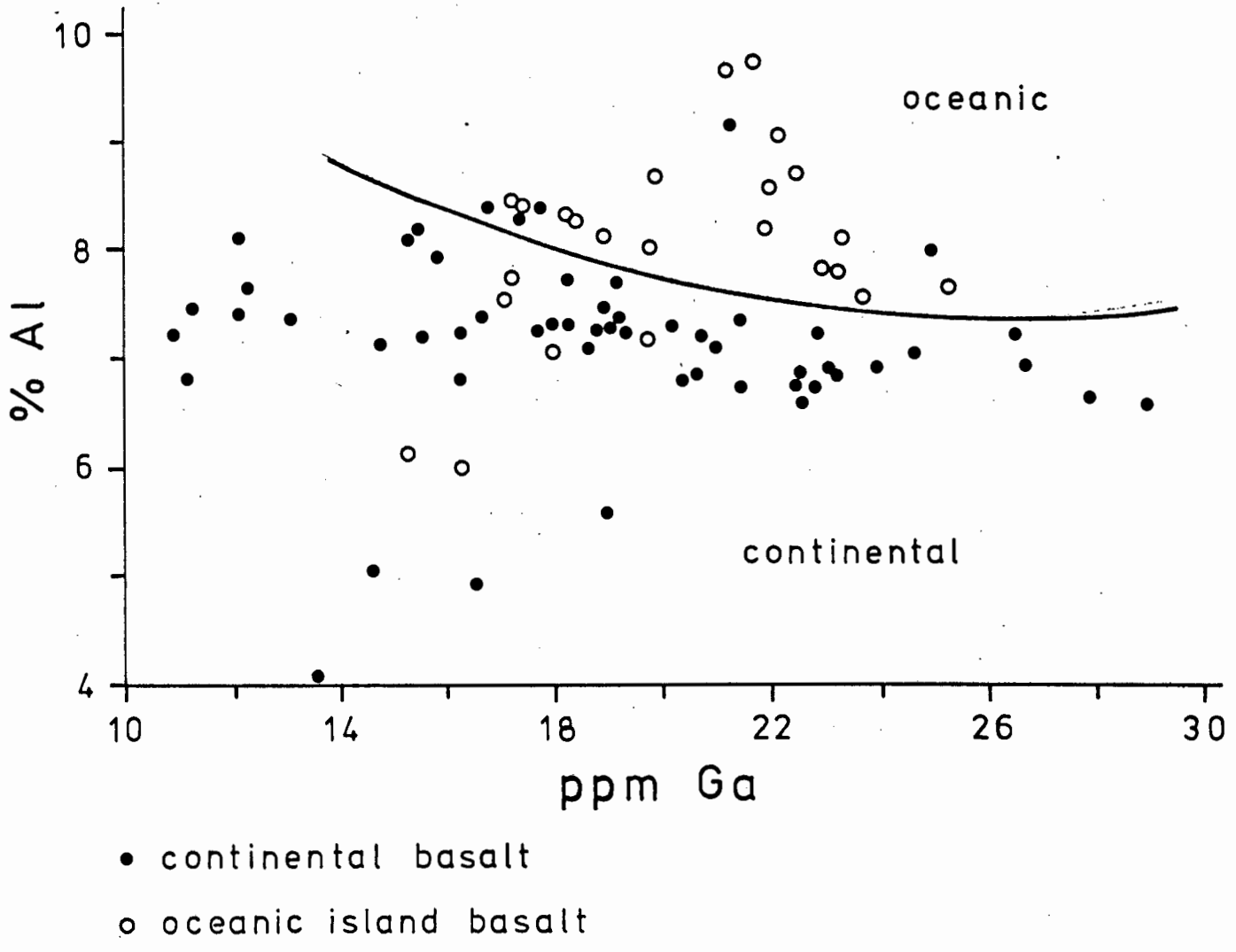

Fig. 74. A Ga - Al plot for oceanic island and continental basalts.

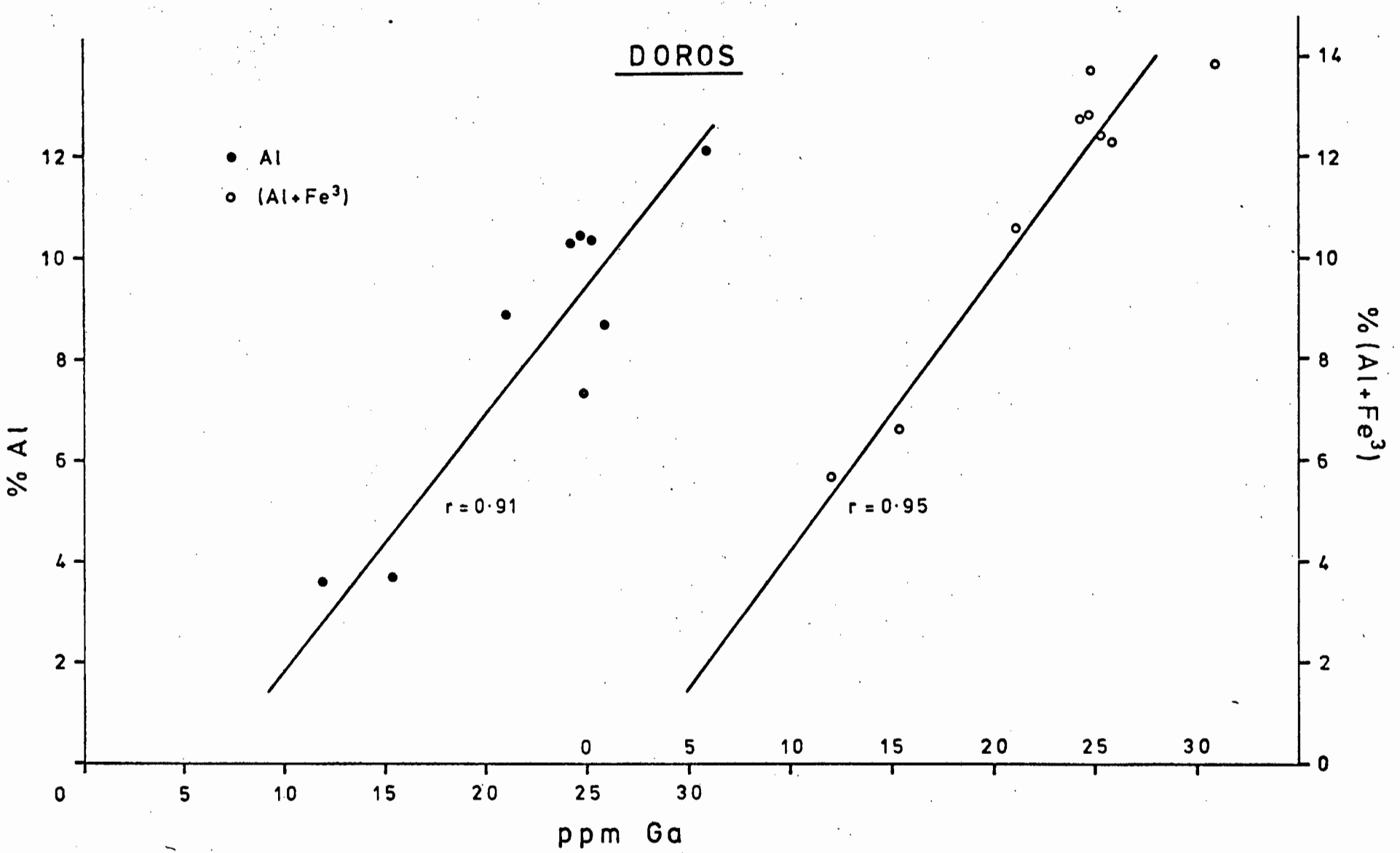

Fig. 75. A Ga - Al and Ga - ($Al + Fe^{3}$) plot for rocks from the Doros Igneous Complex, S.W.A.

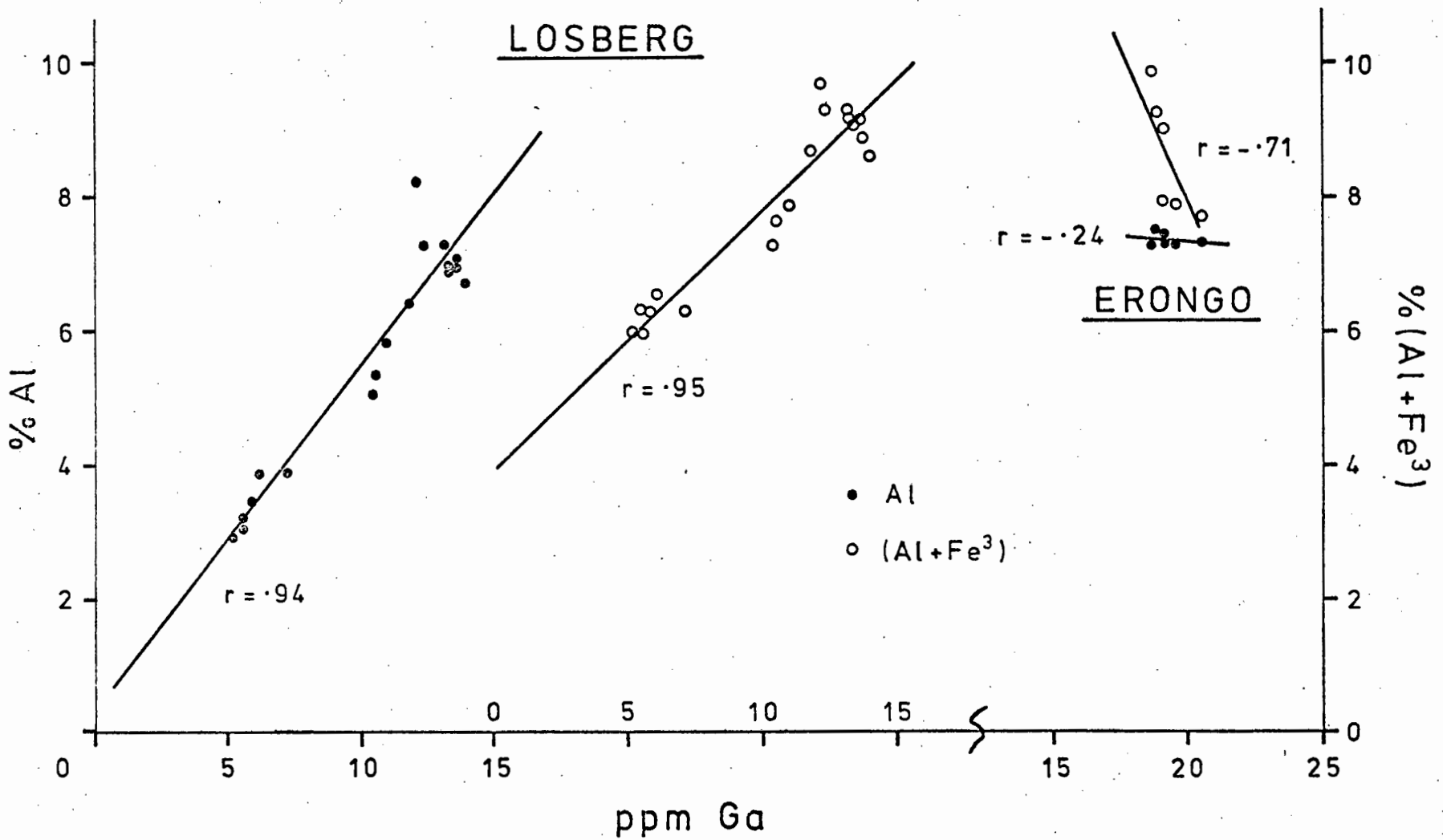

Fig. 76. Ga - Al and Ga - ($Al + Fe^3$) plots for rocks from the Erongo (S.W.A.) and Losberg (Transvaal) Igneous Complexes.

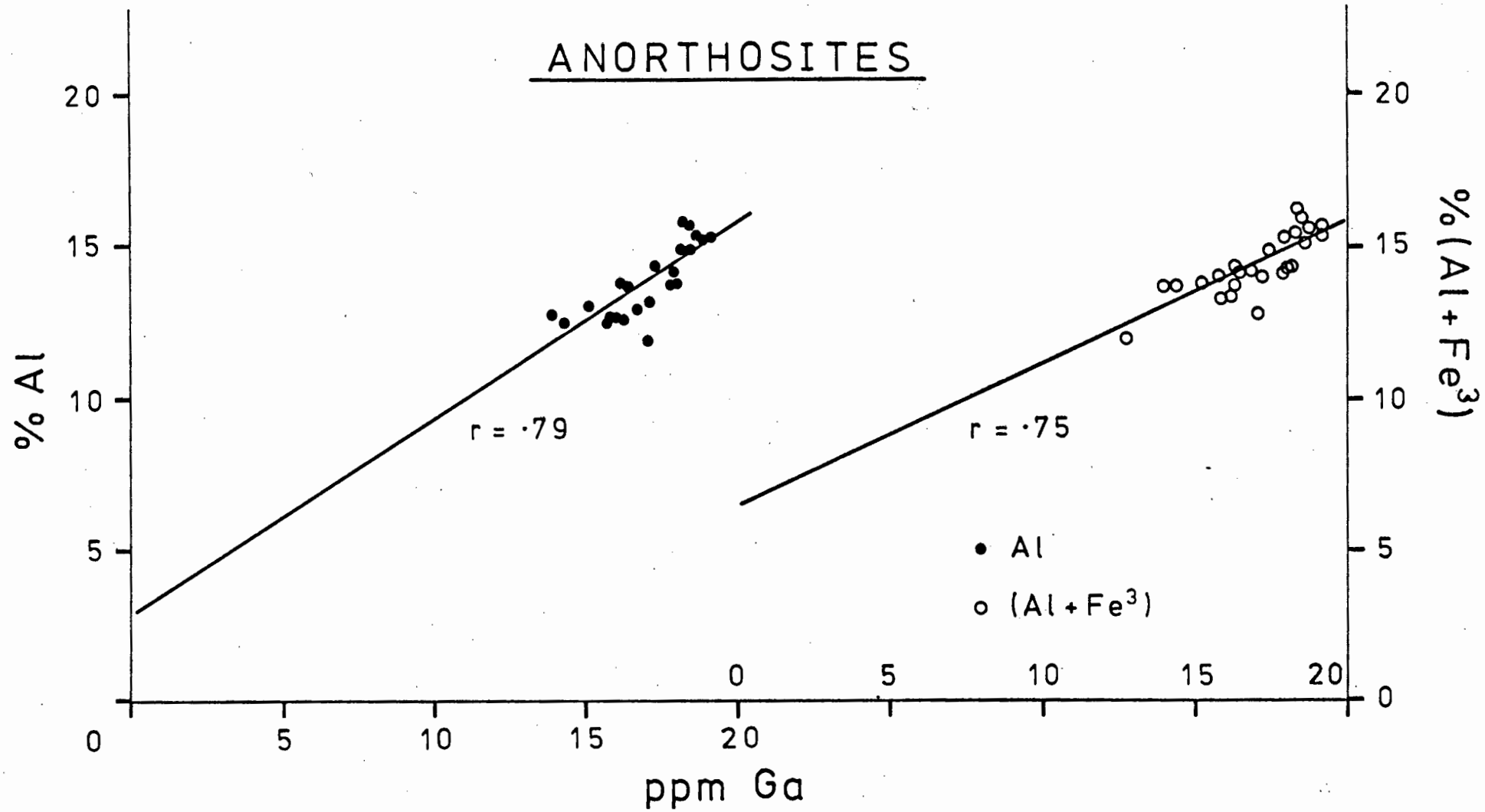

Fig. 77. Ga - Al and Ga - (Al + Fe^3) plot for anorthosites from the Kunene Basic Complex, S.W.A.

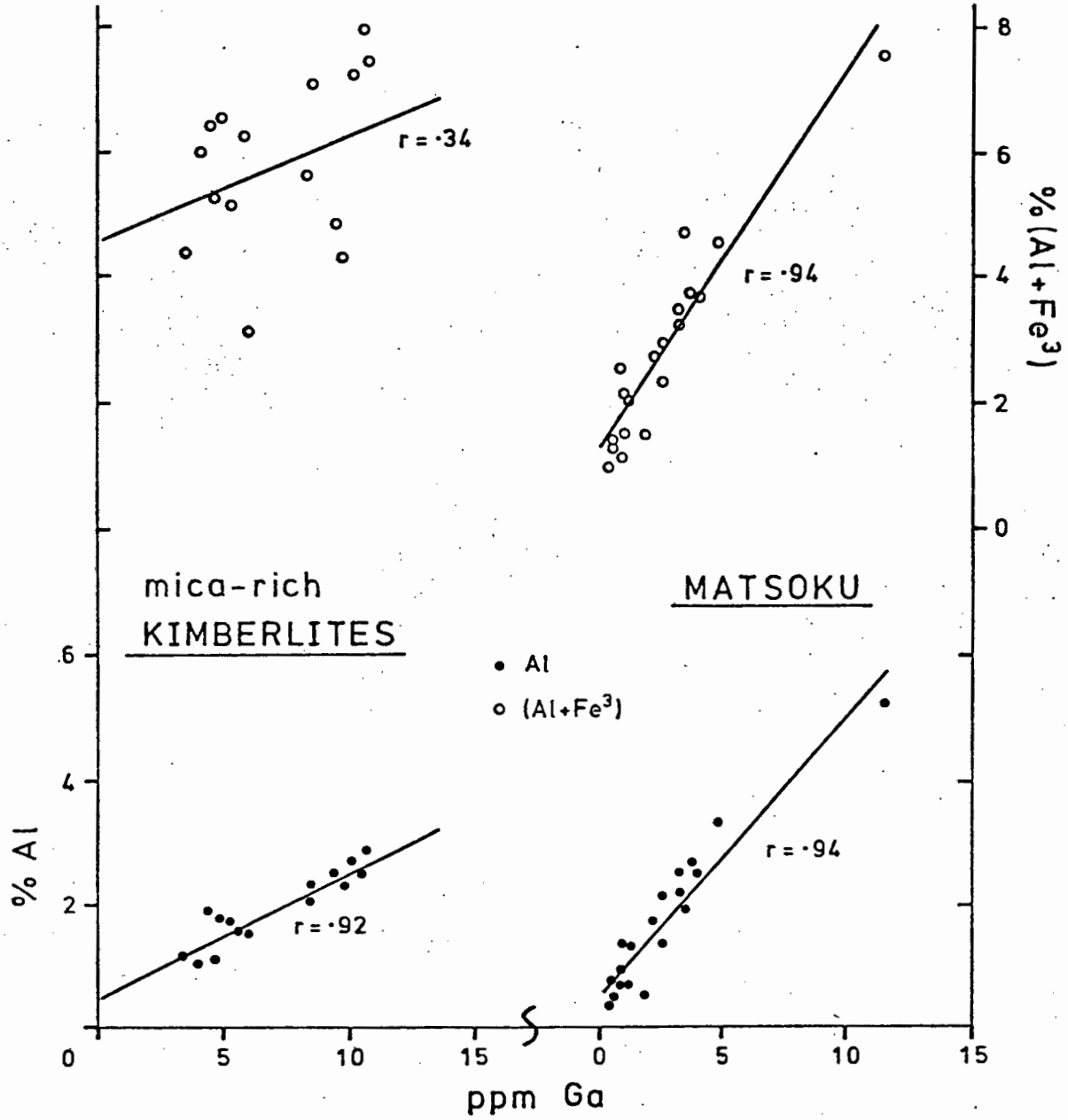

Fig. 78. Ga - Al and Ga - ($Al + Fe^3$) plots for mica-rich kimberlites and for xenoliths from the Matsoku Pipe.

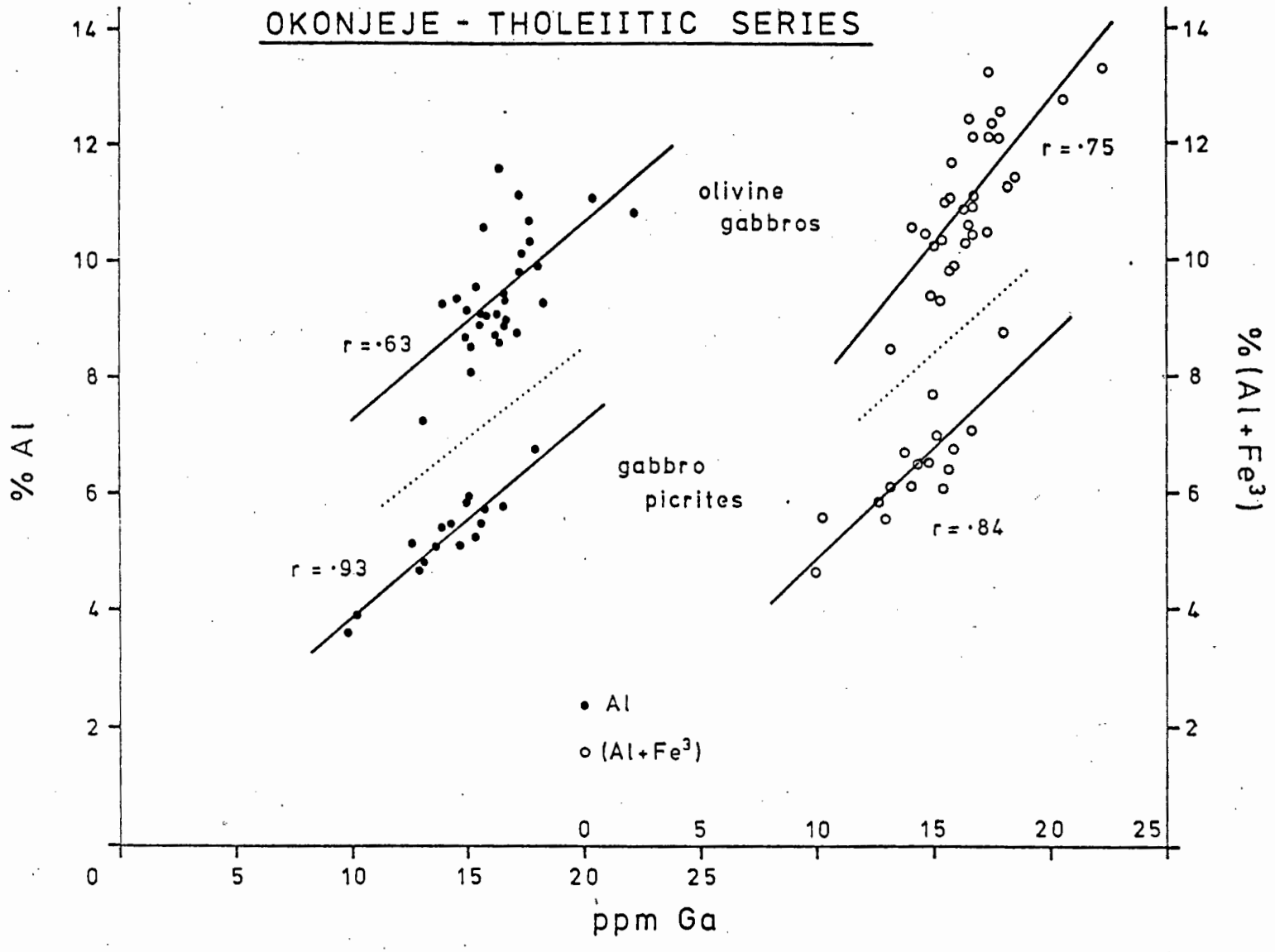

Fig. 79. Ga - Al and Ga - (Al + Fe^{3}) plots for gabbro-picrites and olivine gabbros from the Tholeiitic Series, Okonjeje Igneous Complex, S.W.A.

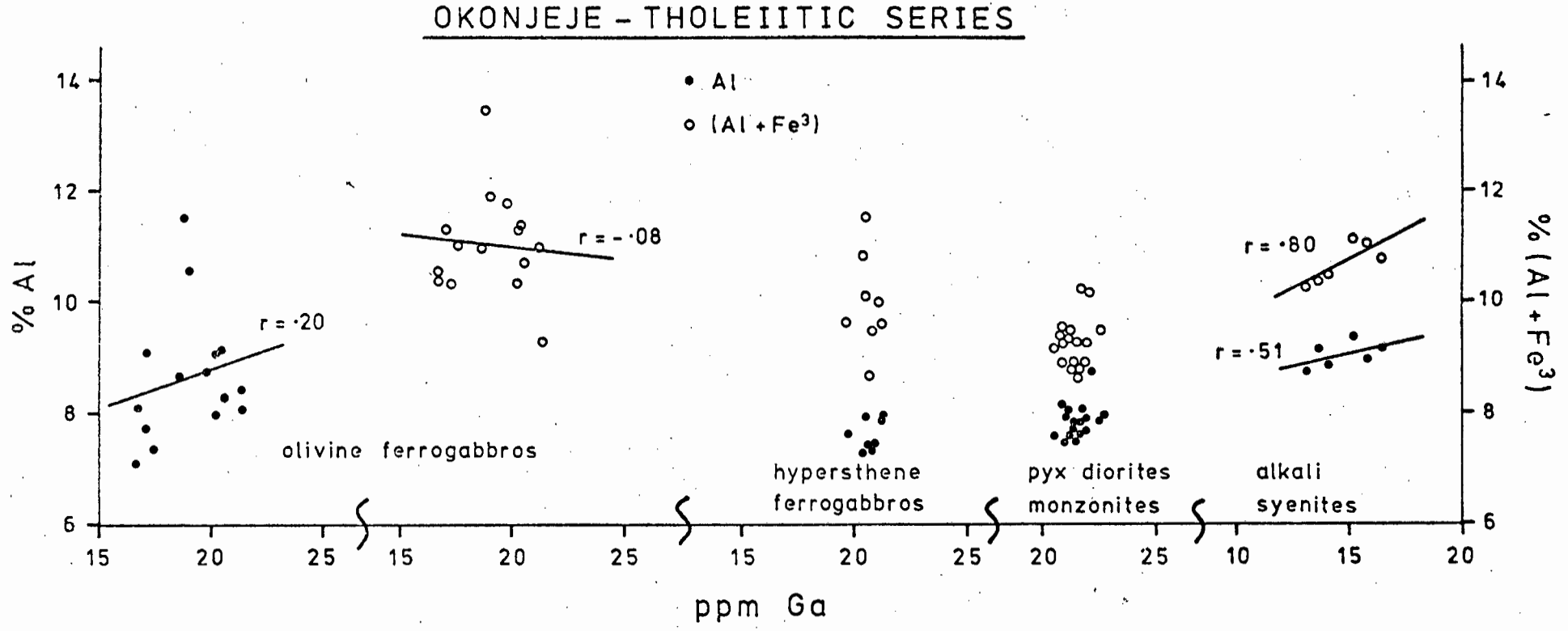

Fig. 80. Ga - Al and Ga - (Al + Fe^3) plots for olivine ferrogabbros, hypersthene ferrogabbros, pyroxene diorites, monzonites and adamellites, and alkali syenites from the Tholeiitic Series, Okonjeje Igneous Complex, S.W.A.

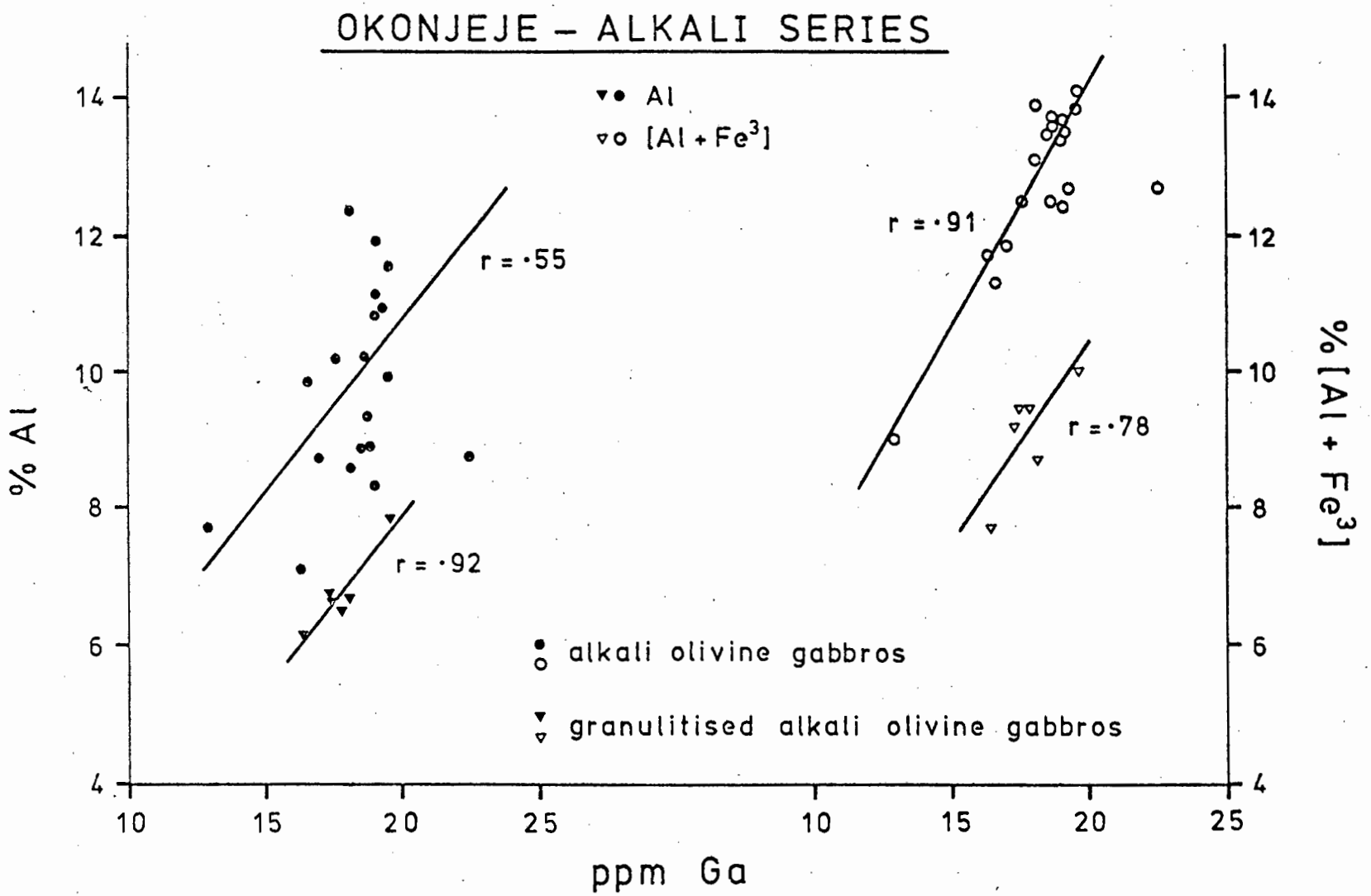

Fig. 81. Ga - Al and Ga - (Al + Fe^3) plots for granulitised alkali olivine gabbros and alkali olivine gabbros from the Alkali Series, Okonjeje Igneous Complex, S.W.A.

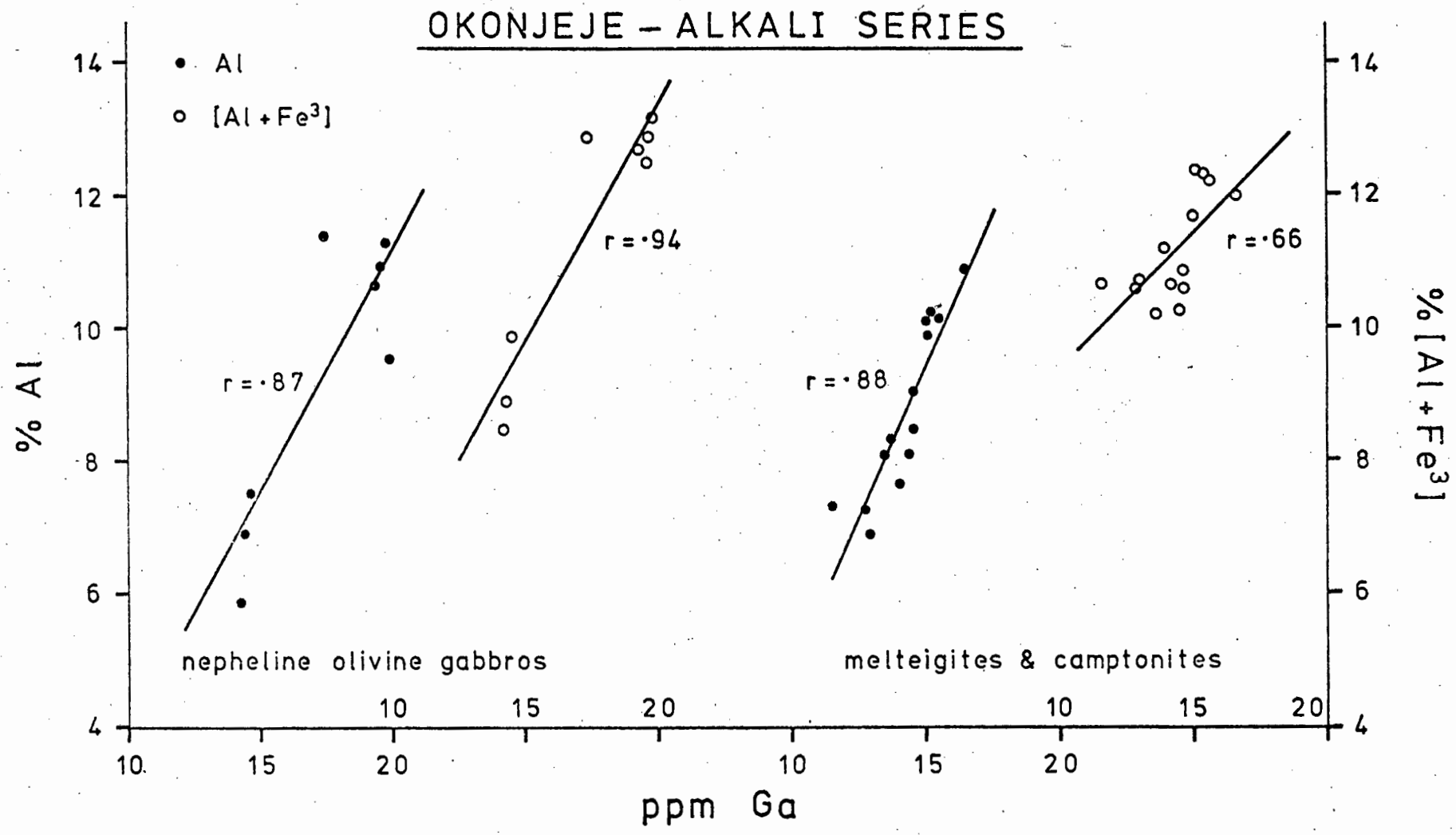

Fig. 82. Ga - Al and Ga - (Al + Fe^3) plots for nepheline olivine gabbros and melteigites and camptonites from the Alkali Series, Okonjeje Igneous Complex, S.W.A.

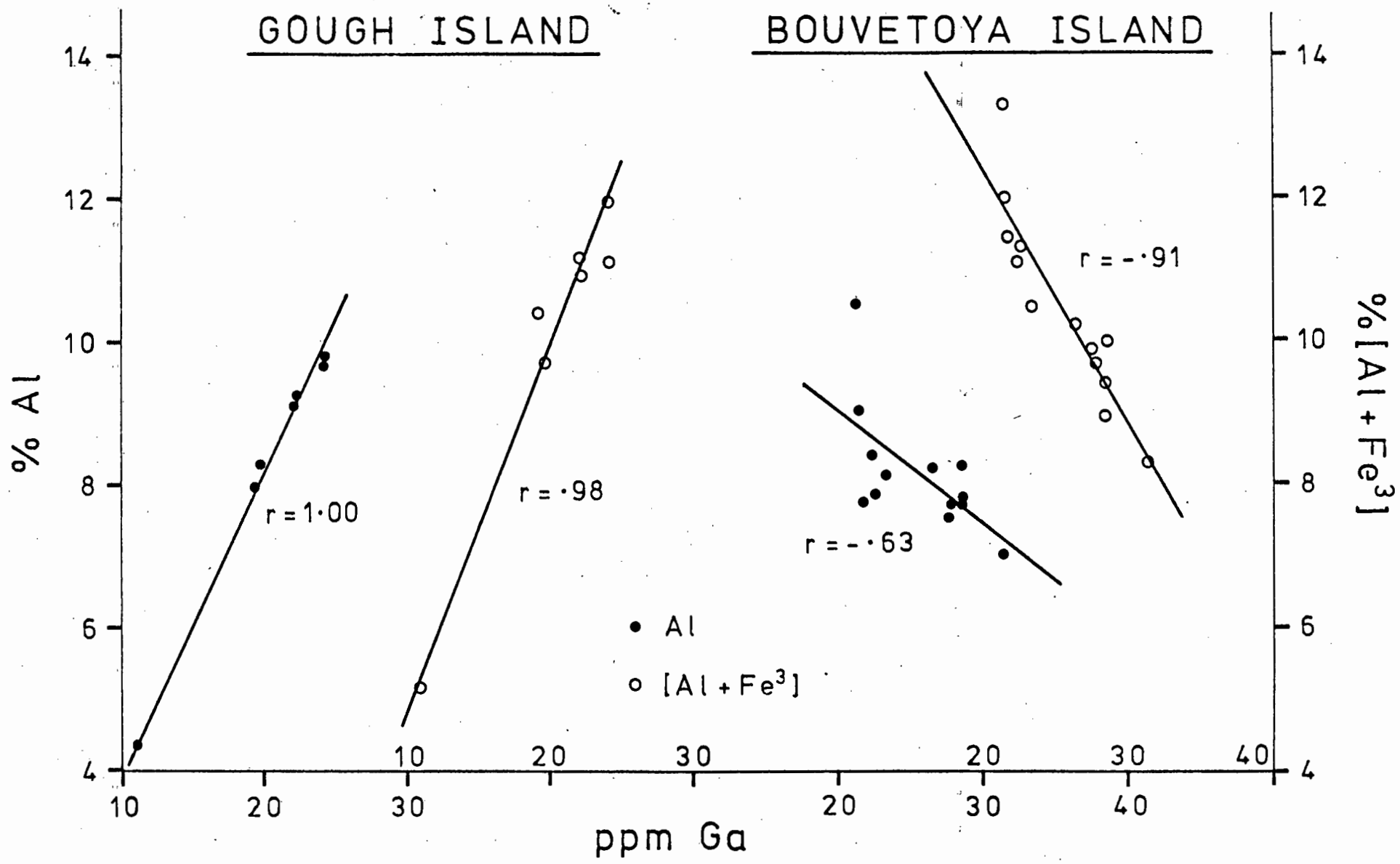

Fig. 83. Ga - Al and Ga - ($Al + Fe^3$) plots for rocks from Bouvetoya Island and from Gough Island.

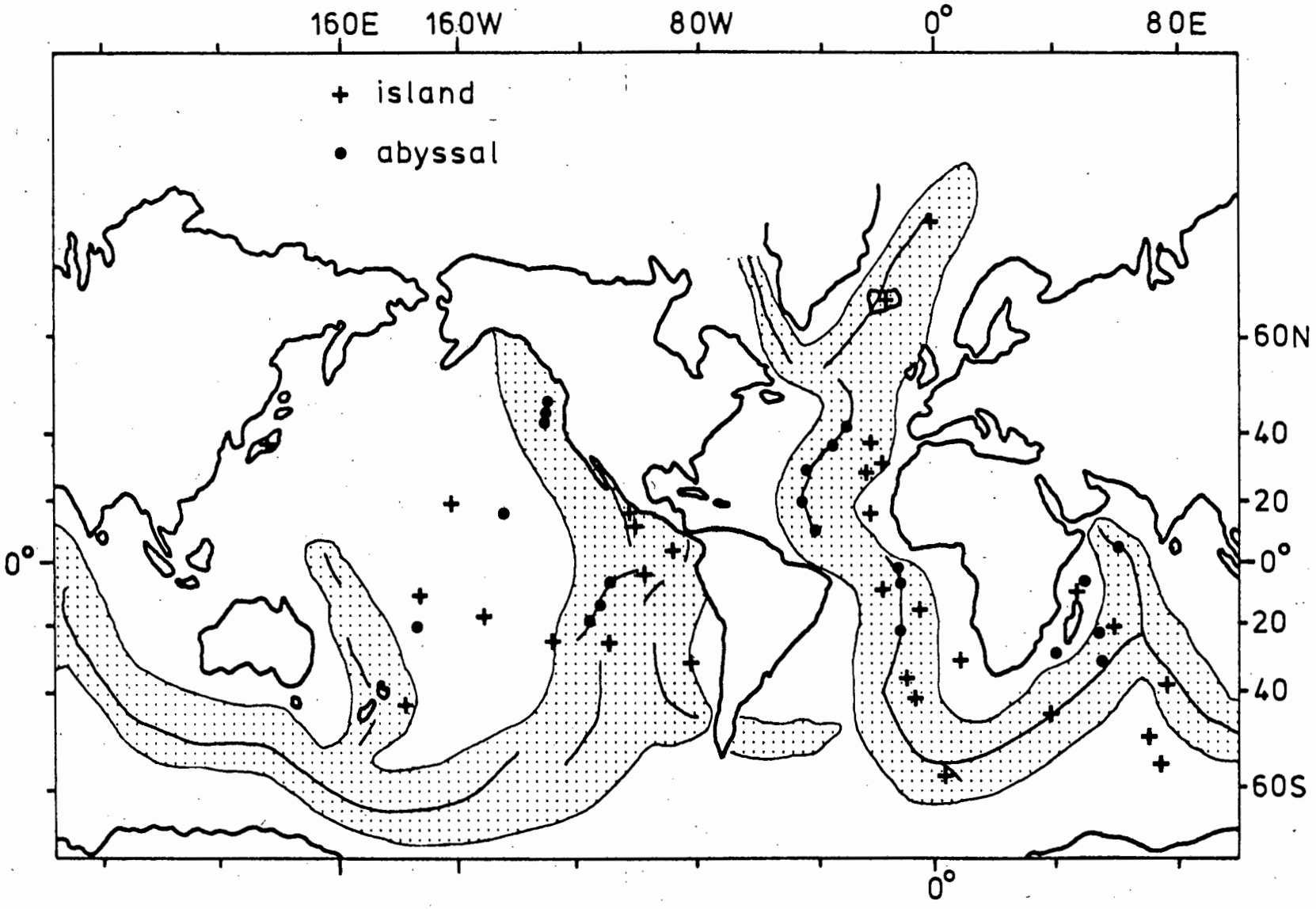

Fig. 84. Map indicating locations of rocks from abyssal sites and islands in which Ga has been determined in this work. Stippled areas indicate oceanic rise and ridge systems. (After Engel et al., 1965)

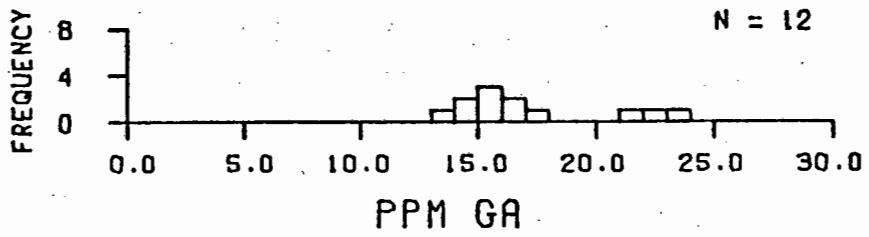

ABYSSAL INDIAN THOLEIITES.

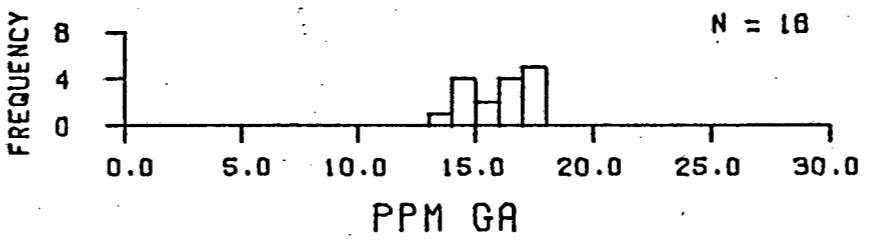

ABYSSAL PACIFIC THOLEIITES.

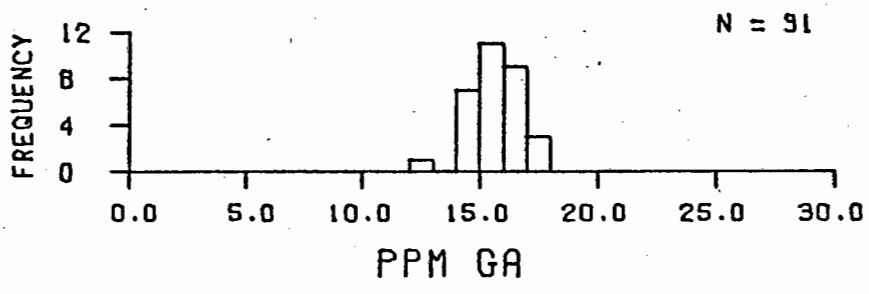

ABYSSAL ATLANTIC THOLEIITES.

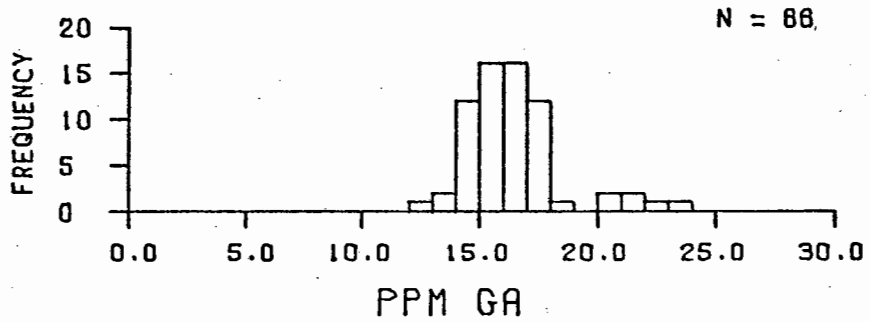

ALL OCEANIC THOLEIITES.

FIG. 85A. OCEANIC THOLEIITES.

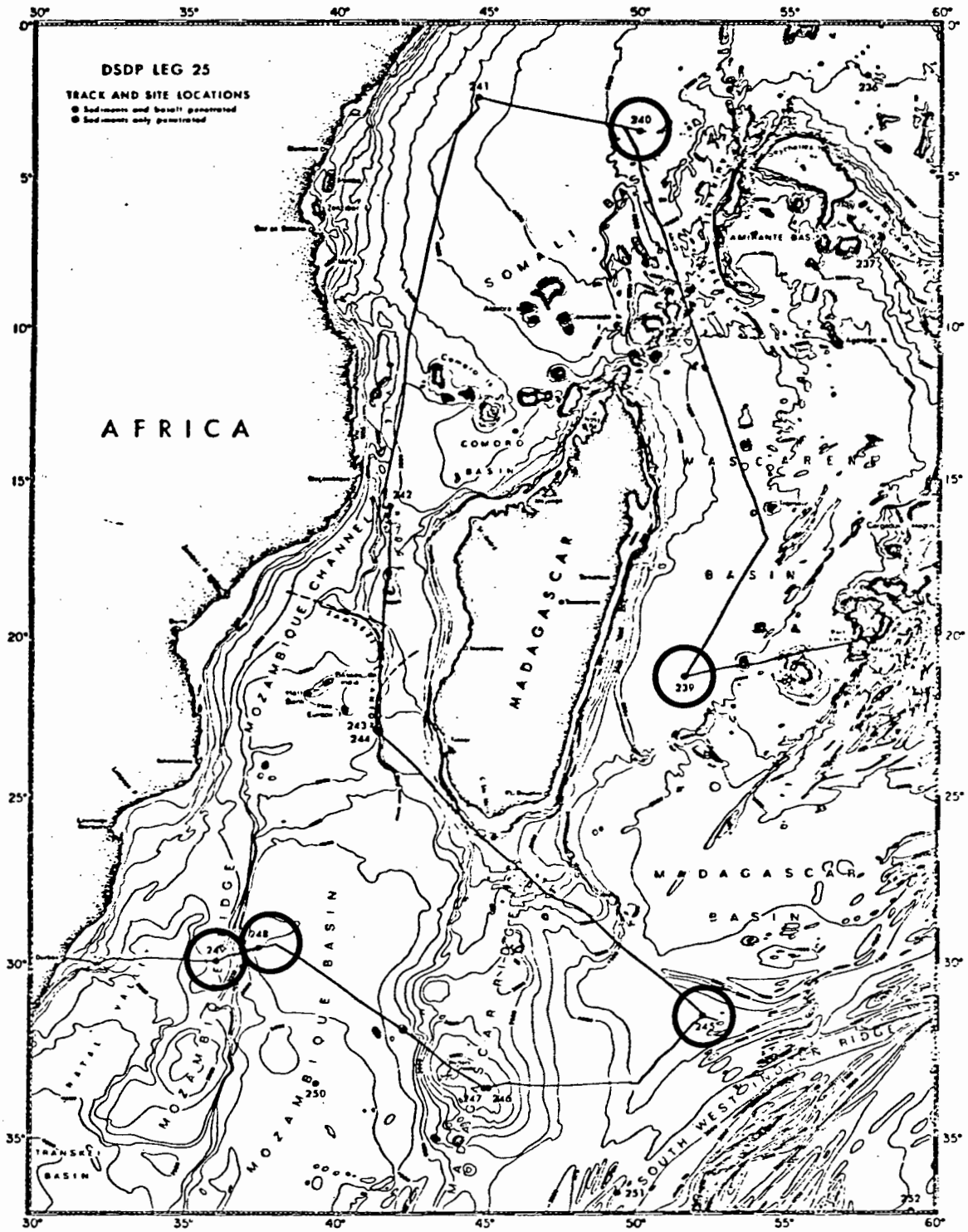

Fig. 86. Drill sites for DSDP Leg 25 in the western Indian Ocean.

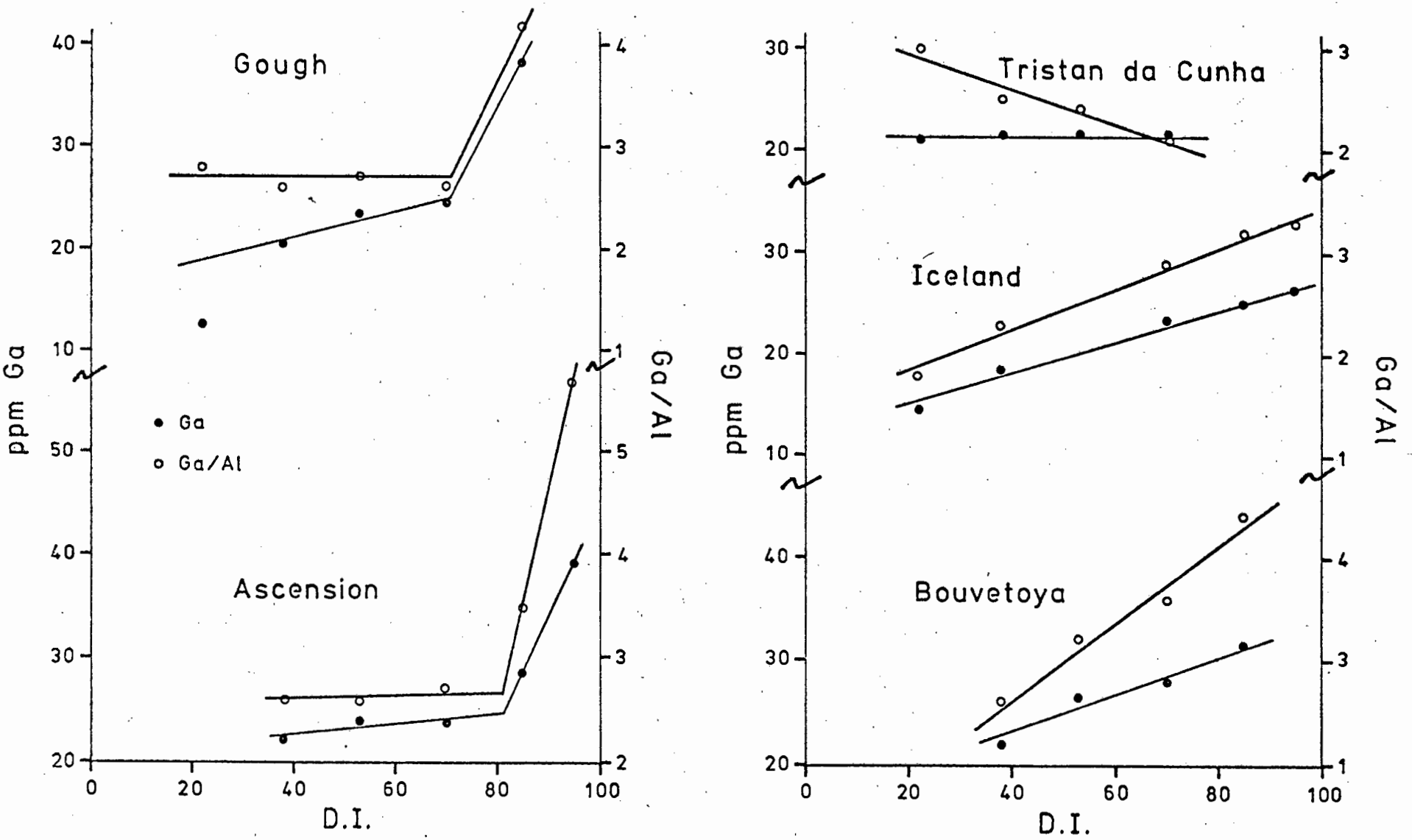

Fig. 87. Plot of Ga and Ga/Al ratio against differentiation index for rocks from islands in the Atlantic Ocean.

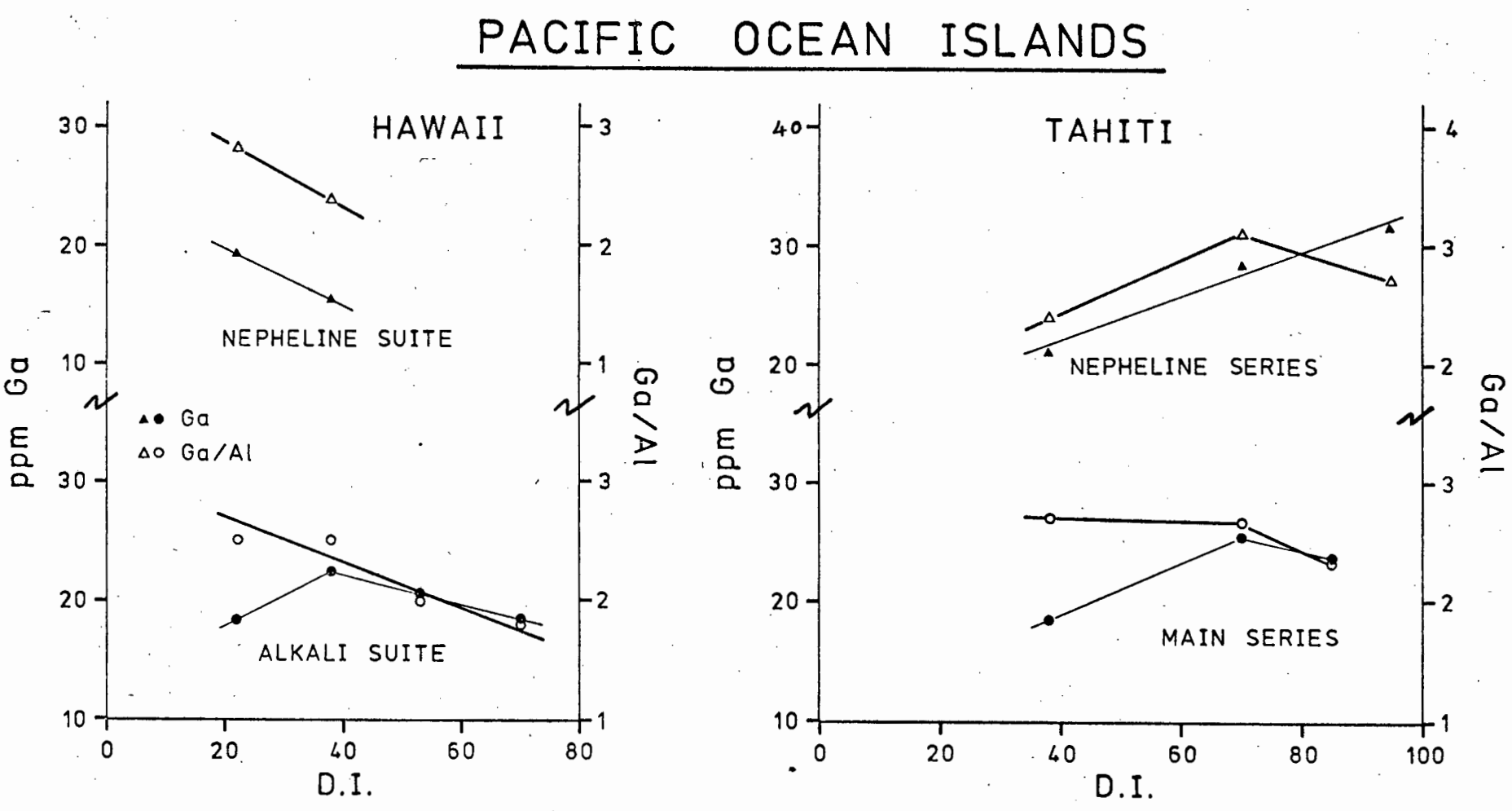

Fig. 88B. Plot of Ga and Ga/Al ratio against D.I. for rocks from islands in the Pacific Ocean.

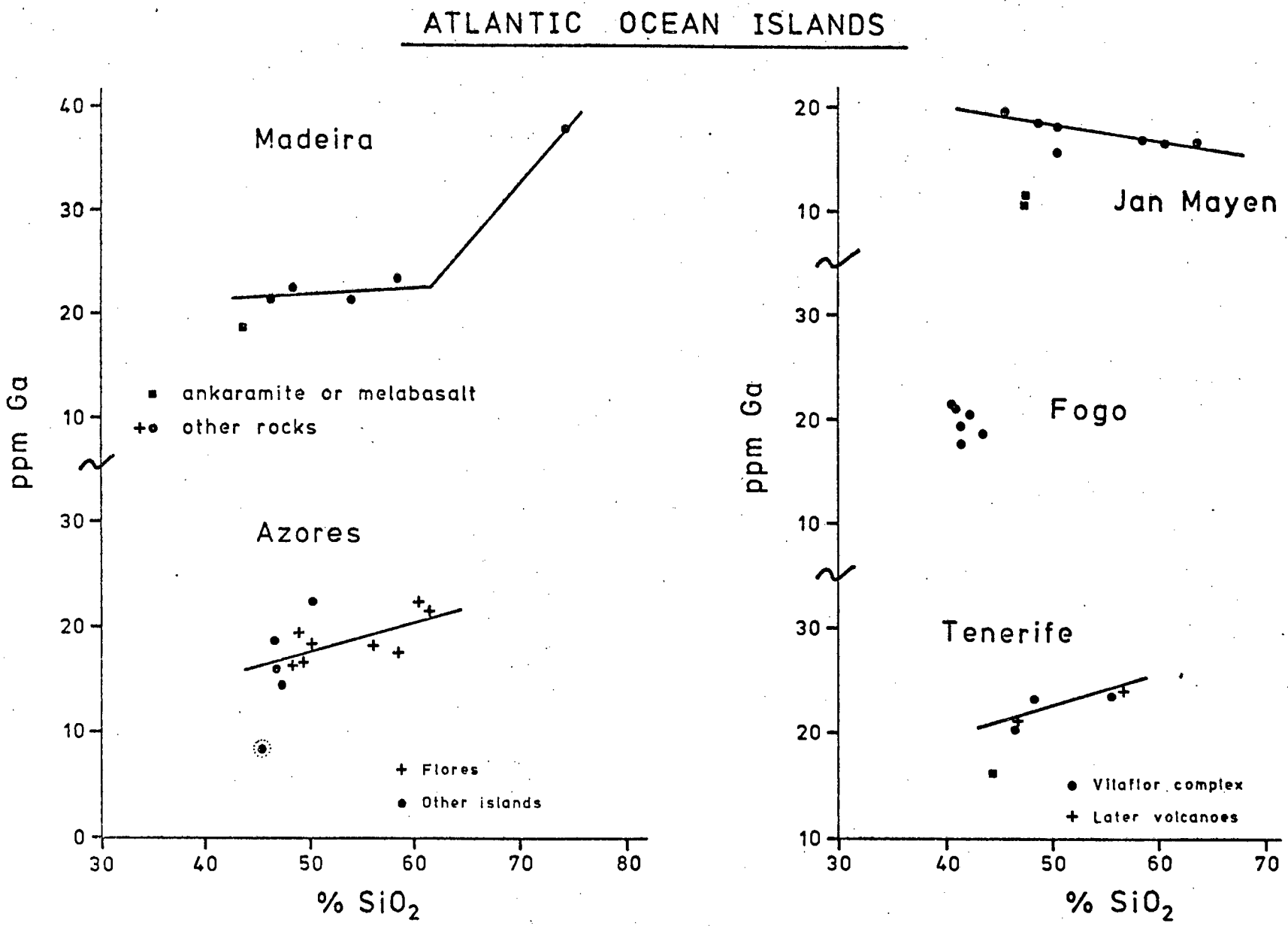

Fig. 90A. Plot of Ga against SiO_2 for rocks, for which D.I's were not known, from islands in the Atlantic Ocean.

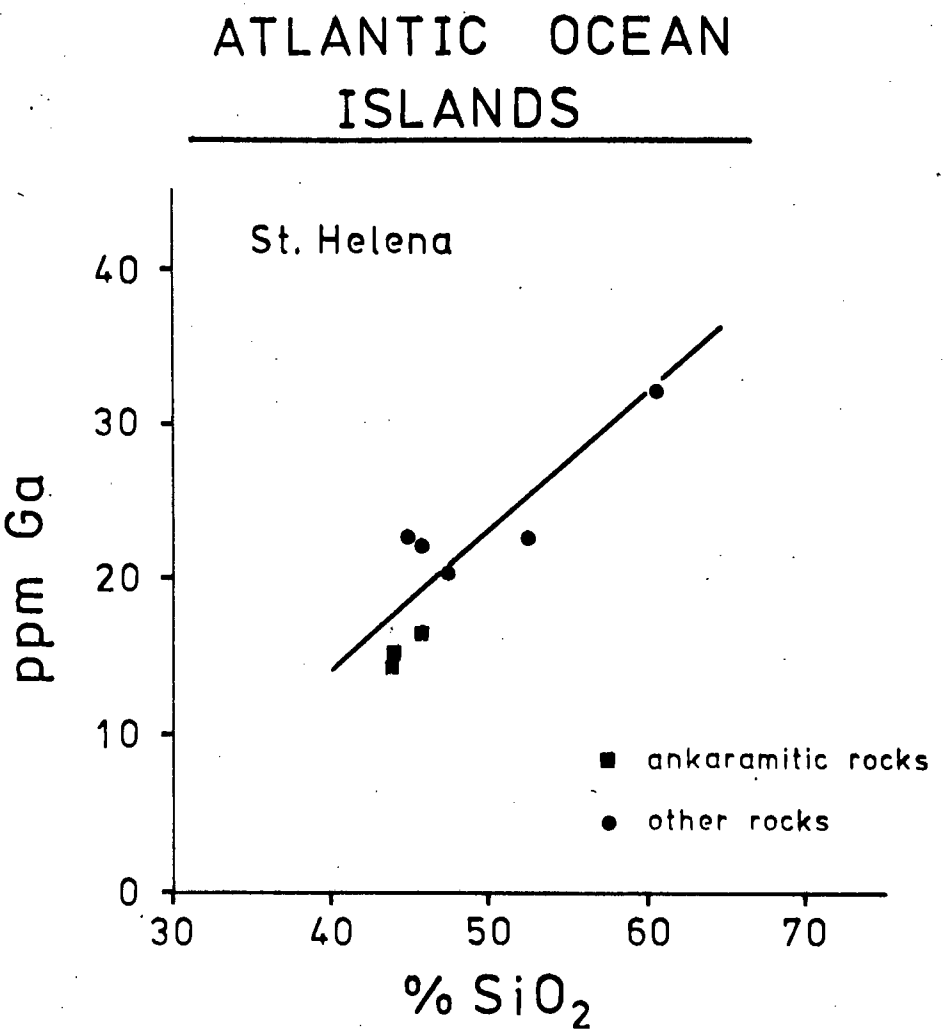

Fig. 90B. Plot of Ga against SiO_2 for rocks, for which D.I's were not known, from islands in the Atlantic Ocean.

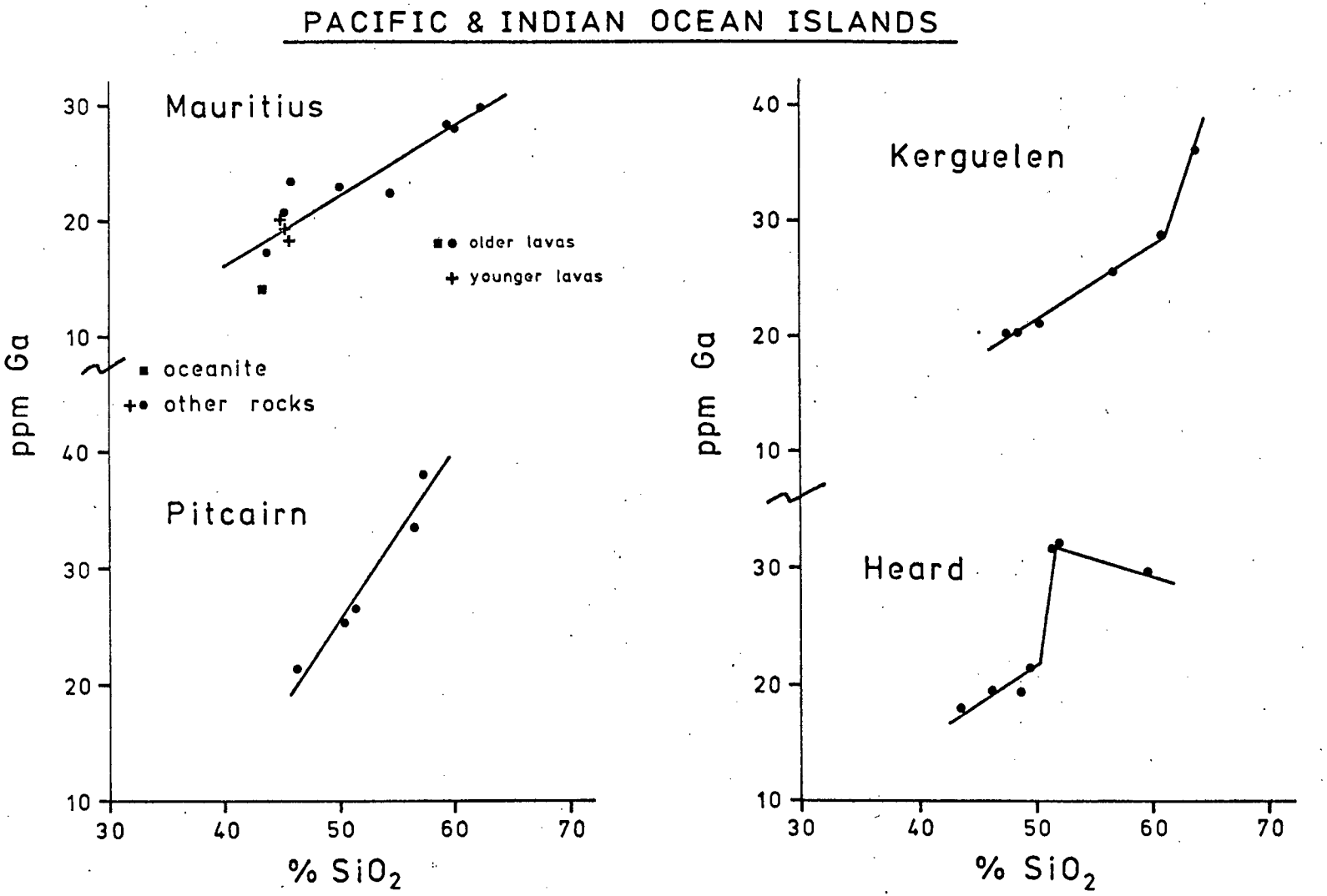

Fig. 91. Plot of Ga against SiO_2 for rocks, for which D.I's were not known, from islands in the Pacific and Indian Oceans.

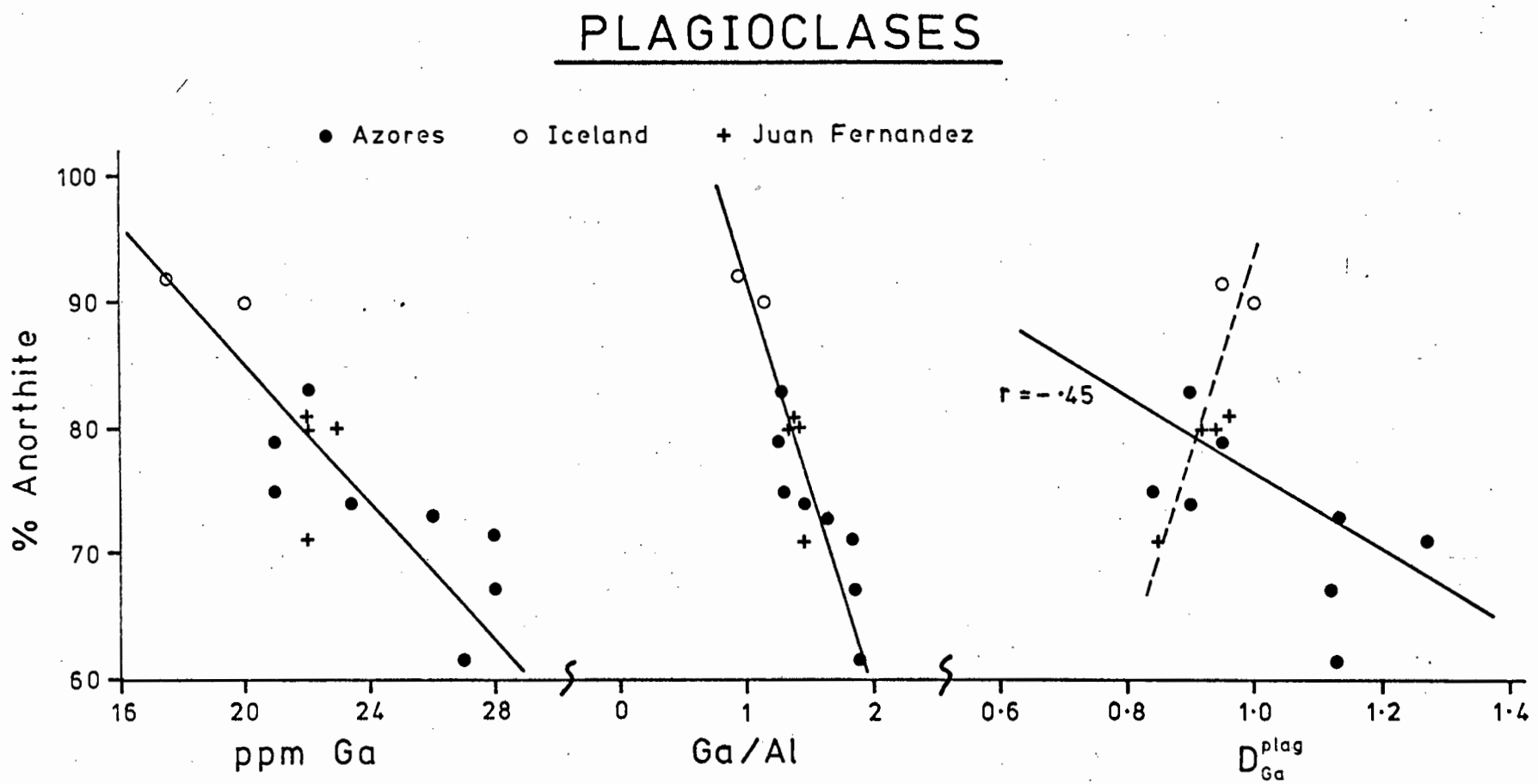

Fig. 92. Plot of Ga, Ga/Al ratio and D_{Ga}^{plag} against percent Anorthite for plagioclases from basic lavas (data from Goodman, 1972).

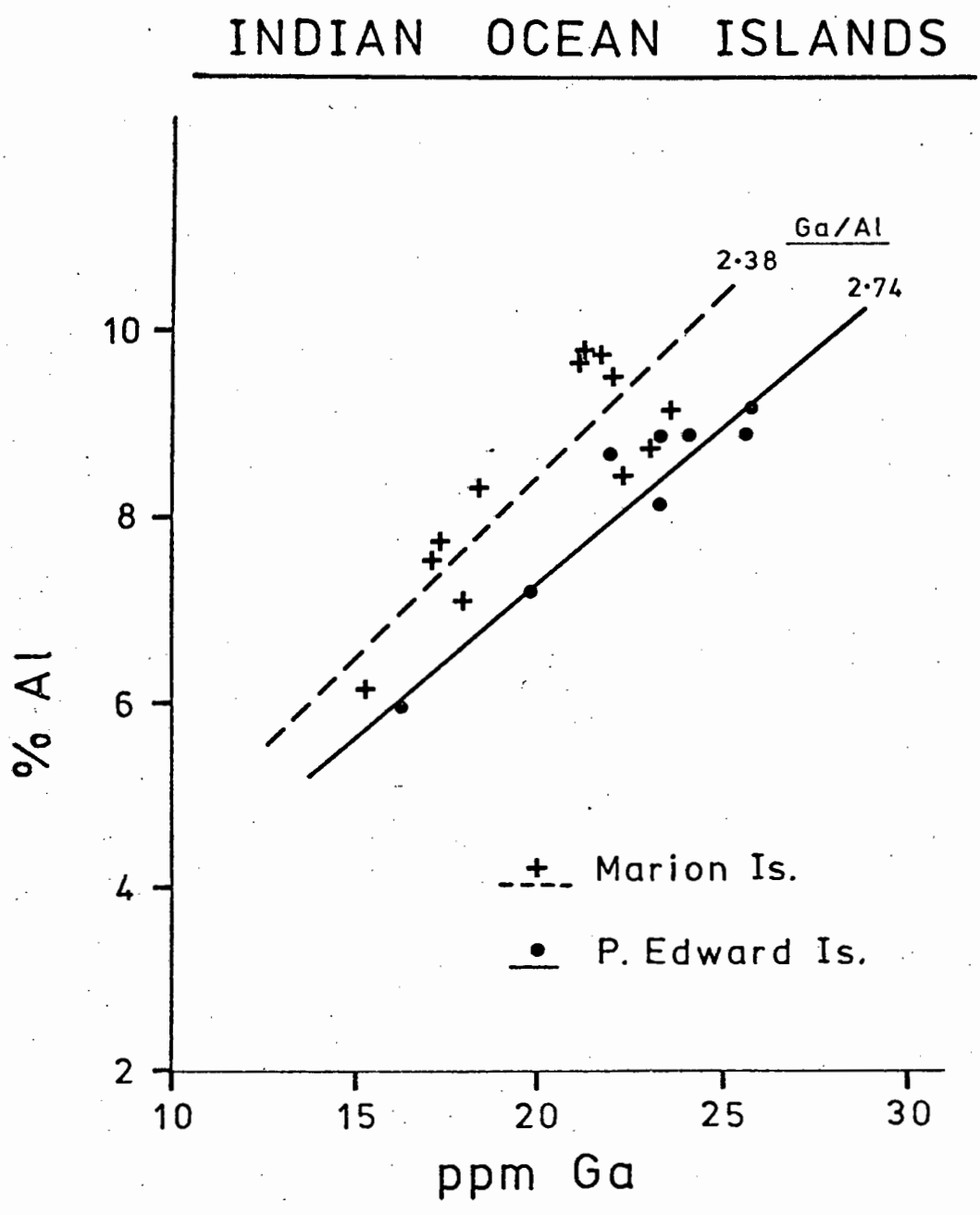

Fig. 93. Plot of Ga against Al for rocks from Marion and Prince Edward Islands, Indian Ocean.

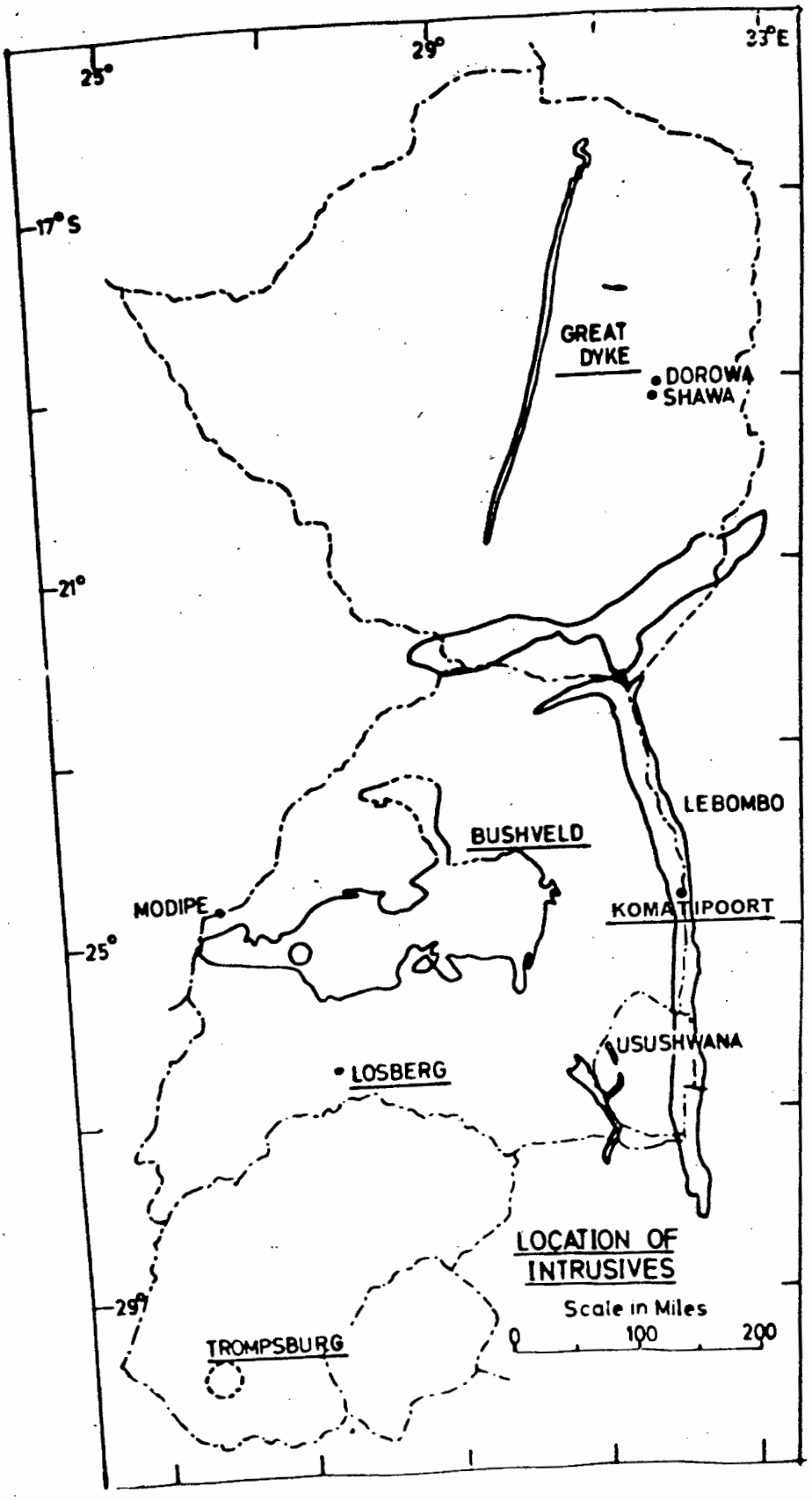

Fig. 94. Map of southern Africa showing the locations and extent of some intrusive bodies in Rhodesia, Transvaal and Orange Free State (after Davies et al., 1970).

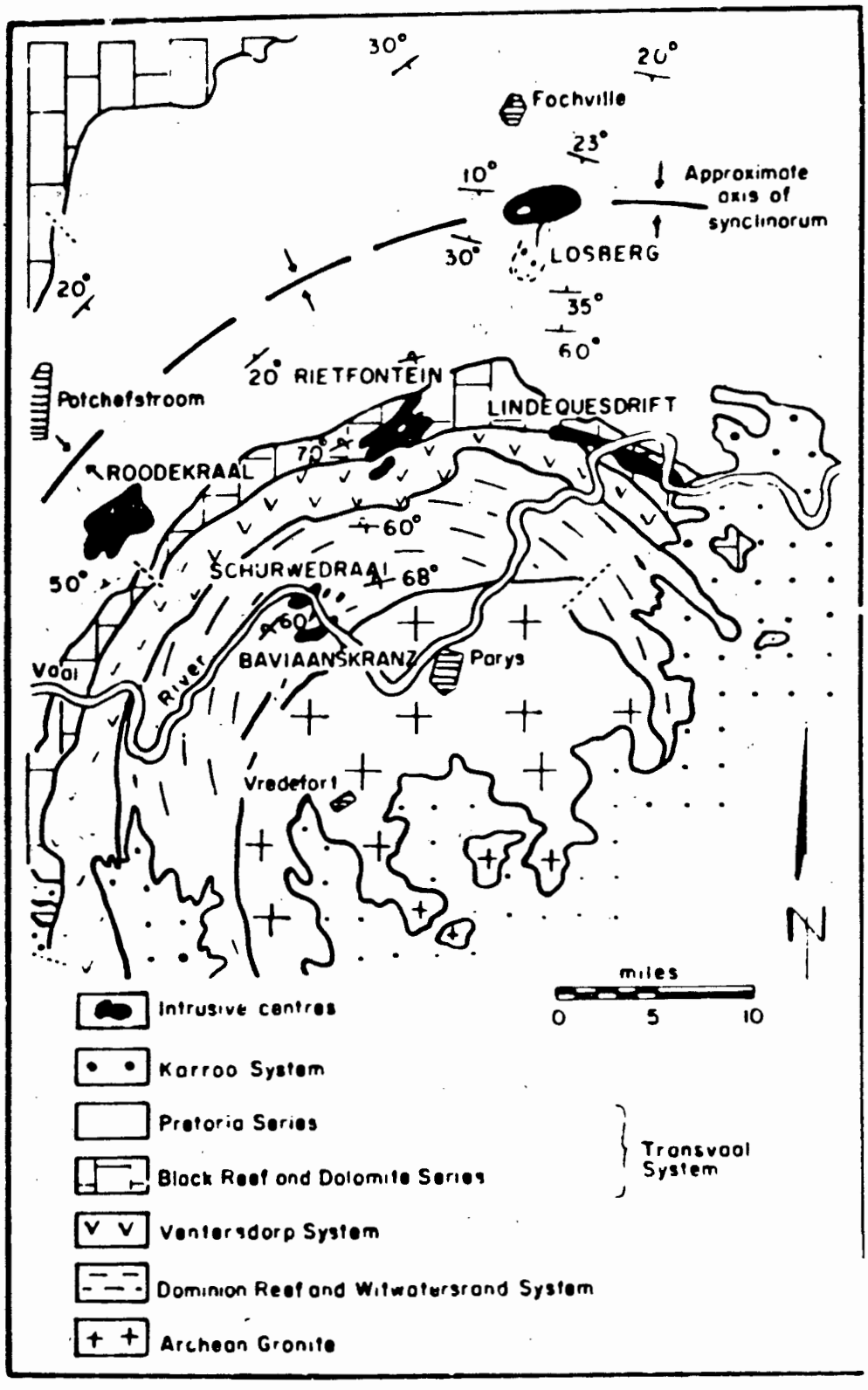

Fig. 95. Geological map of the Vredefort Dome area showing the location of the Losberg Intrusion (from Danchin and Ferguson, 1970).

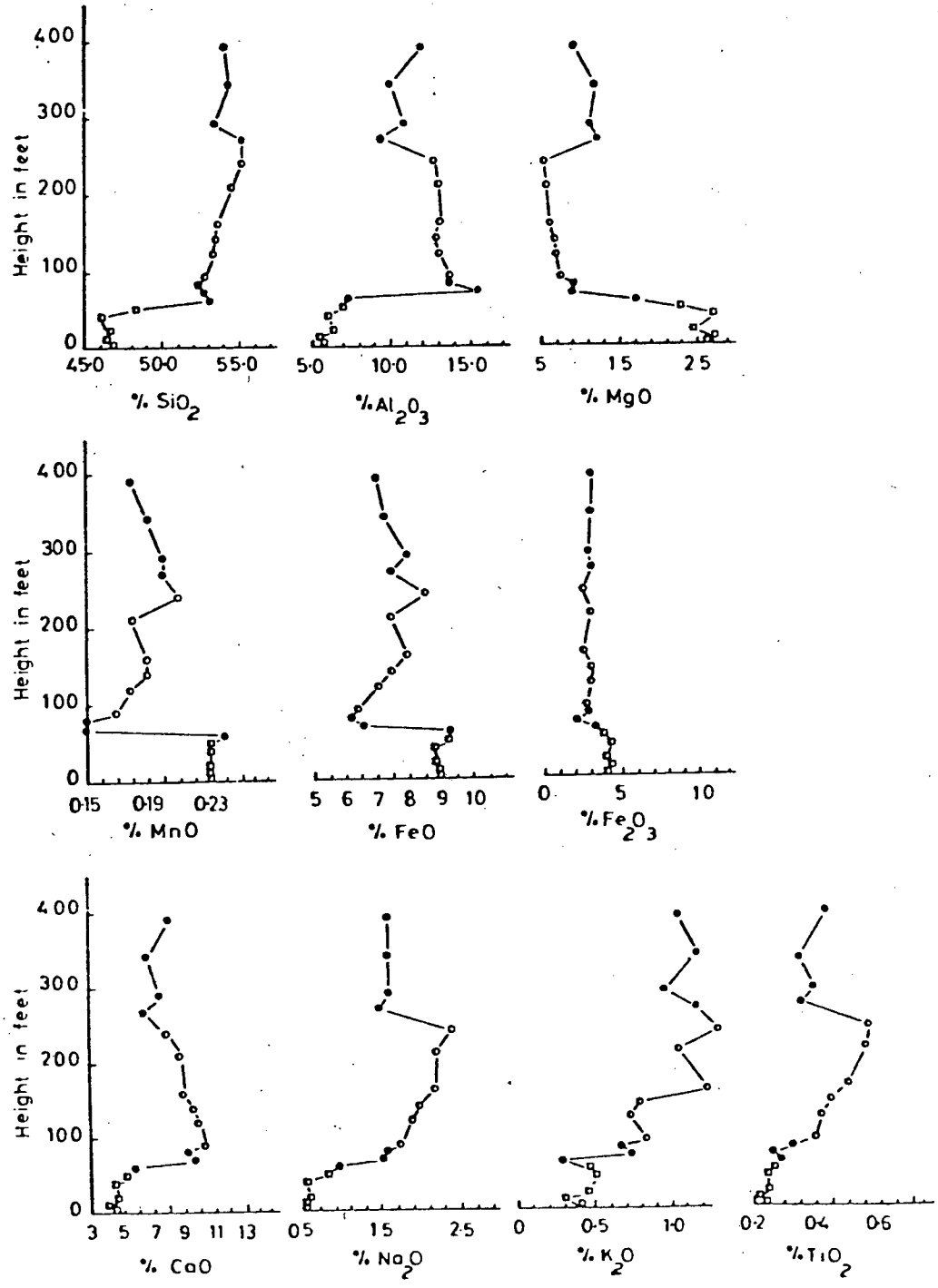

Fig. 96. Variation of major element oxides with height in the Losberg Intrusion (from Danchin and Ferguson, 1970).

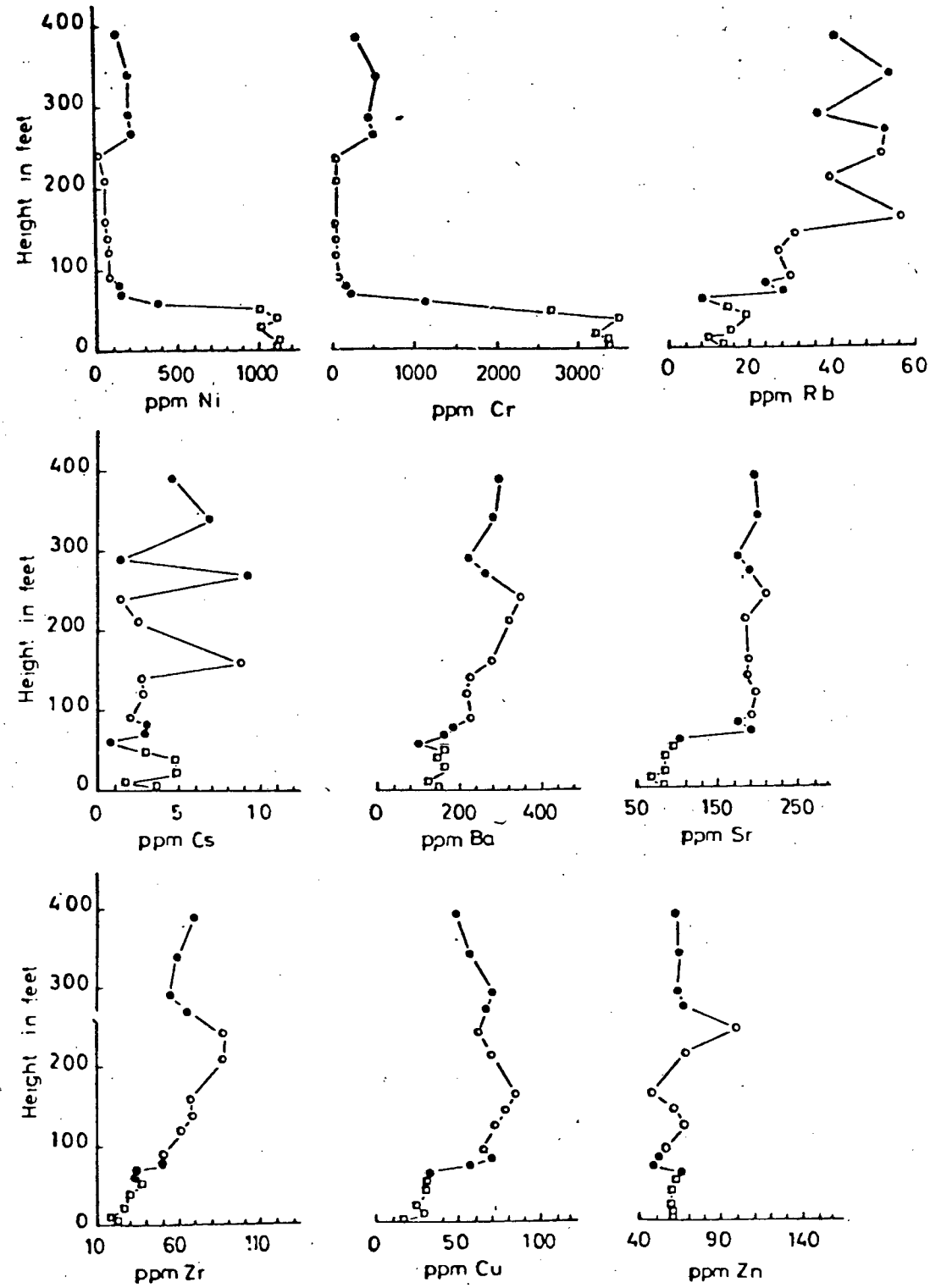

Fig. 97. Variation of trace elements with height in the Losberg Intrusion (from Danchin and Ferguson, 1970).

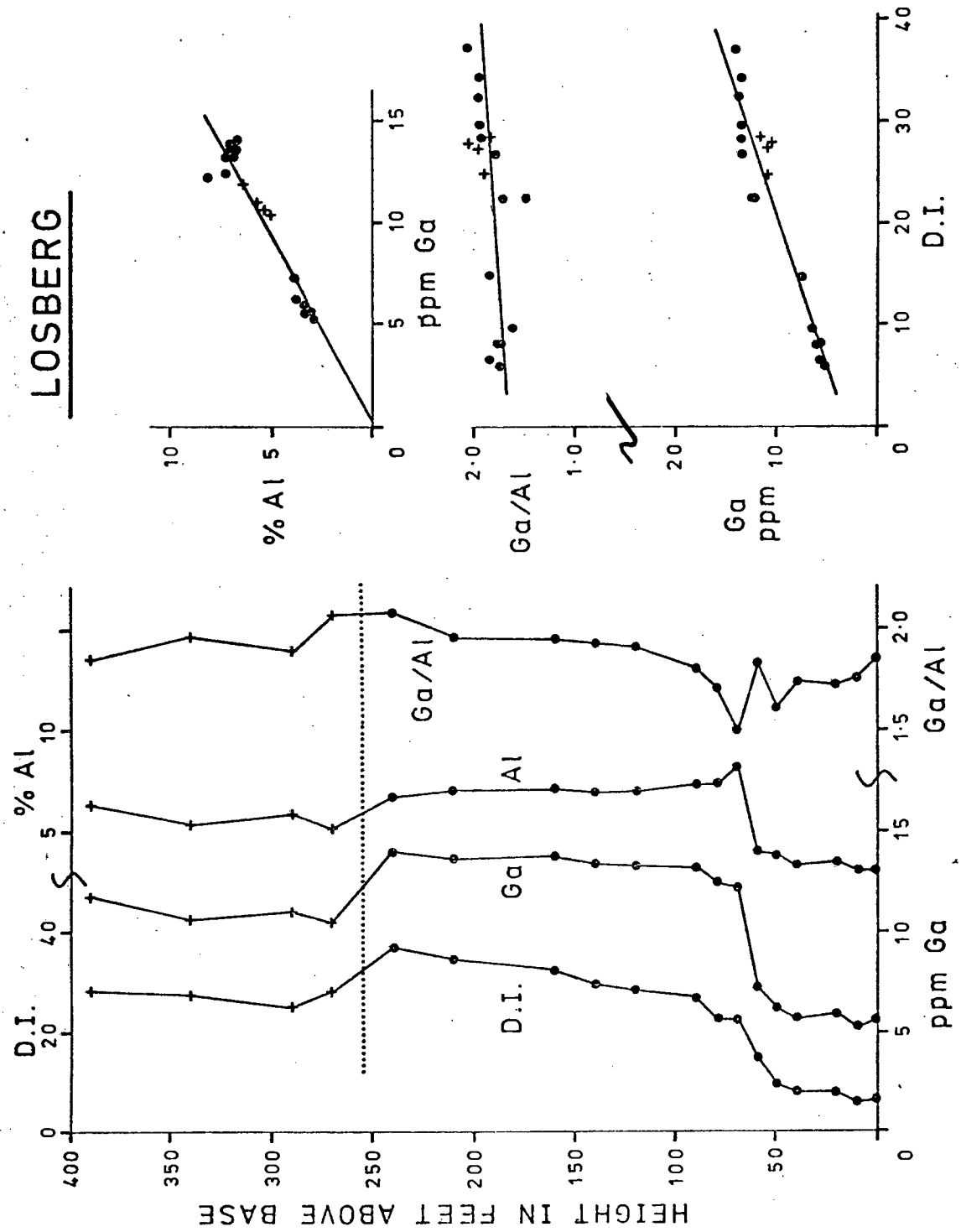

Fig. 98. Plots of Ga, Al, Ga/Al ratio and D.I. against height in the Losberg Intrusion, and plots of Ga - D.I., Ga/Al - D.I. and Ga - Al.

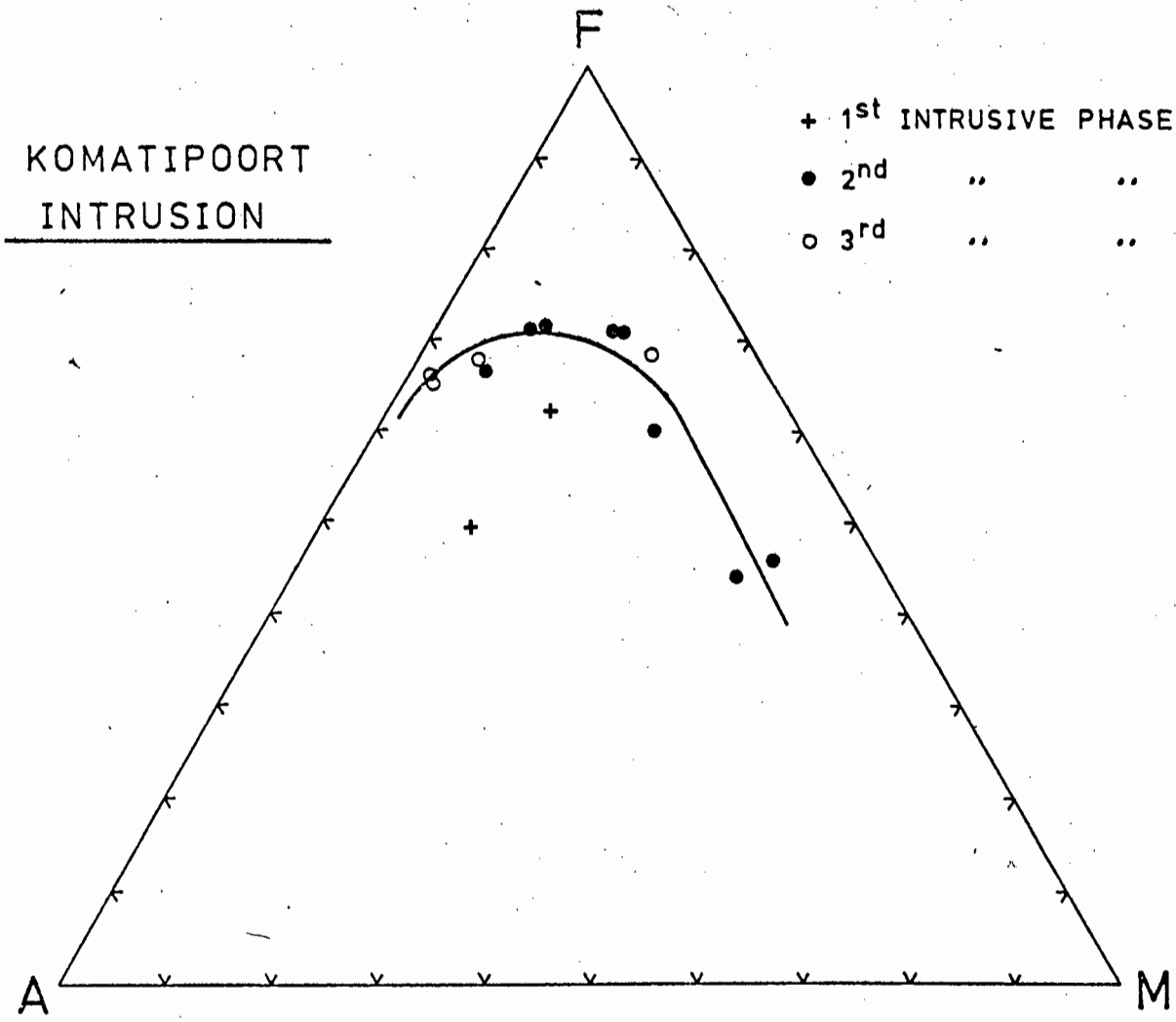

Fig. 99. FMA diagram for rocks from the Komatipoort Intrusion. Data from A.J. Erlank (pers. comm.).

KOMATIPOORT INTRUSION

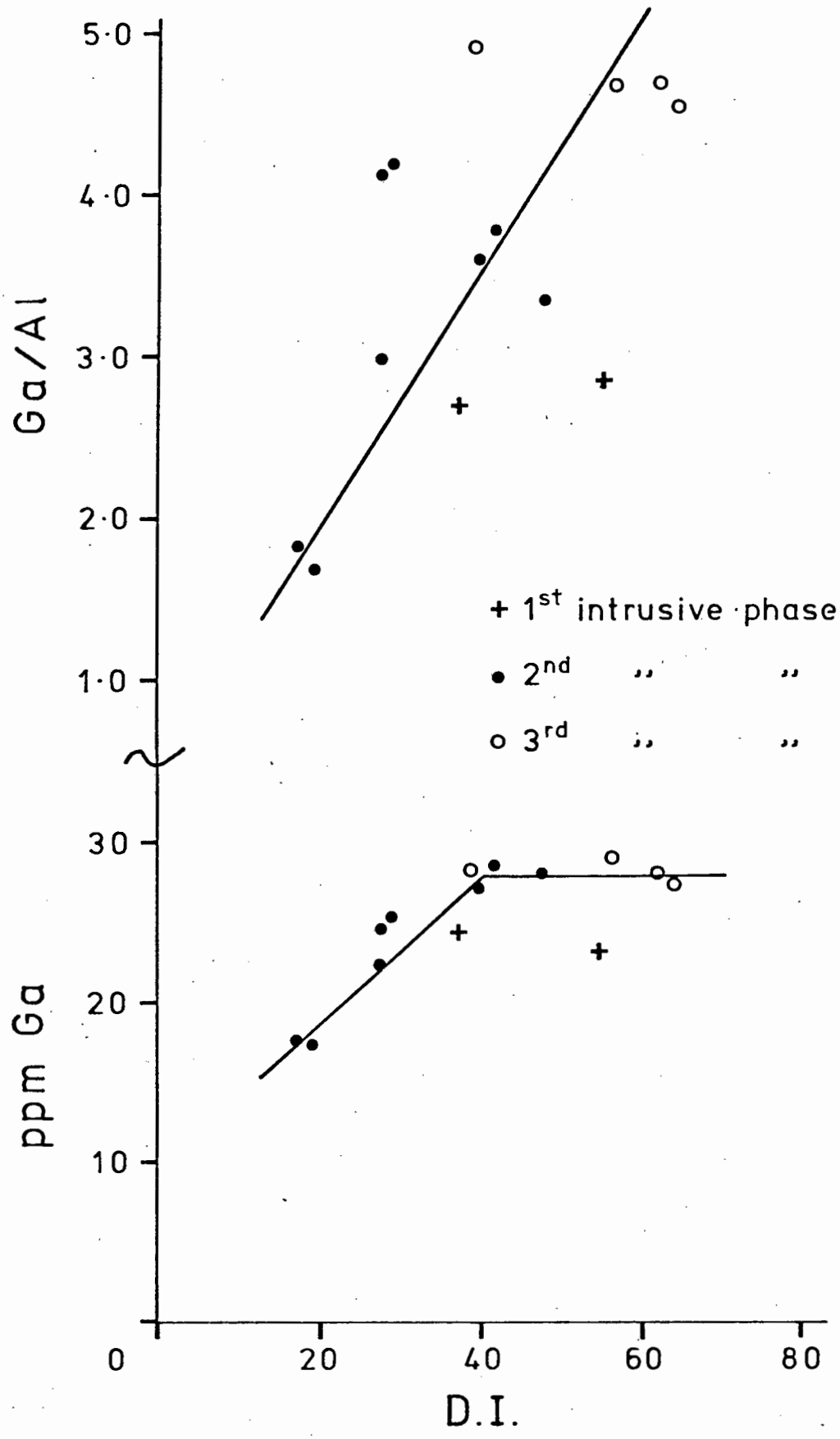

Fig. 100. Ga - D.I. and Ga/Al - D.I. plots for rocks from the Komatipoort Intrusion.

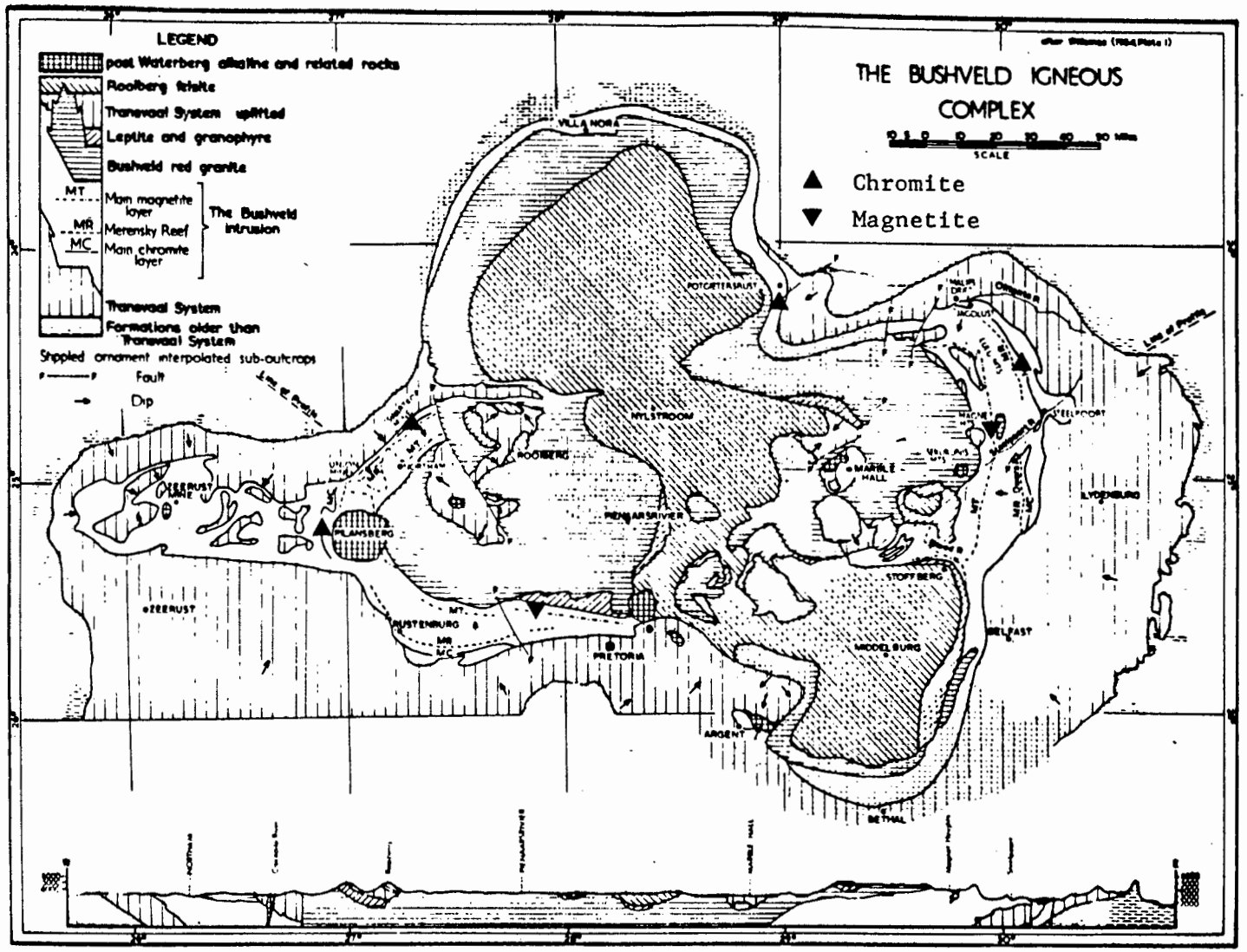

Fig. 101. Map of the B.I.C. showing locations of chromite and magnetite samples analysed in this work (map from Wager and Brown, 1968).

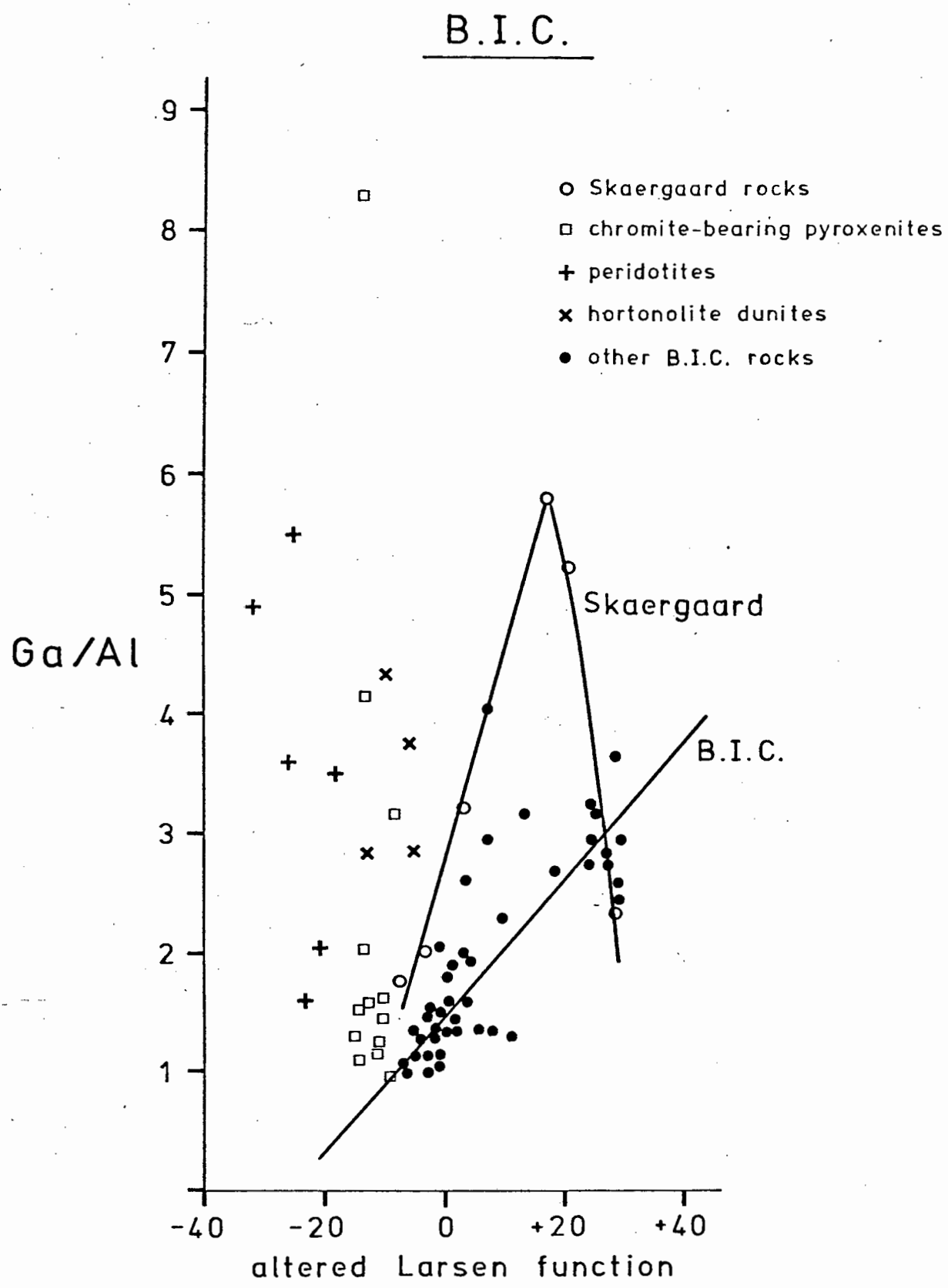

Fig. 102. Ga/Al ratios plotted against the altered Larsen function for rocks from the B.I.C. Data taken from Liebenberg (1960). Data for rocks from the Skaergaard Intrusion are included for comparison.

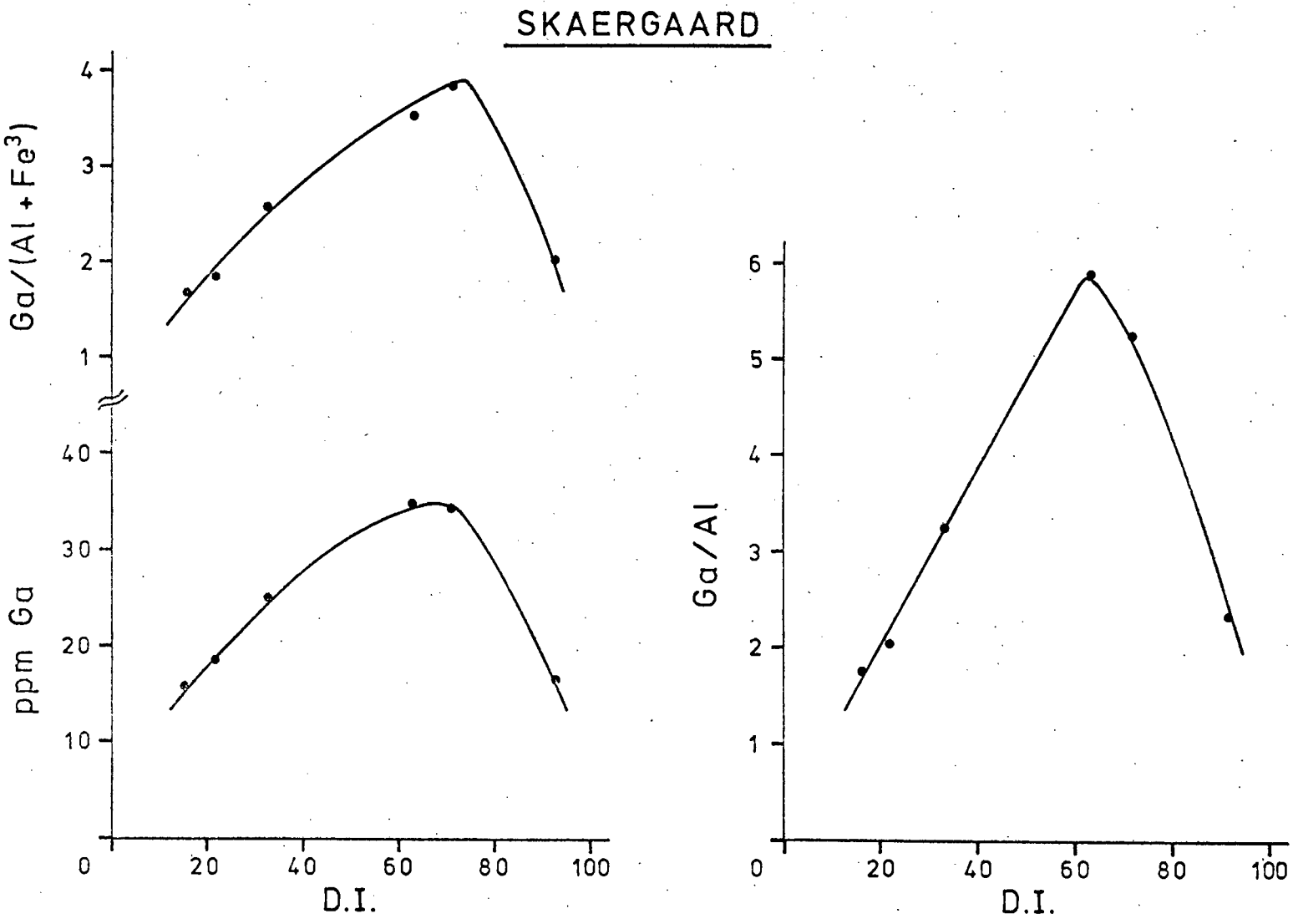

Fig. 103. Plots of Ga, Ga/Al and Ga/(Al + Fe^3) against D.I. for rocks from the Skaergaard Intrusion. Data from this work.

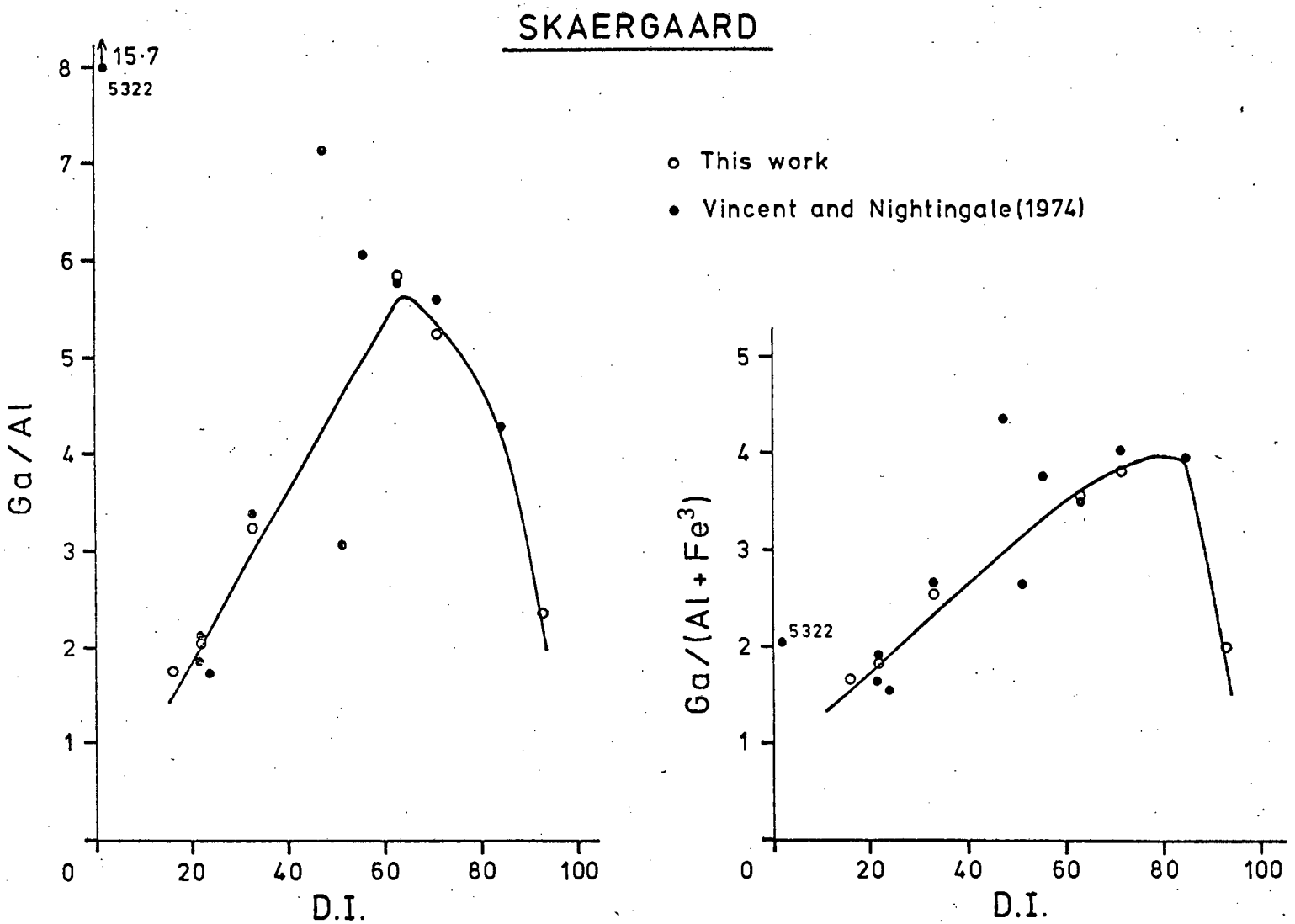

Fig. 104. Plots of Ga/Al and Ga/(Al + Fe^3) for rocks from the Skaergaard Intrusion, showing combined data from this work and Vincent and Nightingale (1974).

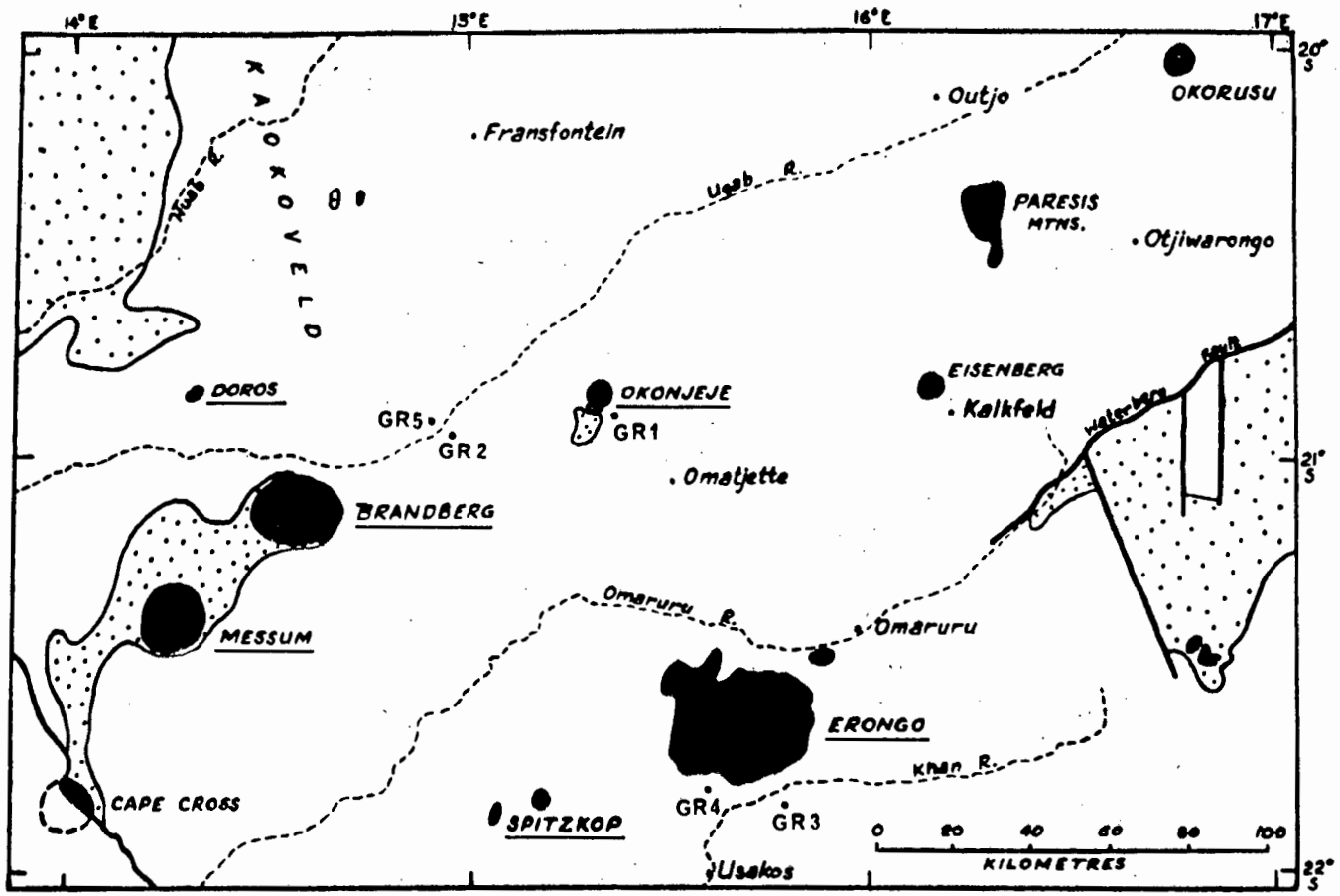

Fig. 105. Sketch map showing the distribution of post-Karroo igneous complexes (solid black) and Karroo sediments and lavas (stippled) in northern Damaraland, S.W.A., and the locations of some granite samples (after Simpson, 1954).

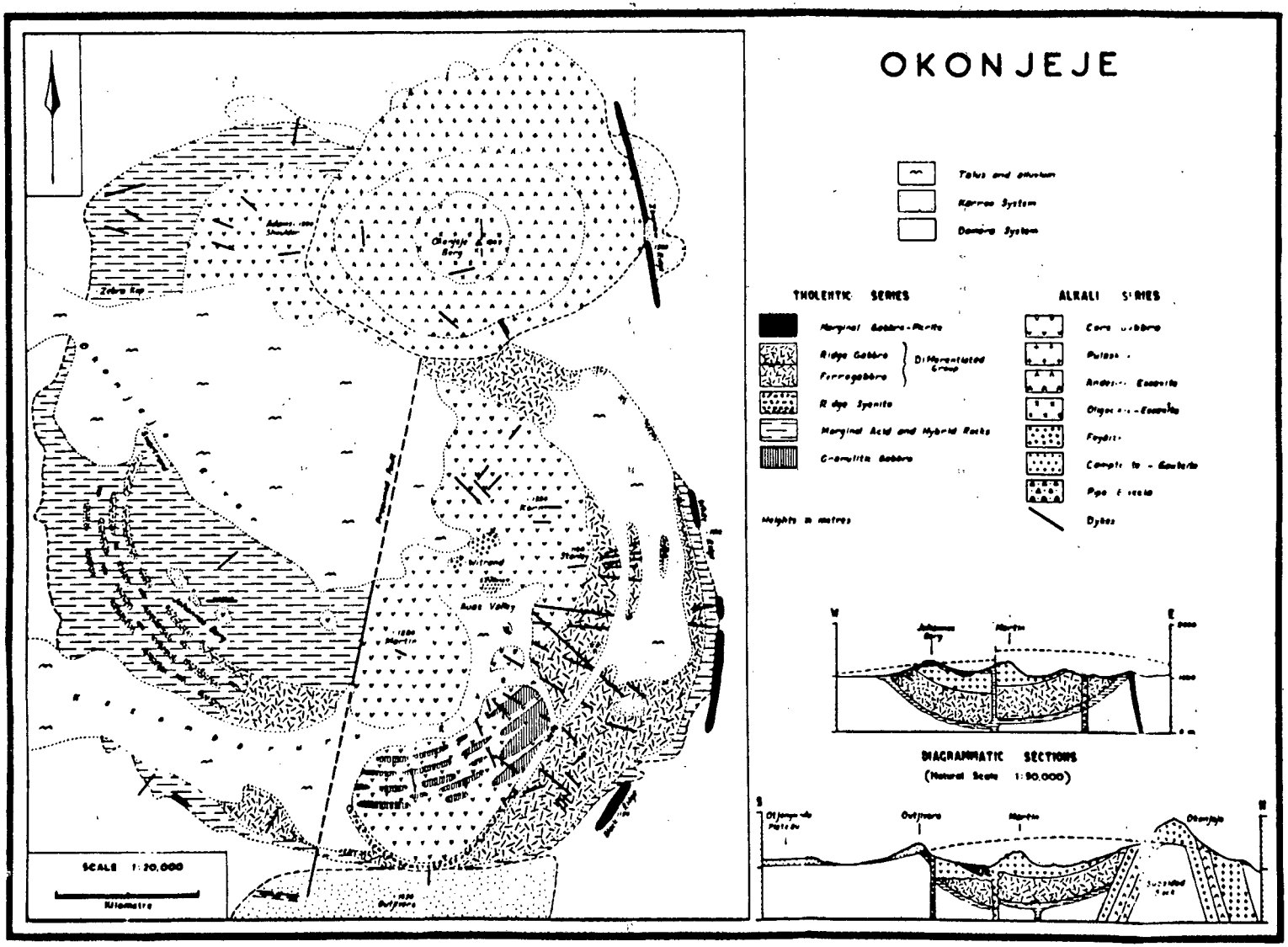

Fig. 106. Geological map of the Okonjeje Igneous Complex, S.W.A., from Simpson (1954).

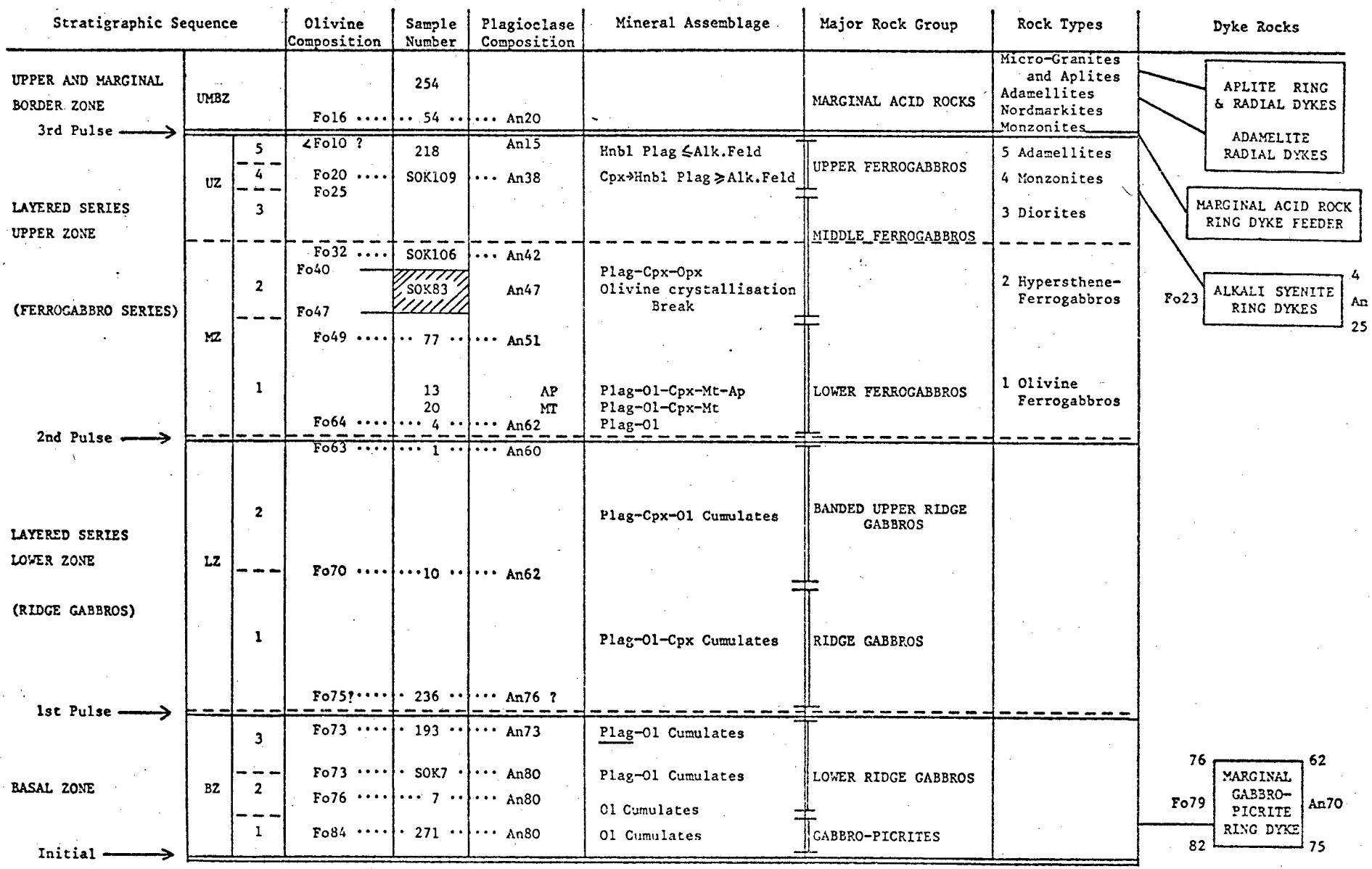

Fig. 107. Schematic representation of the layered tholeiitic series and its dyke equivalents, Okonjeje Igneous Complex (after Fesq, pers. comm.).

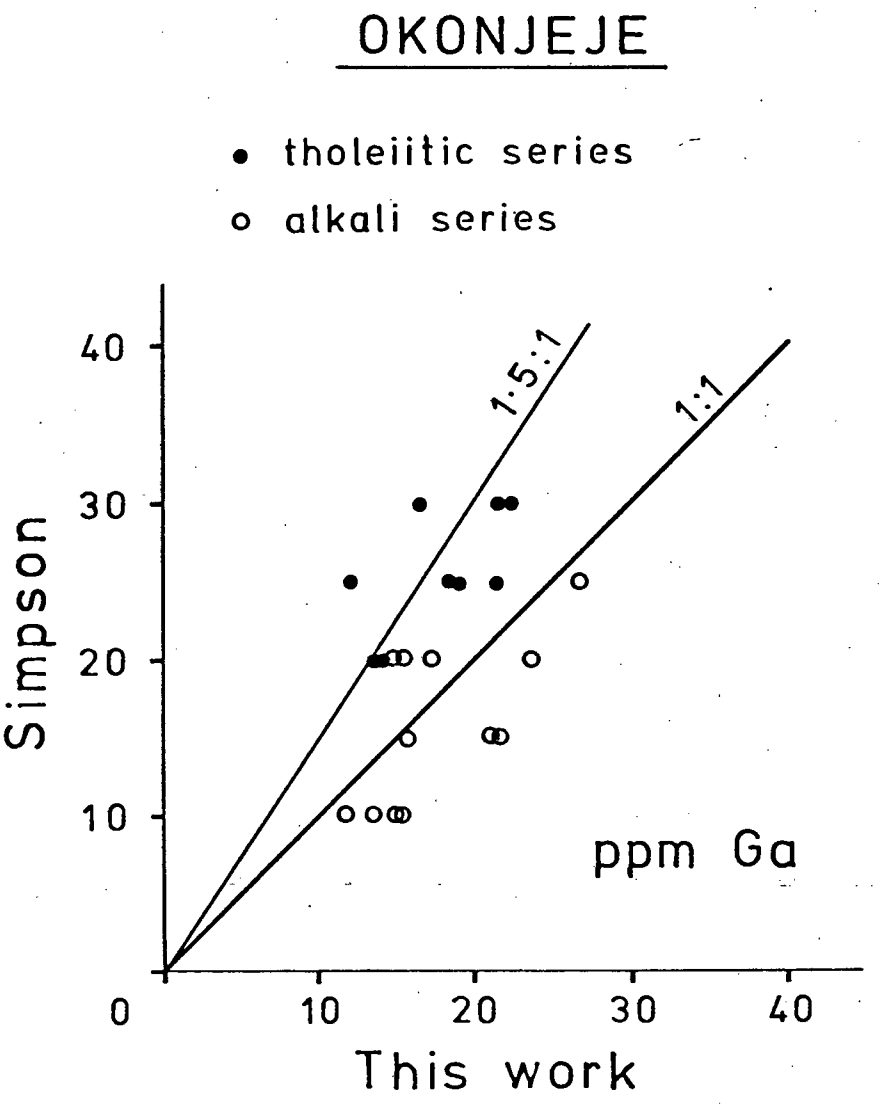

Fig. 108. Plot of Ga data from this work against those from Simpson (1954) for rocks from the Okonjeje Igneous Complex.

Fig. 109. Plots of Ga and Ga/Al ratio against D.I. for all rocks from the tholeiitic and alkali series and granites from the Okonjeje Igneous Complex.

KEY:

Tholeiitic Series

- ● Mafic cumulates (gabbro-picrites)
- ○ Olivine gabbros (Ridge gabbros)
- □ Olivine ferrogabbros
- + Ferrogabbros
- ■ Alkali syenites
- ▼ Quartz syenites
- △ Marginal acid rocks
- ⁘ Plagioclase cumulate

Alkali Series

- ● Contaminated olivine gabbros
- ○ Olivine gabbros (Core gabbros)
- □ Nepheline olivine gabbros
- + Melteigites
- ■ Lamprophyres
- ▼ Essexites and pulaskites
- △ Foyaites and tinguaites

- × Granites

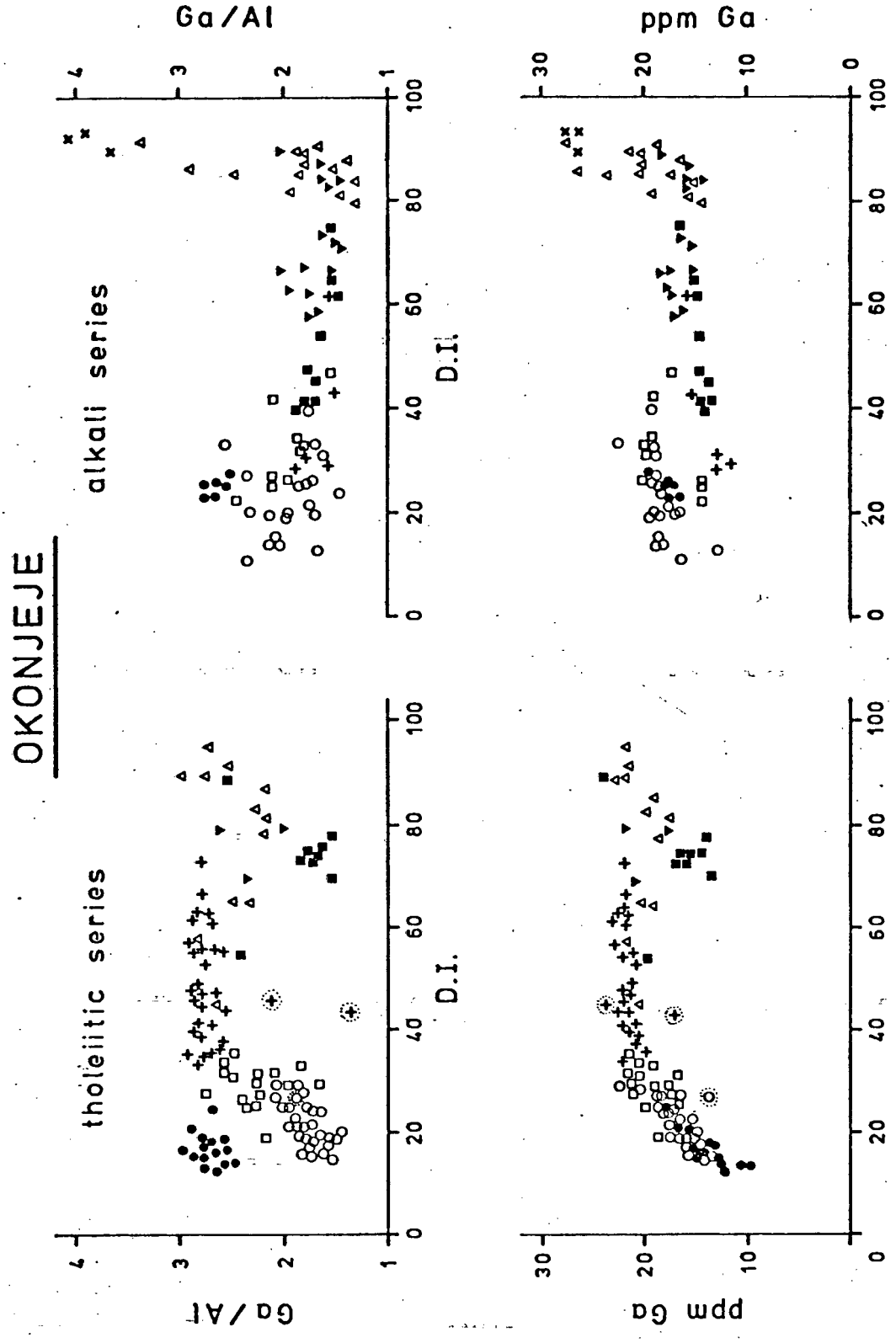

Fig. 109. Plots of Ga and Ga/Al ratio against D.I. for all rocks from the tholeiitic and alkali series of the Okonjeje Igneous Complex.

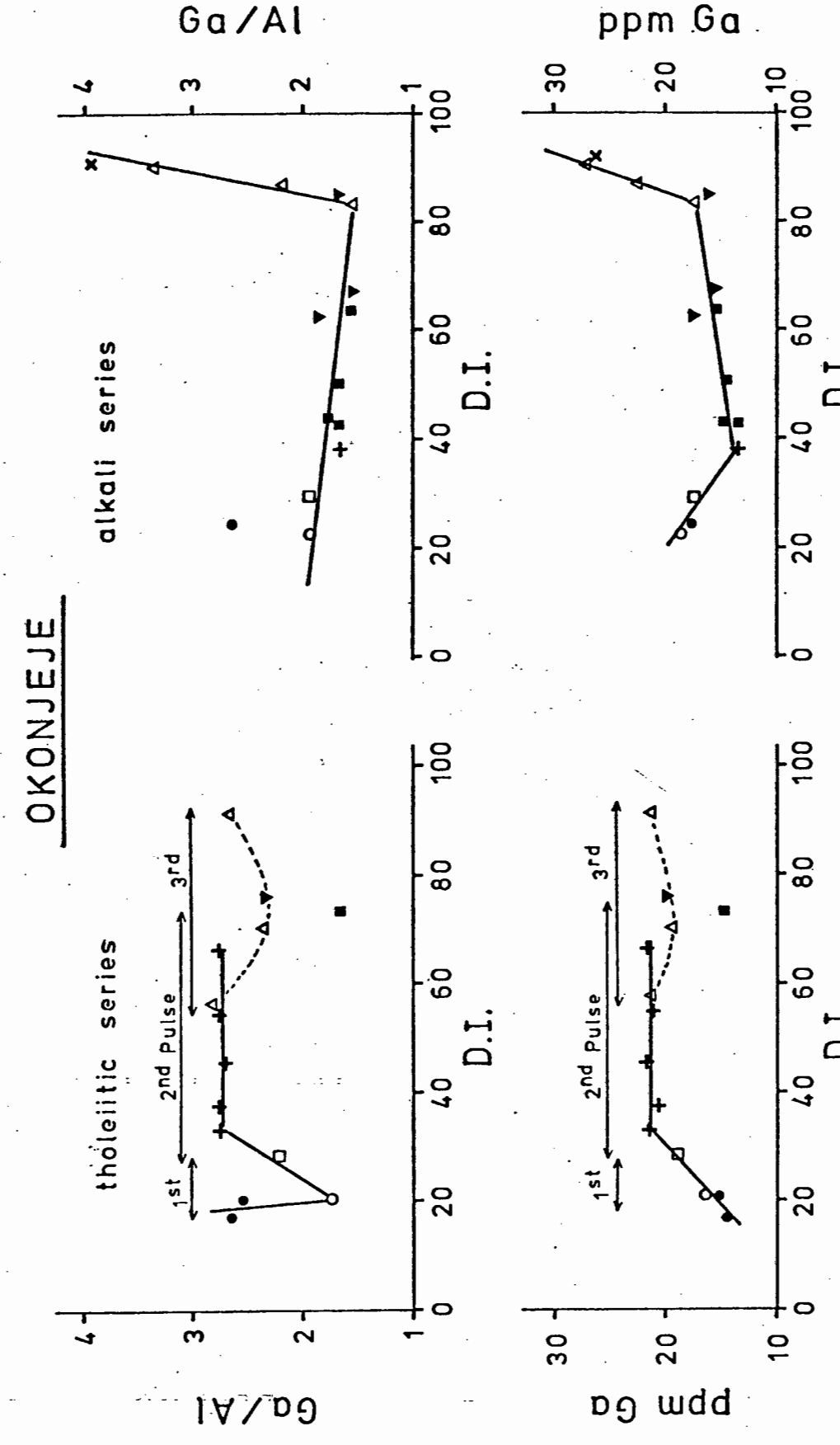

Fig. 110. Plots of mean values for Ga and the Ga/Al ratio against D.I. for individual rock types from the tholeiitic and alkali series of the Okonjeje Igneous Comples. Key: as for Fig. 109.

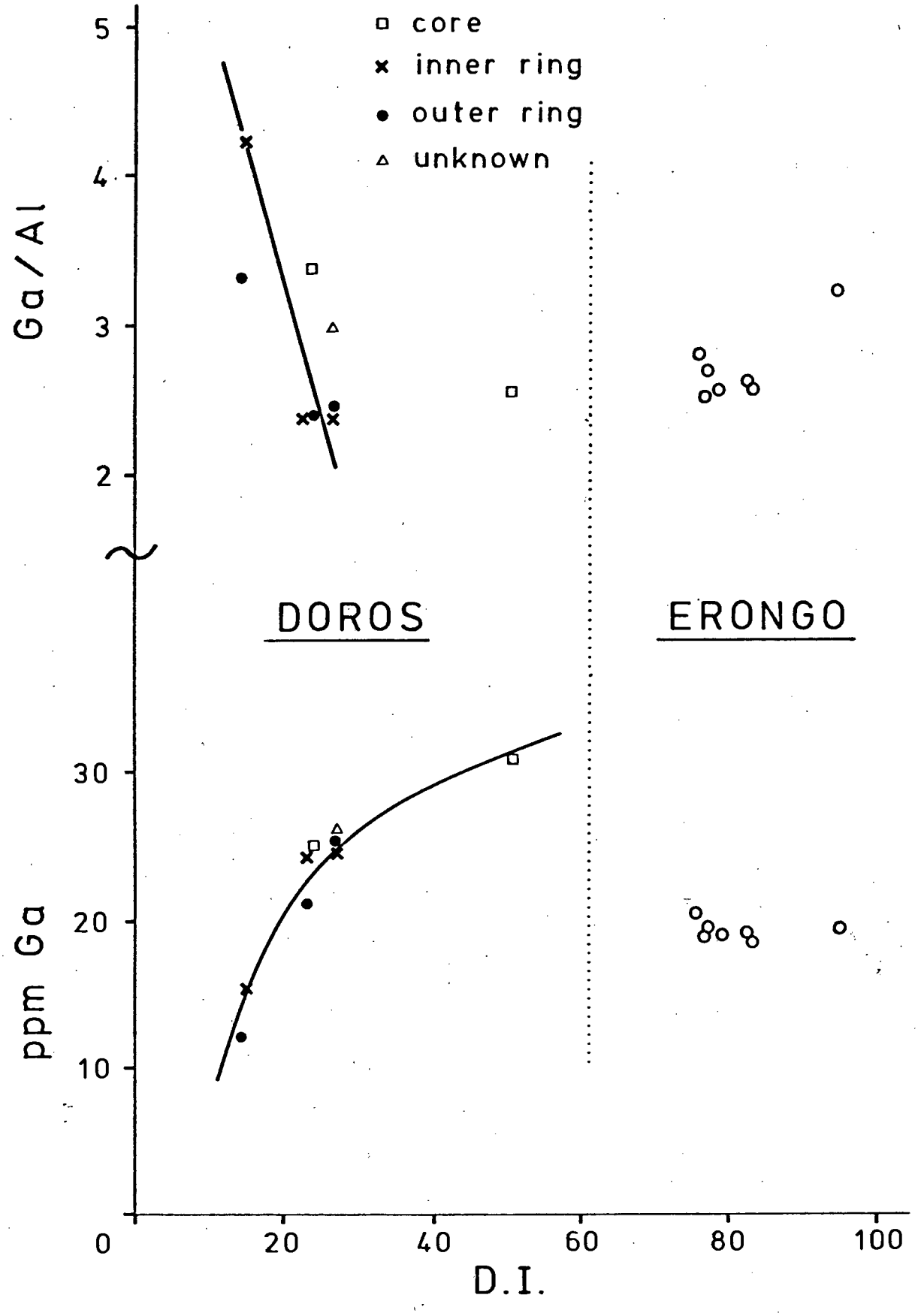

Fig. 111. Plots of Ga and Ga/Al ratio against D.I. for rocks from the Doros and Erongo Igneous Complexes, S.W.A.

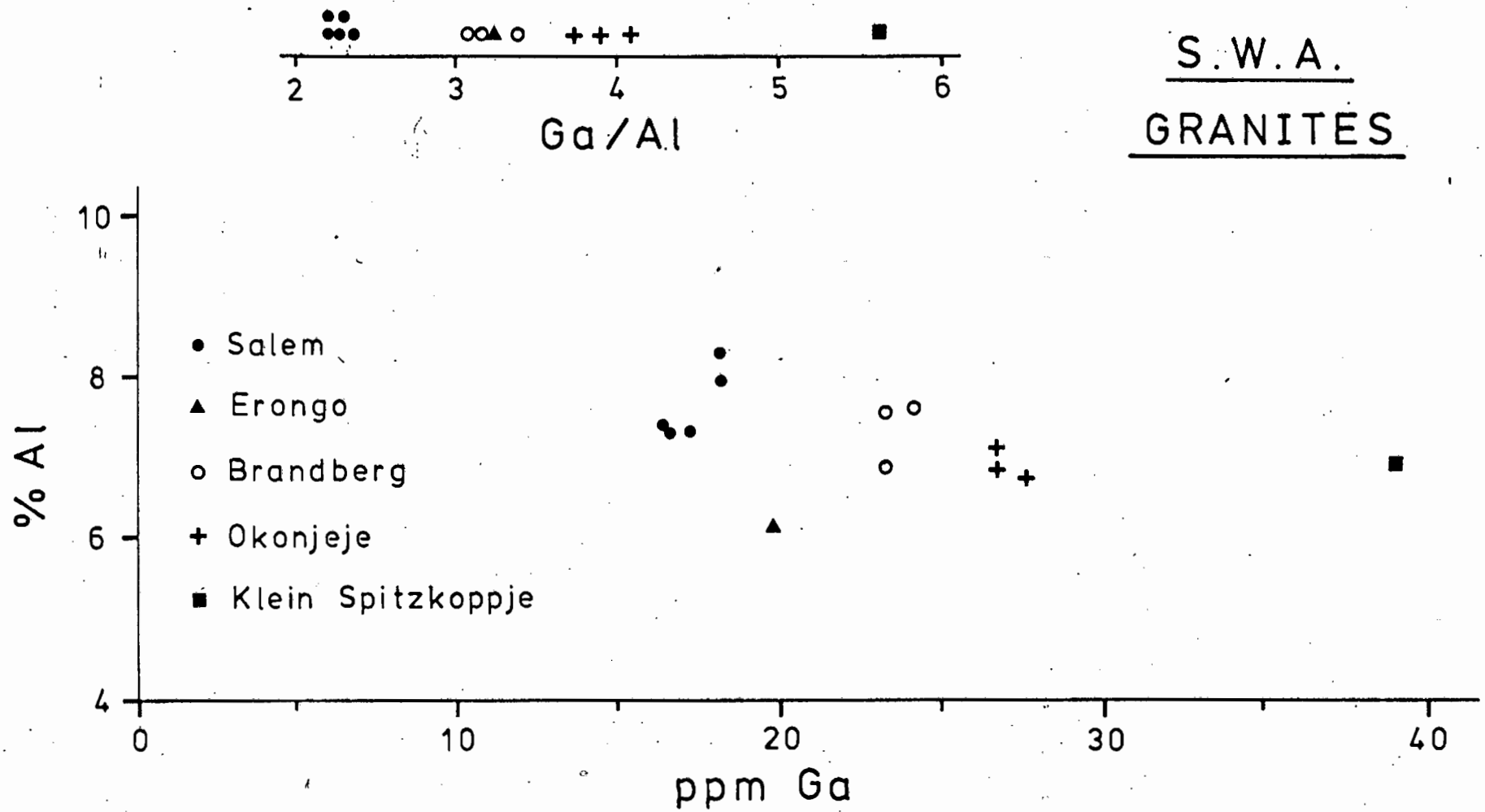

Fig. 112. Plot of Ga against Al, and Ga/Al distribution for granites from S.W.A.

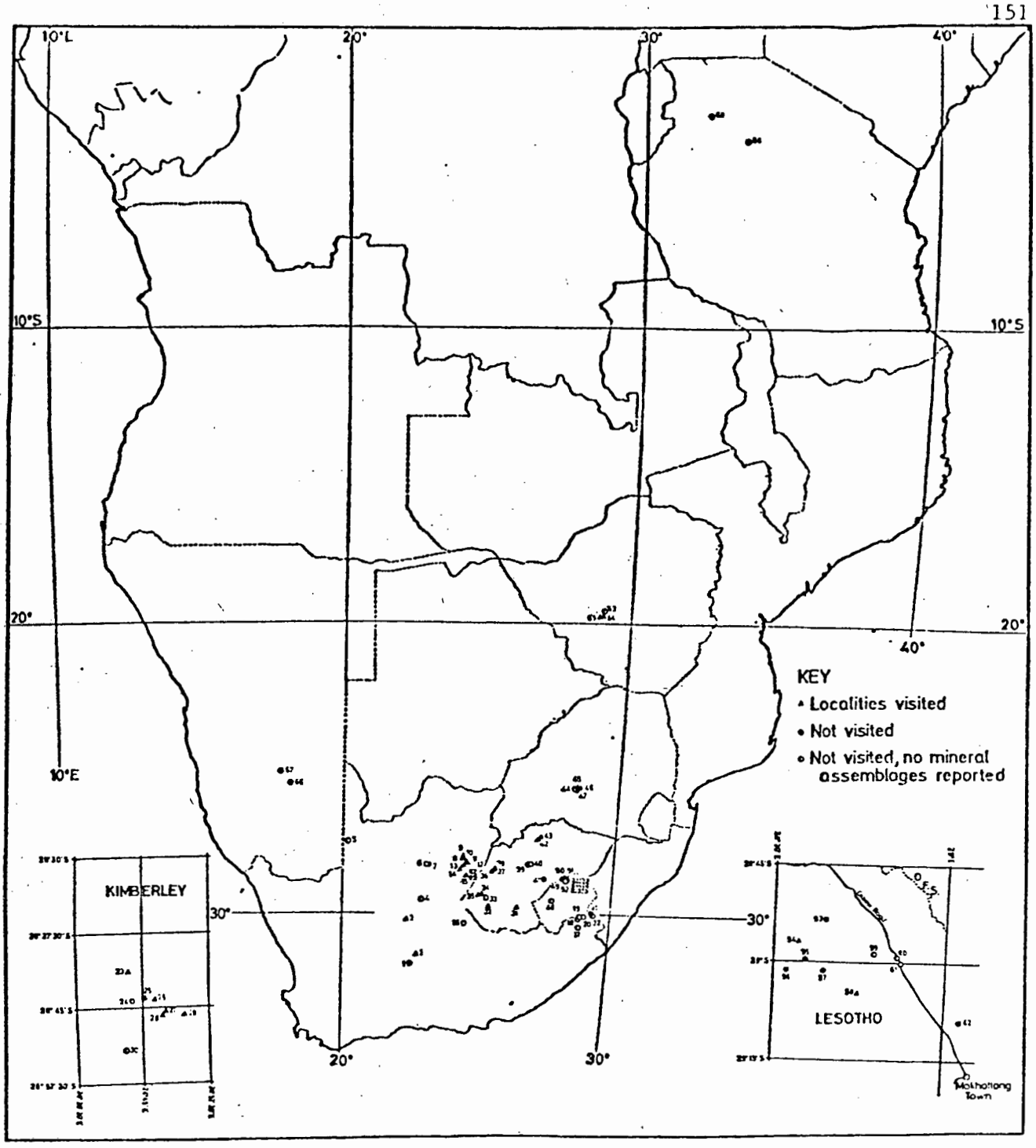

A map of the kimberlite localities in Southern Africa which contain non-eclogitic ultramafic xenoliths.

Locality Numbers:

Cape Province. 1. Gansfontein, 2. Melton Wold, 3. Markt, 4. Sanddrift, 5. Nooniput, 6. West End, 7. Postmasburg, 8. Bobbejaan, 9. Bellsbank, 10. Excelsior, 11. Mitchemanskraal, 12. Frank Smith, 13. Newlands, 14. Sydney-on-Vaal, 15. Secretaris, 16. Lekkerfontein, 17. Abbotsford, 18. Sibi, 19. Robertdale, 20. Hlangwini Location, 21. New Bristol, 2.. Clarkton.

Insert map of Kimberley Area:
23. Kamfersdam, 24. Taylor's Kopje, 25. Kimberley Mine ('Big Hole'), 26. De Beers, 27. Du Toitspan, 28. Bultfontein, 29. Wesselton, 30. Wimbledon Siding.

Orange Free State:
31. Leeufontein, 32. Jagersfontein, 33. Zwartrandsdam, 34. Poortje, 35. Koffiefontein, 36. Blaaubosch, 37. New Elands, 38. Roberts Victor, 39. Phoenix, 40. Star, 41. Monastry, 42. Crown, 43. Voorspoed.

Transvaal:
44. Derdepoort, 45. Premier, 46. Zonderwater, 47. Montrose No. 2.

Lesotho:
48. Ngopetšoeu, 49. Koenaneng, 50. Lipelaneng, 51. Sekameng, 52. Khabos.

Inset Map of Maluti Mountains:
53. Thaba Putsoa, 54. Lemphane, 55. Liqhobong, 46. Malibamatso, 57. Kao, 58. Matsoku, 59. Motai, 60. Qaqa, 61. Letseng-la-Terai, 62. Robert.

Rhodesia:
63. Moffat, 64. Wessels, 65. Colossus.

South West Africa:
66. Mukorub, 67. Louwrencia.

Tanzania:
68. Sultan, 69. Mabuki.

Fig. 113B. Map of kimberlite localities in southern Africa and Tanzania. (From Rickwood, 1969)

Fig. 114. Ga - Al plots for veined and unveined rocks from the Matsoku kimberlite pipe, Lesotho.

KEY:

Veined rocks

- ● Garnet lherzolite (CP)
- ○ Pyroxenite
- □ Cpx-rich zone
- + Opx-rich zone
- ✕ Other zones

Unveined rocks

- ● Garnet lherzolite (CP)
- ○ Pyroxenite
- ⊕ Orthopyroxenite
- ▲ Eclogite and amphibolite
- ■ Kimberlite

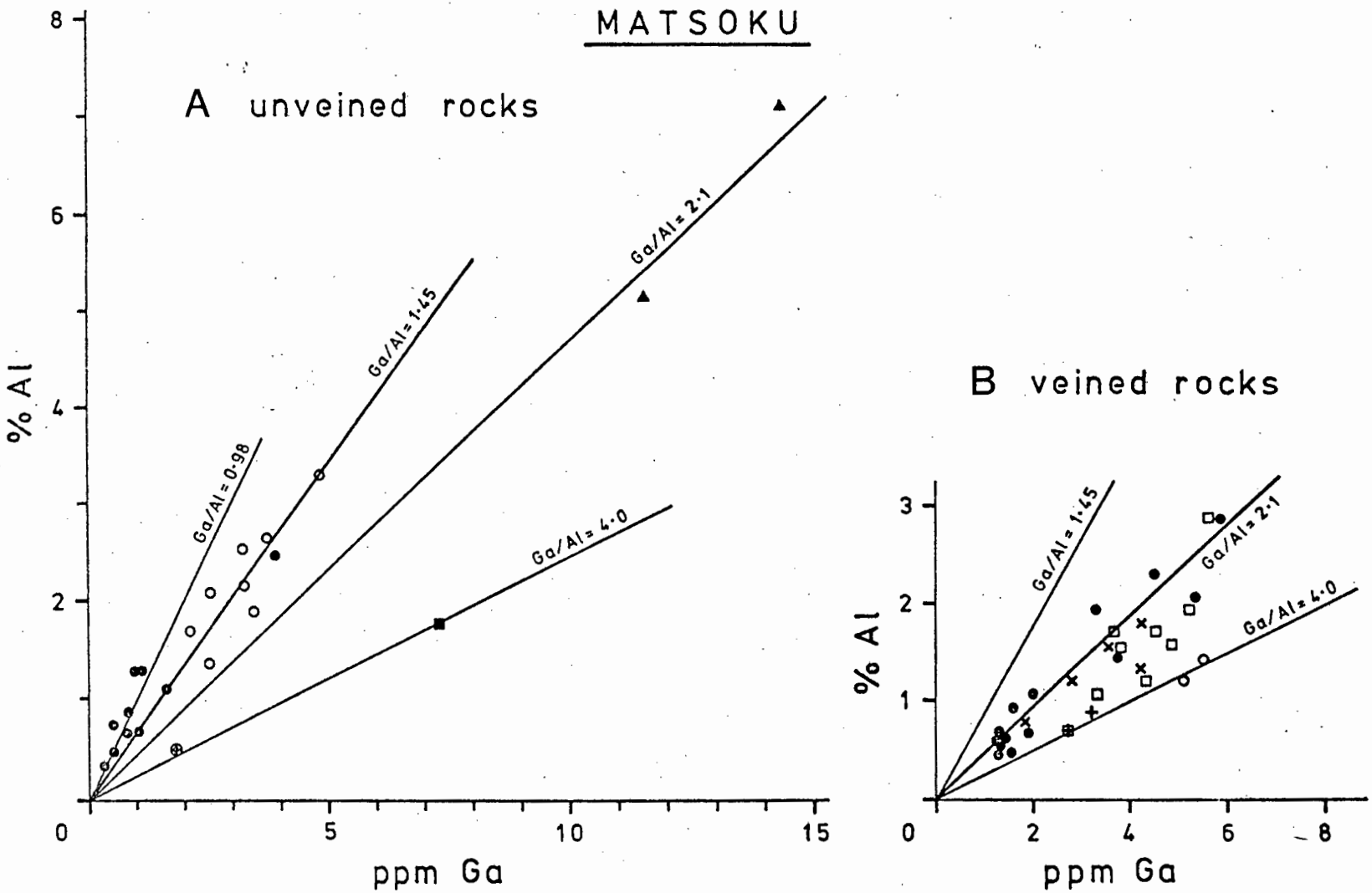

Fig. 114. Ga - Al plots for veined and unveined rocks from the Matsoku kimberlite pipe, Lesotho.

Fig. 115. Cross-section sketch diagrams of veined nodules from Matsoku Pipe.

LBM 33 A: coarse banded pyroxenite; 4% olivine, 40% opx, 33% Cr-diopside, 23% garnet (by volume)

33 B: coarse banded pyroxenite; 14% olivine, 72% opx, 7% Cr-diopside, 7% garnet

33 C: coarse banded pyroxenite; 14% olivine, 21% opx, 49% Cr-diopside, 16% garnet

LBM 36 A: coarse banded pyroxenite; 54% olivine, 23% opx, 12% Cr-diopside, 11% garnet

36 B: coarse banded pyroxenite; 34% olivine, 8% opx, 44% Cr-diopside, 14% garnet

LBM 38 A: coarse CP; 67% olivine, 23% opx, 2% Cr-diopside, 8% garnet

38 B: even textured, gneissose pyroxenite; 14% olivine, 47% opx, 24% Cr-diopside, 6% garnet, 7% ore

LBM 88 b.a.2: garnet lherzolite (CP)

b.a.1: opx- and cpx-rich vein or sheet

b.a.3: garnet lherzolite (CP)

LBM 90 b.a.2: garnet lherzolite (coarse CP), 'host'

b.a.3: 'upper' marginal cpx-rich zone

b.a.4: 'upper' inner cpx-poor ol-rich zone

b.a.5: 'lower' inner cpx-poor opx-rich zone

b.a.6: 'lower' marginal cpx-rich zone

b.a.1: whole of sheet, composite of b.a.2-6

Diagrams from J.J. Gurney (pers. comm.).

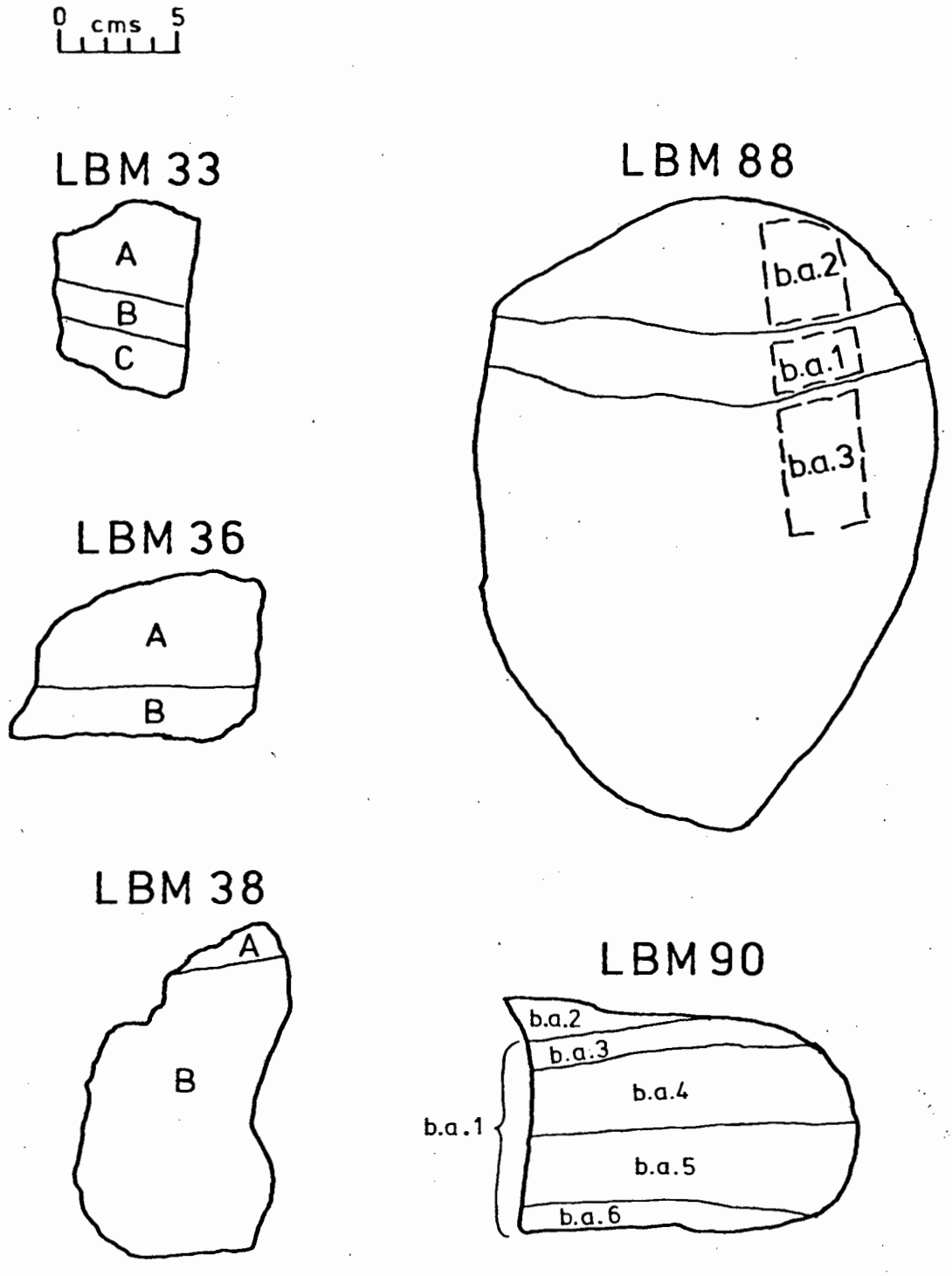

Fig. 115. Sketches of veined nodules from Matsoku Pipe.

Fig. 116. Cross-section sketch diagrams of veined nodules from Matsoku Pipe.

LBM 87 b.a.1: fine-grained garnet lherzolite (CP) unusually rich in garnet and opx

b.a.2: porphyroblastic (flaser) garnet lherzolite (CP) adjacent to b.a.1

b.a.3: porphyroblastic garnet lherzolite (CP) away from b.a.1

LBM 101 b.a.1: 'host' garnet lherzolite (CP)

b.a.2: metasomatic vein containing phlogopite, ilmenite and rutile in addition to ol, opx and cpx

LBM 131 b.a.2: cpx-rich marginal zone of presumed sheet

b.a.3: inner zone richer in opx and olivine

b.a.1: whole cross-section of cpx-rich sheet

LBM 139 CP: 'host' garnet lherzolite (coarse CP) (not available for analysis)

b.a.2: cpx-rich marginal zone of sheet

b.a.3: inner zone, fairly rich in opx with moderate cpx, some olivine and very little garnet

b.a.1: whole of sheet

Diagrams from J.J. Gurney (pers. comm.).

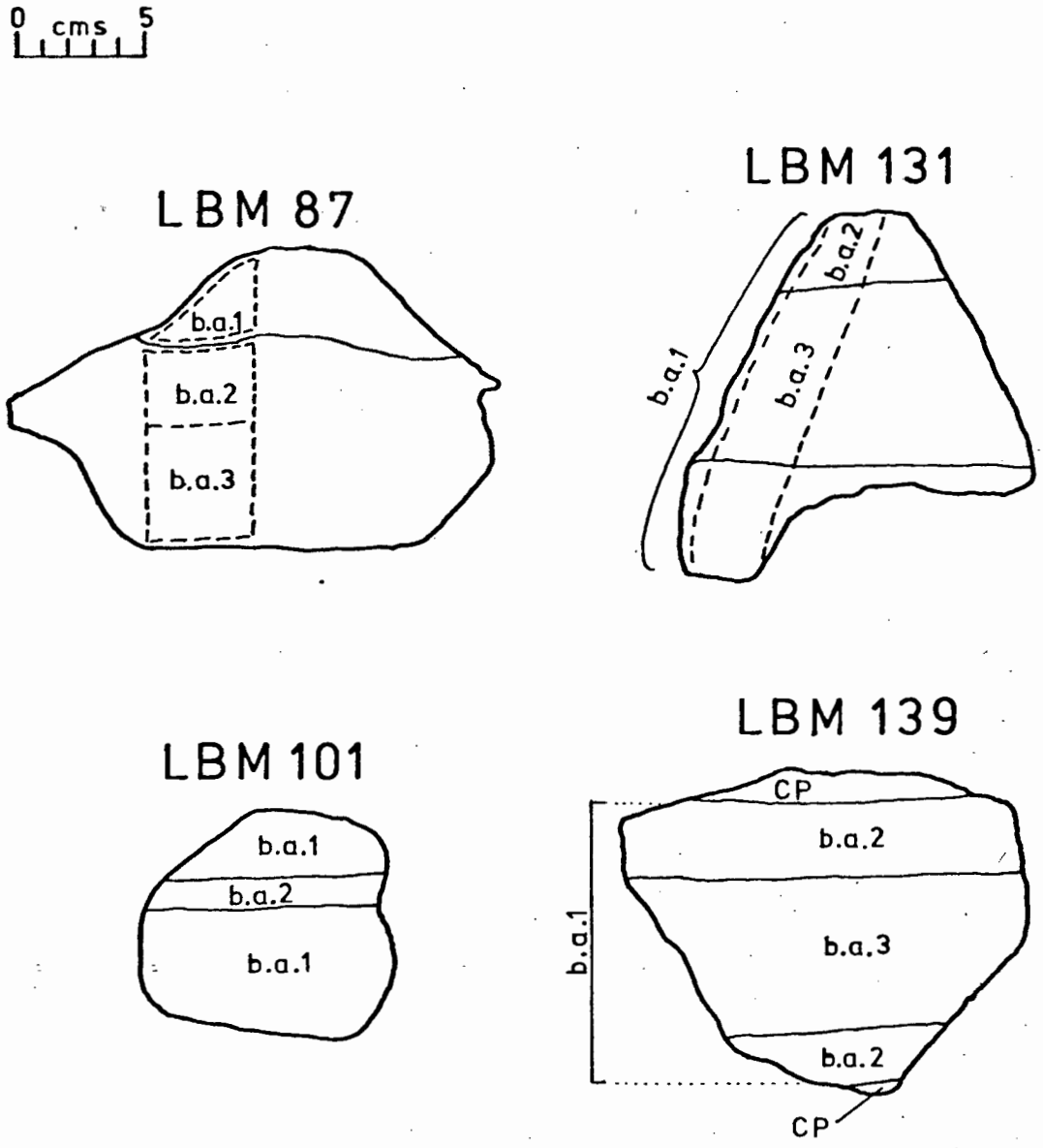

Fig. 116. Sketches of veined nodules from Matsoku Pipe.

Fig. 117. Plots of Ga, Al, Ga/Al ratio and Cr_2O_3 against Mg number (100 MgO / (MgO + FeO*)) for some Matsoku nodules. FeO* is total Fe expressed as FeO. Mg numbers and Cr_2O_3 data from Dr. J.J. Gurney (pers. comm).

KEY:

- o garnet lherzolites (CP) - depleted
- O garnet lherzolites (CP) - flaser texture
- □ metasomatised garnet lherzolites (CP)
- ● cumulate pyroxenites
- ■ CP in contact with cpx-rich sheets
- △ cpx-rich margins in contact with cpx-rich sheets
- ✖ inner zones of cpx-rich sheets
- ▼ complete sections across cpx-rich sheets
- + veins

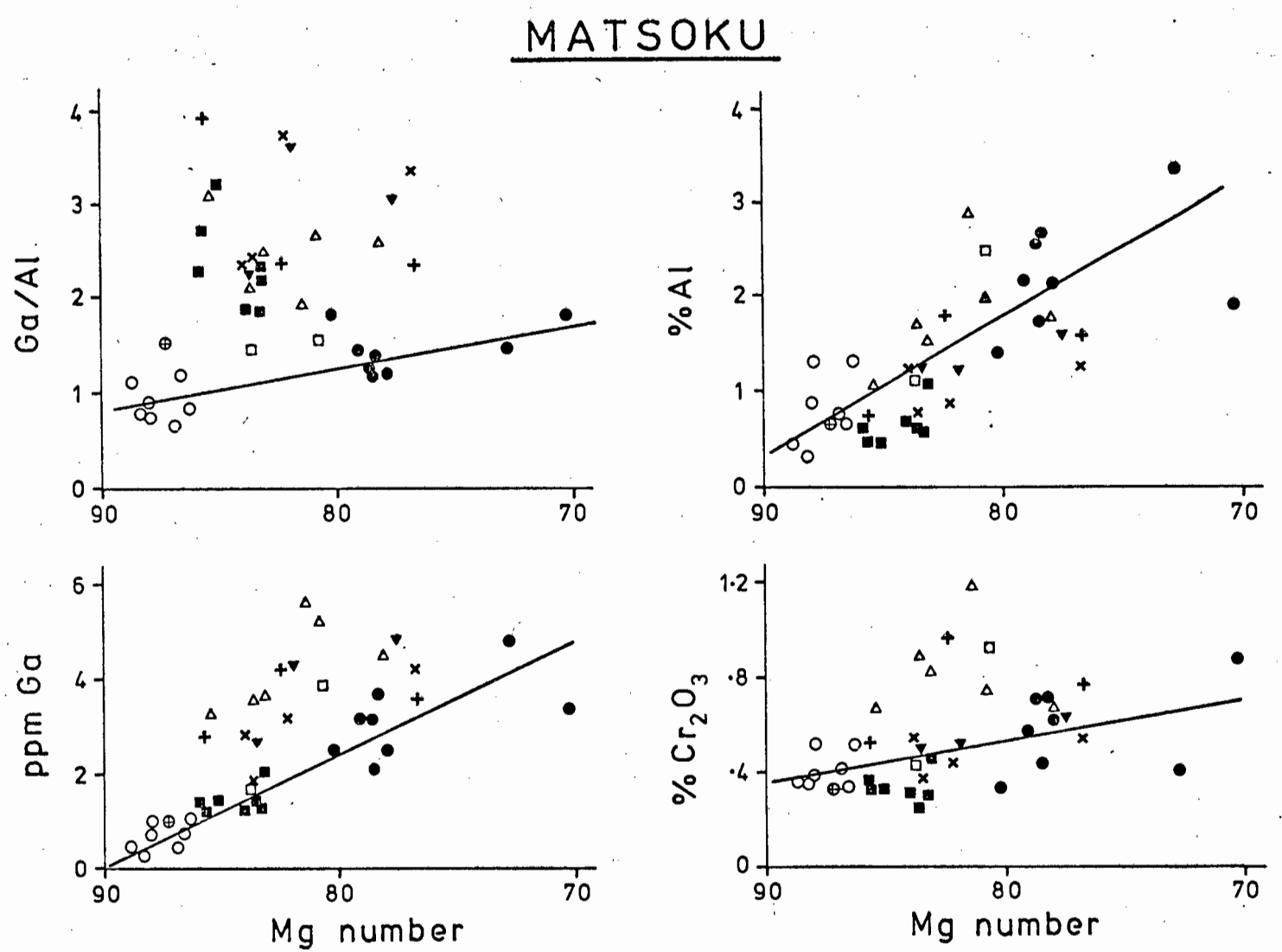

Fig. 117. Plots of Ga, Al, Ga/Al ratio and Cr_2O_3 against Mg number for some Matsoku nodules.

Fig. 118. A plot of Ga against Al for xenoliths from kimberlite pipes other than Matsoku.

KEY:

- ● Roberts Victor eclogites
- ⊙ Roberts Victor eclogites, Ca-rich (1 or 2 = class I or II)
- ⊡ Roberts Victor eclogites, Mg-rich
- ◬ Roberts Victor eclogites, Fe-rich
- □ Rietfontein pipe
- o Bultfontein pipe, garnet lherzolites and harzburgites
- × Bultfontein pipe, richterite and phlogopite peridotites
- ▲ Jagersfontein pipe
- ■ Monastery Mine
- ▽ De Beers Mine
- ▼ Kamfersdown Mine
- \+ Tanzanian eclogites
- K kyanite eclogite
- C corundum eclogite
- cpx clinopyroxene megacryst
- ilm ilmenite megacryst
- gt garnet megacryst
- ☆ eclogitic garnet

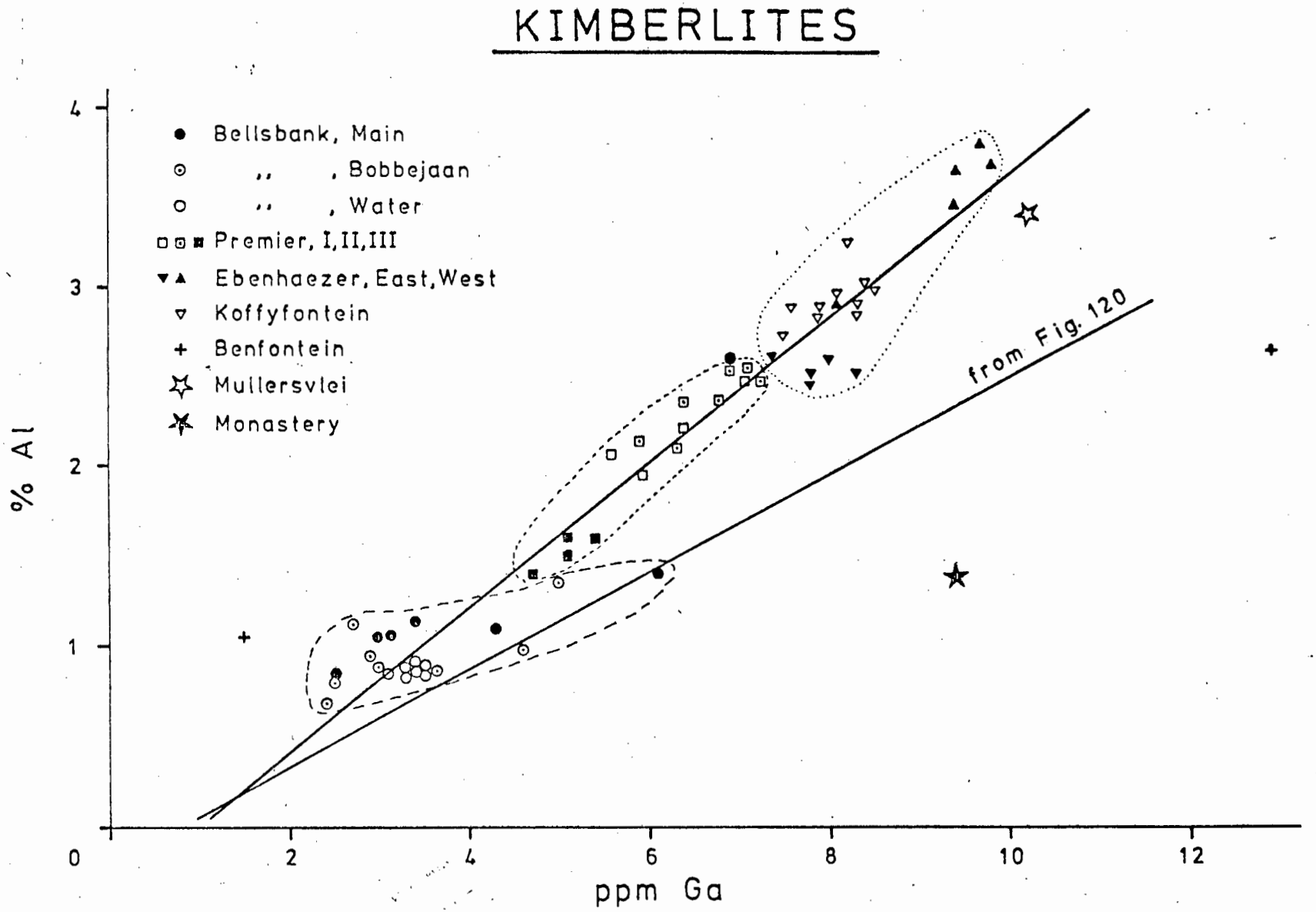

Fig. 119. A plot of Ga against Al for kimberlites from southern Africa, most of which are contaminated with crustal rocks.

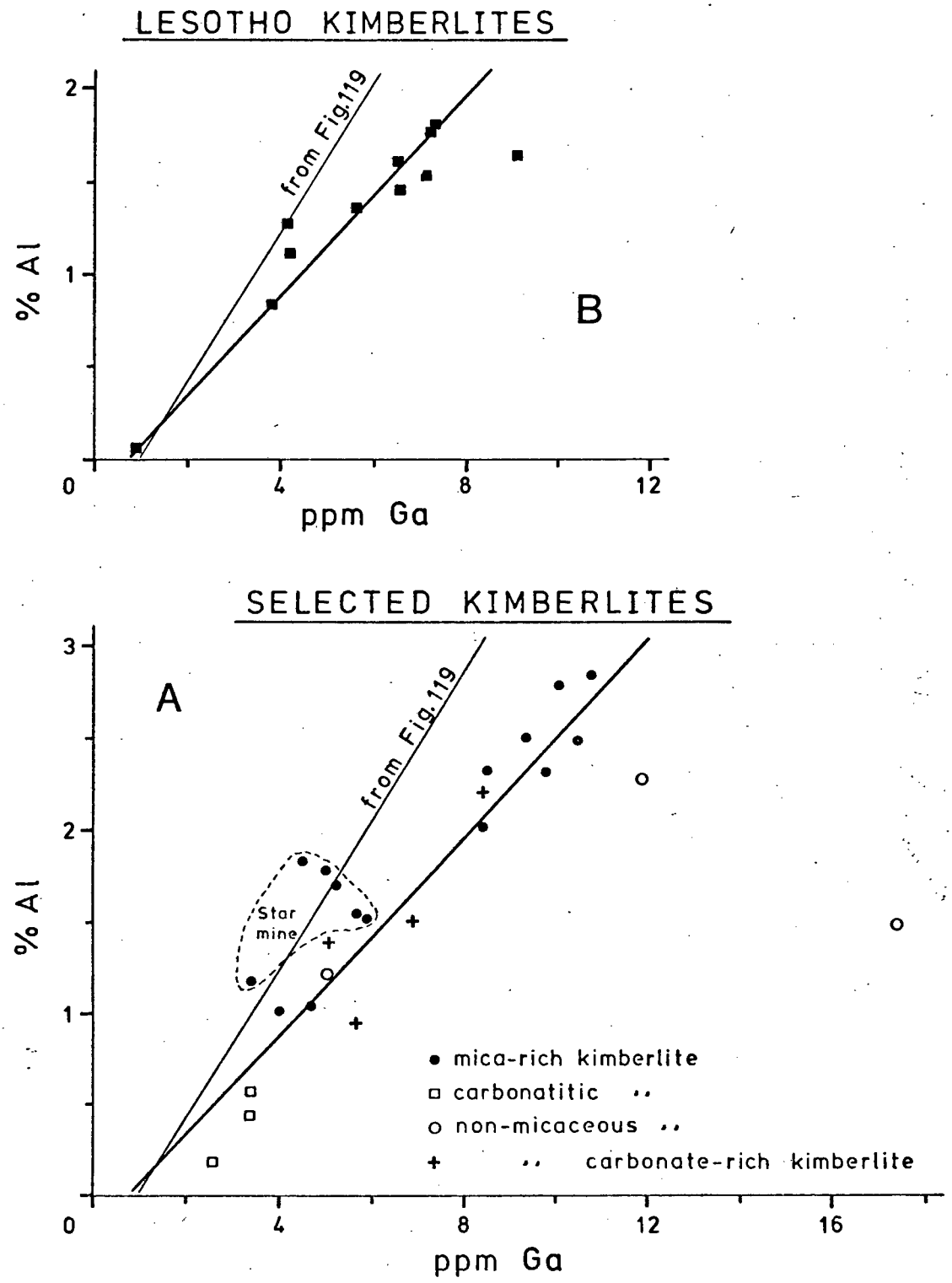

Fig. 120. Plots of Ga against Al for kimberlites from southern Africa specially selected to be free from crustal contamination, and for some Lesotho kimberlites.

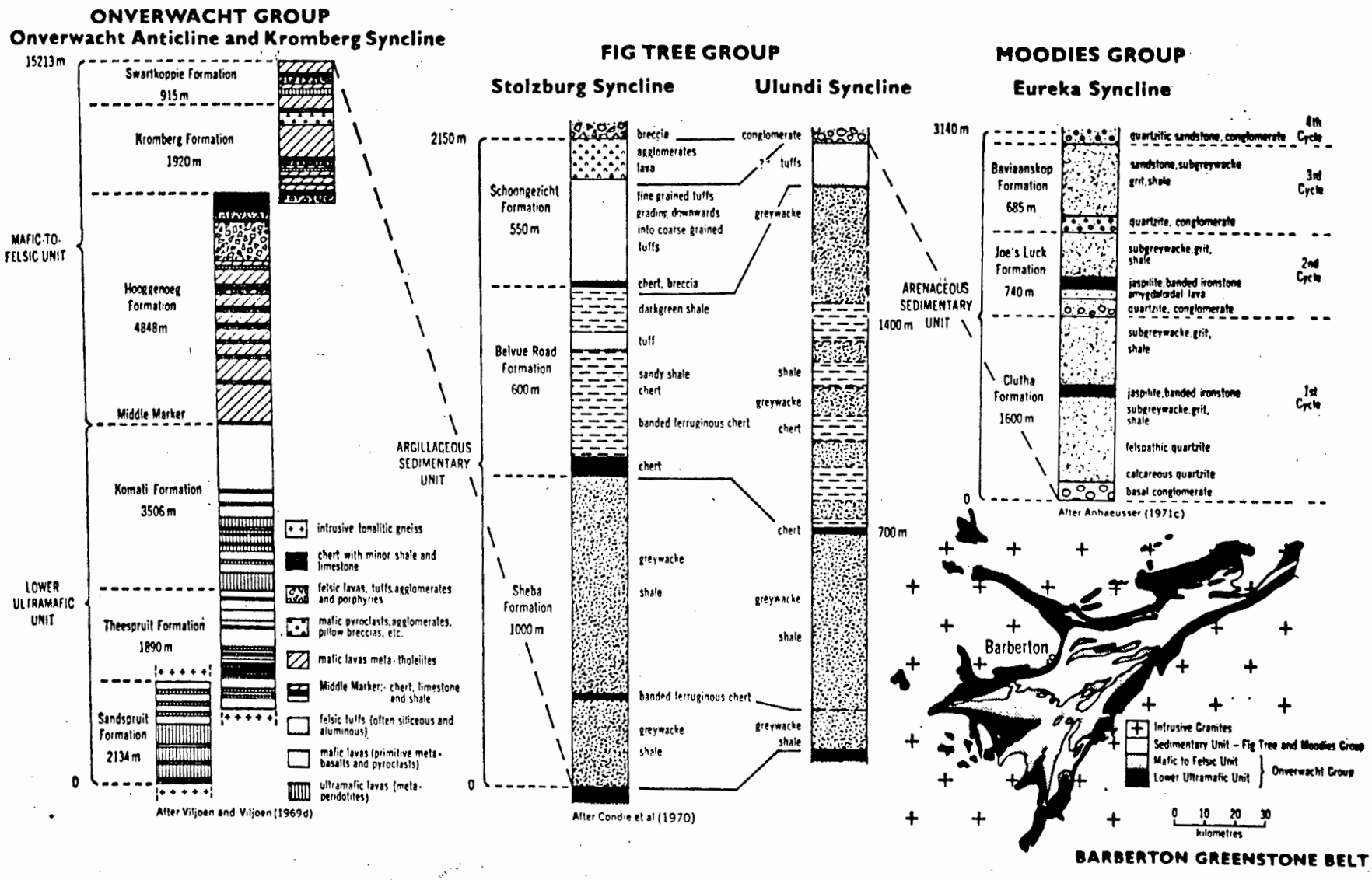

Fig. 121. The distribution and stratigraphy of the Swaziland Sequence in the Barberton Mountain Land, South Africa (from Anhaeusser, 1973).

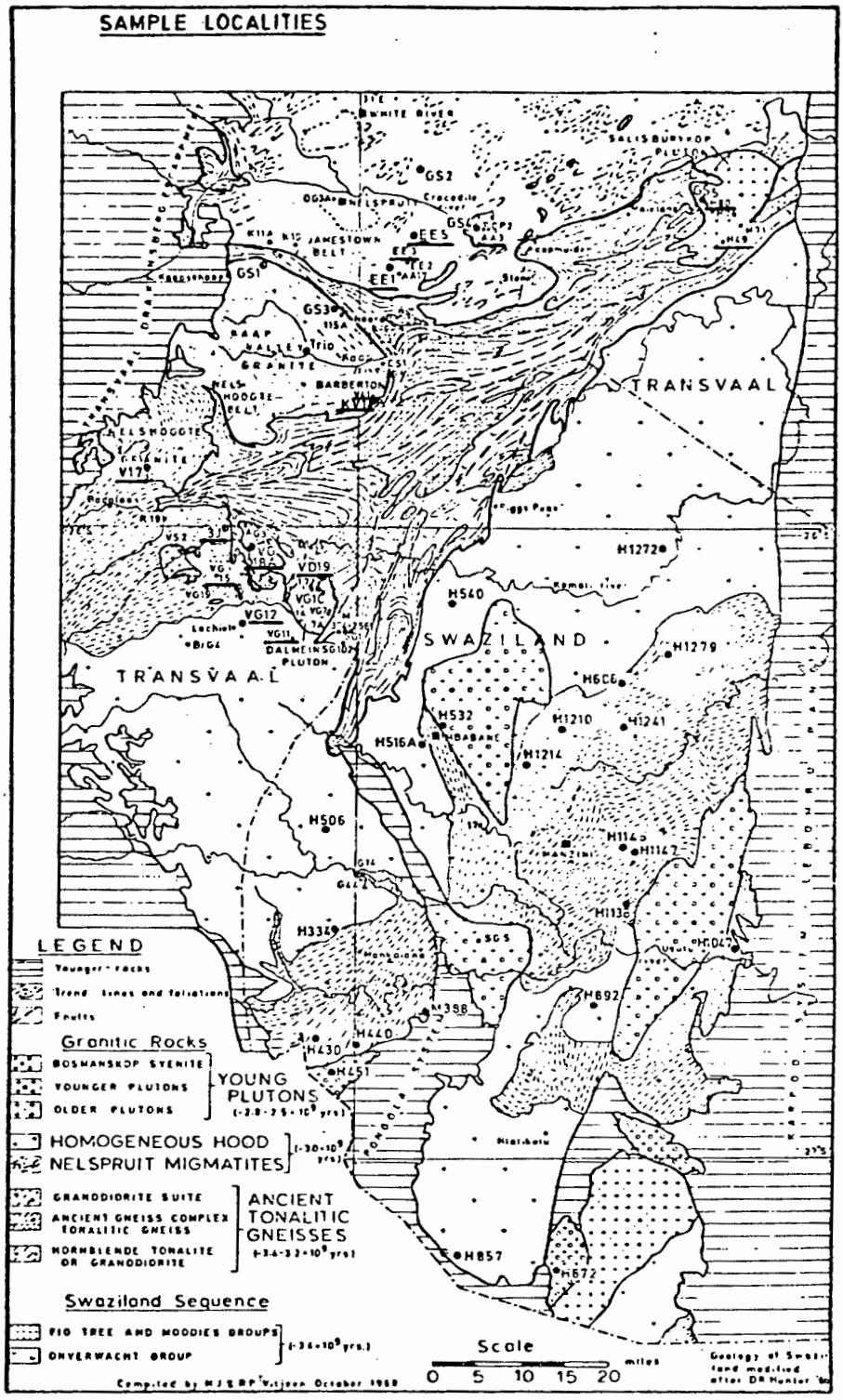

Fig. 122. Geological map of the granitic rocks of the Barberton region showing localities (underlined) of rocks analysed in this work.

Fig. 123. Plot of Ga against Al for rocks from the Barberton Mountain Land.

KEY:

△ Peridotitic komatiite

▲ Basaltic komatiite, Geluk type

▼ Basaltic komatiite, Badplaas type

● Basaltic komatiite, Barberton type, massive

○ Basaltic komatiite, Barberton type, pillow margin

(◎ = epidotised)

⊙ Basaltic komatiite, Barberton type, pillow core

□ Metatholeiite

■ Metabasalt

+ Acid intrusives

▽ Intermediate lava

⩛ Andesite

× Acid lava

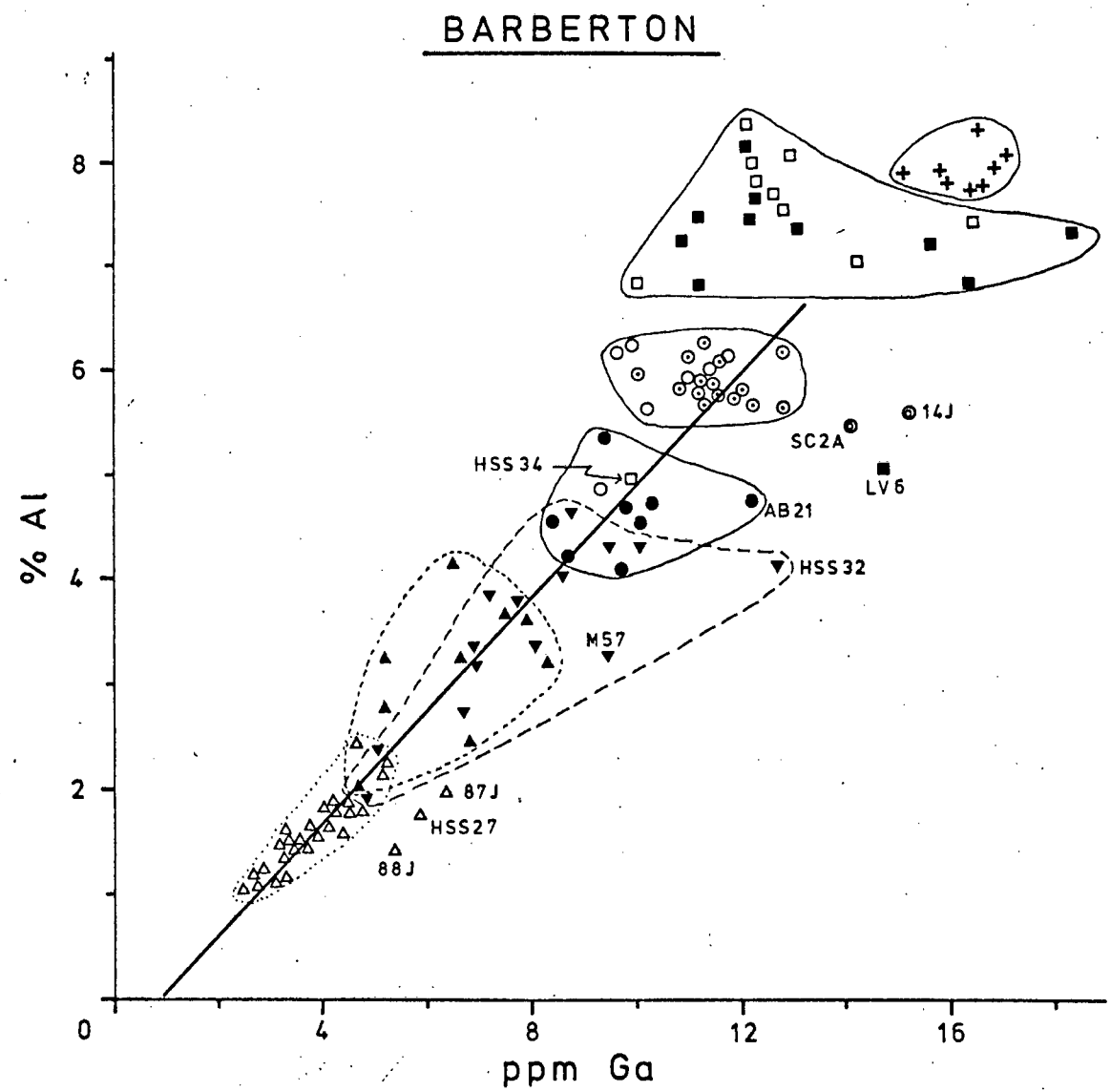

Fig. 123. Plot of Ga against Al for rocks from the Barberton Mountain Land.

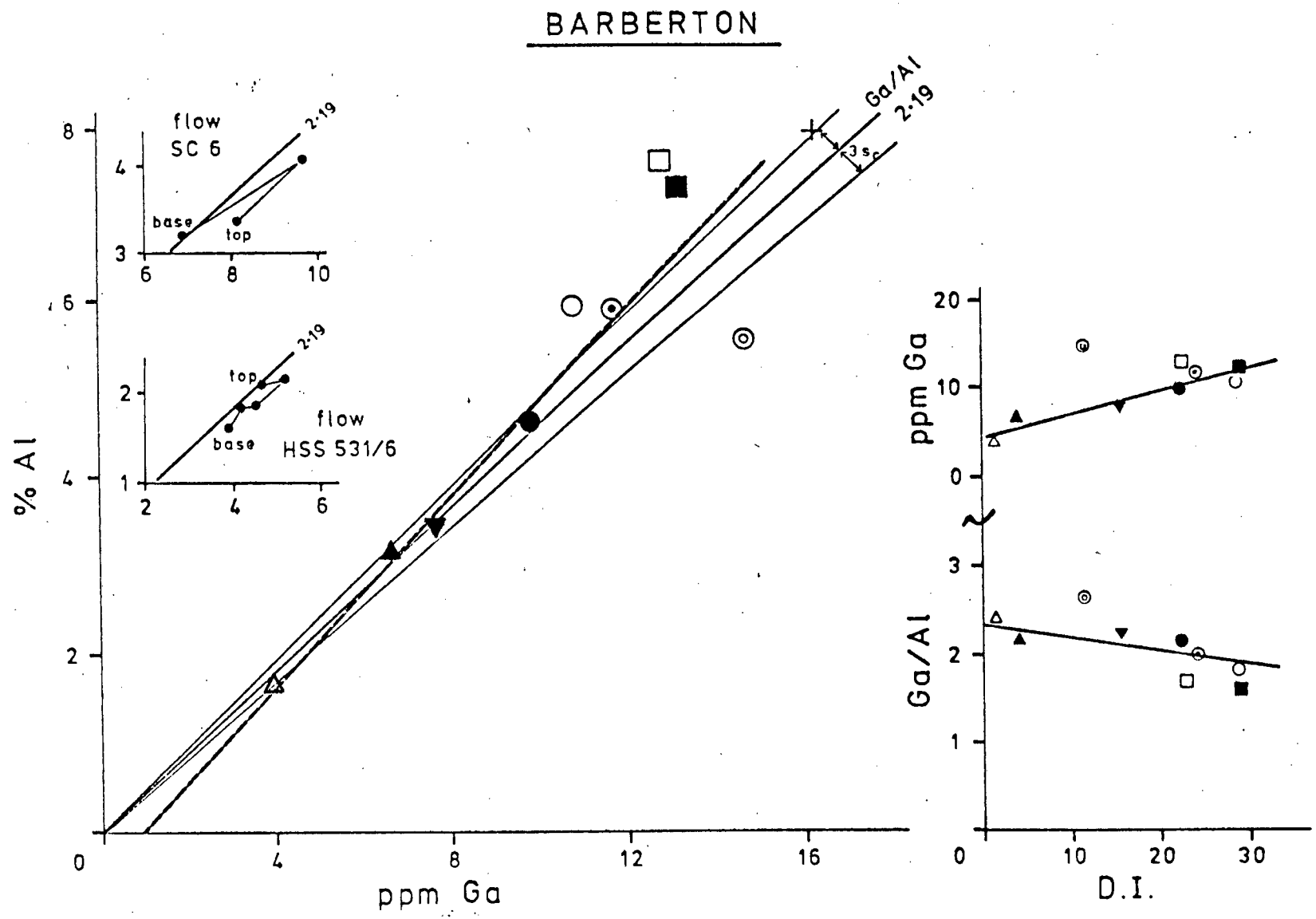

Fig. 124. Plots of average values of Ga - Al, Ga - D.I., Ga/Al - D.I. for the main rock types from the Barberton Mountain Land. Ga - Al plots are included for rocks sampled vertically across two flows. Key as for Fig. 123.

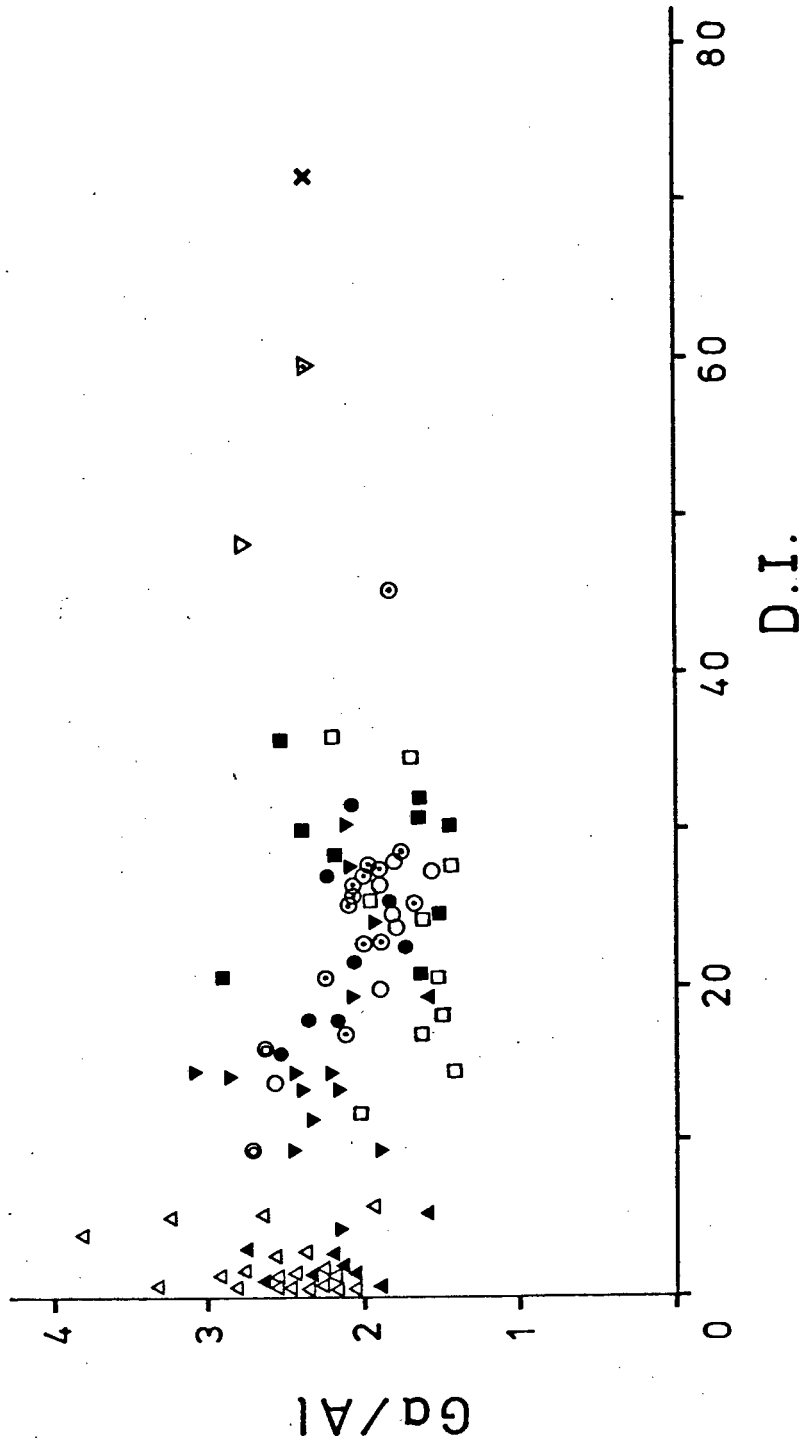

Fig. 125. A Ga/Al - D.I. plot for individual samples from the Swaziland Sequence, Barberton Mountain Land. Key as for Fig. 123.

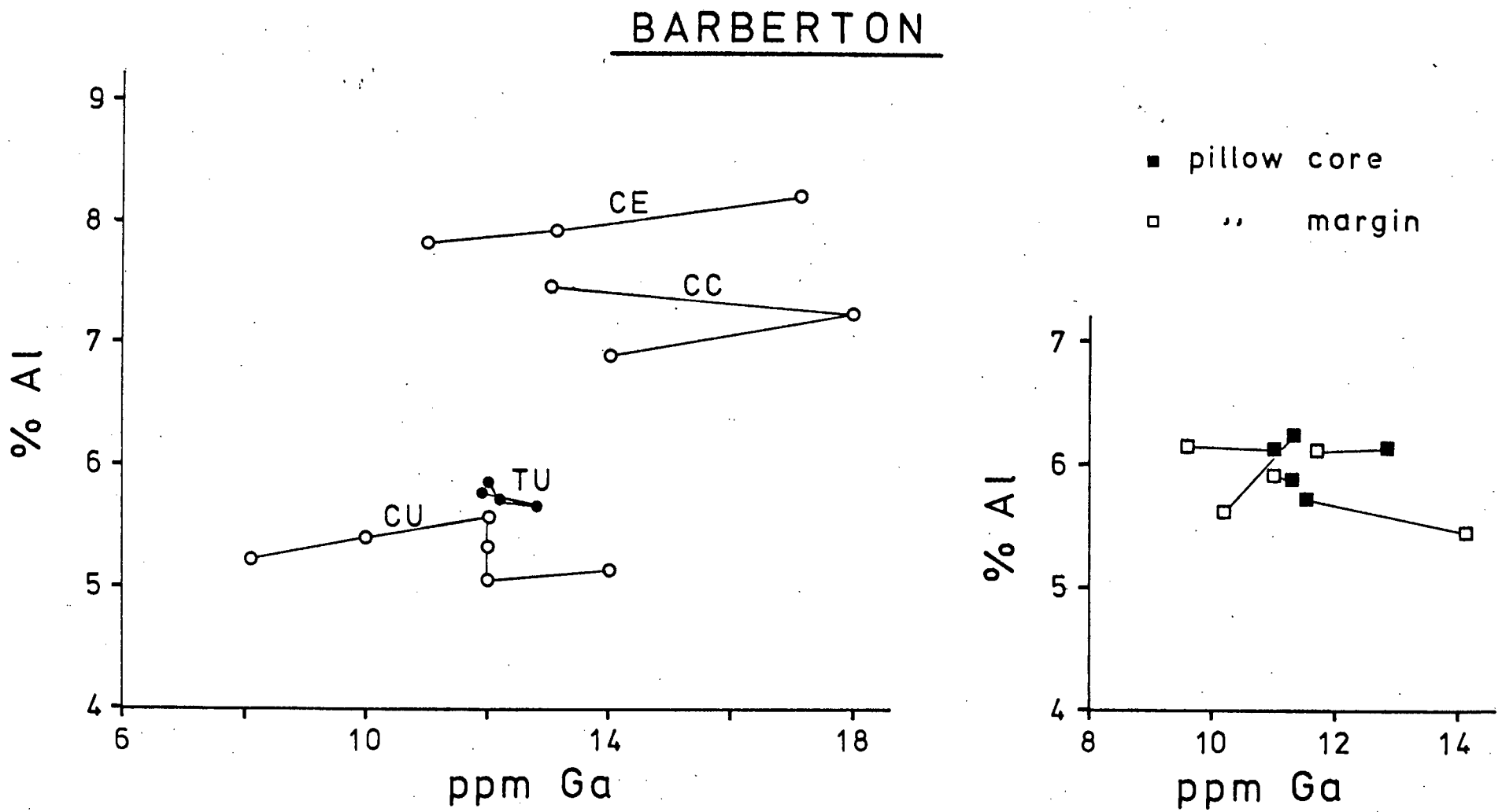

Fig. 126. Ga - Al plots for rocks sampled along flows. Data from this work and Condie et al. (1977). Data are also plotted for core-margin pairs from lava pillows. CE = Condie, epidotised flow; CC = Condie, carbonated flow; CU = Condie, unaltered flow; TU = this work, unaltered flow.

Fig. 127. Simplified geological map of southern Africa showing sample locations of Karroo-Stormberg volcanic rocks (after Erlank, 1971).

1. Central area
2. Southern Lebombo
3. Nuanetsi
4. Northern Province
   - A. Tuli
   - B. Featherstone
   - C. Nyamandhlovu
   - D. Wankie
   - E. Botswana
5. Southern South West Africa
6. Northern South West Africa (Etendeka plateau)

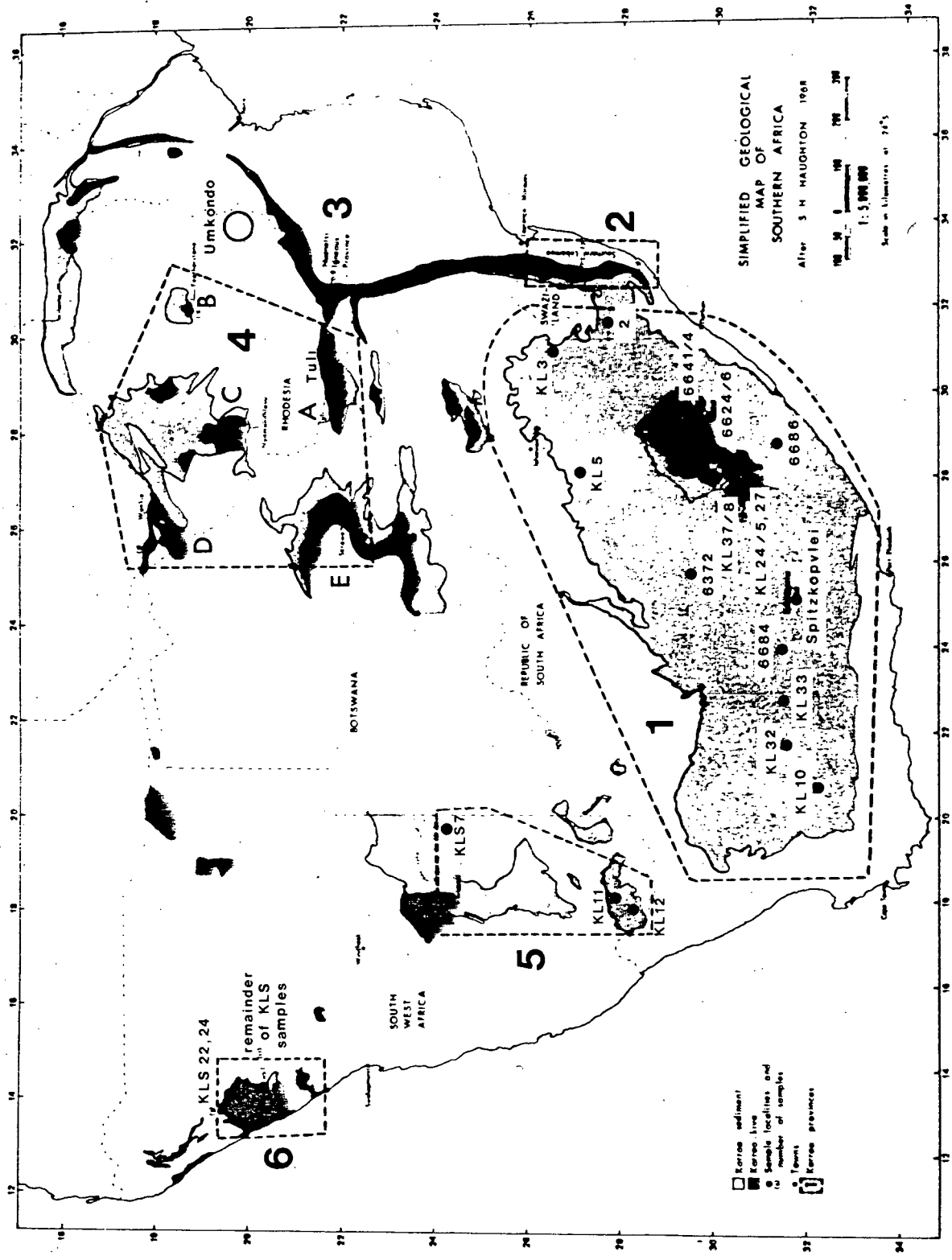

Fig. 127. Simplified geological map of southern Africa showing sample locations of Karroo-Stormberg volcanic rocks (after Erlank, 1971).

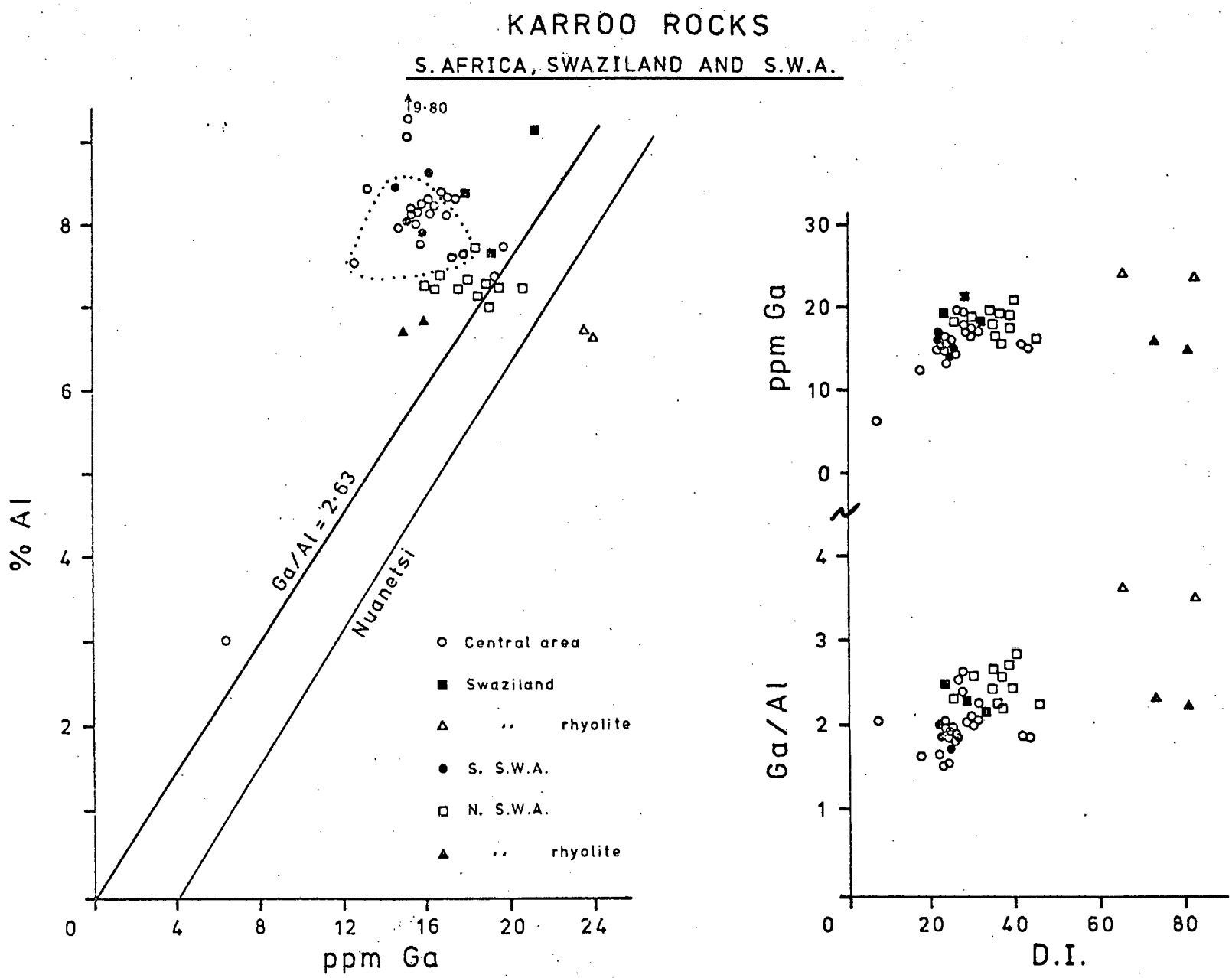

Fig. 128. Ga - Al, Ga - D.I. and Ga/Al - D.I. plots for Karroo rocks from South Africa, Swaziland and South West Africa. Dotted area = Umkondo dolerites (see text and Fig. 130).

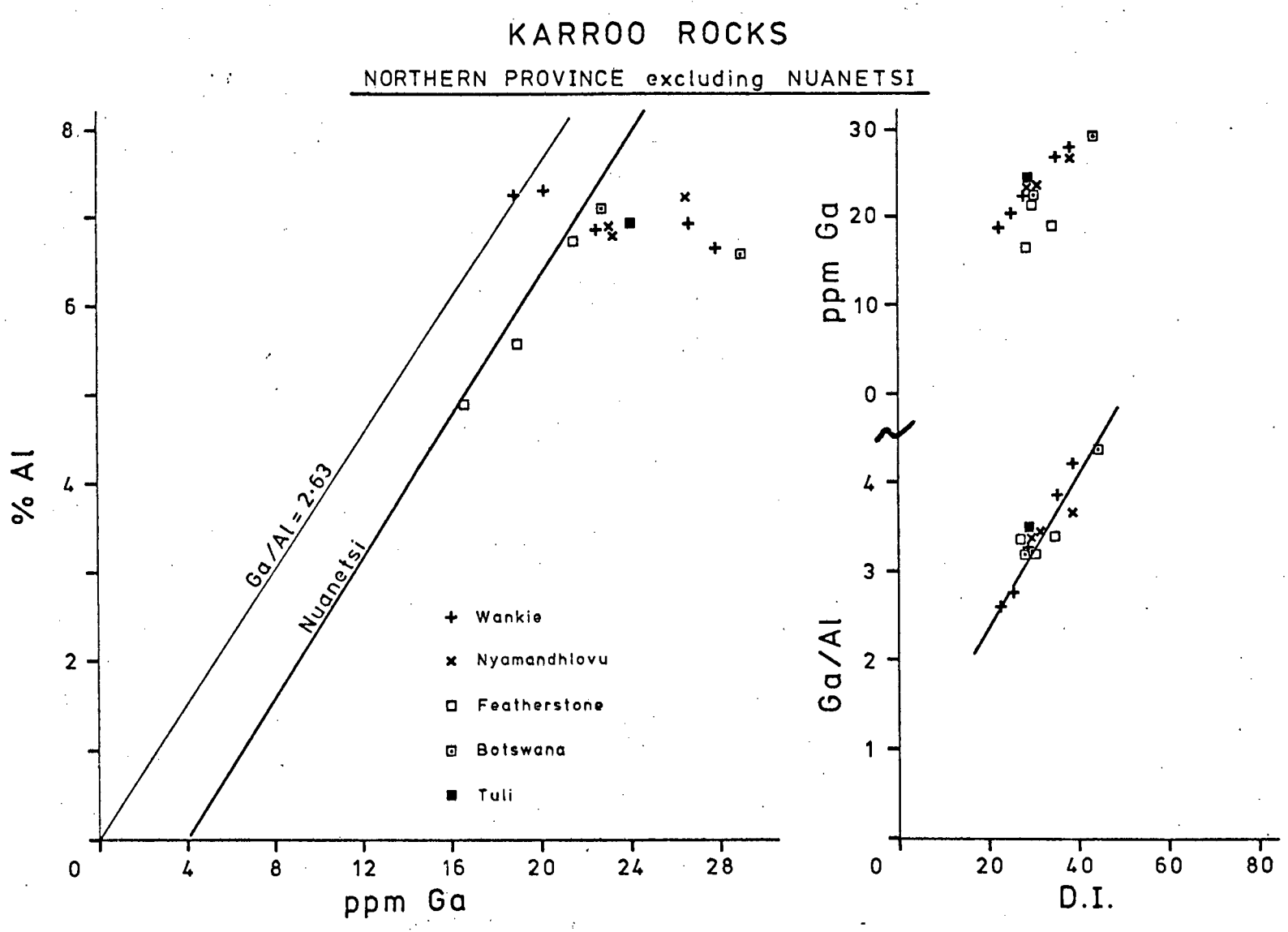

Fig. 129. Ga - Al, Ga - D.I. and Ga/Al - D.I. plots for Karroo rocks from Rhodesia and Botswana (Northern Province) excluding those from the Nuanetsi Igneous Province.

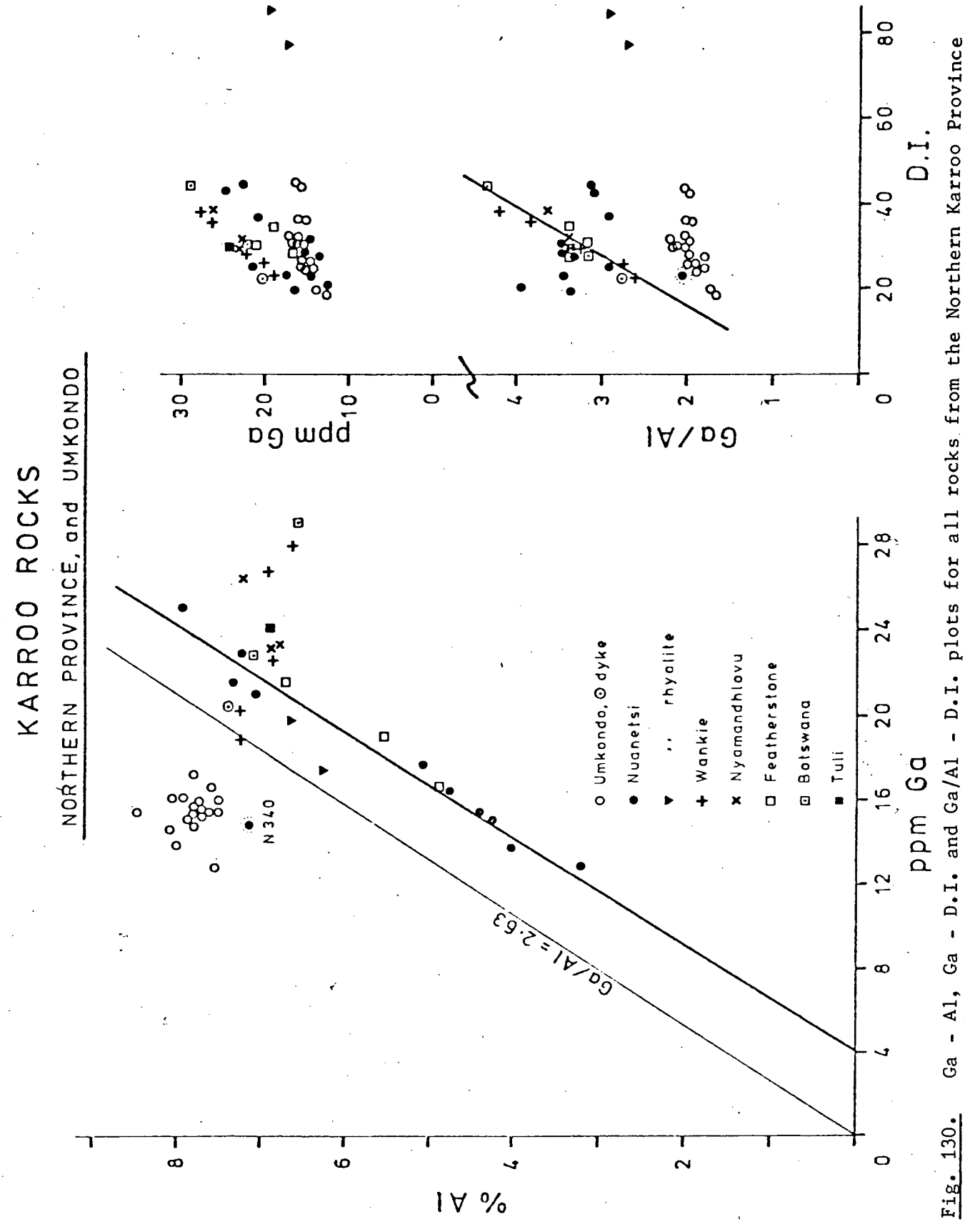

Fig. 130. Ga - Al, Ga - D.I. and Ga/Al - D.I. plots for all rocks from the Northern Karroo Province and the Umkondo dolerites.

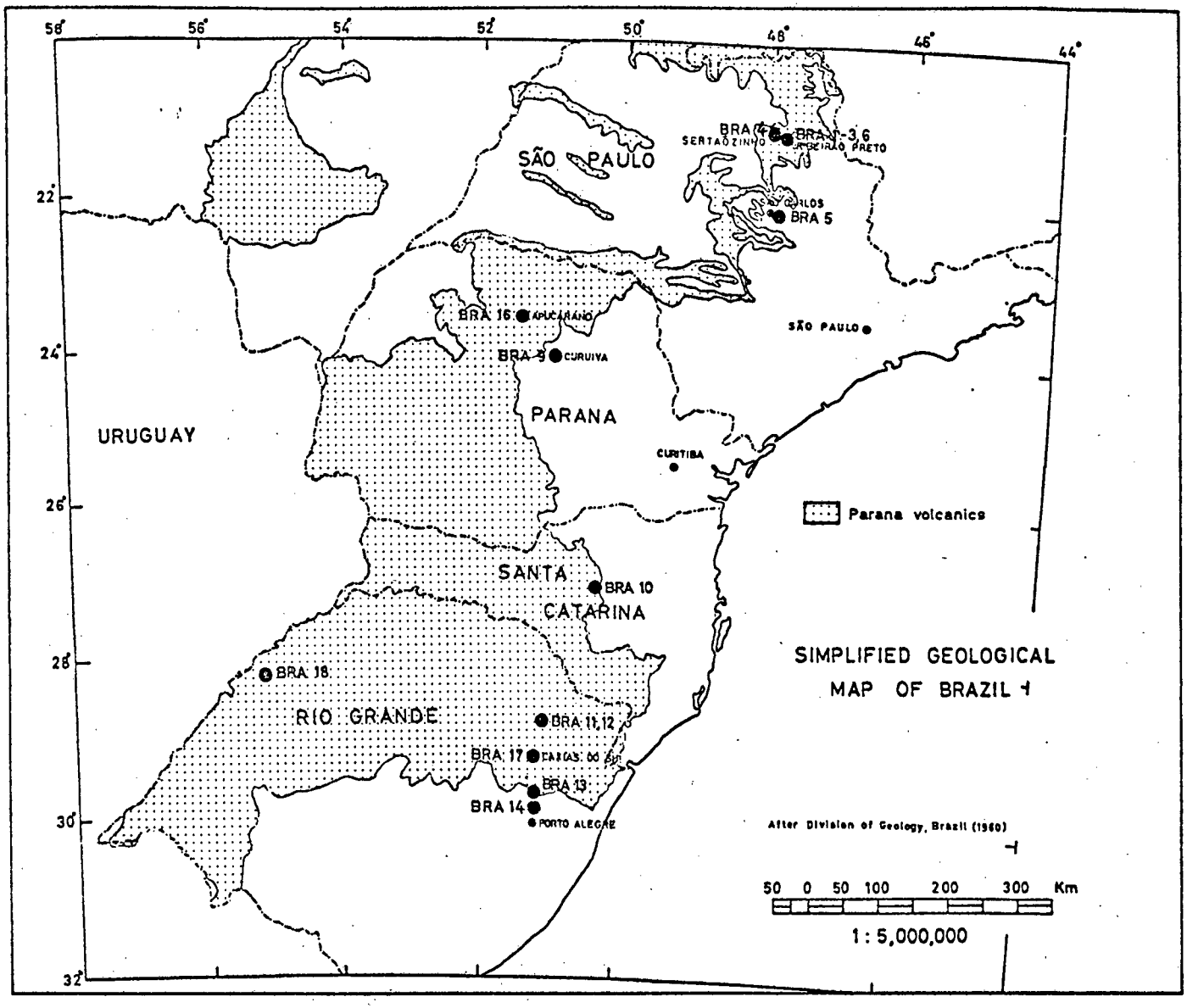

Fig. 131. A simplified geological map of Brazil indicating the distribution of the Parana volcanics and sample localities (from Erlank, 1971).

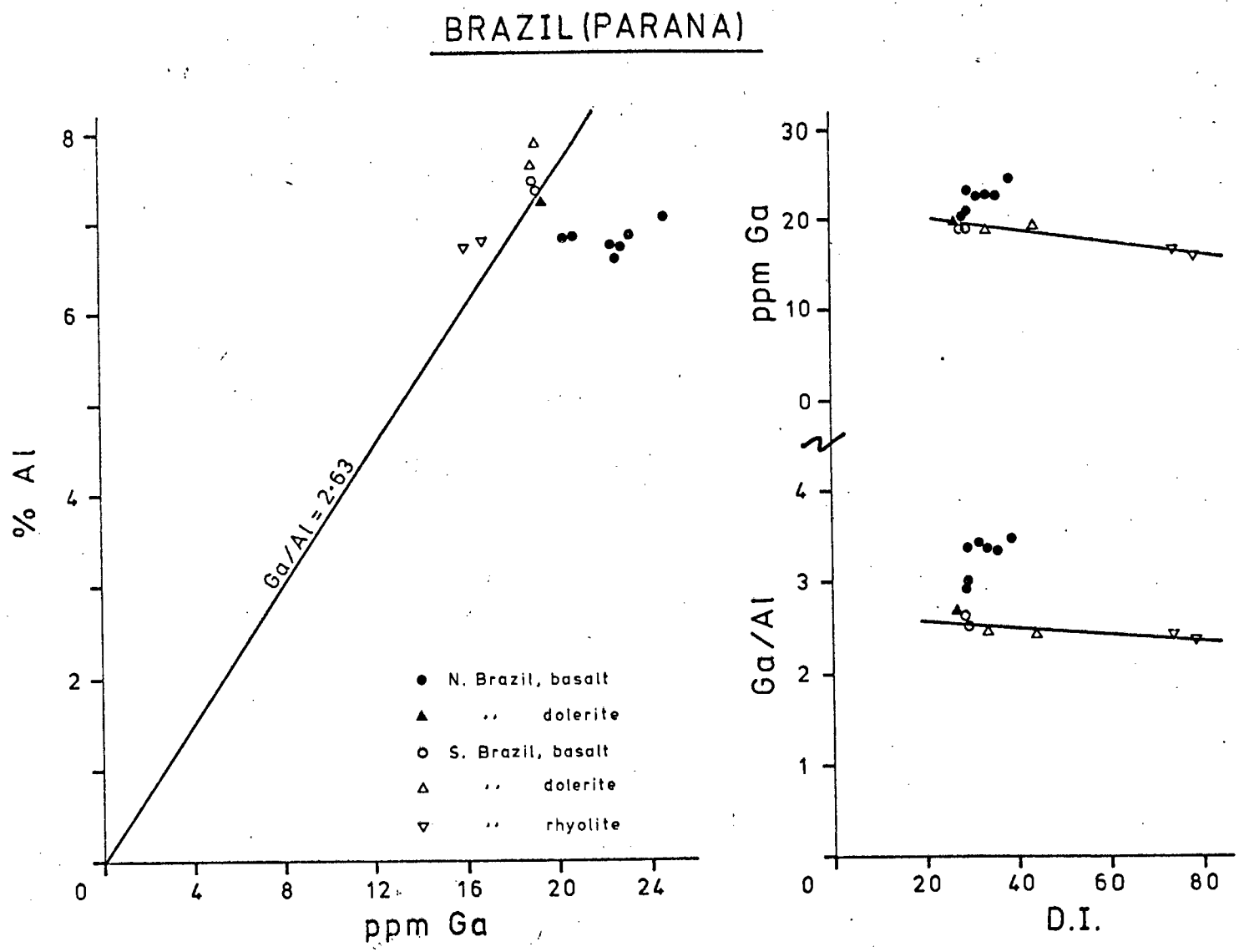

Fig. 132. Ga - Al, Ga - D.I. and Ga/Al - D.I. plots for Brazilian (Parana) volcanic rocks.

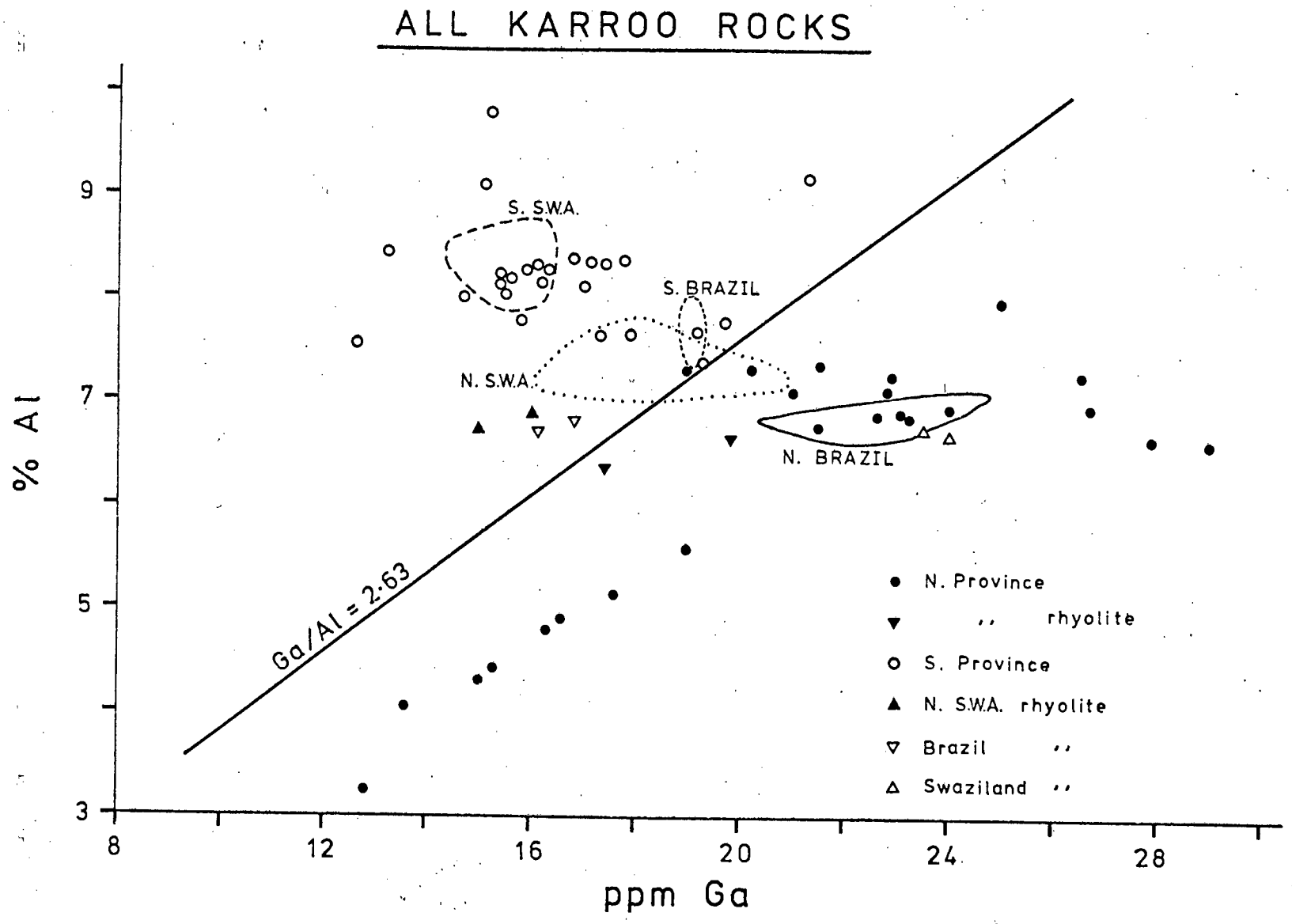

Fig. 133. A Ga - Al plot for all Karroo rocks from southern Africa and Brazil.

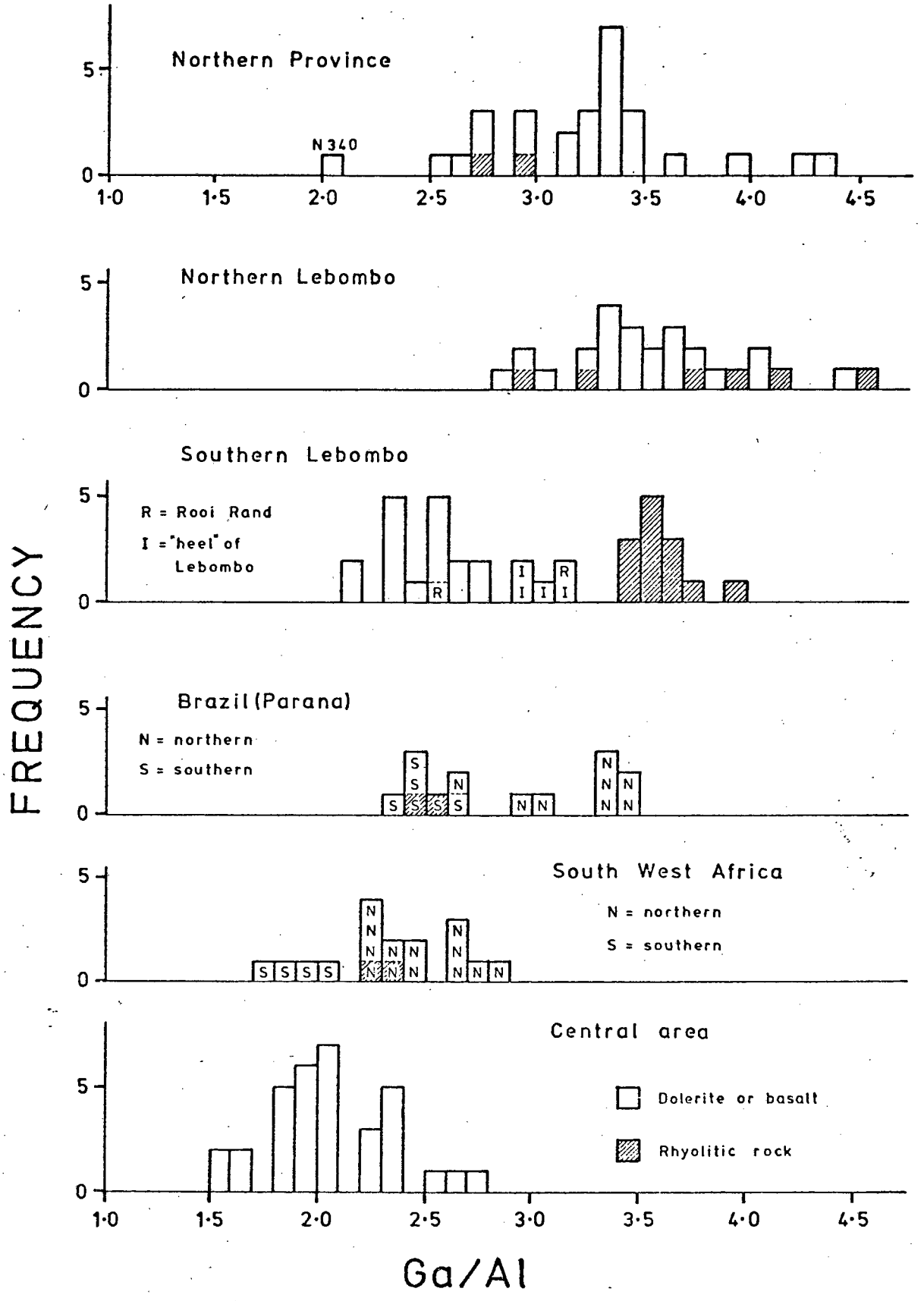

Fig. 134. Frequency distribution diagrams of the Ga/Al ratio in Karroo rocks from southern Africa and Brazil.

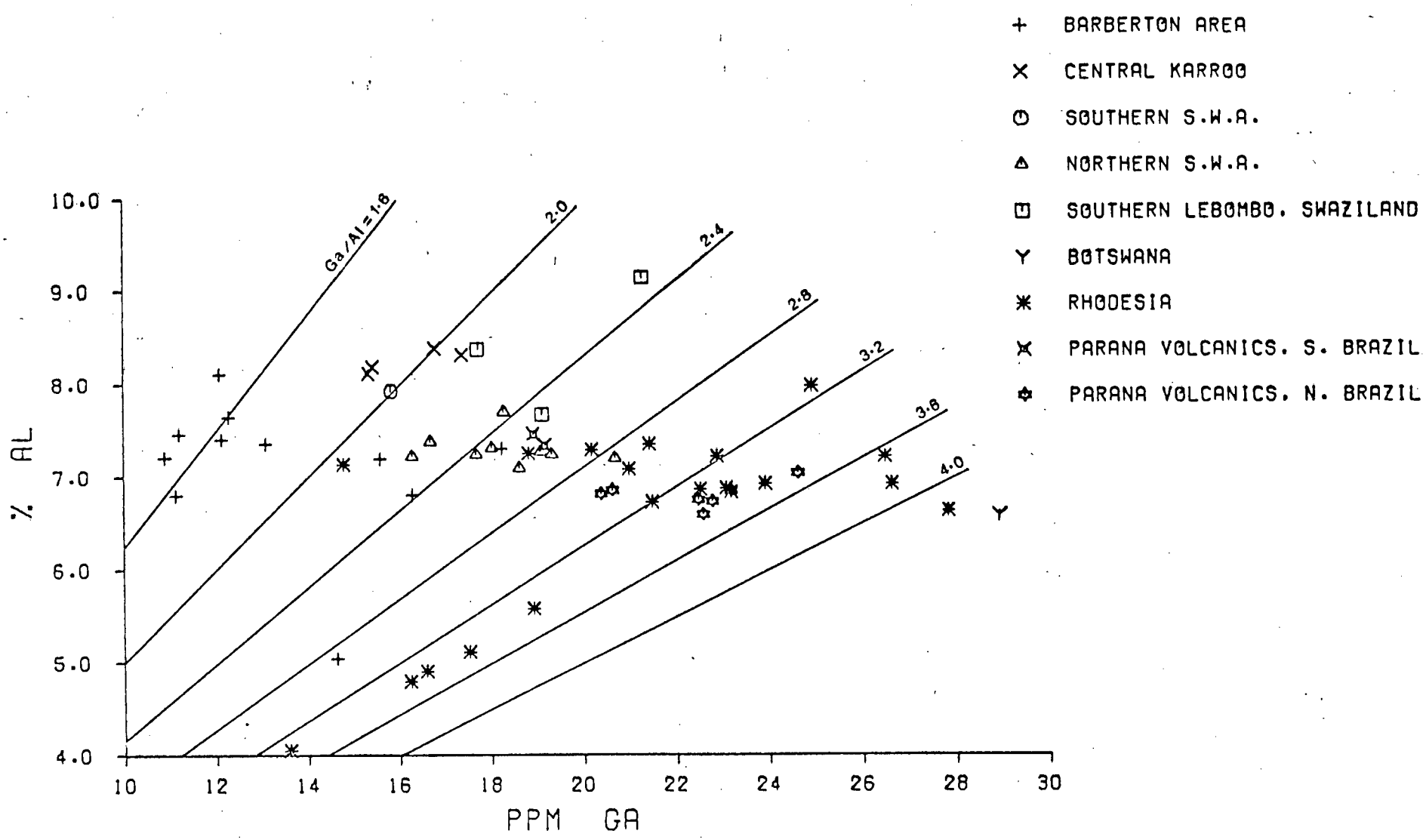

FIG. 135. GA - AL PLOT FOR CONTINENTAL BASALTS.

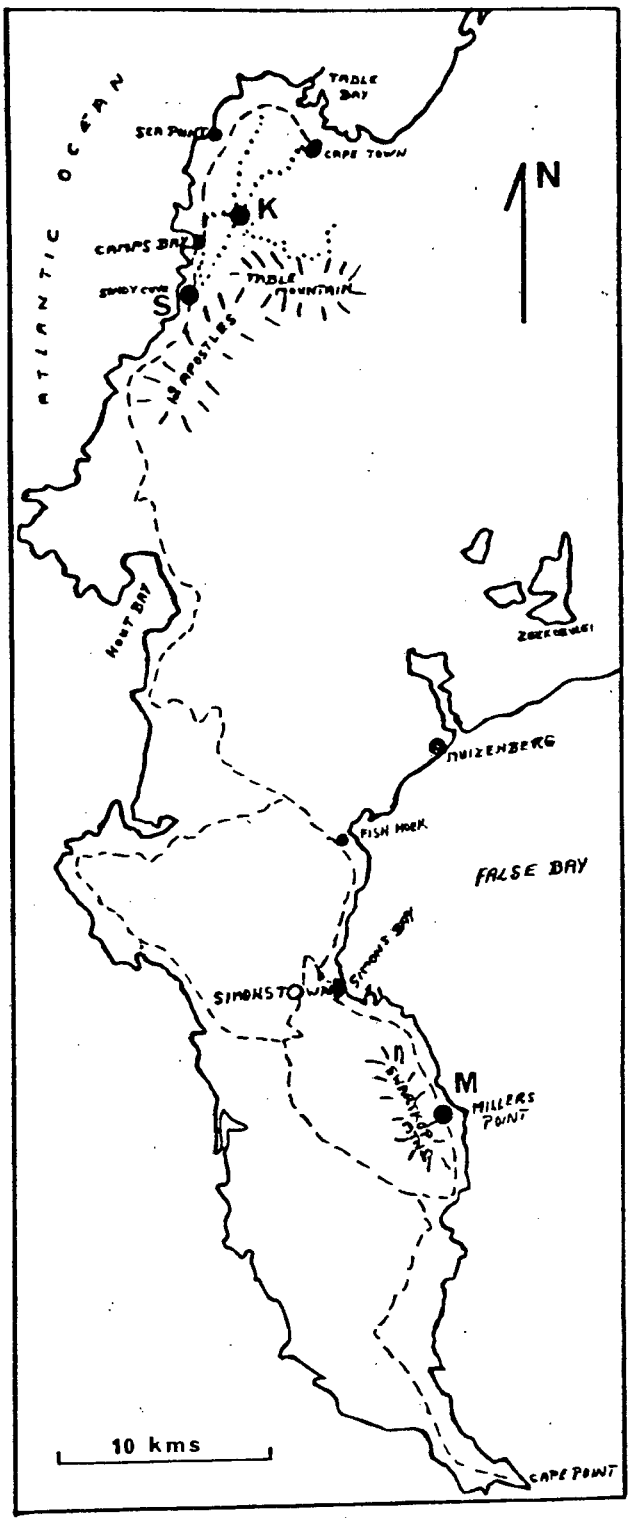

Fig. 136. Sample sites of granites in the Cape Peninsula (from Brunke, 1973).

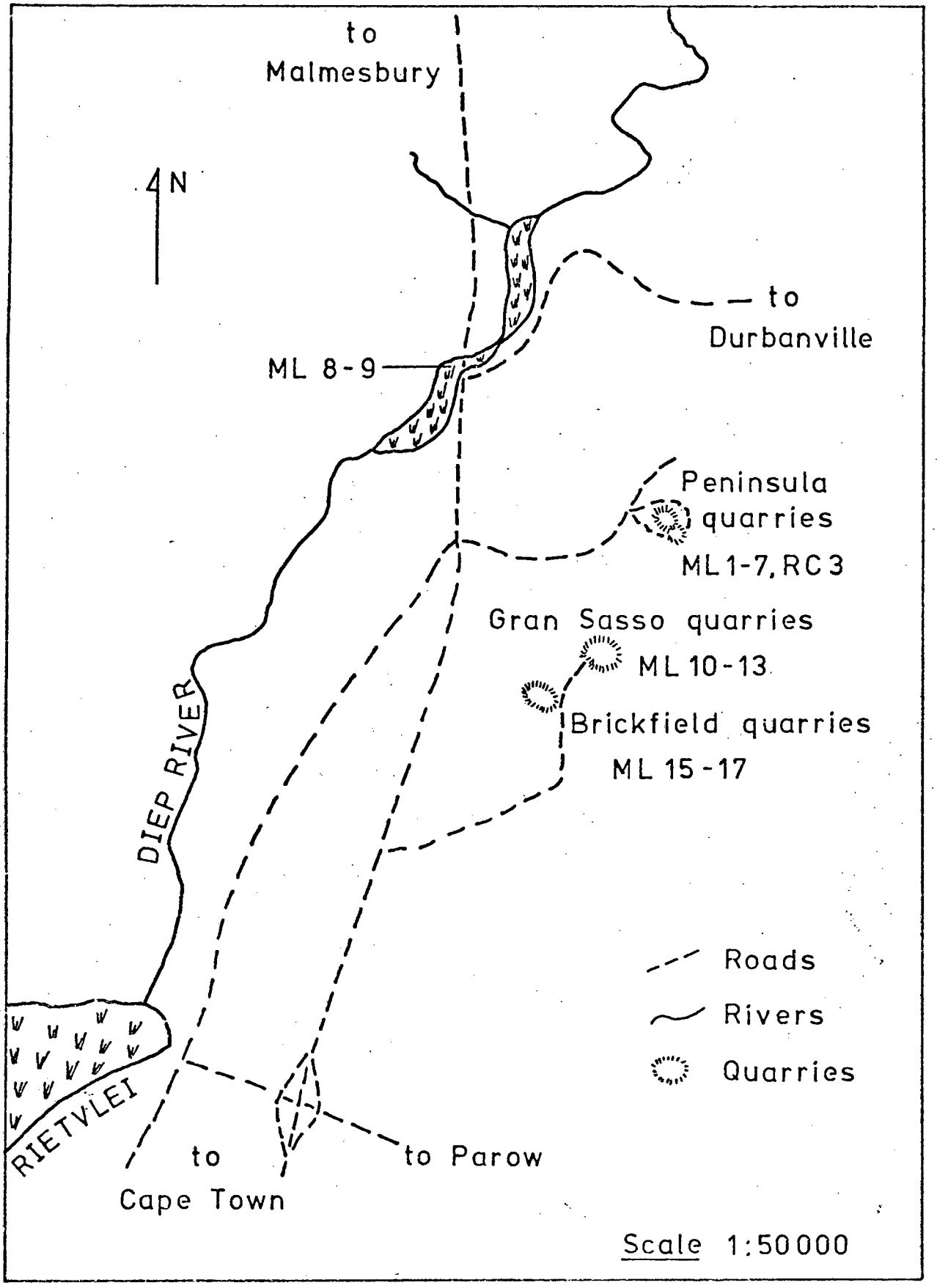

Fig. 137. Location of sample sites of sedimentary rocks from the Malmesbury Series, Cape Province, South Africa.

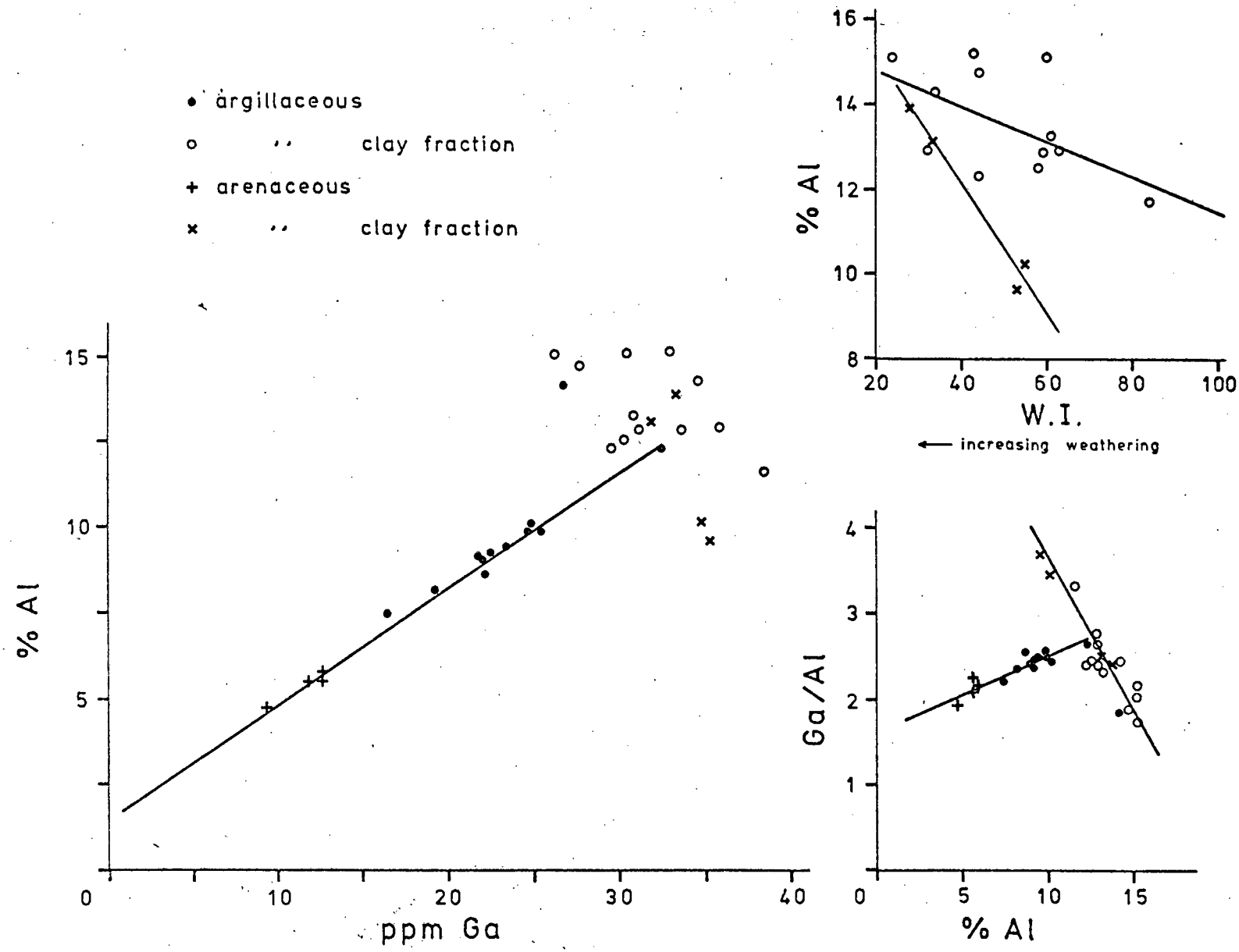

Fig. 138. Ga - Al, Ga/Al - Al and Al - W.I. (weathering index) plots for Malmesbury sediments and separated clay fractions.

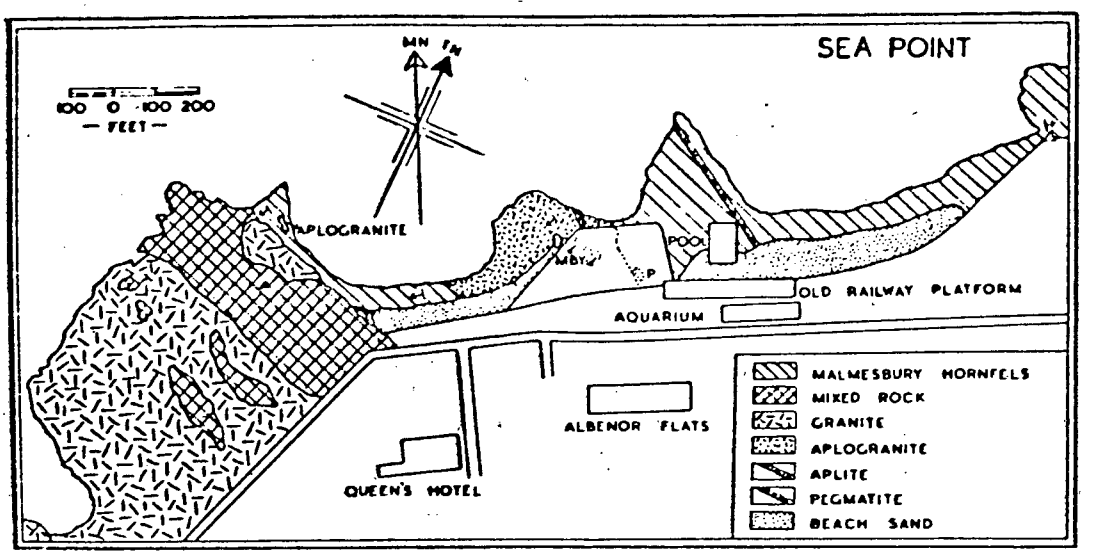

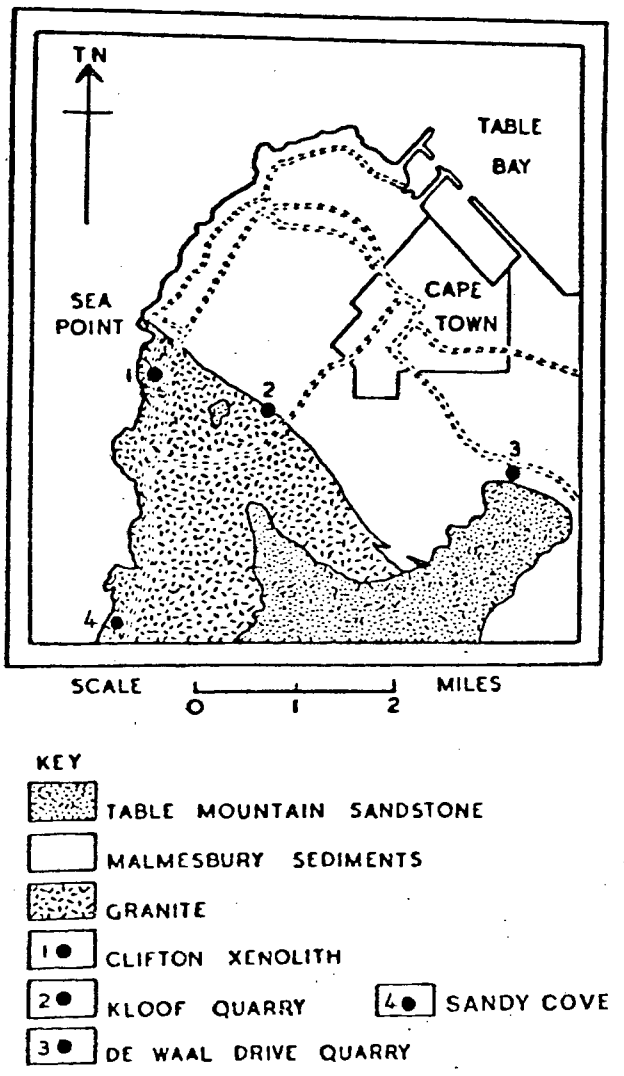

Fig. 139. Sketch diagrams showing the location and general geology of the Sea Point contact, Cape Town, South Africa (from Walker and Mathias, 1947).

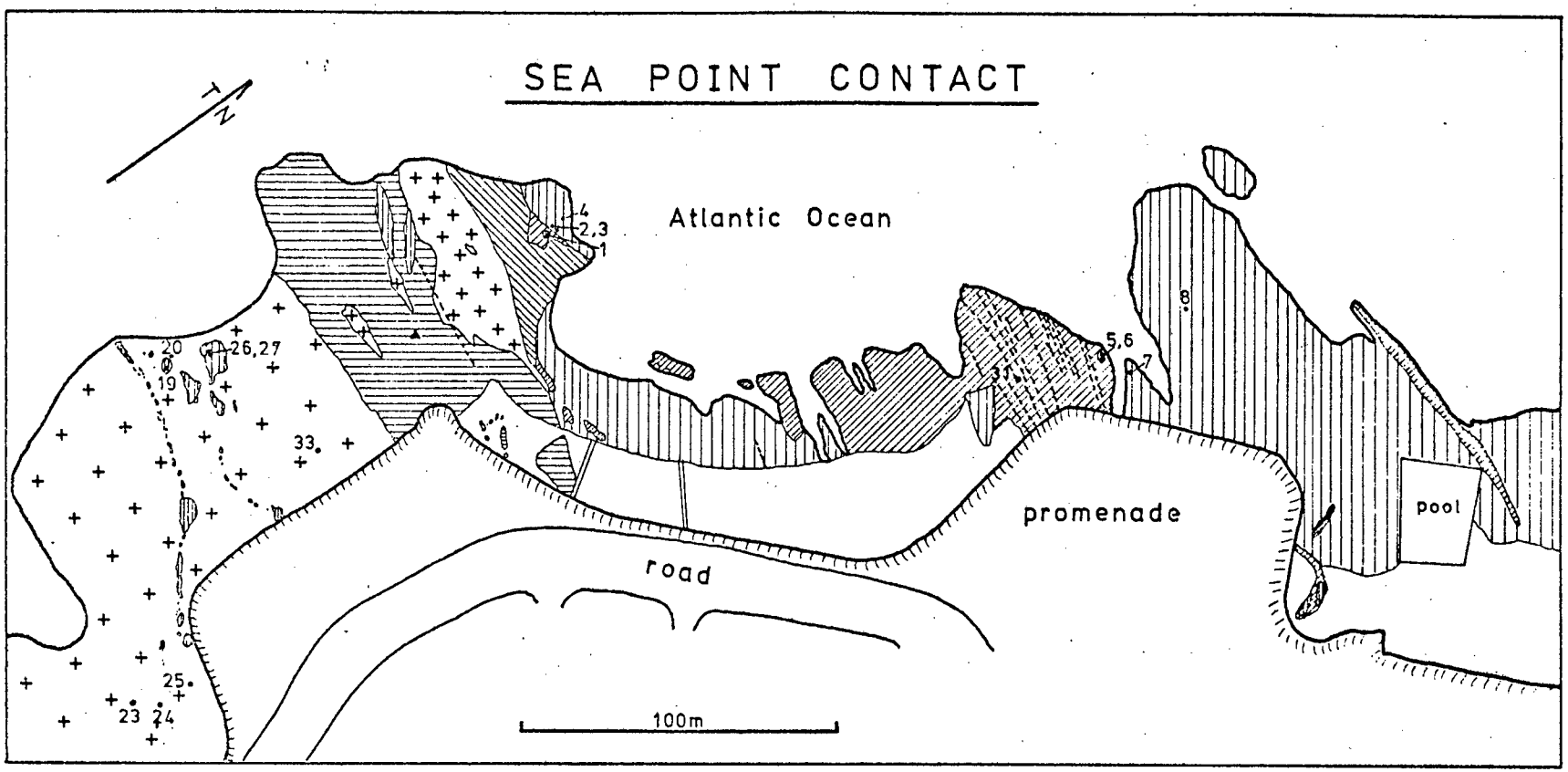

Fig. 140. Sketch map giving sample localities and geological details of the Sea Point contact zone (after van Coller, 1958).

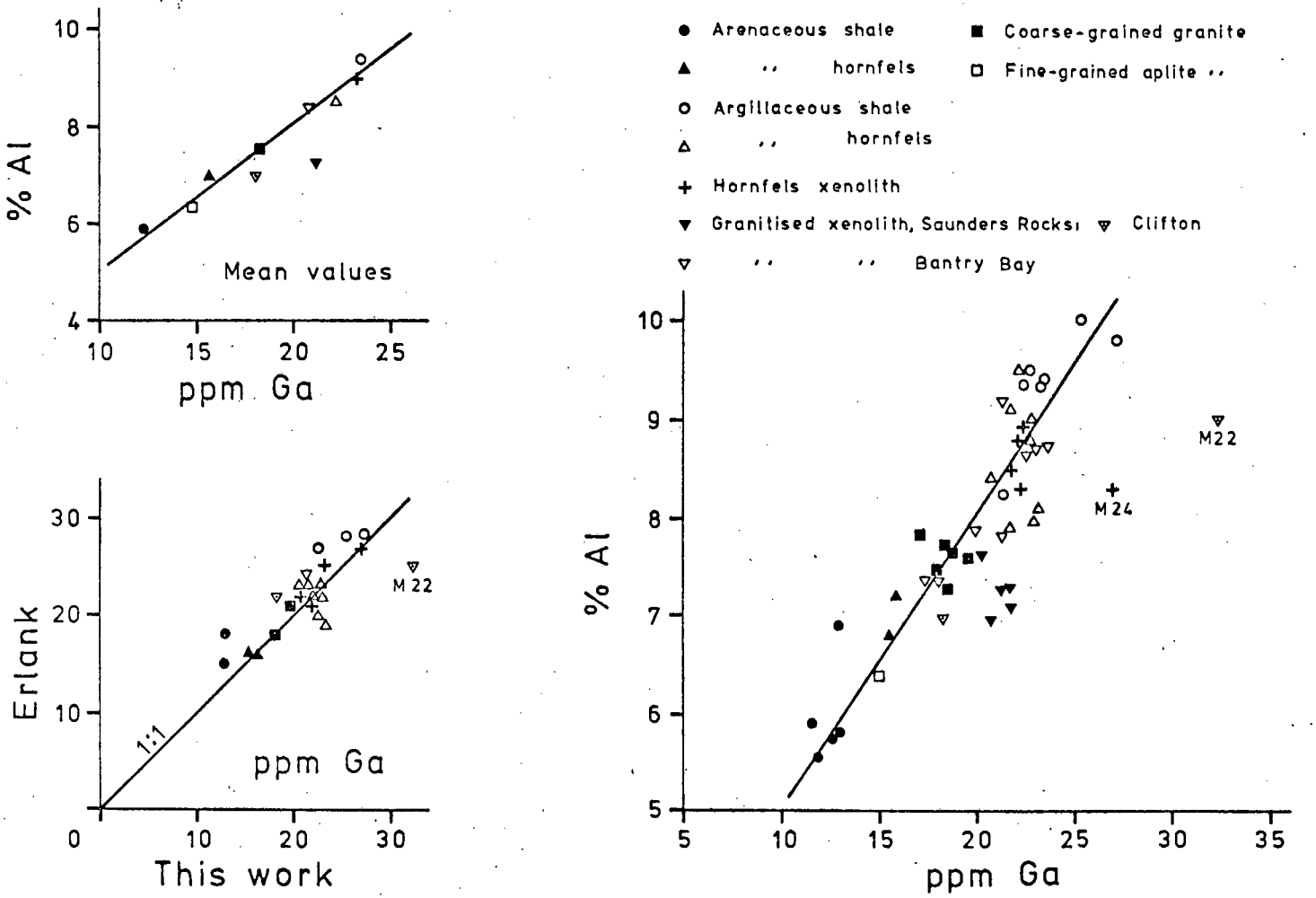

Fig. 141. Ga - Al plots for rocks from the Sea Point contact, and a comparison between optical emission spectrographic (Erlank, pers. comm.) and XRF Ga data for rocks from the area.

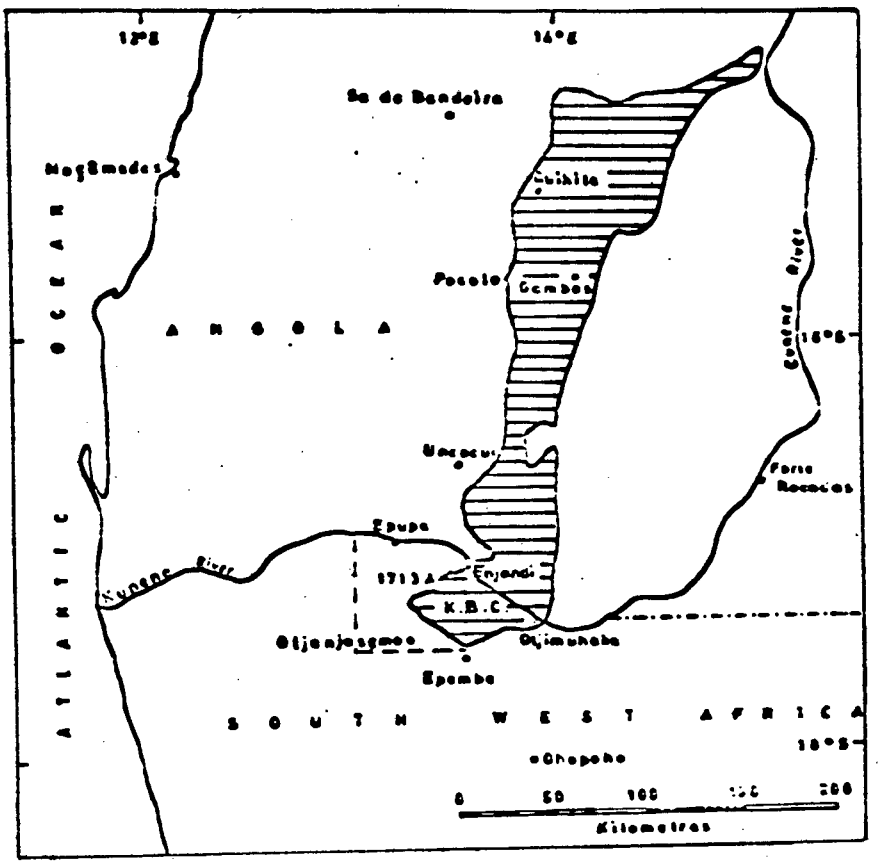

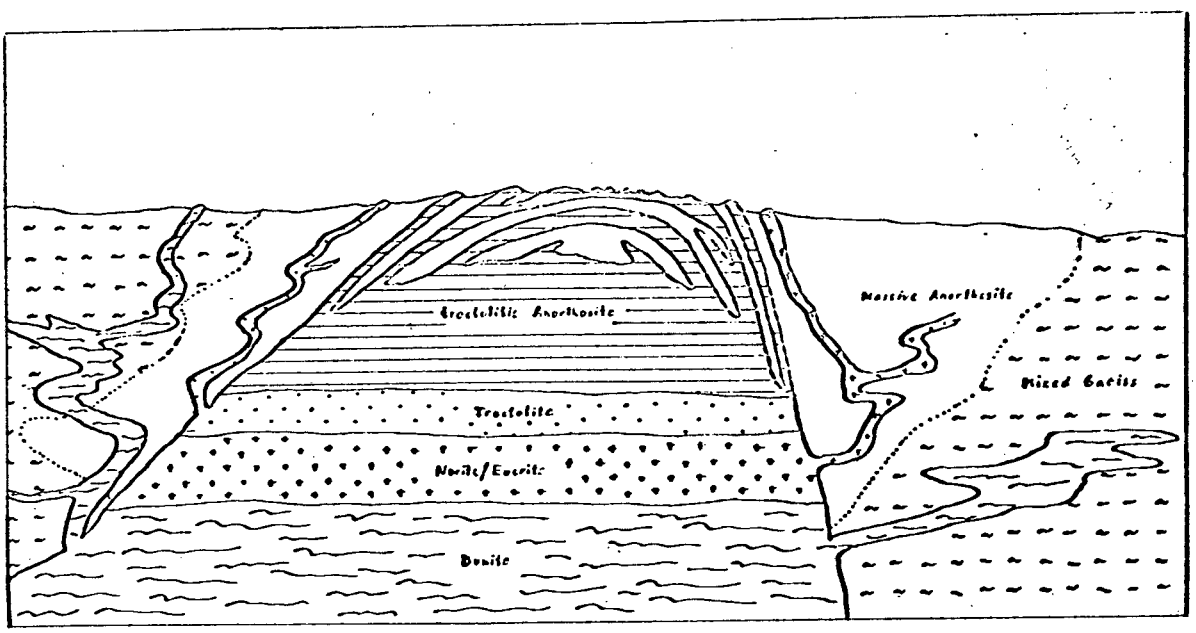

Fig. 142. Location and schematic section of the Kunene Basic Complex, Kaokoveld, S.W.A. (from Köstlin, 1967).

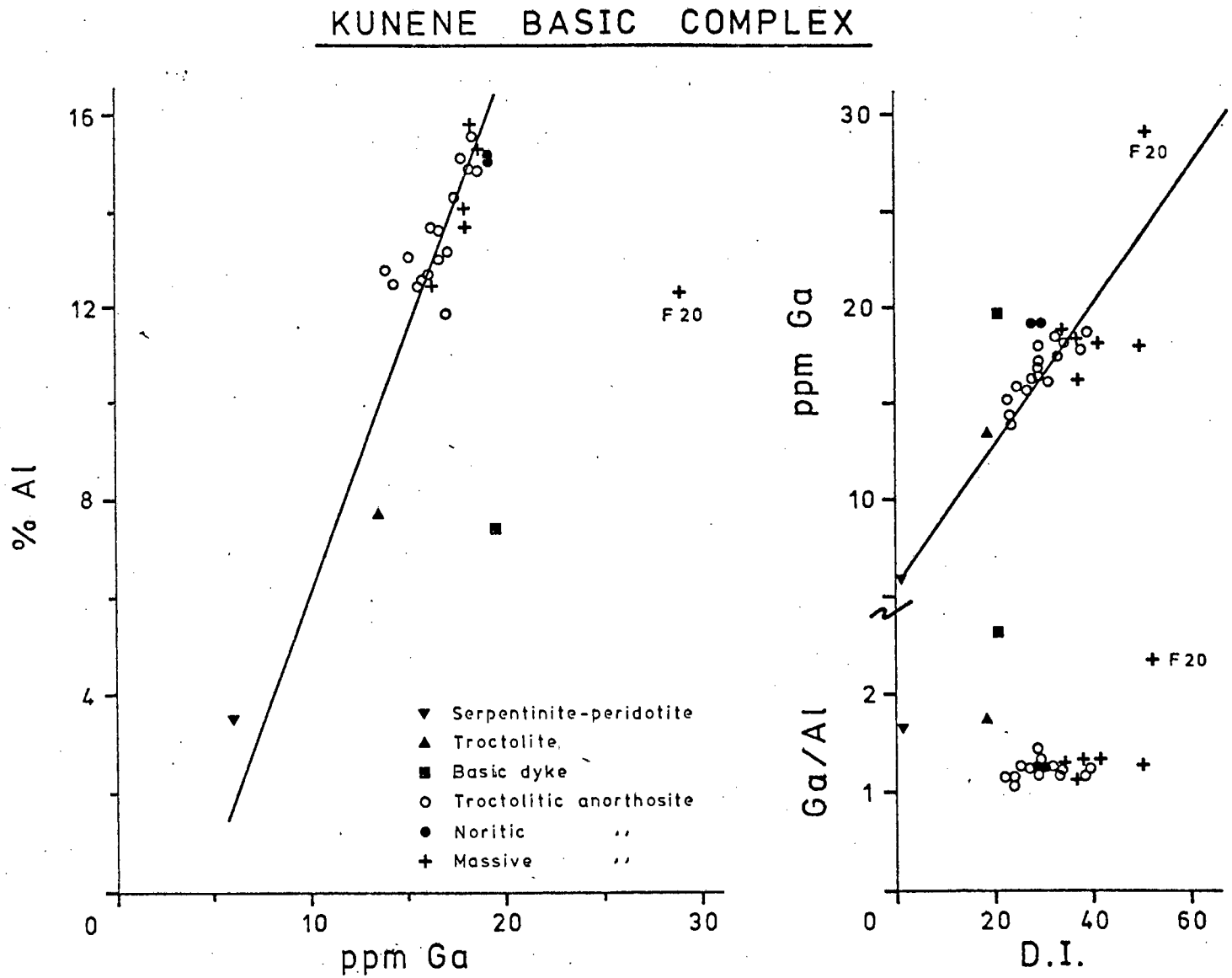

Fig. 143. Ga - Al, Ga - D.I. and Ga/Al - D.I. plots for rocks from the Kunene Basic Complex.

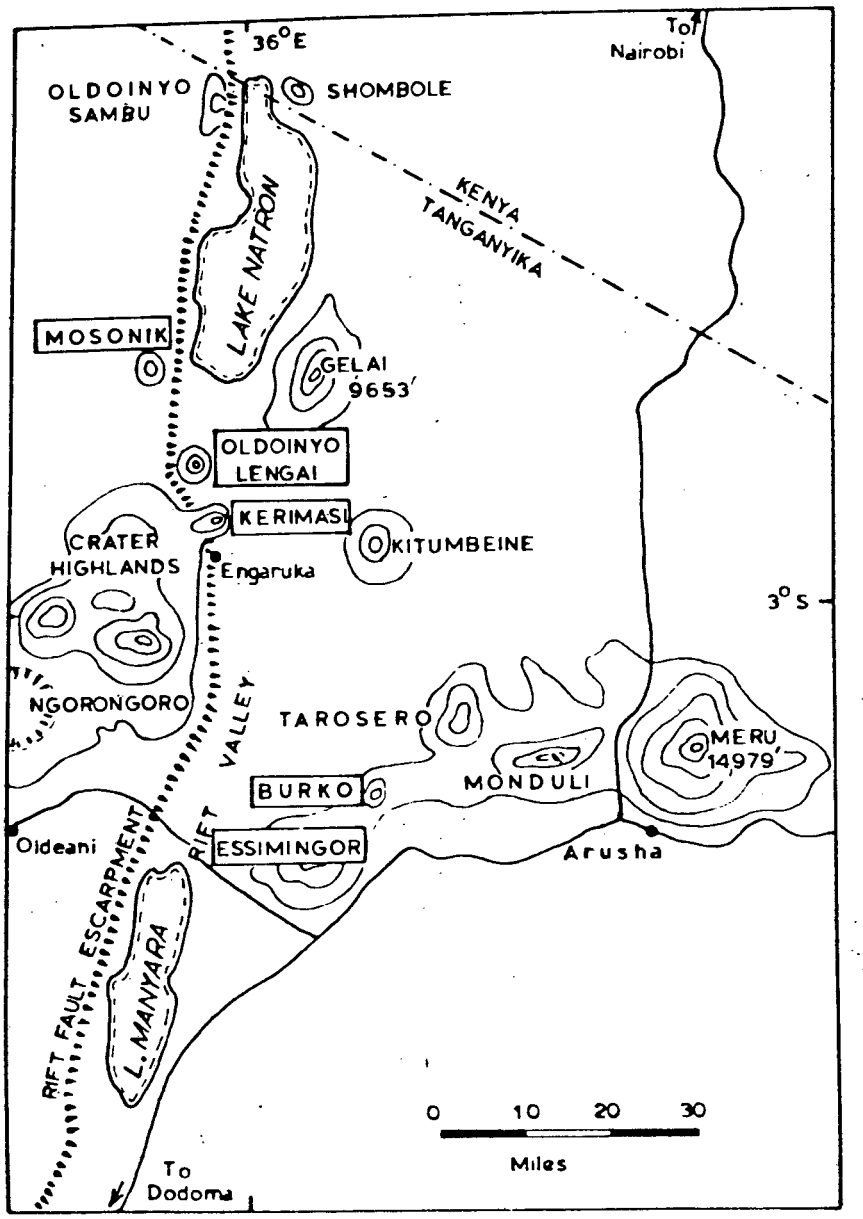

Fig. 144. Map showing location of Oldoinyo Lengai, Tanzania (from Dawson, 1966).

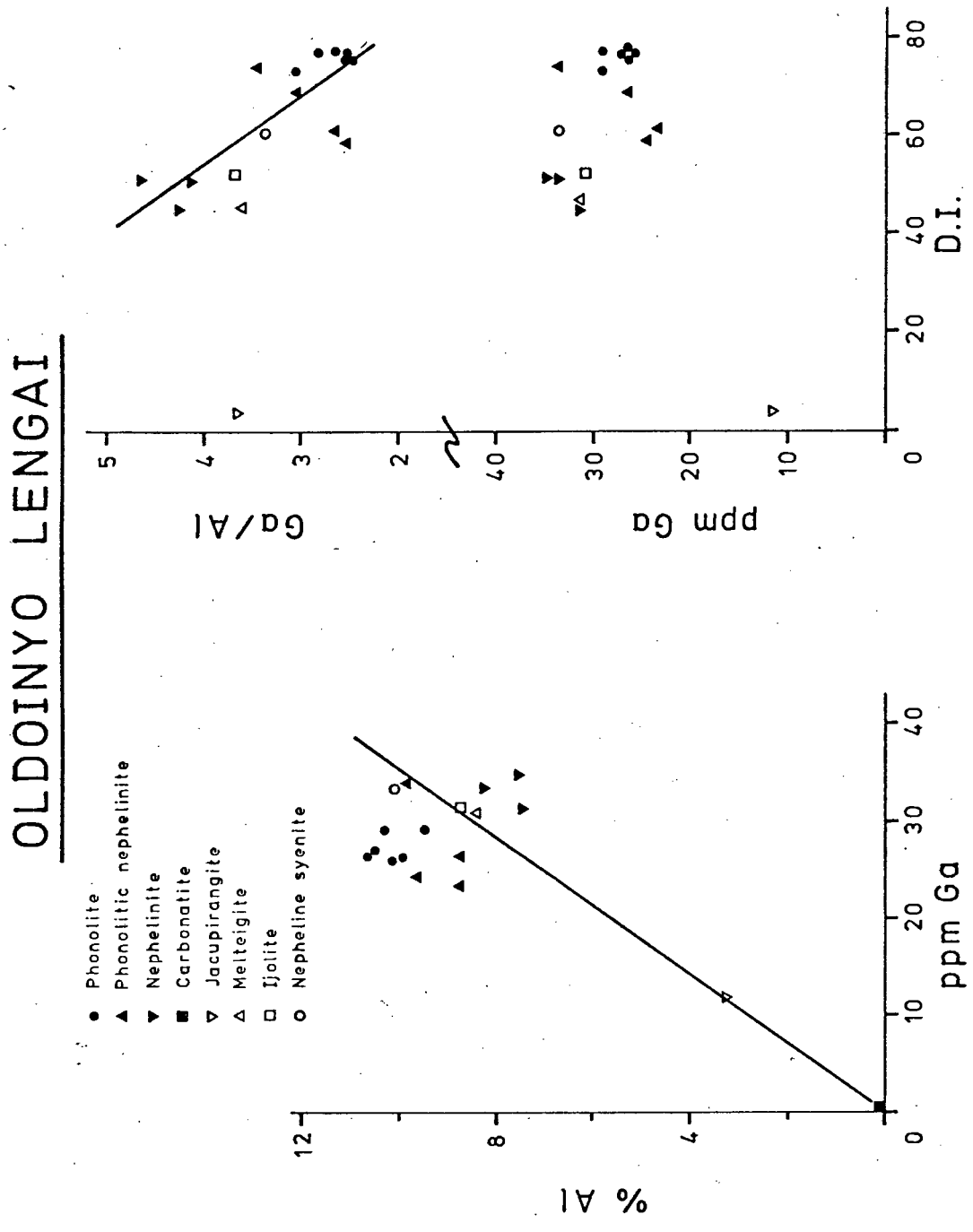

Fig. 145. Ga - Al, Ga - D.I. and Ga/Al - D.I. plots for rocks from Oldoinyo Lengai.

GEOLOGICAL MAP OF THE NEJOIO AREA, ANGOLA

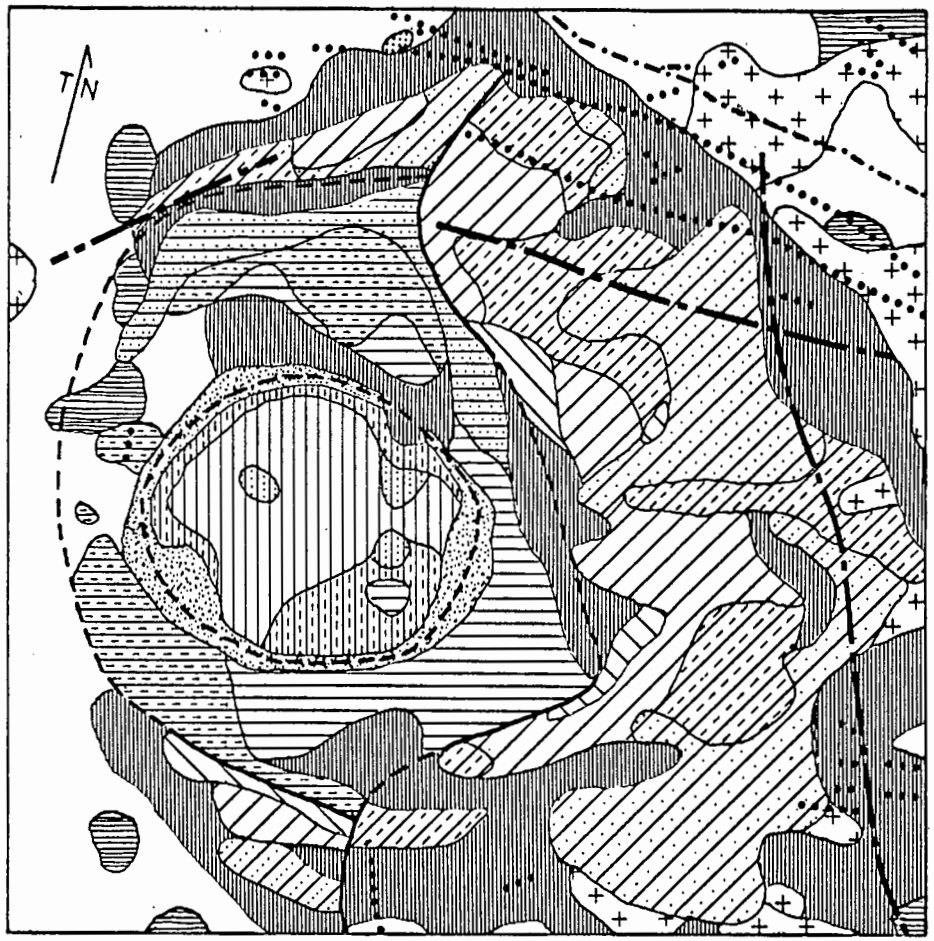

- Recent eluvium or alluvium
- Scree
- Laterite
- Rheomorphic fenites
- Fenites 3
- Fenites 2
- Fenites 1

  (Fenites 3, Fenites 2, Fenites 1: metasomatic fenites)

- Alkaline trachytes
- Phonolites and tinguaites
- Dolerites
- Eruptive breccia
- Cancrinite-hackmanite syenite
- Nepheline-cancrinite-hackmanite syenite
- Nepheline syenite

  (Cancrinite-hackmanite syenite, Nepheline-cancrinite-hackmanite syenite, Nepheline syenite: Outer zone)

- Nepheline-cancrinite-pyroxene syenite
- Nepheline-amphibole-pyroxene syenite
- Amphibole-nepheline syenite

  (Nepheline-cancrinite-pyroxene syenite, Nepheline-amphibole-pyroxene syenite, Amphibole-nepheline syenite: Inner zone)

- Regional granitic rocks
- Fault
- Probable fault

Fig. 147. Geological map of the Nejoio area, Angola (after Rodrigues, 1973).

Fig. 148. Plots of Ga and Ga/Al ratio against E.I. (endofenitization index, see text) for rocks from the Nejoio Ring Complex, Angola.

KEY:

- ● S1, amphibole-nepheline syenites
- ▼ S2, nepheline-amphibole-pyroxene syenites
- ▲ S3, nepheline-cancrinite-pyroxene syenites

(First Intrusion)

- o S4, nepheline syenites
- + S5, nepheline-cancrinite-hackmanite syenites
- × S6, cancrinite-hackmanite syenites

(Second Intrusion)

- △ PT, phonolites and tinguaites
- ▽ AT, alkali trachytes
- ■ dolerites
- □ cone-sheet (eruptive) breccias

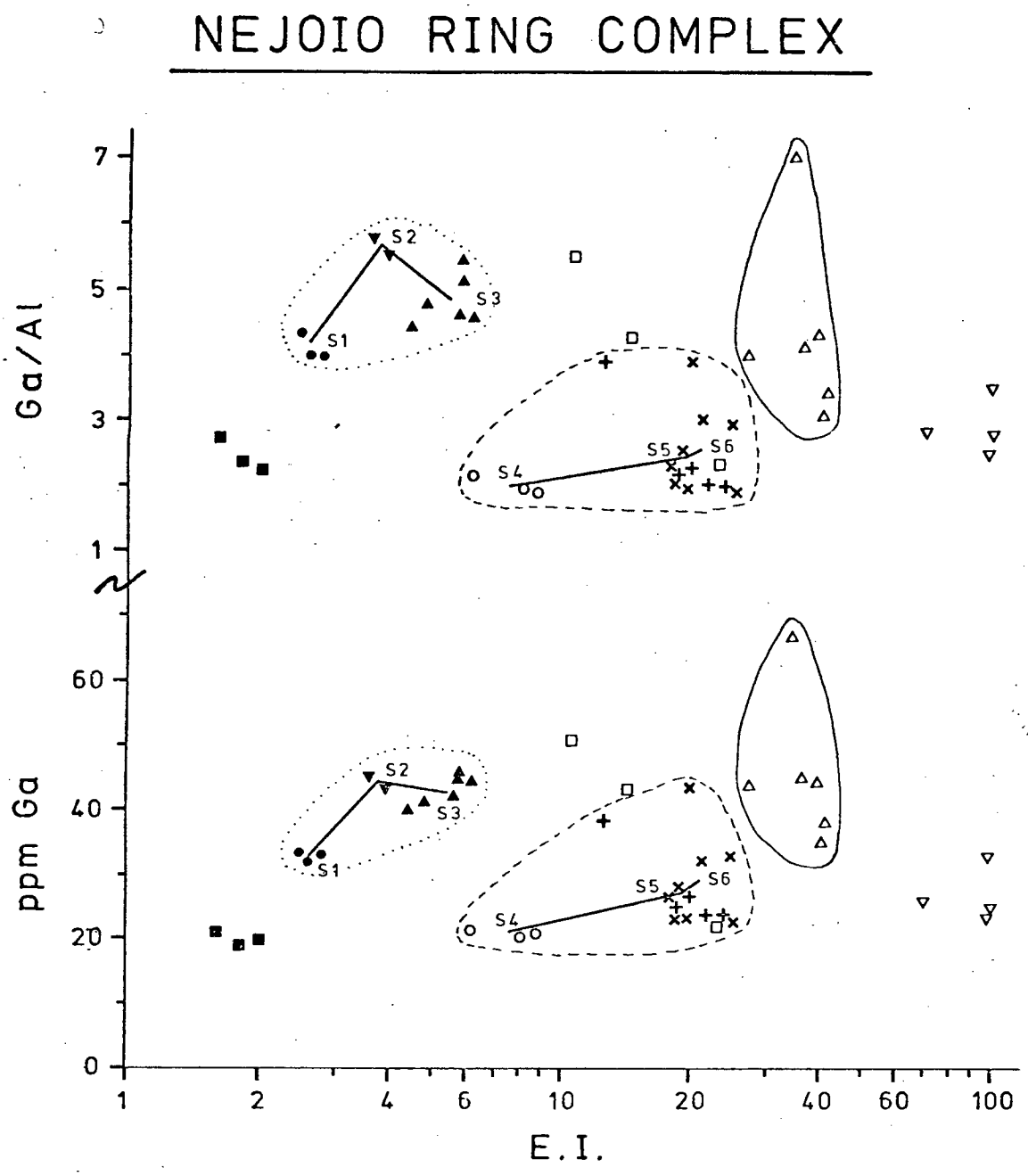

Fig. 148. Plots of Ga and Ga/Al ratio against E.I. (endofenitization index, see text) for rocks from the Nejoio Ring Complex, Angola.

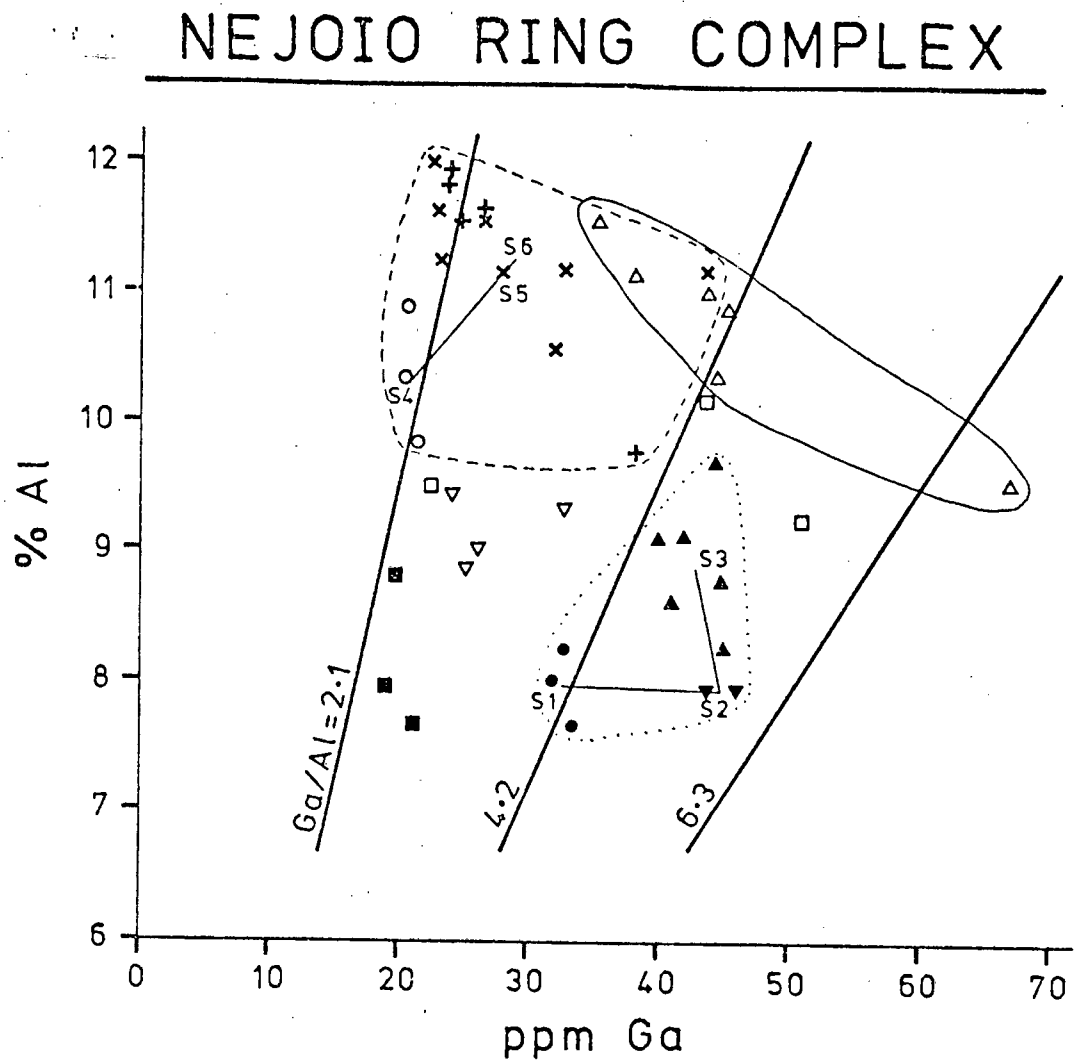

Fig. 149. A Ga - Al plot for rocks from the Nejoio Ring Complex. Key as for Fig. 148.

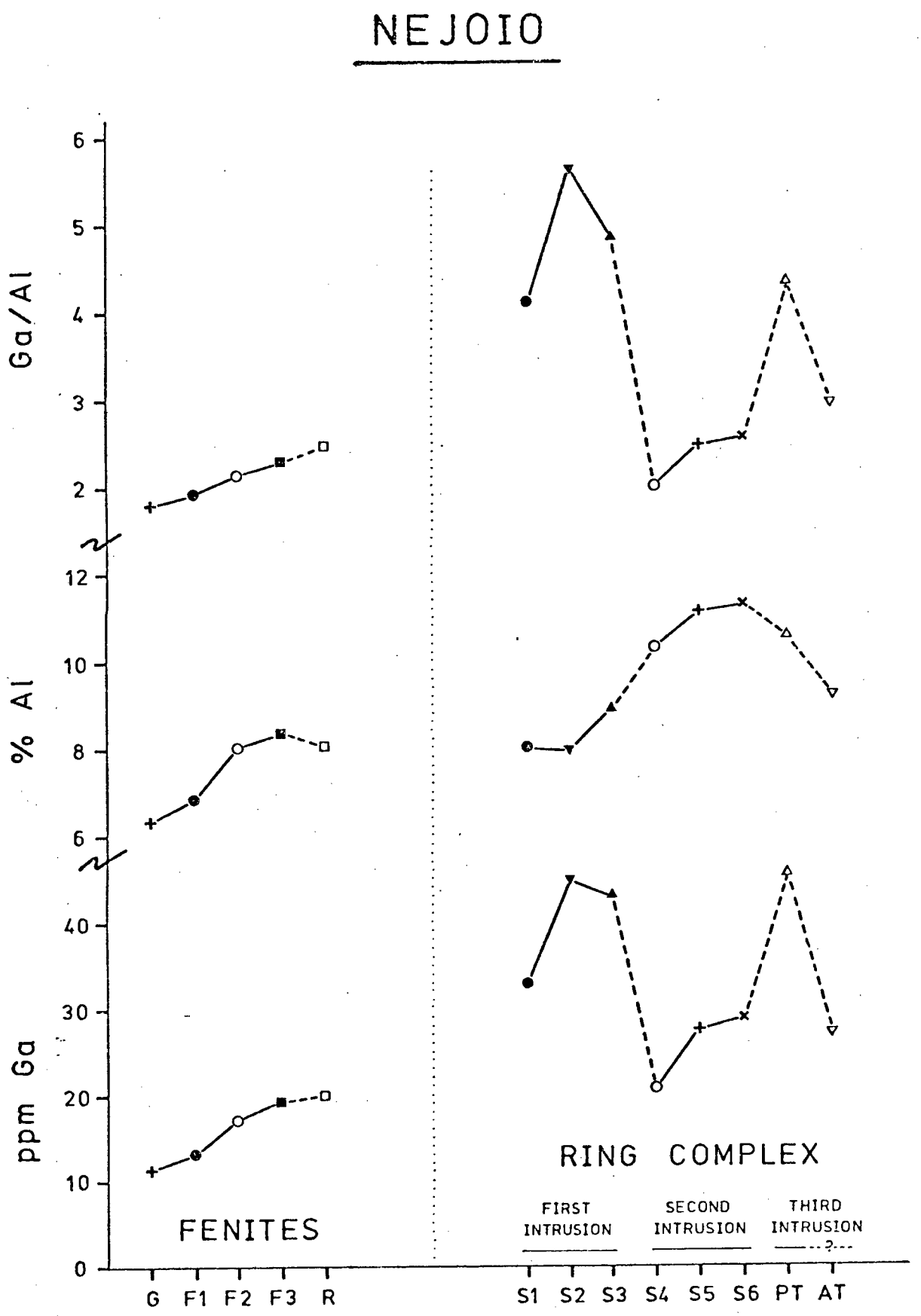

Fig. 150. Plot of mean values of Ga, Al and Ga/Al ratio for different rock types from the Nejoio area, Angola. Keys as for Figs 148 and 151.

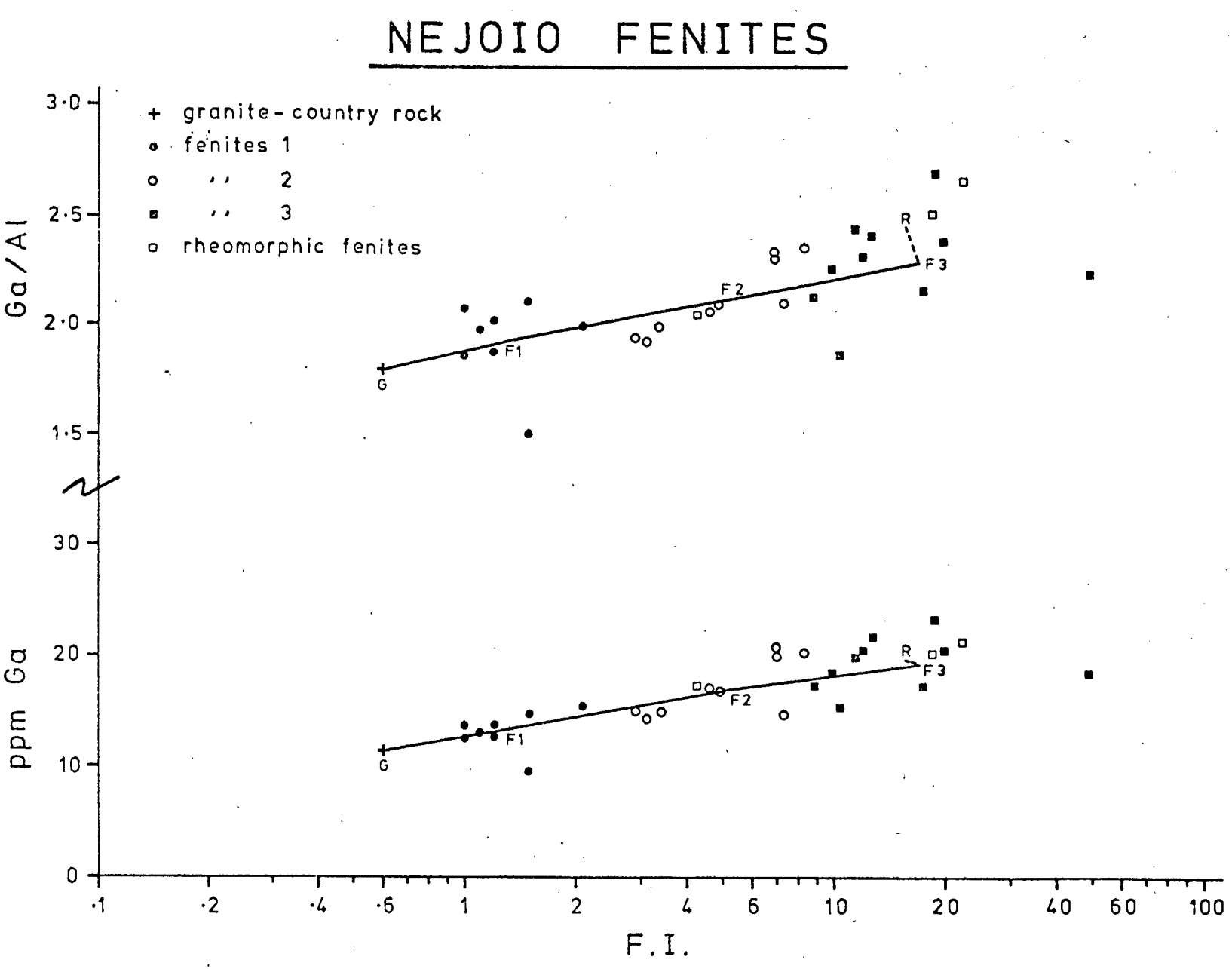

Fig. 151. Ga - F.I. (fenitisation index, see text) and Ga/Al - F.I. plots for fenites from the Nejoio area, Angola.